THE *SACCHAROMYCES CEREVISIAE PSO2/SNM1* GENE AND REPAIR OF ANTICANCER DRUG-INDUCED DNA INTERSTRAND CROSS-LINKS

LOUISE JANE BARBER

A thesis submitted for the Degree of Doctor of Philosophy

Cancer Research UK

Drug-DNA Interactions Research Group

Department of Oncology

Royal Free and University College Medical School

University College London

2004

UMI Number: U602828

All rights reserved

INFORMATION TO ALL USERS
The quality of this reproduction is dependent upon the quality of the copy submitted.

In the unlikely event that the author did not send a complete manuscript
and there are missing pages, these will be noted. Also, if material had to be removed,
a note will indicate the deletion.

UMI U602828
Published by ProQuest LLC 2014. Copyright in the Dissertation held by the Author.
Microform Edition © ProQuest LLC.
All rights reserved. This work is protected against
unauthorized copying under Title 17, United States Code.

ProQuest LLC
789 East Eisenhower Parkway
P.O. Box 1346
Ann Arbor, MI 48106-1346

ABSTRACT

Saccharomyces cerevisiae (budding yeast) cells defective for the *PSO2/SNM1* gene are uniquely sensitive to agents that produce DNA interstrand cross-links (ICLs), but not other forms of DNA damage. In the absence of Pso2, repair is stalled after the initial incision of ICLs, resulting in an accumulation of DNA double strand breaks (DSBs). The Pso2 protein is a member of the β-CASP metallo-β-lactamase family of hydrolytic enzymes, that include the mRNA processing enzyme CPSF, and Artemis, a human V(D)J recombination factor demonstrating single-strand DNA specific 5'-to-3' exonuclease and a hairpin endonuclease activity. Given the genetic epistasis of *PSO2* with the nucleotide excision repair pathway (NER) confirmed here in an isogenic background, it is probable that Pso2 is involved in the processing of ICL-repair intermediates arising from NER. Consequently, the genetic interactions between *PSO2* and yeast nucleases implicated in DNA repair and recombination have been characterised. *PSO2* demonstrates a striking synergistic relationship with the 5'-to-3' exonuclease *EXO1*. Double disruptant *pso2 exo1* yeast cells are significantly more sensitive to the cross-linking drug nitrogen mustard, relative to the single mutants, and accumulate a higher proportion of DSBs, which fail to be repaired. Furthermore, loss of both *pso2* and *exo1* results in a moderate sensitivity to ionising radiation, and a deficiency in spontaneous homologous recombination at a chromosomal inverted-repeat substrate. *EXO1* is known to interact, both genetically and physically, with the mismatch repair factor *MSH2*. In this study, it has been established that *pso2 msh2* double disruptants phenocopy *pso2 exo1*, consistent with an overlap of activity of Pso2 with the Exo1-Msh2 complex. This relationship involves a requirement for both MutS complexes (Msh2-Msh3 and Msh2-Msh6), but does not extend to spontaneous mismatch correction. It is proposed that Pso2 plays a role in the processing of repair intermediates for downstream recombination events, that is functionally redundant with Exo1-MutS during spontaneous recombination and double-strand break repair. As a conclusion to this study, FLAG-tagged Pso2 protein has been successfully purified from budding yeast. Western blotting shows this protein to be larger than expected, and cross-reactivity of purified Pso2 with a human polyclonal αSUMO antibody suggests a role for sumoylation in the regulation of Pso2 activity.

ACKNOWLEDGEMENTS

All hail the *SNM1*-God, Peter McHugh. You are an inspiration, and never cease to amaze me! Thanks for everything.

Also, great appreciation goes to Professor John Hartley, without whose support and advice this thesis would not have been possible.

Sincere gratitude to Cancer Research UK for funding this work.

Many thanks to all the members of the Drug-DNA Interactions Group for their help and friendship. But most of all to my yeastie partner, Ali Hazrati – only you can liven up even the most mundane task (cleaning incubators springs to mind!) and make me smile.

And last, but by no means least, thanks to my parents and Parjam for their constant love and support, especially in those dark moments when all the experiments seemed to fail. Thanks for not asking too often: 'Is it finished yet?' Well, here it is .....

TABLE OF CONTENTS

TITLE		**1**
ABSTRACT		**2**
ACKNOWLEDGEMENTS		**3**
TABLE OF CONTENTS		**4**
LIST OF FIGURES		**10**
LIST OF TABLES		**12**
ABBREVIATIONS		**13**
Chapter 1	**INTRODUCTION**	**16**
1.1	**DNA damaging agents**	**16**
1.1.1	Alkylating agents	17
1.1.1.1	Nitrogen mustards	22
1.1.2	Platinum-based compounds	23
1.1.3	Psoralens	26
1.1.4	Mitomycin C	28
1.1.5	DNA strand breaks	29
1.2	**DNA repair**	**30**
1.2.1	Nucleotide Excision Repair (NER)	31
1.2.2	Mismatch Repair (MMR)	35
1.2.3	Double Strand Break Repair Pathways	40
1.2.3.1	Homologous Recombination (HR)	41
1.2.3.1.1	Mechanisms of homologous DSB repair	43
1.2.3.1.1.1	Gene conversion	43
1.2.3.1.1.2	Break-induced replication (BIR)	47
1.2.3.1.1.3	Single-strand annealing (SSA)	47
1.2.3.2	Nonhomologous end-joining (NHEJ)	48
1.2.4	Post-replication repair (PRR)	52
1.2.5	Other repair pathways	56
1.3	**Repair of DNA interstrand cross-links**	**57**
1.3.1	*Escherichia coli*	58
1.3.2	*Saccharomyces cerevisiae*	59

1.3.3	Mammals (Higher eukaryotes)	65
1.4	***PSO2/SNM1***	**70**
1.4.1	Identification as a gene involved in ICL repair	70
1.4.2	Homology	71
1.4.3	Transcription and Inducibility	74
1.4.4	Intracellular localisation	75
1.4.5	Metallo-β-lactamase superfamily	76
1.4.6	Epistasis and functional analysis	79
1.5	**Objectives of this study**	**80**
Chapter 2	**MATERIALS AND METHODS**	**81**
2.1	**Chemicals and enzymes**	**81**
2.2	**Media and cell culture conditions**	**81**
2.2.1	*Saccharomyces cerevisiae*	81
2.2.1.1	Alpha factor growth arrest	82
2.2.2	*Schizosaccharomyces pombe*	82
2.2.3	*Escherichia coli*	83
2.3	**Production of yeast gene disruptants**	**83**
2.3.1	PCR-based production of the disruption cassette	86
2.3.2	Transformation of *S. cerevisiae*	87
2.3.3	Confirmation of gene disruption	88
2.3.3.1	Isolation of yeast genomic DNA	89
2.3.3.2	Yeast Colony PCR	89
2.4	**Analysis of growth rate and cell cycle phase**	**90**
2.5	**Colony-based survival assays**	**90**
2.5.1	Nitrogen mustard treatment	91
2.5.2	X-irradiation	91
2.5.3	UVC	92
2.5.4	Colony spotting assay	92
2.6	**Analysis of mutagenesis**	**93**
2.6.1	Spontaneous mutagenesis	94
2.6.2	HN2-induced mutagenesis	95
2.6.3	PCR-based analysis of mutagenesis	95

2.7	**CHEF analysis of DSB repair**	**96**
2.7.1	HN2-induced DSBs	96
2.7.2	Irradiated cells	97
2.7.3	Quantification of results	98
2.7.3.1	Gel Pro Analyser	98
2.7.3.2	Southern blotting	99
2.7.3.2.1	Preparation of probes	99
2.7.3.2.2	Southern blotting of CHEF agarose gel	100
2.7.3.2.3	Hybridisation	101
2.8	**Recombination at an *ADE2* inverted repeat construct**	**102**
2.8.1	Determination of spontaneous mitotic recombination frequency	102
2.8.2	Analysis of HN2-induced mitotic recombination frequency	103
2.8.3	PCR-based analysis of recombination events	104
2.9	**NHEJ assay**	**105**
2.10	**Plasmids and Complementation Analysis**	**106**
2.10.1	Cloning of *PSO2* and *EXO1* into pYES2	107
2.10.1.1	Gene amplification	107
2.10.1.2	Restriction enzyme-based cloning of gene into pYES2	108
2.10.1.3	Transformation of *E. coli*	109
2.10.1.4	Confirmation of gene cloning into pYES2	110
2.10.1.5	Isolation of plasmid DNA	110
2.10.2	Complementation using a galactose-inducible system	111
2.10.3	Complementation using a constitutive expression system	111
2.10.4	Confirmation of gene overexpression by RT-PCR	111
2.11	**Protein analysis**	**113**
2.11.1	Protein extraction and quantification	113
2.11.1.1	Whole-cell protein extraction	114
2.11.1.2	Immunoprecipitation	114
2.11.1.3	Large scale Pso2 protein extraction	115
2.11.1.4	Quantification of protein concentration	116
2.11.2	Analysis of post-translational modifications	116
2.11.2.1	Phosphorylation	116

2.11.2.2	Glycosylation	116
2.11.3	Polyacrylamide Gel Electrophoresis (PAGE)	117
2.11.4	Western blotting	117
2.11.5	Immunoblotting	118
Chapter 3	**CHARACTERISATION OF YEAST STRAINS DEFICIENT FOR *PSO2***	**120**
3.1	**Disruption of the *PSO2* gene**	**121**
3.2	***PSO2* is not required for normal growth and cell cycle kinetics**	**123**
3.2.1	Loss of *PSO2* does not disrupt the normal pattern of cell division	123
3.2.2	Loss of *PSO2* does not prevent or render cells sensitive to cell cycle arrest	125
3.2.3	*PSO2* is not essential for mitochondrial function	128
3.3	**Confirmation that loss of *PSO2* results in specific sensitivity to DNA ICL but not other forms of DNA damage**	**130**
3.4	**The *Schizosaccharomyces pombe pso2* mutant phenotype reflects that of *S. cerevisiae pso2***	**133**
3.5	**Creation of a panel of single and multiple gene disruption strains in a defined isogenic background in *S. cerevisiae***	**135**
3.5.1	*PSO2* is epistatic to the NER pathway for ICL repair	136
3.5.2	Both *PSO2* and NER exhibit a non-epistatic relationship with homologous recombination for the repair of cross-links	138
3.5.3	*PSO2* acts synergistically with the *RAD6*/post-replication repair pathway	141
3.5.4	Loss of *PSO2* leads to increased mutagenesis, dependent on *REV3*	143
3.6	**DSB repair is deficient in the absence of *PSO2***	**146**
3.7	**Discussion**	**148**

Chapter 4	**INTERACTIONS OF *PSO2* WITH YEAST REPAIR NUCLEASES**	**156**
4.1	**Repair of nitrogen mustard-induced DNA ICL**	**157**
4.1.1	*PSO2* exhibits significant synergism with *EXO1*	157
4.1.2	*PSO2* also acts synergistically with *MSH2*	161
4.2	**Sensitivity to other DNA damaging agents**	**163**
4.2.1	Loss of both *PSO2* and *EXO1/MSH2* causes increased sensitivity to ionising radiation	164
4.2.2	*PSO2* and *EXO1/MSH2* are not synergistic for the repair of DNA damage associated with UVC	167
4.2.3	*PSO2* and *EXO1/MSH2* do not function in the S-phase or mitotic checkpoints	169
4.3	**Analysis of DSB repair by CHEF**	**172**
4.3.1	DSB repair intermediates fail to be repaired and accumulate after HN2 treatment	173
4.3.2	CHEF analysis of X- and γ-irradiated cells	177
4.4	**Recombination at an inverted repeat substrate**	**181**
4.4.1	Spontaneous intrachromosomal recombination	182
4.4.2	Analysis of spontaneous recombination events in the absence of *PSO2*	186
4.4.3	HN2-induced recombination at the inverted repeat construct	190
4.5	**Non-homologous end joining**	**193**
4.6	**Complementation studies**	**196**
4.6.1	Overexpression of *EXO1* or *MSH2* does not compensate for loss of *PSO2*	196
4.6.2	The HN2 sensitivity of *pso2 exo1* and *pso2 msh2* can be rescued by plasmid expression of the disrupted genes	202
4.7	**Further analysis of the relationship between *PSO2* and Mismatch repair**	**204**
4.7.1	Other MMR factors show an intermediate phenotype for the modification of *pso2* sensitivity to HN2	205
4.7.2	An intermediate phenotype is also observed for sensitivity to ionising radiation in *pso2*-MMR double disruptants	207

4.7.3	No deficiency in recombination is observed for other MMR factors in combination with *pso2*	207
4.7.4	Increased spontaneous mutation is not further affected in *exo1* and *msh2* mutants by the loss of *PSO2*	211
4.8	**Discussion**	**213**
Chapter 5	**BIOCHEMICAL ANALYSIS**	**224**
5.1	**Verification of FLAG-Pso2 activity**	**225**
5.2	**Optimisation of protein extraction**	**228**
5.2.1	Protein extraction techniques	228
5.2.2	Galactose inducibility	230
5.3	**Isolation of FLAG-Pso2 by immunoprecipitation**	**233**
5.4	**Large-scale purification of Pso2**	**235**
5.5	**Analysis of post-translational modifications of the Pso2 protein**	**239**
5.5.1	Phosphorylation	240
5.5.2	Glycosylation	243
5.5.3	Sumoylation	245
5.6	**Discussion**	**246**
Chapter 6	**GENERAL DISCUSSION**	**254**
REFERENCES		**262**
APPENDIX		**306**
PUBLICATIONS ASSOCIATED WITH THIS THESIS		**309**

LIST OF FIGURES

1.1	Types of DNA adduct formed by cross-linking agents	18
1.2	Structure of nitrogen mustard	19
1.3	Alkylation sites of DNA bases	21
1.4	Structures of platinum compounds	24
1.5	Structures of other cross-linking compounds	27
1.6	Mechanism of NER in yeast	33
1.7	Mechanism of MMR in yeast	36
1.8	Models of DSB repair by homologous recombination in yeast	45
1.9	Mechanism of Non-Homologous end joining in yeast	50
1.10	Schematic of Post-replication repair	53
1.11	Model of ICL repair in yeast	61
1.12	Multiple protein sequence alignment of members of the Pso2/Snm1 family	72
1.13	Graphical representation of proteins of the β-CASP family	78
3.1	*PSO2* gene disruption	122
3.2	Analysis of the growth profile of *pso2* deficient cells	124
3.3	Sensitivity to HU and Benomyl	127
3.4	Analysis of growth on non-fermentable media	129
3.5	Sensitivity to HN2	131
3.6	Sensitivity to UVC and X-irradiation	132
3.7	*S. pombe pso2* sensitivity to HN2 and HN1	134
3.8	Comparison of HN2 sensitivity in *pso2* and *rad4* (NER) deficient cells	137
3.9	Comparison of HN2 sensitivity in *pso2* and HR mutants	139
3.10	Comparison of HN2 sensitivity in *pso2* and *rev3*, or *rad18* (PRR) deficient cells	142
3.11	Mutagenesis in *pso2*, PRR, and NER mutants	144
3.12	HN2-induced DSB repair in *pso2*, NER and HR mutants	147
4.1	Comparison of HN2 sensitivity in *pso2* and nuclease mutants	158

4.2	Comparison of HN2 sensitivity in *pso2*, *exo1*, *msh2*, and *rad52* mutants	162
4.3	Comparison of X-irradiation sensitivity in *pso2*, *exo1*, *msh2* and *rad52* mutants	165
4.4	Comparison of UVC sensitivity in *pso2*, *exo1*, and *msh2* mutants	168
4.5	Comparison of HU and Benomyl sensitivity in *pso2*, *exo1*, and *msh2* mutants	170
4.6	HN2-induced DSB repair in *pso2*, *exo1*, and *msh2* mutants	174
4.7	X-irradiation-induced DSB repair	178
4.8	γ-irradiation-induced DSB repair	180
4.9	Spontaneous recombination at an inverted repeat substrate	183
4.10	Representation of the classes of recombination event	187
4.11	Analysis of spontaneous recombination events	189
4.12	HN2-induced recombination at an inverted repeat construct	192
4.13	Non-homologous end joining assay	195
4.14	Complementation analysis of a *pso2* mutant	197
4.15	Confirmation of *MSH2* gene expression by RT-PCR	200
4.16	Simultaneous complementation analysis of a *pso2* mutant by *EXO1* and *MSH2*	201
4.17	Complementation analysis in the *pso2 exo1* and *pso2 msh2* double disruptants	203
4.18	Comparison of HN2 sensitivity in *pso2* and MMR mutants	206
4.19	Comparison of X-irradiation sensitivity in *pso2* and MMR mutants	208
4.20	Comparison of spontaneous recombination in *pso2* and MMR mutants	210
4.21	Analysis of mutagenesis in *pso2*, *exo1*, and *msh2* mutants	212
5.1	Complementation of a *pso2* mutant by FLAG-*PSO2* expression	227
5.2	Analysis of galactose-inducible FLAG-*PSO2* expression	232
5.3	FLAG-Pso2 immunoprecipitation	234
5.4	Purification of FLAG-Pso2	238

5.5	Sequence-based prediction of post-translational modifications	242
5.6	Biochemical analysis of post-translation modifications	244
5.7	Putative sumoylation of FLAG-Pso2	247
6.1	Revised model of ICL repair in yeast	258

LIST OF TABLES

1.1	Conservation of NER genes between yeast and humans	34
2.1	*S. cerevisiae* strains used in this study	84
2.2	Primers used in the cloning of *PSO2* and *EXO1*	108
3.1	Microscopic analysis of cell cycle phase	125
4.1	DSB repair efficiencies	176
4.2	Number of DSBs per 1 Mb DNA induced by 200 Gy X-irradiation	181
4.3	Spontaneous recombination rates at an inverted repeat substrate	184
4.4	Classification of recombination events	190
4.5	Spontaneous recombination rates in *pso2*-MMR defective strains	209
5.1	Comparison of protein yields obtained using different extraction techniques	230
5.2	Putative Pso2 phosphorylation sites	241
5.3	Putative Pso2 sumoylation sites	246

ABBREVIATIONS

8-MOP	8-methoxypsoralen
ade	Adenine
arg	Arginine
BER	Base excision repair
BIR	Break-induced replication
bp	Base pair
BSA	Bovine serum albumin
CDS	Coding sequence
CHEF	Contour-clamped homogenous field electrophoresis
CHEF	Contour-clamped homogenous field electrophoresis
CHO	Chinese Hamster Ovary
chrom	Chromosome
CIAP	Calf intestinal alkaline phosphatase
CPD	Cyclobutane pyrimidine dimer
dHJ	Double Holliday Junction
DNA-PK	DNA protein kinase
dNTP	Dinucleotide triphosphate
DSB	Double-strand break
dsDNA	Double-stranded DNA
EUROSCARF	European *Saccharomyces cerevisiae* Archives for Functional analysis
FA	Fanconi anaemia
GGR	Global genome repair
HN1	Mono-nitrogen mustard (2-dimethylaminoethylchloride hydrochloride)
HN2	Nitrogen mustard (Mechlorethamine)
HNPCC	Hereditary non-polyposis colorectal cancer
HR	Homologous recombination
HU	Hydroxyurea
ICL	Interstrand cross-link
IDL	Insertion-deletion loop

LB	Luria-Bertani
leu	Leucine
MAT	Mating-type genes
MM	Minimal media
MMC	Mitomycin C
MMR	Mismatch repair
MMS	Methyl methane sulfonate
MRX	Mre11-Rad50-Xrs2
MWCO	Molecular weight cut-off
NEF	Nucleotide excision repair factor
NER	Nucleotide excision repair
NHEJ	Non-homologous end joining
nt	Nucleotide
OD	Optical density
ORF	Open reading frame
PAGE	Polyacrylamide gel electrophoresis
PBS	Phosphate-buffered saline
PCR	Polymerase chain reaction
PEG	Polyethylene glycol
PFGE	Pulsed field electrophoresis
PRR	Post-replication repair
RS-SCID	Radiation Sensitive Severe Combined Immune Deficiency
RT-PCR	Reverse transcription PCR
SC	Synthetic complete
SDSA	Synthesis-dependent strand annealing
SEM	Standard error of the mean
SSA	Single-strand annealing
SSB	Single-strand break
SSC	Sorbitol-sodium citrate-EDTA
ssDNA	Single-stranded DNA
SSPE	Sodium chloride-sodium phosphate-EDTA
TBE	Tris-Borate-EDTA
TCR	Transcription coupled repair

TCR	Transcription-coupled repair
TE	Tris-EDTA
TLS	Translesion synthesis
trp	Tryptophan
ura	Uracil
UV	Ultraviolet light
wt	Wild-type
XP	Xeroderma pigmentosum
YEPD	Yeast extract-peptone-dextrose
YES	Yeast extract with supplements
YPAD	Yeast extract-peptone-adenine-dextrose
YPG	Yeast extract-peptone-glycerol

CHAPTER 1 INTRODUCTION

Cancer is a complex disease arising from genetic mutations that confer a selective advantage for disregulated cell growth and development. Yet DNA is also the target for many of the current cancer therapies, as critical DNA damage can cause cell death. Hence, genomic integrity represents a crucial determinant in cancer progression, and therefore our understanding of normal DNA metabolism and repair is central to the development of successful treatments for this disease.

1.1 DNA damaging agents

The DNA of any organism is under constant assault from both the environment and reactive species generated within the cell (reviewed in Friedberg *et al.*, 1995). Spontaneous damage occurs frequently during normal DNA metabolism and may result in strand breakage, mismatches, or alterations in the chemistry of DNA bases (e.g. tautomeric shifts, deamination, depurination, depyrimidination). Environmental stress may be chemical (e.g. alkylating agents, benzo(α) pyrenes, aflatoxins) or physical (e.g. ultraviolet light, ionising radiation), and can inflict a similarly diverse range of DNA lesions. Examples include: covalent linkage of adjacent pyrimidines (cyclobutane pyrimidine dimers and 6-4 photoproducts) resulting from UV exposure; ionising radiation-induced strand breaks; and DNA base adducts formed by aflatoxin and alkylating agents. Furthermore, reactive oxygen species arising both endogenously and exogenously cause a variety of DNA damage including fragmentation and base loss.

Many clinically relevant chemicals, including many common chemotherapeutic agents, cause damage to DNA through the formation of cross-links. For example, nitrogen mustards, platinum drugs, photoactivated psoralens, and the natural compound mitomycin C (Metzler, 1986). Cross-links are produced when a monoadduct that is covalently attached to DNA undergoes a second reaction with the same DNA strand (intrastrand), the complementary DNA strand (interstrand), or in some cases with a protein (Fig. 1.1). These lesions can be highly cytotoxic as a result of the inhibition of essential cellular processes such as transcription and replication, particularly the interstrand cross-link (ICL), as it prevents separation of the two DNA strands. Furthermore, if allowed to persist, cross-links can cause further damage, such as the formation of DNA strand breaks (reviewed in Hartley, 2001).

1.1.1 Alkylating agents

Alkylating agents are electrophilic compounds that can substitute a proton with an alkyl group to form covalent adducts with DNA, RNA, or protein. The alkylation reaction may occur either by first (S_N1) or second (S_N2) order nucleophilic substitution. The rate of $S_N1$reactions is limited by the formation of a highly reactive positively charged intermediate, whereas the S_N2 mechanism involves bimolecular nucleophilic displacement. Some alkylating drugs act preferentially by one mechanism (SN_1 for nitrogen mustards, SN_2 for the alkylalkanesulphonate, busulfan), whereas others appear to utilise both (Hartley, 2001). In the case of nitrogen mustards, loss of chloride results in the formation of a highly electrophilic aziridinium ion intermediate, which reacts covalently with DNA (Fig. 1.2). This can be repeated with the other chloroethyl group

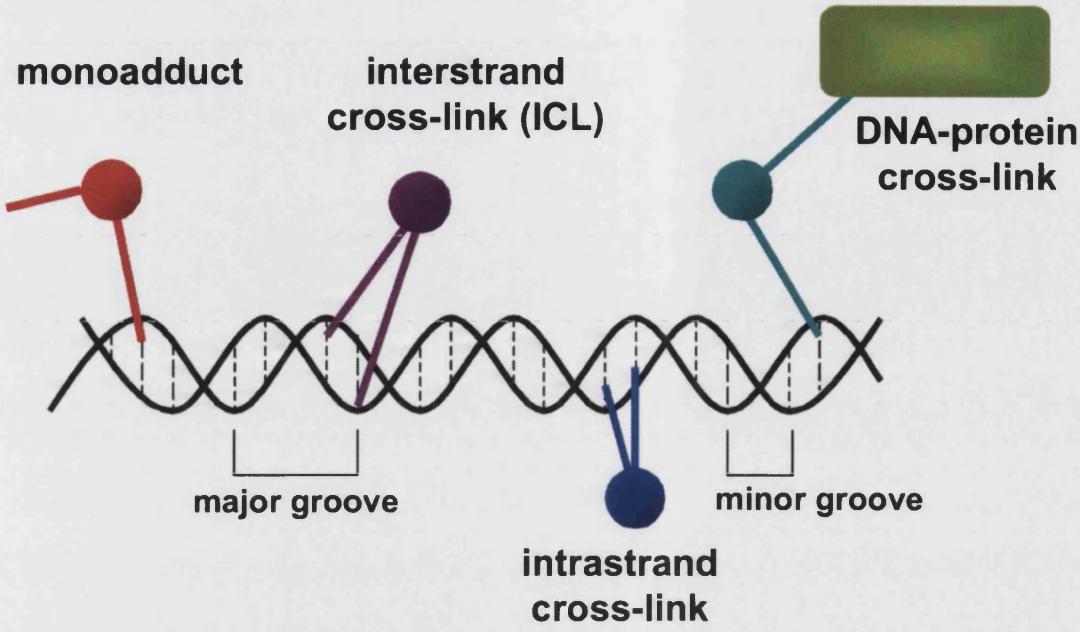

Figure 1.1 Types of DNA adduct formed by cross-linking agents. A covalent attachment to a single strand of DNA results in a monoadduct. Bifunctional compounds have the ability to react a second time, either with the same DNA strand (intrastrand cross-link), the complementary strand (interstrand, ICL), or with a protein. (Adapted from McHugh *et al.*, 2001)

A. Mechlorethamine (HN2)

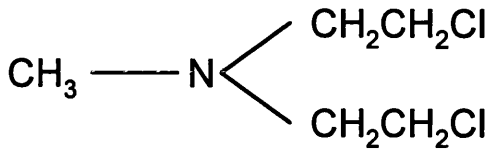

B. Reactive aziridinium ion intermediate

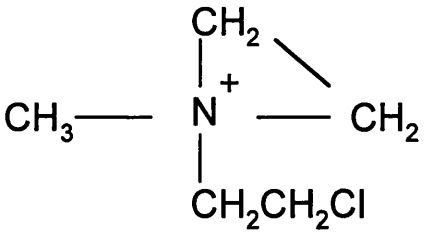

Figure 1.2 Structure of nitrogen mustard. **A.** The simple nitrogen mustard (mechlorethamine, HN2). The non-alkylating methyl group is substituted in mustard analogues. **B.** Loss of a chloride ion produces the electrophilic aziridinium ion intermediate, which can react with DNA to form monoadducts. An analogous reaction at the other chloroethyl group results in a DNA cross-link.

and a second nucleophile, resulting in the formation of a cross-link (Fig. 1.1). Such compounds are known as bifunctional alkylating agents, as a result of their ability to form two alkylation reactions (Hartley, 2001).

DNA contains a number of nucleophilic centres, although some sites, particularly the ring nitrogens of the bases, are more susceptible to alkylation. The preferential site of attack is the N7 position of guanine in the major groove, producing a 7-alkylguanine adduct (Hartley, 2001) (Fig. 1.3). However, this is a relatively harmless lesion that does not alter normal base pairing, and is slowly hydrolysed to leave an apurinic site, which can be readily repaired. The other frequently occurring monoadducts, 3-alkyladenine, are formed at the N3 position of adenine in the minor groove, and cause a greater obstruction to the progression of DNA polymerase, so are more toxic (Hartley, 2001). A further adduct is O6-alkylguanine, an enol-tautomeric base that is highly mutagenic as a result of erroneous DNA synthesis (Hartley, 2001) (Fig. 1.3).

The preference for particular nucleophilic sites largely reflects their molecular electrostatic potential, with the N7 position of guanine being the most negative site within the bases of DNA. However, not all guanines will be alkylated to the same extent, because the electrostatic potential of any one site is affected by its flanking bases. Two adjacent guanine bases constitute the greatest electrostatic potential, and as such, alkylation by simple agents such as mechlorethamine occurs predominantly in guanine-rich regions of DNA.

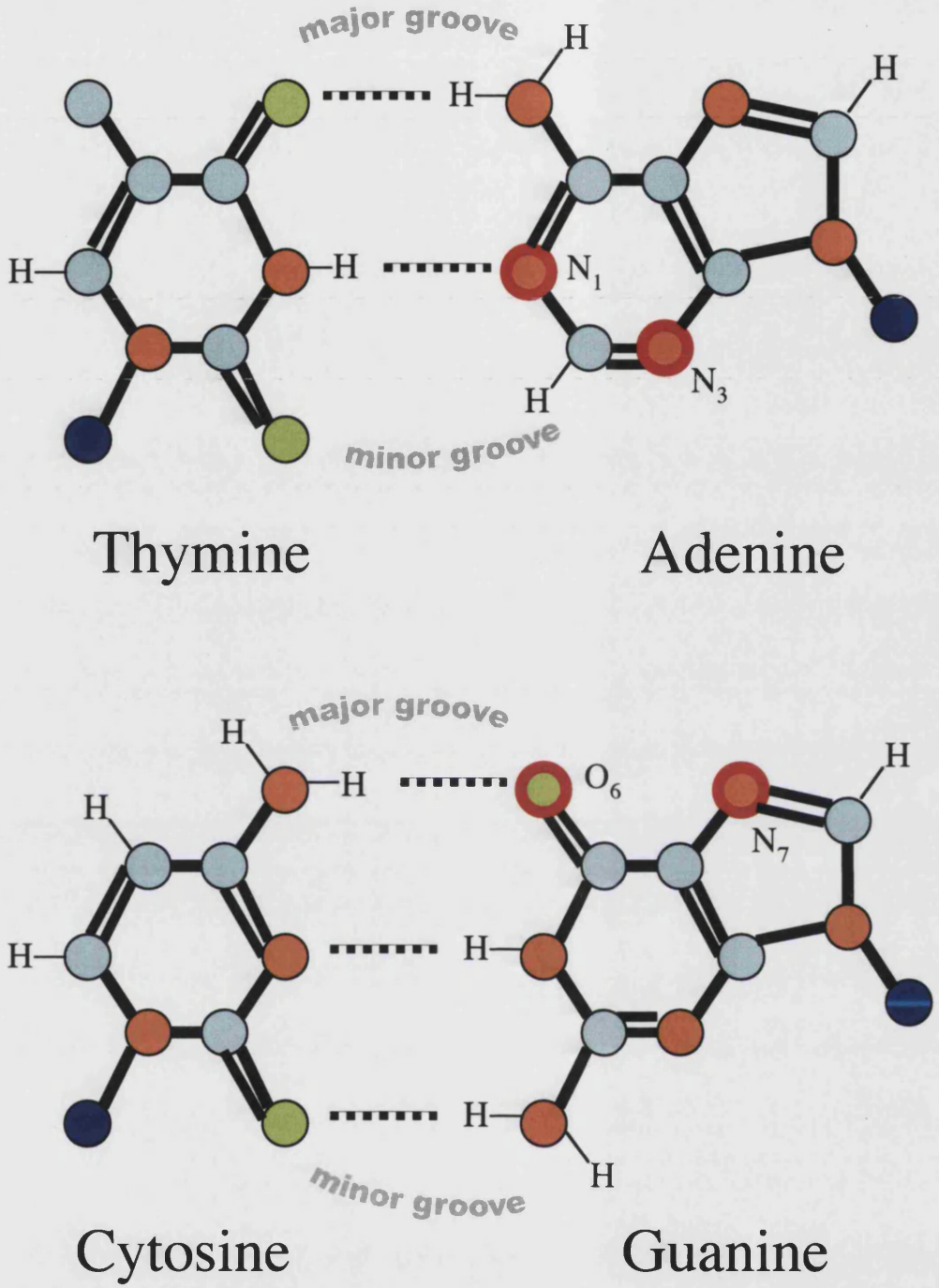

Figure 1.3 Alkylation sites of DNA bases. The reactive sites of adenine (N_1 and N_3) and guanine (O_6 and N_7) are highlighted with a red outline. The different atoms within the bases are colour coded: carbon in pale blue, nitrogen in orange, and oxygen in green. The C_1 site of deoxyribose is depicted in dark blue. (Adapted from Hartley, 2001)

1.1.1.1 Nitrogen mustards

The alkylating agent mechlorethamine (nitrogen mustard, HN2; Fig. 1.2) was the first antitumour drug to be administered, more than fifty years ago, following observations that the related compound, di(2-chloroethyl)sulphide (sulphur mustard, used as a war gas) was toxic to the haematopoetic system (Jacobson *et al.*, 1946; Goodman *et al.*, 1946). Today, the clinical application of HN2 is restricted largely to the treatment of Hodgkin's lymphoma as a result of its high systemic toxicity. However, a range of bifunctional nitrogen mustard derivatives including melphalan, chlorambucil, cyclophosphamide, and ifosfamide are widely used. In these compounds, the simple methyl group is substituted with alternative organic chains and rings. Even small changes in these non-alkylating regions can significantly affect biological properties, such as compound stability, metabolic bioactivation, cellular uptake, sequence specificity, and cross-resistance. This facilitates the use of different alkylating agents in combination chemotherapy to more effectively treat a range of tumours (reviewed in Hartley, 2001).

The production of cross-links first requires the formation of a monoadduct. The second alkylation event is slow, and not all monoadducts will react to form cross-links. The ratio of monoadducts to cross-links is usually in the region of 20:1 (Hartley, 2001), and for HN2, ICLs only account for 1-4 % of the total adducts formed (Dronkert and Kanaar, 2001). Bifunctional mustard compounds form DNA intra- and interstrand cross-links between guanine N7 residues, most often at the recognition sequence 5'-GNC-3'/3'-CNG-5' (Ojwang *et al.*, 1989). The ICL is generally regarded to be the critical cytotoxic lesion for members of the nitrogen mustard class, as the extent of interstrand cross-linking correlates well with cytotoxicity (O'Connor and Kohn, 1990;

Sunters *et al.*, 1992). Furthermore, there is growing evidence that clinically-acquired drug resistance may specifically be the result of increased repair of these lesions (Chaney and Sancar, 1996; Spanswick *et al.*, 2002).

1.1.2 Platinum-based compounds

Platinum complexes are DNA cross-linking agents that have a similar mechanism of action to the alkylating agents. The biological activity of platinum compounds was discovered fortuitously forty years ago by Rosenberg, who observed that platinum salts produced during electrolysis caused filamentation in *E. coli* (due to the inhibition of cell division) (Rosenberg *et al.*, 1967). Depending on the oxidation state of the platinum ion, complexes may have either four (Pt(II) complex) or six (Pt(IV)) coordination sites. These coordination complexes are fixed, giving rise to distinct cis (cisplatin) and trans (transplatin) isomers (Fig. 1.4 A). Transplatin has a much lower cytotoxicity compared to cisplatin, and has no anti-tumour activity (Jakupec *et al.*, 2003). There are a number of reasons that have been demonstrated to account for this crucial difference, including less inhibition of DNA replication and transcription by transplatin adducts, a slower rate of monoadduct to cross-link conversion, and the inability of transplatin to produce 1,2-intrastrand cross-links (Jakupec *et al.*, 2003). The anti-cancer agent cis-diamminedichloroplatinum(II) (cis-DDP, cisplatin) possesses two chloride ions, which can be displaced in aqueous solution to form a reactive electrophilic species (Fig. 1.4 A) (Jakupec *et al.*, 2003). Activated cisplatin will efficiently attack any cellular nucleophile, including DNA, RNA, and protein, and the sequential displacement of both

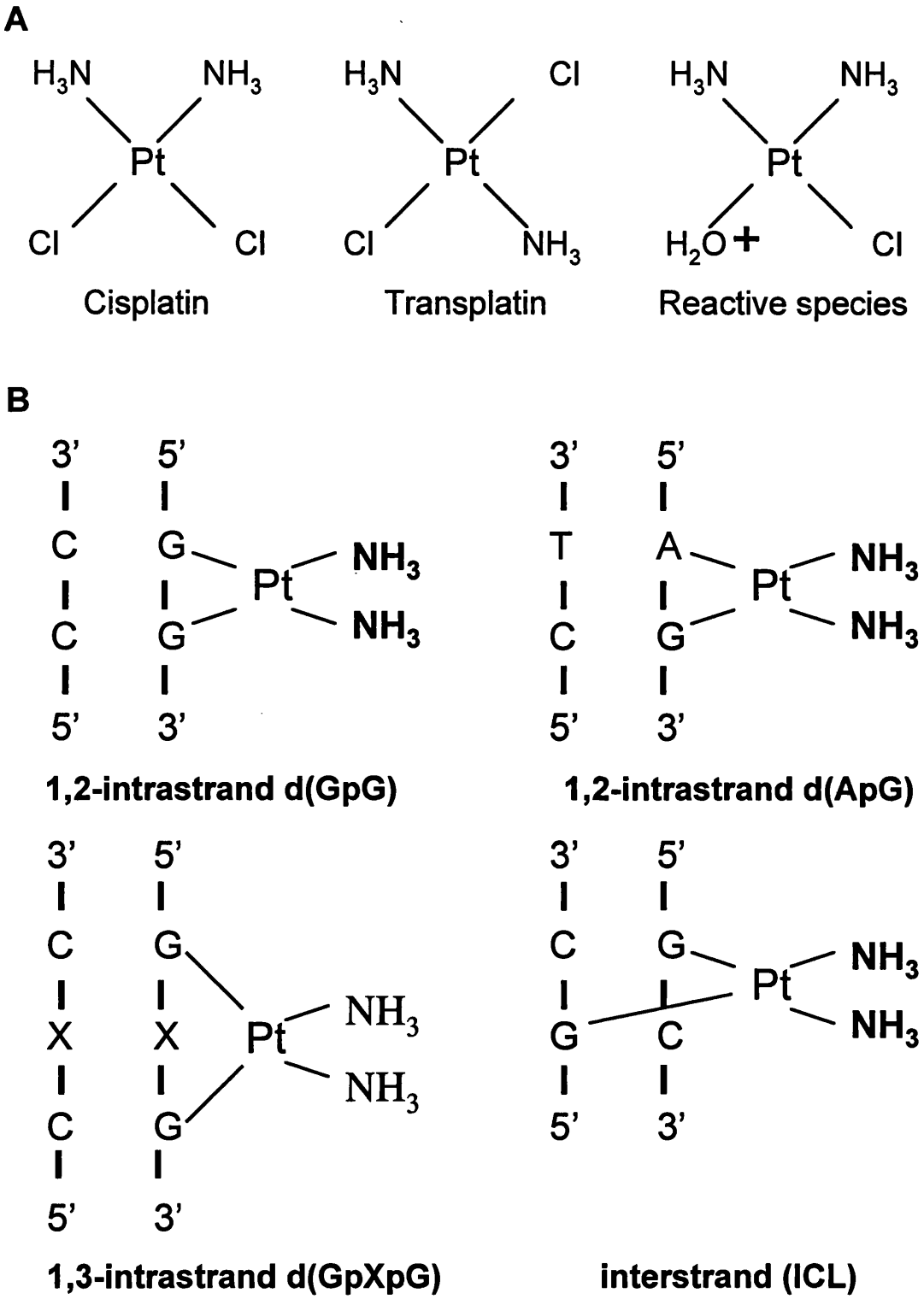

Figure 1.4 Structures of platinum compounds. **A.** Structures of cis- and trans-platin. In an aqueous solution, the chloride ions can be displaced to leave an electrophilic aquated species, which is the reactive form of these compounds. **B.** Schematic of the different bifunctional adducts formed by cisplatin on DNA.

chloride groups will result in a bifunctional agent, capable of forming covalent cross-links (Fig. 1.1) (Jakupec *et al.*, 2003).

Cisplatin primarily reacts with the N7 atom of purine bases in the DNA major groove resulting in the formation of 1,2-d(GpG), 1,2-d(ApG), and 1,3-d(GpNpG) intrastrand cross-links, and interstrand cross-links between guanines in the complementary DNA strands (Fig 1.4 B) (Pinto and Lippard, 1985; Comess and Lippard, 1993). The 1,2cisplatin intrastrand adducts (d(GpG) and d(ApG)) account for around 90 % of the DNA damage (Fichtinger-Schepman *et al.*, 1985), and are less well recognised by the mammalian Nucleotide Excision Repair (NER) apparatus than the rarer (approximately 6 %) 1,3-intrastrand cross-links, probably as a result of the smaller degree of helical distortion induced (Zamble *et al.*, 1996; Moggs *et al.*, 1997). The cisplatin ICLs and monoadducts are even more rare, occurring only at a frequency of around 1-2 % (Fichtinger-Schepman *et al.*, 1985).

It is clear that the clinical effectiveness of cisplatin is a result of the DNA, rather than RNA and protein lesions (Jakupec *et al.*, 2003). The critical cytotoxic lesion is likely to be the predominant 1,2-intrastrand cross-links (Fichtinger-Schepman *et al.*, 1995), although evidence has also been presented regarding the cytotoxicity of ICLs (Zwelling *et al.*, 1979). An ELISA-based quantitation of the level of intrastrand adducts has shown a correlation with clinical response in testicular and ovarian cancer cells (Reed *et al.*, 1986). Furthermore, all components of the NER machinery are required for the unhooking of cisplatin ICL *in vivo*, yet in some mutants this results in only a modest increase in sensitivity (De Silva *et al.*, 2002).

Cisplatin was approved for clinical use in anti-cancer therapy in 1979 (Loehrer and Einhorn, 1984), and it remains one of the most utilised agents. It is an effective component of several different combination drug protocols used to treat a variety of solid tumours, including testicular, ovarian, and bladder cancers. However, acquired resistance is frequently observed, and some tumours, such as liver and colon, appear to be intrinsically resistant to cisplatin chemotherapy (reviewed in Ho *et al.*, 2003). A number of factors are thought to contribute to resistance, including increased DNA repair, and tolerance due the binding of cellular proteins to platinum adducts. Hence, research is being conducted to identify new compounds with distinct chemical and biological properties. Platinum (II) complexes essentially have two stable carrier ligands (the amine groups in cisplatin), and two anionic leaving groups (cisplatin chloride ions). It is thought that the carrier group determines the structure of the adduct bound to DNA, whereas the reactivity of the leaving group affects drug toxicity, and can also influence tissue and intracellular distribution (reviewed in Ho *et al.*, 2003). A number of cisplatin analogues are now in clinical use, including carboplatin and oxaliplatin. Carboplatin has been found to exhibit reduced side effects compared to cisplatin, probably as a result of the less labile cyclobutanedicarboxyl leaving group (Ho *et al.*, 2003). Oxaliplatin demonstrates enhanced activity and a lack of cross-resistance to cisplatin, which may be due to the inhibition of DNA repair by the bulky diaminocyclohexane carrier ligand (Ho *et al.*, 2003).

1.1.3 Psoralens

DNA cross-links can also be formed as a result of the photoaddition of bifunctional psoralens to pyrimidine bases. Psoralens are planar tricyclic furocoumarins (Fig. 1.5 A)

A

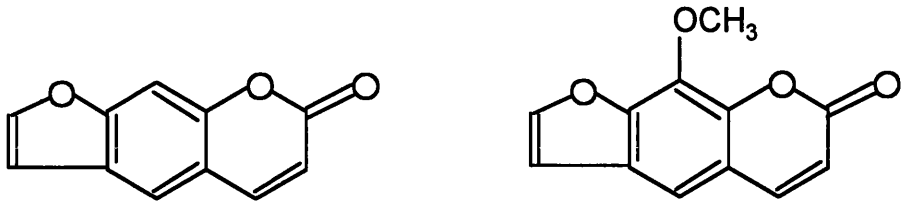

Psoralen 8-Methoxypsoralen

B

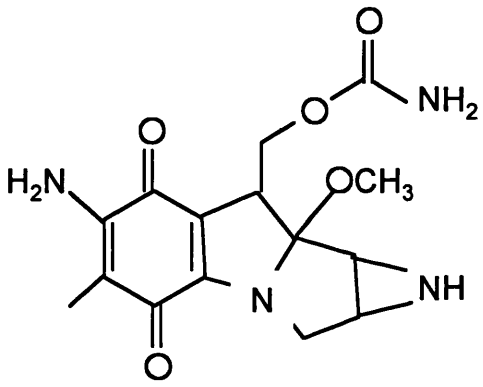

Mitomycin C

Figure 1.5 Structures of other cross-linking compounds. **A.** Psoralen and its derivative 8-methoxypsoralen. **B.** Mitomycin C.

that can intercalate with DNA, and become covalently bound to pyrimidine bases after photoactivation by UVA radiation. The principal site of attack is the 5,6 double bond of thymine, and two sequential UV absorption events will result in the formation of a stable interstrand cross-link between thymines above and below the plane of the psoralen molecule (Friedberg *et al.*, 1995). These ICLs cause significant distortion to the helix, as well as inducing the unwinding of DNA. Three times as many monoadducts are produced compared to ICLs, yet, as for other classes of compound, the cross-link has been shown to be the crucial determinant of cellular toxicity (Brendel and Ruhland, 1984). Due to the planar structure of psoralens, intrastrand cross-links cannot be formed in DNA, but photoreactivation with proteins has been observed after prolonged exposure to UVA (Brendel and Ruhland, 1984).

The inhibition of DNA replication by psoralen in combination with high-intensity UVA radiation is widely utilised in the treatment of psoriasis and other skin diseases, which are characterised by a marked proliferation of certain skin epithelial cells (Friedberg *et al.*, 1995). More recently, psoralens have been found to act as effective chemoprotective agents against non-melanoma skin cancers (Pathak and Fitzpatrick, 1992).

1.1.4 Mitomycin C

Mitomycin C is a natural antibiotic compound (Fig. 1.5 B), isolated from *Streptomyces caespitosus*, that is used to treat a wide spectrum of tumours including breast, gastric, oesophageal, and bladder cancer (reviewed in Hartley, 2001). It requires bioactivation by reduction of the quinone moiety, in order to function as an alkylating agent (Hartley, 2001). All monoalkylation and cross-linking occurs in the minor groove of DNA.

Activated mitomycin C forms monoadducts at the N7 and N2 positions of guanine, with a preference for the DNA sequence 5'-CGN-3' (where N is C>T>G>A), compared to 5'-GGN-3' (Kumar *et al.*, 1992). Intrastrand cross-links are formed between guanine N2 residues at d(GpG) sites, whereas ICLs occur at d(CpG) sequences (Tomasz, 1995). Unlike the cross-links produced by nitrogen mustards and platinum compounds, mitomycin C-induced ICL cause relatively little DNA distortion (Tomasz, 1995). Monoadducts are also formed without significantly affecting DNA conformation, however, the intrastrand cross-link has been shown to result in bending of the DNA (Rink *et al.*, 1996). Mitomycin C monoadducts react slowly to form cross-links, and ICLs are believed to constitute 5-13 % of the total adducts (Dronkert and Kanaar, 2001). However, the ICL has been shown to be the critical determinant of cytotoxicity (Palom *et al.*, 2002).

1.1.5 DNA strand breaks

Single (SSBs) and double (DSBs) strand breaks occur frequently in DNA, as a result of both endogenous and exogenous assault (Friedberg *et al.*, 1995; Paques and Haber, 1999). SSBs occur during replication and repair, for example, by the action of type I topoisomerases, or where a replication fork encounters an unrepaired adduct, and they are also one of the lesions induced by UV and ionizing radiation. DSBs are a consequence of ionizing radiation, radiomimetic drugs such as bleomycin, mechanical stress, and endonuclease digestion. These lesions are also produced as a consequence of oxidative damage or unrepaired nicks occurring during normal metabolic processes, and are thought to arise at stalled replication forks (Cox *et al.*, 2000). Of particular significance to this study, DSBs are known to occur during the repair of DNA ICL (Section 1.3). Strand breaks, especially DSBs, have the potential to cause considerable

cytotoxicity as a result of increased genomic instability and the inhibition of cellular processes such as replication.

The exact nature of a strand break can vary, depending on the causative agent. Endo- and exonucleases, such as those employed in DNA recombination and repair pathways (Section 1.2), hydrolyse the phosphodiester linkages in DNA, causing a range of discrete nicks and longer digested regions, often with a complementary single strand overhang. In contrast, ionizing radiation-induced DSBs exhibit additional damage (e.g. fragmentation, loss) to the terminal bases and sugars of the DNA helix, and the anti-cancer drug bleomycin produces breaks with phosphoglycolate-modified 3'-termini. These differences can have major implications for the mechanism of repair employed by the cell, as the damage may not be completely restored by simple end joining.

1.2 DNA repair

As already described, the DNA in any organism is constantly subject to many different types of damage. It follows that cells have evolved a complex system of repair pathways to counteract this assault. Many of the factors involved in these mechanisms were identified by the analysis of genetic mutants, both in model organisms such as *E. coli* and *Saccharomyces cerevisiae*, and more recently, higher eukaryotes. Classically, these repair factors have been allocated into independent genetic epistasis groups, for example the *RAD3*/nucleotide excision repair and *RAD52*/homologous recombination pathways of budding yeast. However, research now suggests that these well-characterized pathways also form part of a composite system in which repair proteins interact with multiple partners to process different types of lesion. The co-operation of

various factors and pathways is exemplified by the case of DNA interstrand cross-link repair (Section 1.3).

1.2.1 Nucleotide Excision Repair (NER)

The nucleotide excision repair pathway is proficient in the repair of a variety of DNA lesions, particularly those that are bulky and distort the DNA helix, such as UV-induced dipyrimidine photoproducts (Prakash and Prakash, 2000). NER is also likely to be the major determinant of cellular sensitivity to bifunctional chemotherapeutic agents, such as cisplatin, that predominantly produce intrastrand cross-links as opposed to ICL (Section 1.1.2). The NER pathway was initially deciphered in *E. coli*, and identification of NER genes in both yeast and mammalian cells has relied upon the identification of UV-sensitive mutants, such as those isolated from Xeroderma pigmentosum (XP) patients. The genes involved in yeast repair are designated *RAD* as a result of these studies into radiation sensitivity, and those that are associated with UV sensitivity form the *RAD3* group. A combination of genetic and biochemical analyses has identified specific interactions between these factors to form functional complexes. Physical associations between more diverse members of the NER group have also been suggested, as a result of the co-purification of large protein complexes from yeast. These complexes have been designated 'nucleotide excision repair factors' (NEF; Guzder *et al.*, 1996).

In *S. cerevisiae*, global genome NER (GGR, Fig. 1.6), the initial recognition of a DNA lesion is probably mediated by the Rad4-Rad23 (NEF2) and Rad7-Rad16 (NEF4) complexes. It has been suggested that these complexes interact in the presence of ATP, enhancing binding to the damaged site (Guzder *et al.*, 1999). Recent research has

shown that binding of Rad7-Rad16 to DNA also generates helical torsion that is essential for the excision reaction to proceed (Yu S. *et al.*, 2004). The single-stranded DNA-binding protein, RPA, is thought to be involved in both damage binding and the subsequent incision step (Huang *et al.*, 1998; Prakash and Prakash, 2000). The remaining NER proteins are probably recruited to the lesion through the interaction of Rad23 with the transcription factor TFIIH (NEF3) and Rad14 (NEF1) (Prakash and Prakash, 2000). The helicases Rad3 and Rad25 (part of the NEF3 complex) unwind the DNA at the damaged site by translocating along ssDNA in the 5'-3' and 3'-5' directions, respectively, creating an open "bubble" around the lesion (Sung *et al.*, 1996). This provides access to the single-strand/double-strand DNA junctions that are substrates for the dual endonuclease incisions, made 5' to the lesion by the Rad1-Rad10 heterodimer (NEF1) and 3' to the lesion by the Rad2 protein (NEF3) (Bardwell *et al.*, 1994; Habraken *et al.*, 1995). An oligonucleotide of 24-32 nt containing the damaged region is released (Guzder *et al.*, 1995), leaving a gap, which is restored by DNA synthesis, performed by DNA polymerase δ and ε, and ligation by DNA ligase I (Cdc9) (Prakash and Prakash, 2000).

NER operates in essentially the same manner in mammalian cells as in yeast, and human homologues of most of the yeast NER factors have been identified (Table 1.1), particularly from studies in Xeroderma pigmentosum (XP) patients, who display an

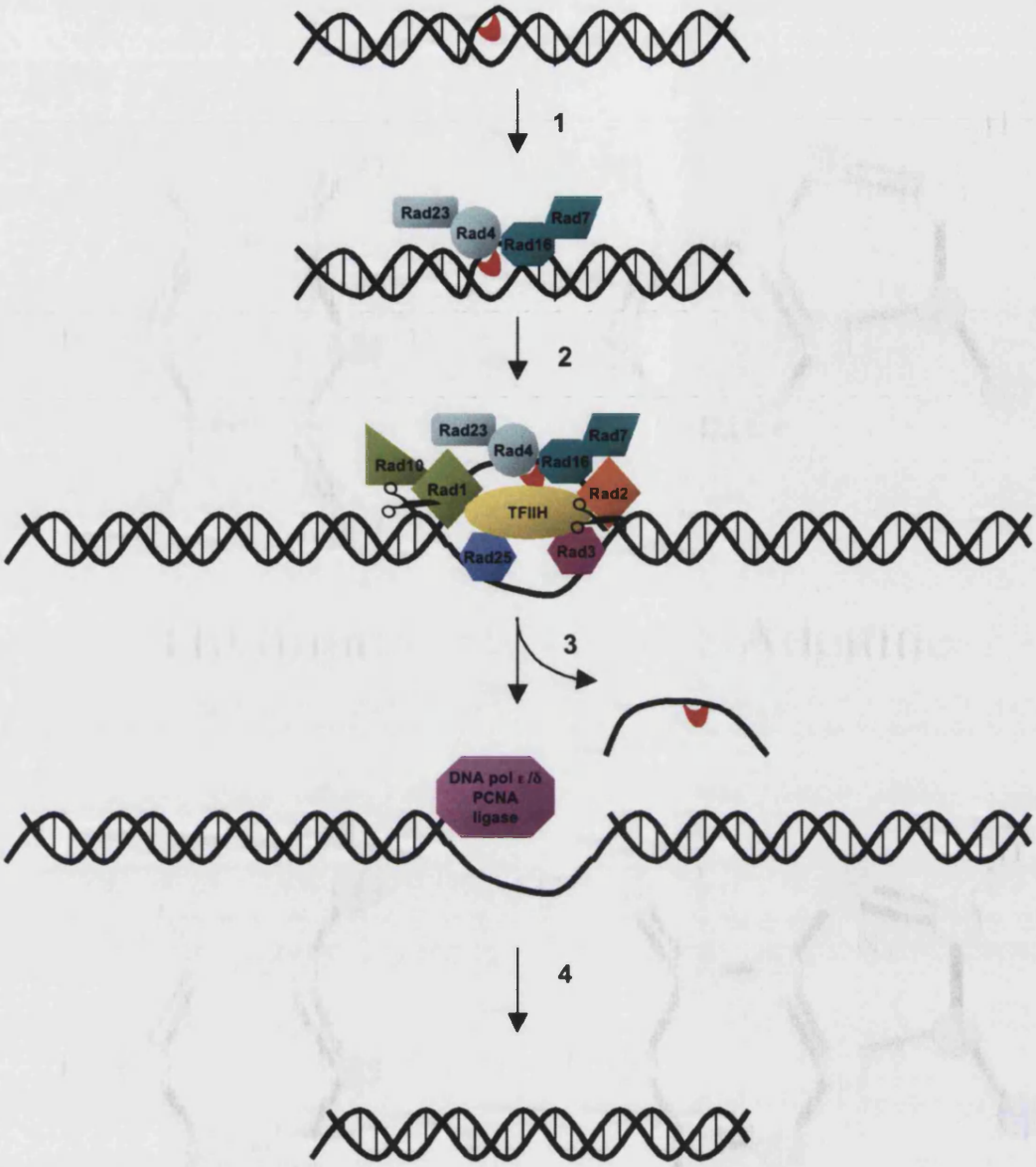

Figure 1.6 Mechanism of NER in yeast. Following damage recognition by Rad4-Rad23 and/or Rad7-Rad16 (1), the double helix is unwound around the lesion by the helicases Rad3 and Rad25, and components of the TFIIH complex are recruited (2). The resulting bubble structure provides the substrate for the structure-specific endonucleases Rad2 (cleaving first, 3' to the lesion) and Rad1-Rad10 (subsequently cleaves 5' to the lesion) (3). A lesion-containing oligomer is released, and the remaining gap reconstituted by DNA synthesis (DNA polymerase ε/δ and PCNA) and ligation (DNA ligase), using the undamaged strand as a template (4). (Adapted from McHugh *et al.*, 2001)

Table 1.1 **Conservation of NER genes between yeast and humans**

S. cerevisiae	Human	Function
Rad4-Rad23	XPC-hHR23B	Lesion recognition
Rad7-Rad16	None identified	Lesion recognition
Rad14	XPA	Lesion recognition
Rad3, Rad25	XPD, XPB	DNA unwinding
Rad1-Rad10	XPF-ERCC1	Lesion excision
Rad2	XPG	Lesion excision
Rad26, Rad28	CSB, CSA	TCR

extreme sensitivity to sunlight and a predisposition to skin cancer. Recognition of DNA lesions is thought to require the XPC-hHR23B complex, possibly assisted by XPA in combination with RPA (replication protein A) (Batty and Wood, 2000). However, studies using immunofluorescent labelling to determine the assembly of NER proteins in UV-irradiated human cells indicate a later role for XPA, promoting the recruitment and activation of the nucleolytic factors XPF-ERCC1 and XPG (Volker *et al.*, 2001). As in *S. cerevisiae*, the helicases XPD and XPB are believed to associate at the damaged site as part of a complex with TFIIH, leading to the local unwinding of 10-20 nt in an ATP-dependent fashion (Evans *et al.*, 1997). This enables the release of a damage-containing oligonucleotide by sequential asymmetric incision reactions, first 3' (XPG) and then 5' (XPF-ERCC1) to the lesion (Sancar, 1996). It has even been suggested that XPG is involved in the recruitment of XPF-ERCC1 (Wakasugi and Sancar, 1998). Repair is completed by the activities of PCNA, DNA polymerases δ and ε, and DNA ligase.

Recognition of damaged sites in actively transcribed regions of DNA is specifically achieved by the interaction of the Rad26-Rad28 complex with stalled RNA polymerase

II (Transcription Coupled Repair, TCR) (van Gool *et al.*, 1994; Bhatia *et al.*, 1996). In humans, Cockayne's syndrome is associated with a deficiency in TCR, and two of the associated gene disruptants correlate with Rad26 (CSB) and Rad28 (CSA). These factors may stimulate the removal of the RNA pol II complex in order to facilitate binding of the downstream NER factors (Balajee and Bohr, 2000).

1.2.2 Mismatch Repair

The identification and repair of single nucleotide mismatches and small insertion/deletion loops (IDLs) of DNA is achieved through the combined activity of the Mismatch repair (MMR) family of proteins (Hansen and Kelley, 2000; Hoeijmakers, 2001). This pathway was originally characterized in *E. coli*, which has served as the model for elucidation of eukaryotic systems (such as yeast, shown in Fig. 1.7). In *E. coli*, a homodimer of MutS protein binds non-specifically to DNA, and scans the DNA until it encounters a mismatch, stimulating a conformational change into the recognition complex (Wang *et al.*, 2003). In the presence of ATP, MutS translocates along the DNA, forming a loop structure with the mismatch at its apex. The recruitment of MutL and MutH into the MutS-DNA complex activates the endonuclease activity of MutH, which nicks the newly-replicated unmethylated DNA strand (MutH recognises hemi-methylated *dam* sites that exist transiently after replication). This nick may occur on either side of the mismatch, and so the single-strand exonuclease responsible for further degradation is specific to this polarity: ExoI, ExoX, or ExoVII if

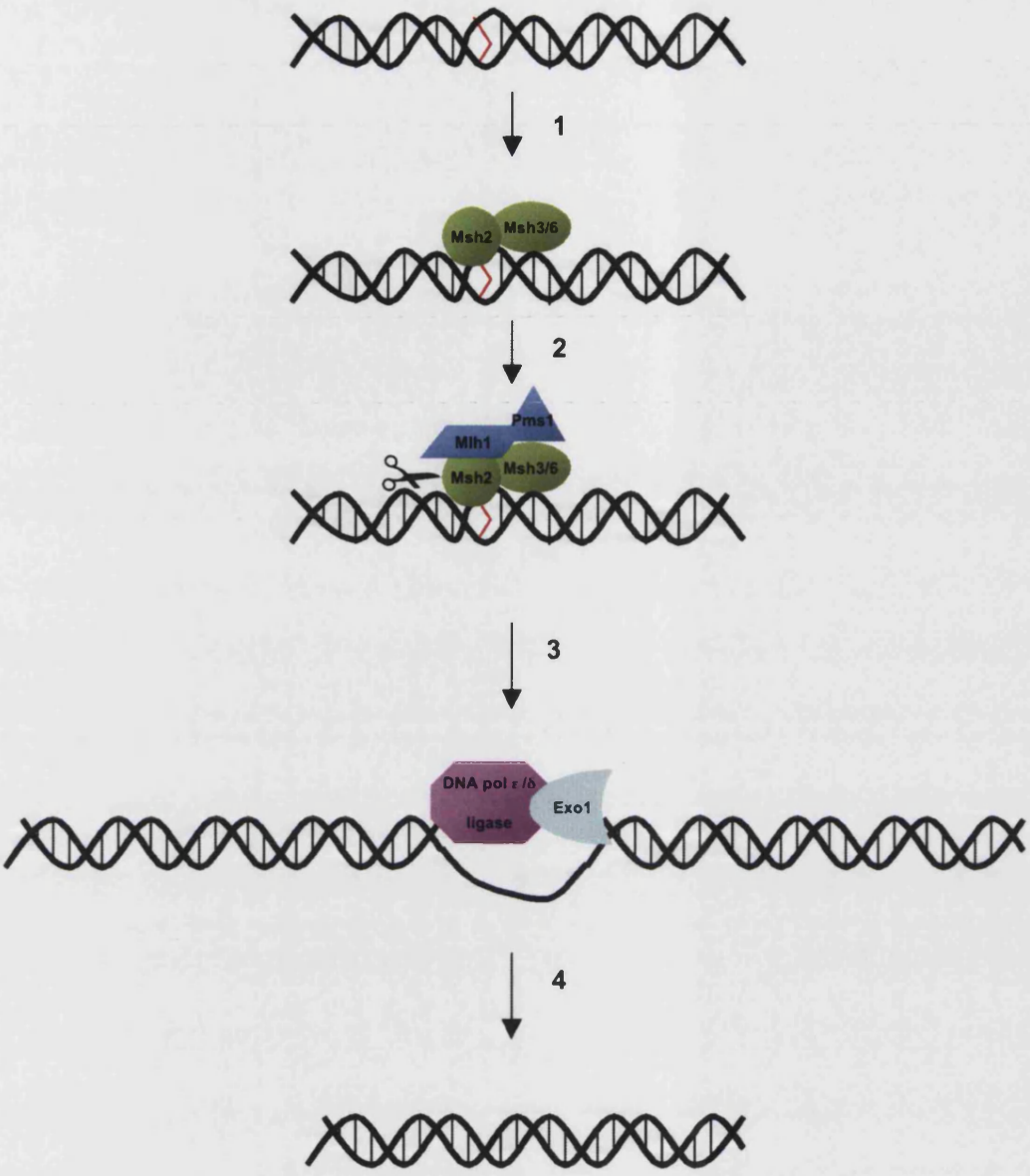

Figure 1.7 Mechanism of MMR in yeast. The mismatched DNA base or insertion/deletion loop is recognised by either Msh2-Msh6 or Msh2-Msh3, respectively (1). The Mlh1-Pms1 heterodimer is then recruited, resulting in the formation of a 5' or 3' nick (2). The exonuclease activities of Exo1 and DNA pol δ/ε leads to the creation of a 100-1000 nt gap (3), which is repaired by DNA synthesis and ligation (4).

the nick occurs 3' to the mismatch, and either ExoVII or RecJ for 5' nicks. MutL recruits helicase II, which unwinds a repair patch up to 1 kb long, and DNA polymerase III replicates across the gap resulting from exonuclease digestion. The remaining nick is sealed by DNA ligase (reviewed in Marti *et al.*, 2002).

Eukaryotic MMR proteins have been classified by analogy to their bacterial counterparts MutS and MutL. Six MutS (Msh1-6) and four MutL (Mlh1-3, Pms1) homologues have been identified in *S. cerevisiae*, some of which are specific to meiotic recombination (Msh4, Msh5) and mitochondrial repair (Msh1) (Hollingsworth *et al.*, 1995; Ross-Macdonald and Roeder, 1994; Reenen and Kolodner, 1992). Mitotic mismatch repair is governed by Msh2, which functions as a heterodimer with Msh3 or Msh6 to specify recognition of either IDLs, or base substitutions and 1-2 nt loops, respectively. These complexes are known as MutSβ (Msh2-Msh3) and MutSα (Msh2-Msh6), and have also been identified in mammalian cells (Genschel *et al.* 1998). The function of bacterial MutL is primarily accomplished by a heterodimer of Mlh1 and Pms1 in yeast (Prolla *et al.*, 1994). However, Mlh1 may also complex with Mlh2 or Mlh3, possibly to repair certain intermediates arising from the activity of MutSα. It has also been suggested that different Mlh1 heterodimers may exist at distinct stages of the cell cycle (reviewed in Harfe and Jinks-Robinson, 2000). No eukaryotic homologues of MutH have been identified, despite extensive screening. However, the sliding clamp protein, PCNA (proliferating cell nuclear antigen), has been shown to physically interact with Msh2 and Mlh1, and it has been suggested that through its interaction with the replication machinery could provide the means to discriminate between the newly synthesized and template DNA strands (Harfe and Jinks-Robinson, 2000). Nick-directed mismatch processing is believed to occur in the 5'-3' direction by means of the

exonuclease Exo1, and 3'-5' through exonuclease activities associated with the replicative DNA polymerases ε and δ (Harfe and Jinks-Robinson, 2000).

The yeast MMR factors have also been implicated in recombination events, some of which also involve interactions with members of the NER family. MutSβ in combination with the Rad1-Rad10 complex, has been shown to be involved in the removal of 3' non-homologous tails arising during gene conversion and single-strand annealing (described in more detail in Section 1.2.3.1.1) (Sugawara *et al.*, 1997). It has been suggested that Msh2-Msh3 bind and stabilise single-strand/double-strand DNA junctions, enabling nicking by Rad1-Rad10. The NER endonuclease Rad1 is also required for the Msh3-dependent repair of a 95 nt loop between direct repeats during DNA replication, as well as the Msh2-dependent removal of a 26 nt loop during meiotic recombination (Harfe and Jinks-Robinson, 2000). It is believed that Msh2-Msh3 and Rad1-Rad10 may form a novel complex that is responsible for the excision of heterologies larger than a few nucleotides. In addition, one report has shown that MutSα may bind and influence the resolution of Holliday junctions *in vitro*, analogous to the role of Msh4 and Msh5 in meiosis (Marsischky *et al.*, 1999).

An additional responsibility of some of the MMR proteins is the suppression of homeologous recombination (between diverged sequences). Recent research suggests that Msh2 and Msh6 are required to prevent single-strand annealing between moderately divergent sequences, whereas the full complement of MMR factors are utilised in the correction of mismatches in the heteroduplex intermediate (Sugawara *et al.*, 2004). However, Msh3 and Pms1 have also been implicated in rejecting other

homeologous recombination events (Paques and Haber, 1999). Msh2 may be especially important in the regulation of homeologous recombination in mammalian cells, due to the large fraction of the genome that is comprised of repetitive elements (Abuin *et al.*, 2000).

Defective MMR results in both an accumulation of replication errors and inappropriate recombination events, hence is highly mutagenic. In humans, MMR deficiency, particularly due to mutated *MSH2* or *MLH1* alleles, is associated with a large proportion of hereditary non-polyposis colorectal cancer (HNPCC) (Muller and Fischel, 2002). MMR defects have also been detected in a number of sporadic tumours (Hoeijmakers, 2001), with hypermethylation silencing of the *MLH1* promoter occurring at high frequency. This hypermethylation has also been observed in cisplatin resistant ovarian tumour cell lines (Strathdee *et al.*, 1999). An MMR deficiency has been shown to correlate with resistance to a number of anti-tumour agents including cisplatin, carboplatin, busulphan, temozolomide, etoposide, and doxorubicin (Fink *et al.*, 1998). Furthermore, Msh2 expression is elevated in both testicular and ovarian tissue, corresponding with the tumour types most successfully treated by cisplatin (Mello *et al.*, 1996). In the same report, analysis of hMsh2 binding to cisplatin-modified DNA has shown an affinity for 1,2-intrastrand cross-links (although recognition of the interstrand adduct was solely excluded on the basis of its infrequent occurrence). The authors suggest that Msh2 mediates cisplatin toxicity either by initiating futile MMR resulting in lethal DNA-strand breaks, or by preventing the recognition of cisplatin adducts by appropriate NER factors. However, Moggs *et al.* have shown that mismatched 1,2-intrastrand cross-links are in fact repaired more effectively by NER *in vitro*, and that

this increased repair is not dependent upon MMR factors, as the same NER preference is observed in extracts from cells deficient for hMutSα (Moggs *et al.*, 1997).

1.2.3 Double Strand Break Repair Pathways

Double strand breaks (DSBs) are formed on exposure to agents such as ionising radiation and free radicals, but can also occur naturally in a cell as intermediate structures during meiotic and V(D)J (mammalian immunoglobulin class switching) recombination events. Furthermore, DSBs may arise during the repair of other DNA damage and as a result of replication fork collapse at lesions, single strand breaks or gaps (Paques and Haber, 1999; Cox *et al.* 2000). Unrepaired DSBs lead to gene disruption and chromosomal rearrangements, ultimately increasing the risk of tumour progression. Indeed, human cancer-prone syndromes such as Nijmegen breakage syndrome and ataxia-telangiectasia-like disorder are associated with defects in DSB repair (Karran, 2000).

The two primary pathways for DSB repair are homologous recombination (HR) and nonhomologous end joining (NHEJ), which, as suggested by the nomenclature, are concerned with regions of long (hundreds of base pairs) near-perfect homology, and little or no sequence homology, respectively. In *S. cerevisiae*, HR is the predominant mechanism, although NHEJ can efficiently repair certain classes of DSB, such as those induced by endonuclease digestion retaining complementary single-strand DNA overhangs. In contrast, chemically modified DSB ends (e.g. arising from ionising radiation) are poor substrates for NHEJ (Lewis and Resnick, 2000). In higher eukaryotes, pathway preference may be cell cycle-dependent, with NHEJ favoured during G1/early S phase, and HR in late S-G2 (Takata *et al.*, 1998). Furthermore, the

conceived boundaries between these pathways may prove to be flexible, as cooperation between NHEJ and homology-driven processes has been observed in the repair of DSBs in murine cells (Richardson and Jasin, 2000).

1.2.3.1 Homologous recombination

Many of the genes involved in HR were originally identified from *S. cerevisiae* mutants displaying a hypersensitive phenotype to ionising radiation, and are collectively known as the *RAD52* epistasis group. To date, the known HR factors are Rad50, Rad51, Rad52, Rad54, Rad55, Rad57, Rad59, Mre11 (originally Rad58), and Xrs2, of which *rad51*, *rad52* and *rad54* mutants are associated with the most severe deficiencies in recombination and DSB repair (reviewed in Pastink and Lohman, 1999). Rad52 is the central recombination factor, and is required in all known mechanisms of HR in budding yeast. Rad52 forms ring structures that interact with ssDNA, promoting the efficient annealing of complementary strands (Shinohara *et al.*, 1998). Rad51, Rad55 and Rad57 are homologues of the *E. coli* recombination factor, RecA, which catalyses the pairing of ssDNA with complementary dsDNA. Rad51 polymerizes on DNA to form nucleoprotein filaments, which initiate pairing between single-strand DNA and duplex DNA to catalyze strand exchange (Sung, 1994). This polymerisation is regulated by the Rad55-Rad57 heterodimer and Rad52, which suppress the inhibitory effects of RPA (Sugawara *et al.*, 2003). A further protein required for efficient strand exchange is Rad54, a DNA-dependent ATPase thought to be involved in chromatin remodelling to 'open up' the DNA helix (Petukhova *et al.*, 1999).

The final three members of the *RAD52* epistasis group, Rad50, Mre11, and Xrs2, function as a complex (MRX), as determined by genetic and protein assays (reviewed in

Haber, 1998). The Mre11 protein alone displays a 3'-5' exonuclease and an endonuclease activity, which is enhanced by binding of the Rad50 and Xrs2 cofactors. Despite this polarity, yeast cells deficient for any of these factors demonstrate a considerably reduced 5'-3' exonuclease activity (Ivanov *et al.*, 1994; Tsubouchi and Ogawa, 1998). One explanation for this apparent contradiction is that the complex may endonucleolytically remove ssDNA tails unwound by an associated helicase, analogous to the activity of the RecBCD complex in *E. coli* (Eggleston and West, 1996). Recent research suggests Xrs2 to be important in the recruitment of the complex to DSB ends (Trujillo *et al.*, 2003), whilst Rad50 is a member of the 'structural maintenance of chromosomes' family of proteins and hence presents a number of DNA binding motifs (de Jager *et al.*, 2001). Rad50 has been shown to bind ATP, causing a conformational change in the MRX complex that appears to regulate the specificity of binding to DNA (de Jager *et al.*, 2002). Furthermore, it has been suggested that Rad50 dimerises upon binding of ATP, and this may be important for the juxtaposition of DSB ends (de Jager *et al.*, 2001; Hopfner *et al.*, 2002; Moncalian *et al.*, 2004). In addition to HR, the MRX complex is involved in a range of other DNA repair and maintenance processes including NHEJ and telomere conservation (Section 1.2.3.2; reviewed in Haber, 1998). Recently, it has been proposed that the MRX complex may perform an important role in the early stages of DSB detection and signalling, acting to co-ordinate repair attempts by the HR and NHEJ pathways (Lisby and Rothstein, 2004).

The key features of HR appear to be conserved in higher eukaryotes, and a number of homologues of the *RAD52* family have been identified, both by sequence analysis and from studies in defective cell lines, such as the X-ray repair cross complementation (XRCC) analysis in rodent cells. Multiple paralogues of the yeast *RAD51* gene have

been discovered, including *XRCC2*, *XRCC3*, *HsRAD51*, *HsRAD51B*, *HsRAD51C*, *HsRAD51D*, and *HsDMC1*, yet it remains to be determined whether any of these additional factors are functionally equivalent to the Rad55-Rad57 heterodimer (Pastink and Lohman, 1999). Sequence homologues of *RAD52*, *RAD54*, *RAD50*, and *MRE11* have also been found, yet only a functional analogue, *NBS1* (Nijmegen Breakage Syndrome factor), has been detected for *XRS2* (Pastink and Lohman, 1999). Discrepancies in mutant phenotypes (for example null lethality and sensitivity to X-irradiation) have been observed between mammalian and yeast recombination factors, although these are probably due to a combination of functional redundancy and an increased repair burden in higher eukaryotic genomes (reviewed in Paques and Haber, 1999; Pastink and Lohman, 1999).

1.2.3.1.1 Models of homologous DSB repair

There are three main models of homologous recombination that are used to explain the repair of chromosomal DSBs in mitotic yeast cells: gene conversion, break-induced replication, and single-strand annealing. Moreover, two models have been proposed to account for gene conversion events (DSB repair, and synthesis-dependent strand-annealing models), and given the substantial supporting experimental data, it is likely that they both represent functional subpathways of repair. Some key features are shared between these mechanisms, namely, resection of the DSB ends, strand invasion, removal of non-homologous tails, and gap repair by DNA synthesis.

1.2.3.1.1.1 Gene conversion

The original mechanism proposed for HR, referred to as the DSB repair or Szostak model (Szostak *et al.*, 1983; although an earlier model was suggested by Resnick,

1976), involves strand exchanges between sister chromatids or homologues (Fig. 1.8 A). This process is initiated by a DSB, the ends of which are first resected to yield 3' single-stranded tails. The Rad51 protein forms a protective filament on the ssDNA, and facilitates the invasion of the homologous duplex by both of the 3' tails, priming DNA synthesis to replace the degraded region. Ligation leads to the formation of a double Holliday Junction (dHJ) structure, which when resolved causes an exchange of genetic material between the damaged and homologous duplexes in the newly-synthesised patches. Depending on the resolution orientation, these products may also exhibit a 'crossover', where the region of genetic exchange extends from the break site along the entire length of the chromosome (Symington, 2002). It is thought that most gene conversion events, where DNA is exchanged in a non-reciprocal manner, occur as a result of mismatch repair activity upon the long heteroduplex tracts that form between the invading and donor sequences (Weng and Nickoloff, 1998).

The second model, synthesis-dependent strand-annealing (SDSA), was proposed to account for DSB gene conversion events that occurred with low levels of associated crossovers, such as HO endonuclease-mediated mating-type switching in yeast (reviewed in Paques and Haber, 1999). In SDSA, only one of the 3' tails resulting from the resected DSB invades the homologous duplex to prime DNA synthesis, resulting in the formation of a displacement (D-) loop (Fig. 1.8 B). Displacement of this nascent strand from the donor duplex provides a template for DNA synthesis from the other 3'

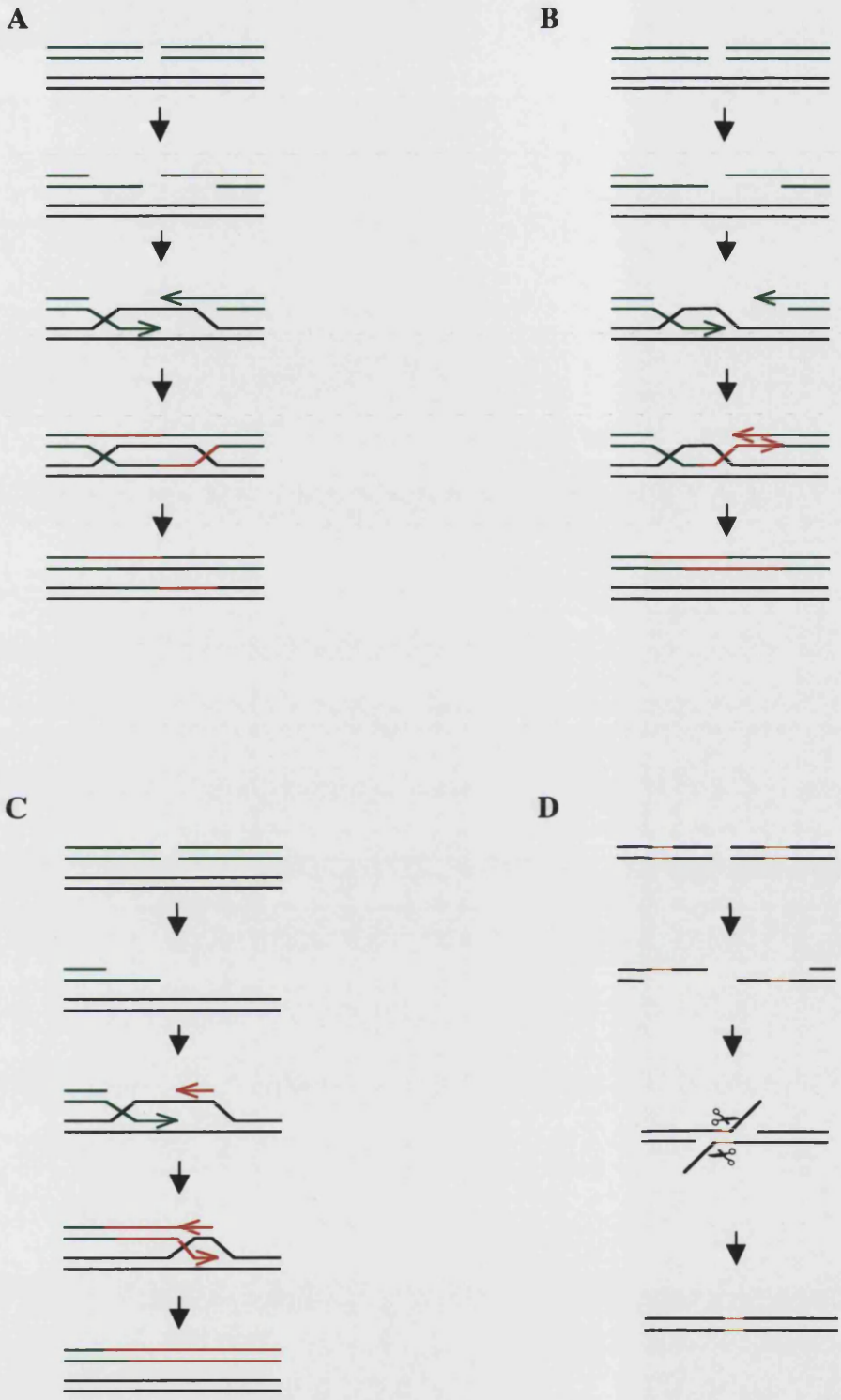

Figure 1.8 Models of DSB repair by homologous recombination in yeast. **A.** Szostak model of gene conversion by Holliday junction formation. **B.** Synthesis-dependent strand-annealing. **C.** Break-induced replication. (homologous chromosomes depicted in black and green, with newly synthesised DNA in red). **D.** Single-strand annealing (homologous region depicted in orange). (Adapted from Haber *et al.*, 2004)

tail, in order to complete repair across the DSB. It follows that only the broken DNA molecule is modified with genetic material from the homologous duplex, whilst the donor remains intact (Symington, 2002). SDSA is also thought to be responsible for the occurrence of a dHJ on one side of a DSB, rather than flanking it, as seen in the Szostak model (Haber *et al.*, 2004). SDSA is thought to be promoted by the helicase, Srs2, possibly by regulation of Rad51 during strand exchange (Ira *et al.*, 2003).

Recent research has shown that the incidence of crossovers is tightly regulated. Crossovers are promoted during meiosis, but are suppressed during mitosis (Allers and Lichten, 2001). Loss of the Sgs1 helicase (homologue of human BLM/WRN) significantly increases the frequency of crossovers (Ira *et al.*, 2003). Hence it was proposed that Sgs1, in combination with its associated topoisomerase Top3, acts to eliminate dHJ intermediates to reduce the crossover occurrence, by a mechanism distinct from SDSA. This hypothesis was corroborated in human cells, where BLM and hTOPOIIIα act to dissolve dHJs arising from the homologous recombination-dependent repair of replicative strand gaps (Wu and Hickson, 2003). This prevents a high frequency of sister chromatid exchange, which is characteristic of Bloom's syndrome cells (BLM deficiency). Crossovers are thought to occur by RuvC-like resolution of dHJs, yet to date no formal HJ resolvase has been identified in eukaryotes. The most likely resolvase candidate is thought to be Xrcc3-Rad51C in human cells (and by analogy, Rad55-Rad57 in yeast, as these are the most conserved paralogues) (Liu *et al.*, 2004).

1.2.3.1.1.2 Break-induced replication

A further mechanism is that of break-induced replication (BIR, Fig. 1.8 C). This results from the synthesis of both leading and lagging strands by the invasion of just one end of a processed DSB. In contrast to gene conversion events, where the second DSB tail eventually engages either the replication fork or the displaced nascent strand, BIR continues to the end of the donor chromosome (Malkova *et al.*, 1996). It has been suggested that BIR provides the means to maintain telomeres in the absence of the dedicated telomerase enzyme (Le *et al.*, 1999). Genetic analysis has revealed two independent branches of BIR in both telomere maintenance and DSB repair in diploid cells (Malkova *et al.*, 1996; Signon *et al.*, 2001). Both demonstrate an absolute requirement for Rad52, however one mechanism involves Rad50-Mre11-Xrs2 and Rad59, whilst the other depends on Rad51, Rad54, Rad55 and Rad57. It has been suggested that Rad51 is inhibitory to recombination in cases where homology is limited, whereas the Rad50-dependent pathway remains efficient, even with only 30 bp of homology on each side of the break (Ira and Haber, 2002).

1.2.3.1.1.3 Single-strand annealing

The subpathway of homology-dependent recombination known as single-strand annealing (SSA), is specific to DSBs occurring between direct repeat sequences (Fig. 1.8 D). Such events have been identified in yeast using artificial repeat substrates (Fishman-Lobell *et al.*, 1992), but may potentially be an important mechanism in higher eukaryotic genomes that contain a high proportion of repeated DNA regions (such as Alu repeats) (Symington, 2002). In SSA, the DSB ends are resected to generate 3' single-stranded regions with sufficient homology to be annealed. The non-complementary ssDNA overhangs are then removed endonucleolytically, and the

resulting gaps are filled in by DNA synthesis and ligation (Sugawara and Haber, 1992). This mechanism of homologous repair is mutagenic, as it results in the deletion of one of the repeat sequences. Rad52, but not Rad51 (nor Rad54, Rad55, and Rad57), has been found to be necessary for SSA (Ivanov *et al.*, 1996). As in gene conversion, the initial step requires resection of the DSB ends to facilitate annealing in the regions of homology. The overhanging 3' tails are then cleaved from the intermediate repair structure by the NER endonuclease complex Rad1-Rad10 (Bardwell *et al.*, 1994). This role is performed by the equivalent heterodimer XPF-ERCC1 in mammalian cells. Furthermore, the mismatch repair complex Msh2-Msh3 has been shown to bind to the branched DNA intermediate and promote cleavage by Rad1-Rad10, especially where the flanking homologous regions are short (Sugawara *et al.*, 1997). It is not yet known whether the role of Msh2-Msh3 is to stabilise the branched structure and facilitate cleavage, or to directly recruit the endonuclease complex.

1.2.3.2 Nonhomologous end-joining (NHEJ)

NHEJ is a lower fidelity repair pathway than HR due to the reduced requirement for homology between DNA ends, and as a consequence of the loss of a few bases at some types of repaired site. However, it is still an important pathway for maintaining genomic integrity, and is utilised more often than HR in higher eukaryotes (Jeggo, 1998). Furthermore, NHEJ is the preferred pathway of DSB in *S. cerevisiae* in cases where the DSB has short (4 bp) complementary ends (Haber, 2000). Most of the repair factors employed in NHEJ are distinct from the protein complement utilised in HR, with only Rad50, Mre11, and Xrs2 required in both processes (reviewed in Paques and Haber, 1999).

In *S. cerevisiae*, the DSB ends are identified and bound by a heterodimer of Yku70 and Yku80, which migrates along the DNA to allow further Ku molecules to be loaded onto the break site (Fig. 1.9). To date, no yeast homologue of the mammalian catalytic subunit of DNA-dependent protein kinase (DNA-PKcs) has been identified, suggesting that the complete DNA-PK complex (regulatory Ku70/Ku80 and DNA-PKcs) performs an additional role in higher eukaryotic NHEJ. The functions of the Yku70/Yku80 complex are believed to include protecting broken DNA ends from cellular nucleases, promoting the association of compatible DNA ends, and recruiting other NHEJ factors for the processing and ligation of the damaged site. The Ku heterodimer has been shown to associate with DNA break sites *in vivo* (Martin *et al.*, 1999). Accurate and efficient end joining also requires the recruitment of downstream factors, namely the DNA ligase, Dnl4, and its cofactor Lif1. Loss of DNA ligase IV in higher eukaryotes has been shown to result in significant sensitivity to ionising radiation (Adachi *et al.*, 2001; Karanjawala *et al.*, 2002). Furthermore, the human homologues, DNA ligase IV and XRCC4 have been found to form a tetramer which is thought to act as a bridge between the DSB ends to facilitate ligation (Lee *et al.*, 2000). Two regulatory factors, Nej1 and Lif2, have also been identified, which repress NHEJ during mating-type switching in yeast diploids (Valencia *et al.*, 2001; Frank-Vaillant and Marcand, 2001).

A further protein complex involved in NHEJ is the MRX (Mre11-Rad50-Xrs2) nuclease, which is considered to be particularly important in the repair of DSBs with damaged termini, such as those arising from ionising radiation. The human *XRS2*

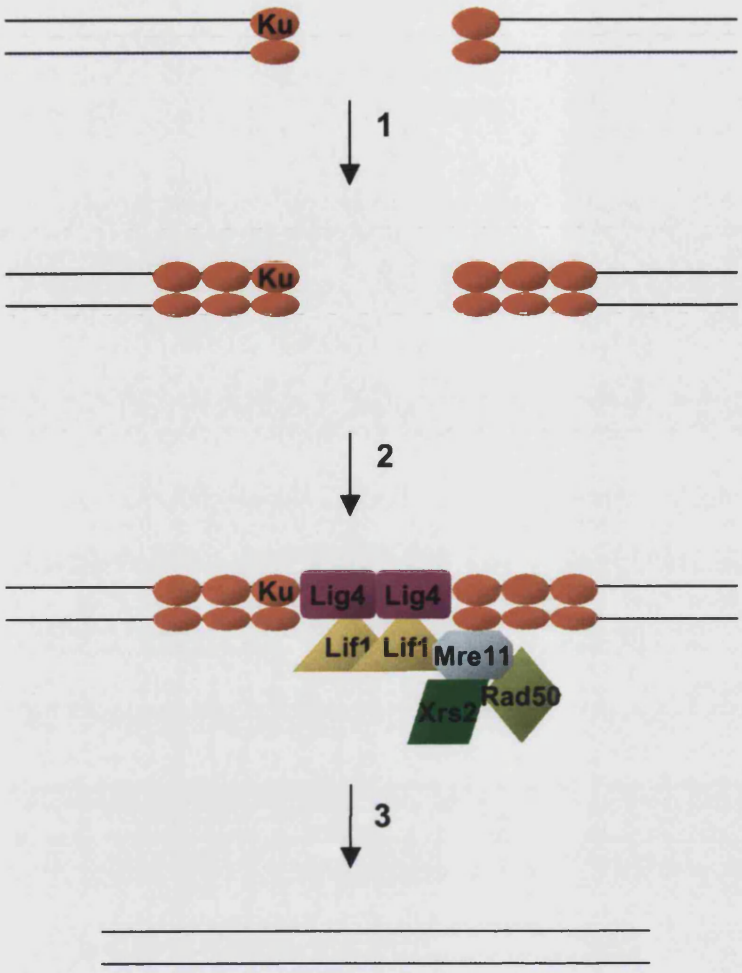

Figure 1.9 Mechanism of Non-Homologous End Joining in yeast. The Ku70-Ku80 heterodimer binds to the DNA ends of a DSB, and migrates along the DNA to allow loading of further Ku molecules (1). A complex of ligase IV (Lig4) and its co-factor Lif1 is recruited to the DSB, and possibly acts as a bridge to facilitate ligation of the ends (2). The Mre11-Rad50-Xrs2 complex is also required for the efficient association and rejoining of the DSB ends.

homologue, *NBS1* (associated with the disorder Nijmegen breakage syndrome), has been shown to be responsible for the localisation of the other subunits to sites of radiation-induced damage (Kobayashi *et al.*, 2004). Plasmid repair assays (which monitor the end-joining of compatible break termini produced by restriction nucleases) have shown that in contrast to a loss of Ku, Dnl4, or Lif1, absence of the MRX complex results in inefficient but predominantly accurate repair. It has been suggested that the MRX complex is involved in the stabilisation of interactions between short homologous sequences, and also the resection of ssDNA overhangs, during NHEJ (Pauli and Gellert, 1998).

In mammalian cells, V(D)J recombination at the immunoglobulin locus is a specialised system of NHEJ reaction in developing B and T lymphocytes that is partially responsible for antibody diversity. The process is initiated by the formation of ssDNA nicks that result in DSBs between variable (V), diversity (D), and joining (J) sub-exon segments of the immunoglobulin genes, and proceeds through a number of intermediate structures, including DNA hairpins (O'Driscoll and Jeggo, 2002). The full complement of NHEJ factors, namely both Ku proteins, DNA-PKcs, and DNA ligase IV, are essential for efficient rejoining of the V(D)J segments to produce the complete variable domain exon. Some of the evidence establishing this link between NHEJ and V(D)J recombination has resulted from studies in SCID (severe combined immunodeficiency) mice, which were found to be deficient in DNA-PKcs or one of the Ku genes (O'Driscoll and Jeggo, 2002).

1.2.4 Post-replication repair

DNA post-replication repair (PRR) is a tolerance pathway, through which single-strand gaps in the nascent DNA can be filled in without removal of the replication-blocking lesion (Fig. 1.10). PRR is known to counter replication obstruction arising from many different types of damage, particularly bulky lesions such as UV photoproducts and alkylation, but also irradiation. In *S. cerevisiae*, the Rad6-Rad18 heterodimer is central to this pathway, with many of the other factors identified as members of the *RAD6* epistasis group through genetic studies for mutagenesis-defective mutant phenotypes (Broomfield *et al.*, 2001). Rad6 is an E2 ubiquitin-conjugating enzyme, which is thought to be targeted to the gaps formed at stalled replication forks by the ssDNA binding capacity of Rad18 (Bailly *et al.*, 1994). Protein modification by ubiquitin (a small peptide) is emerging as an important signal for various cellular processes, including regulated proteolysis, protein localization, DNA repair and regulation of chromatin structure. Binding of Rad6-Rad18 to DNA initiates lesion bypass via one of a number of downstream sub-pathways, which can be error-free or error-prone (mutagenic). Ultimately, all pathways result in the bypass of unrepaired DNA lesions (Johnson *et al.*, 1999).

A subset of the error prone pathway is performed by the translesion polymerase ζ (a heterodimer of Rev3 and Rev7) (Nelson *et al.*, 1996 A), in conjunction with the deoxycitidyl transferase Rev1, which promotes the incorporation of cytosine opposite an abasic site or UV photoproducts (Nelson *et al.*, 1996 B). An alternative mutagenic

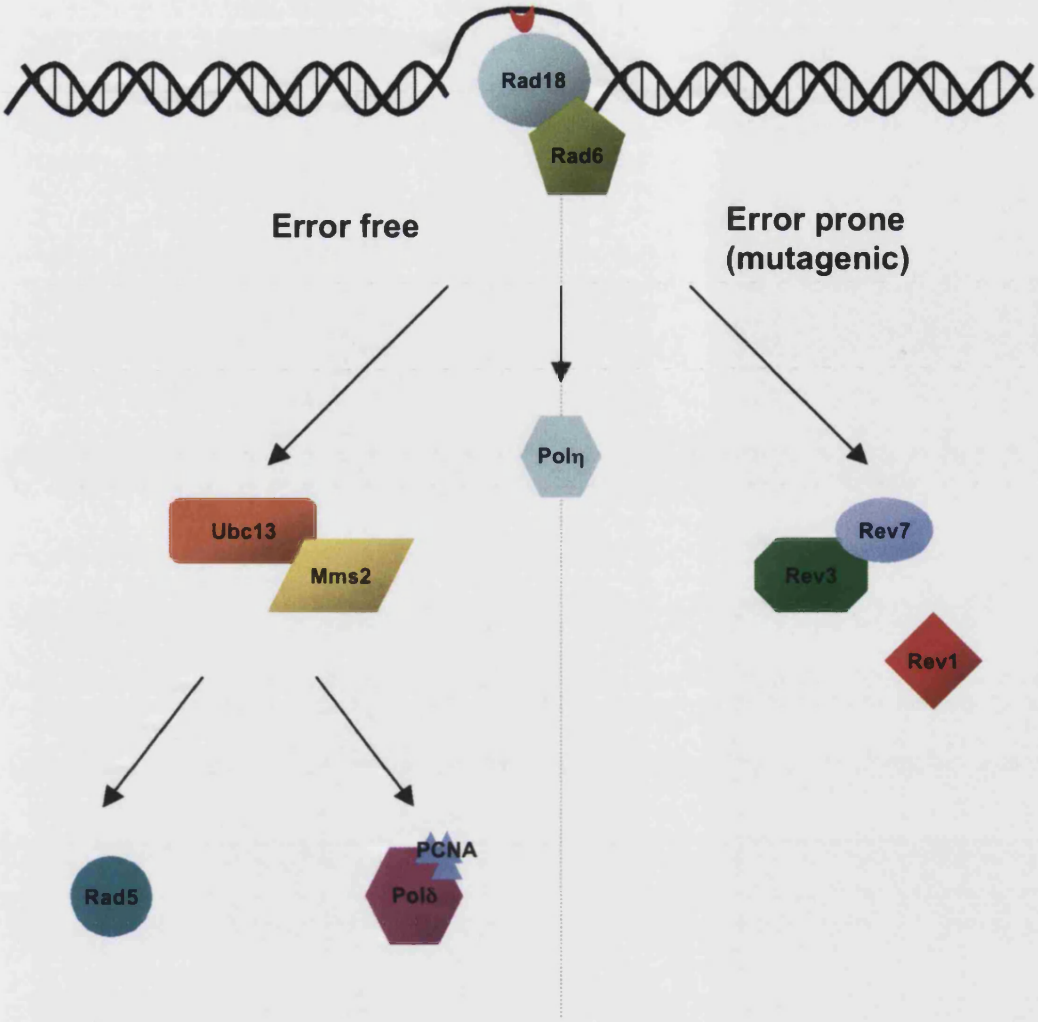

Fig. 1.10 Schematic of Post-replication repair. Initial recognition and binding to DNA damage requires the Rad6-Rad18 heterodimer. Downstream of damage recognition, the pathway divides into error-free and error-prone (mutagenic) branches of repair. The translesion polymerase Polη is involved in both error-free and error-prone mechanisms of repair.

pathway is represented by the repair of N-methyl-N'-nitro-N-nitrosoguanidine (MNNG)-induced lesions, which have been shown to require polymerase η (Haracska *et al.*, 2000). However, the major role of polymerase η is in the error free bypass of UV-induced cyclobutane pyrimidine dimers (CPDs), where it can accurately insert two complementary adenine bases during DNA replication (Masutani *et al.*, 1999; Johnson *et al.*, 1999). Correspondingly, loss of the human gene (*RAD30*) has been implicated in a variant form of Xeroderma pigmentosum, which is associated with an increased incidence of mutations as a result of compensatory use of error-prone polymerases (Johnson *et al.*, 1999; Woodgate, 1999). Hence branches of error free and error prone PRR are not necessarily exclusive, and may depend upon the type of DNA damage.

Another error free pathway requires the ubiquitin conjugating enzymes Ubc13 and Mms2, before further subdivision into branches dependent on either Rad5, a ssDNA ATPase, or the replicative DNA polymerase δ in combination with PCNA (proliferating cell nuclear antigen, a DNA 'sliding clamp' likely to function as a docking platform for replication and repair proteins) (Torres-Ramos *et al.* 2002). Rad5 has been shown to physically interact with both the Ubc13-Mms2 complex and Rad18, and may act to coordinate ubiquitin conjugation (Ulrich and Jentsch, 2000). It is thought that ubiquitination of Rad5 by Ubc13-Mms2 facilitates strand-switching by DNA polymerase δ, in order to replicate past lesions in the original template strand (Torres Ramos *et al.*, 2002). Recent research suggests that ubiquitination of PCNA by Rad6-Rad18 and Ubc13-Mms2 also leads to the activation of translesion synthesis by DNA polymerases ζ and η (Stelter and Ulrich, 2003). Furthermore, the specificity of the various PRR subpathways may be regulated by differential modification of PCNA by

ubiquitin and the ubiquitin-like peptide SUMO (Stelter and Ulrich, 2003; Haracska *et al.*, 2004).

PRR is clearly one of the less well-defined pathways of DNA repair, and much is still to be elucidated. Studies performed in higher eukaryotes have identified homologues to the yeast PRR factors, suggesting that a similar system exists. Moreover, a number of additional translesion polymerases have been discovered, and these are believed to be responsible for the majority of mutations induced by bulky DNA damaging agents (Christmann *et al.*, 2003).

In addition to the translesion synthesis mechanism for resolving stalled replication forks, there is also evidence to suggest a role for sister chromatid exchange recombination events to facilitate replication past the DNA lesion. This may be through strand invasion and the formation of a Holliday junction, or by template switching to provide a 'copy choice' mode of DNA synthesis (Broomfield *et al.*, 2001). In either case, PRR by sister chromatid exchange is considered to be dependent upon Rad52. It is likely that the preference for translesion synthesis or recombination is tightly regulated, potentially through the modification of regulatory factors by ubiquitin and SUMO (Broomfield *et al.*, 2001). The error free branches of PRR appear to be linked to recombination by the helicase Srs2 (Broomfield and Xiao, 2002). Studies of the mutant *srs2* phenotype have revealed that Srs2 acts upon replication-blocking lesions to create a DNA intermediate structure that diverts repair from recombination into the Mms2-dependent branch of error-free PRR (Broomfield and Xiao, 2002).

1.2.5 Other Repair Pathways

Other pathways of DNA repair that have been identified are of less relevance to this study, and so are only reviewed here in brief. Base excision repair (BER) is concerned with the correction of modified DNA base structures arising from endogenous metabolites (such as reactive oxygen species, methylation, deamination) as well as damage produced by ionising radiation and alkylating agents. Recognition of the damaged base is achieved by one of a range of structure-specific DNA glycosylases, which in many cases 'flip' the altered base out of the helix (reviewed in Friedberg *et al.*, 1995). The abasic site is cleaved by either a hydrolytic AP endonuclease (e.g. Apn1) or N-glycosylase associated AP lyases (e.g. Ntg1, Ntg2), and the resulting gap is processed by DNA polymerase β (Memisoglu and Samson, 2000) An alternative 'long patch' gap repair process exists in mammalian cells (particularly at AP sites produced by X-irradiation or chemical agents), in which 2-10 nt are excised and replaced by the combined activity of DNA polymerase, PCNA, replication factor C, and the flap endonuclease FEN1. Corresponding proteins have been identified in yeast, but to date, long patch BER has not been observed (Memisoglu and Samson, 2000). Interestingly, some overlap has been shown between BER, NER recombination, and translesion synthesis pathways for the repair of abasic sites, alkylation, endogenous, and exogenous oxidative damage (Xiao and Chow, 1998; Doetsch *et al.*, 2001).

A number of specific types of DNA damage, either involving abnormal chemical bonds between bases or inappropriate base modifications, can be corrected by direct damage reversal. This repair process requires specialized enzymes to recognise and eliminate the lesion. Examples include the photoreactivation of cyclobutane pyrimidine dimers by DNA photolyase, and the selective removal of methyl groups from the O^6 position of

guanine bases by O^6-methylguanine DNA methyltransferase (MGMT) (Friedberg *et al.*, 1995). Such reactions differ from excision repair pathways in that the modification is repaired without the need to replace the damaged DNA base.

1.3 Repair of DNA interstrand cross-links

The primary process by which DNA interstrand cross-links (ICLs) are repaired, requires the coordinated efforts of factors from the main cellular repair pathways, most notably NER and homologous recombination. An alternative pathway of ICL repair is thought to depend upon the activities of the *RAD6*/post replication repair group. Hence, the elucidation of ICL repair has depended to some extent on the current awareness of these other mechanisms, and as such is less well defined. Studies of ICL repair have also been hampered by the fact that cross-links form only a small fraction of the total DNA damage inflicted by most agents (photoactivated psoralens 30-40 %, cisplatin 5-8 %, nitrogen mustard (mechlorethamine, HN2) 1-5 %) (Dronkert and Kanaar, 2001), hence the cellular response is less easy to decipher. Approaches used to combat this issue include the comparison of repair pathways utilised in response to related bifunctional and monofunctional compounds, and also the production of plasmids with single site-specific ICL. A further caveat is that some of the techniques used to investigate ICL repair, such as alkaline sedimentation, alkaline elution, and gel electrophoresis, have a low sensitivity and require a relatively high concentration of cross-linking agent (reviewed in Hartley *et al.*, 1993; Dronkert and Kanaar, 2001). Such a dose is often extremely toxic, especially considering that a single ICL is lethal to repair-deficient yeast cells (Magana-Schwencke *et al.*, 1982).

1.3.1 *Escherichia coli*

A model for the repair of ICLs in *E. coli* was first outlined by Cole (1973). Genetic and biochemical studies using photoactivated psoralens had shown that the NER factors UvrA, UvrB, UvrC, and UvrD, in conjunction with the recombinase RecA and the polymerase PolA, were required for the repair of ICLs. Cole proposed that repair was initiated by asymmetric dual incisions flanking the cross-link in one strand of the DNA, which 'unhooks' the lesion to leave an 11-base oligonucleotide-drug moiety covalently bound to the complementary strand. These incisions are performed by the UvrABC nuclease complex (Van Houten *et al.*, 1986). It has since been discovered that subsequent processing of the nick 3' to the ICL by the 5'-exonuclease activity of DNA polymerase I (PolA) (Sladek *et al.*, 1989), creates a ssDNA region through which RecA can initiate strand exchange with intact homologous DNA (Cole *et al.*, 1976). The sensitivity of different recombination-deficient bacterial strains to cisplatin suggest that *in vivo*, other factors, including RecFOR and RecBCD, are necessary for efficient recombination at the cross-link (Zdraveski *et al.*, 2000). In normal recombination events, RecFOR promotes the formation of ssDNA-RecA nucleofilaments and stimulates strand invasion, especially in the absence of a DSB (Webb *et al.*, 1997), whereas the RecBCD complex is required to resect DSBs to produce a 3' ssDNA tail that is subsequently bound by RecA (Anderson and Kowalczykowski, 1997). However, the exact roles of these factors in ICL repair remains to be determined. During recombination at the ICL, a three-stranded intermediate structure is formed, in which the predominant base pairing is between the full-length DNA strands. This facilitates access of the UvrABC nuclease to cleave and release the lesion-containing oligonucleotide (Sladek *et al.*, 1989). The resulting gap is repaired by DNA polymerase I, and ligation.

A recombination-independent pathway has been identified in *E. coli*, which requires both the UvrABC nuclease complex, and DNA polymerase II (polB) (Berardini *et al.*, 1999). Repair is similarly initiated by UvrABC incision and unhooking of the cross-link, however, instead of a recombination event, new DNA is subsequently synthesized across the gap by DNA polymerase II. The UvrABC nuclease completes repair by incising the cross-linked oligonucleotide from the complementary strand. The capacity of this pathway to repair ICL appears to vary between agents, with only 2 % of psoralen ICLs repaired in RecA-deficient cells, compared to 30 % of HN2 ICLs (Piette *et al.*, 1988; Berardini *et al.*, 1999). This may reflect differences in pathway preference, with possible variances in the requirement for individual repair factors for each type of ICL (Lage *et al.*, 2003). The reasons for such disparities are as yet unknown, but could conceivably result from restrictions on recognition and access to the various ICLs formed at different sites in the DNA. Furthermore, residual repair is seen in *uvr* mutants, suggesting that recombination or bypass of the ICL may still occur in the absence of cleavage by UvrABC, perhaps through the action of other nucleases such as the newly discovered NER factor Cho (Dronkert and Kanaar, 2001; Van Houten *et al.*, 2002).

1.3.2 *S. cerevisiae*

The yeast *S. cerevisiae* was the first eukaryotic system of ICL repair to be investigated, although it is not yet characterised in as much detail as in *E. coli*. As in bacteria, the major pathway of yeast ICL repair requires elements from both the NER and recombination systems (Fig. 1.11). Genetic studies have shown that loss of genes belonging to either the *RAD3* or *RAD52* epistasis groups renders cells sensitive to cross-

linking agents (Jachymczyk *et al.*, 1981; McHugh *et al.*, 2000). The unhooking of the cross-link from one strand of the DNA involves NER factors (Jachymczyk *et al.*, 1981; Miller *et al.*, 1982), however, the oligonucleotide-drug moiety that remains attached to the complementary strand after incision blocks the normal completion of NER by DNA synthesis and ligation. Furthermore, it has been suggested that the nature of an ICL may even prevent the unwinding of DNA to form a bubble prior to incision (Bessho *et al.*, 1997).

It is well established that NER plays a key role in early ICL repair, since cross-linked DNA from cells deficient in *rad1*, *rad2*, or *rad3* cannot be denatured (Miller *et al.*, 1982; Meniel *et al.*, 1995). This contrasts with the situation in both wild-type and recombination-deficient cells, which exhibit denatured DNA after an appropriate period of incubation for the initial incision events. However, little is known about the nature of these incisions, the resulting repair intermediates, or whether NER factors are also responsible for nuclease activity in the later stages of repair. Further evidence for the involvement of NER factors in ICL repair can be inferred from the observation that repair is faster in transcriptionally active regions, and as mutations induced by psoralen-ICLs are predominantly found in the non-transcribed strand (Meniel *et al.*, 1995; Meniel *et al.*, 1997; Barre *et al.*, 1999 A). The involvement of the NER lesion recognition factors may vary between different types of ICL. Analysis of the sensitivity of mutant

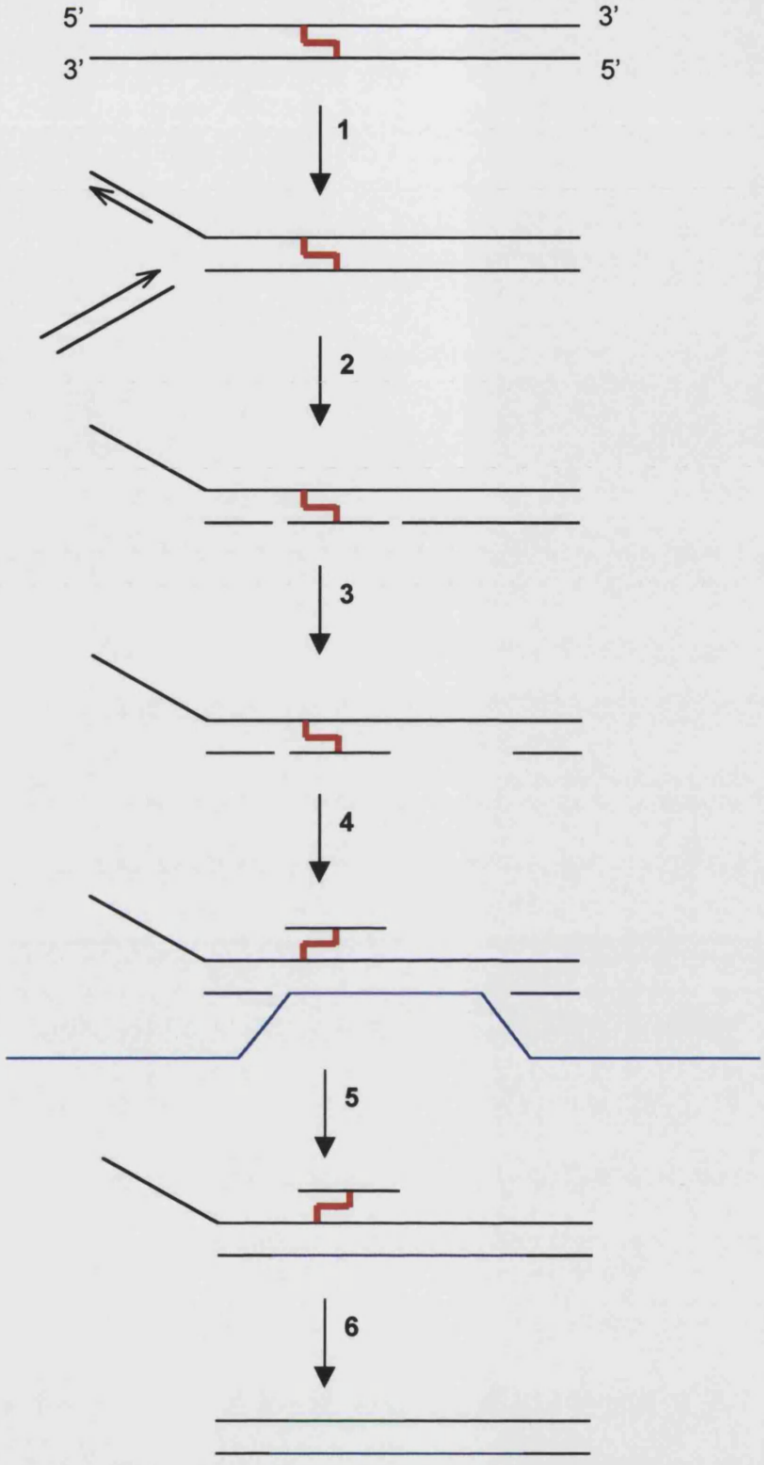

Figure 1.11 Model of ICL repair in yeast, developed from the known mechanism in *E. coli*. (1) Collapse of the replication fork due to torsional stress may result in the formation of a DSB. (2) NER-dependent dual incision reactions leads to the unhooking of the cross-link from one strand. (3) 5'-3' nucleolyitc resection may provide a gap and ssDNA tail for recombination by strand invasion. (4) Homologous recombination. (5) Resolution of recombination. (6) A second incision reaction releases the damaged DNA. Repair is completed by DNA resynthesis across the gap and ligation.

strains to mitomycin C and cisplatin revealed an equal role for *RAD4* and *RAD14* in ICL repair compared to UV, yet an increased requirement for *RAD7* and *RAD16*, and a lesser involvement for *RAD23* (Wu *et al.*, 2004). Interestingly, loss of the TCR recognition factors *RAD26* and *RAD28* did not result in sensitivity to either cross-linking agent.

As in *E. coli*, it is believed that a recombination event occurs post-incision, providing a template to complete the repair process. Indeed, yeast cells deficient in homologous recombination pathways (e.g. *rad51*, *rad52*, *rad54*, *mre11*) are sensitive to agents such as nitrogen mustard and psoralen plus UVA (Henriques and Moustacchi, 1980, 1981), and exhibit a reduced capacity to recover high-molecular weight DNA (i.e. intact chromosomes) after ICL-associated DSB formation (Jachymczyk *et al.*, 1981; Magana-Schwencke *et al.*, 1982; McHugh *et al.*, 2000). No evidence exists as to the exact recombination mechanism involved in ICL repair, and any of the known models (Holliday Junctions, BIR, SSA) could conceivably be utilised (Dronkert and Kanaar, 2001). NHEJ is not thought to be required for ICL repair, as NHEJ mutants are not sensitive to ICL agents, and a *ku70 rad52* double disruptant is only as sensitive as the *rad52* alone (McHugh *et al.*, 2000). Hence, even in the absence of homologous DNA during stationary phase, the NHEJ pathway does not appear able to compensate for loss of HR. One of the caveats of proposed ICL repair by sequential NER and recombination events (Fig. 1.11) is that synergism has been observed between representative factors of these pathways (Chanet *et al.*, 1985; Magana-Schwencke and Averbeck, 1991). This does not exclude the possibility of cooperation in ICL repair, however these pathways are likely to be involved in other independent systems of repair.

A further prominent limitation of the existing model for ICL repair in replicating yeast cells (Fig. 1.11) is that, if the replication fork disintegrates upstream of the cross-link, it precludes the production of a sister chromatid for homologous recombination bypass of the incised adduct. Given that DNA must be unwound a considerable distance ahead of the advancing fork during DNA replication, the resulting torsional stress exerted by an ICL renders fork collapse likely. Hence, in haploid cells that lack homologous chromosomes, some additional mechanism is required to facilitate repair and replication past the cross-link (discussed in more detail in Chapter 6).

The formation of DSBs was first identified during ICL repair in yeast by density gradient DNA sedimentation (Jachymczyk *et al.*, 1981), and initially this was interpreted as evidence for dual incisions on each strand to release the cross-link from both DNA strands. However, it was subsequently suggested that, as in *E. coli*, such dual incisions on both strands do not occur (Dardalhon and Averbeck, 1995; McHugh *et al.*, 2000). Nevertheless, the formation of DSBs is much more prominent in yeast than bacteria, and, as DSBs are potent initiators of recombination in eukaryotic cells they may be an important intermediate for the promotion of efficient post-incision repair events.

DSBs are believed to arise during ICL repair by different means. Firstly, they can occur as a direct result of nuclease activity. Indeed, the NER endonuclease Rad2 (in addition to Rad3) is involved in the production of DSBs during the repair of psoralen-induced cross-links (Jachymczyk *et al.*, 1981; Magana-Schwencke *et al.*, 1982). However, the DSBs observed in the presence of HN2-induced ICL do not depend on functional NER (McHugh *et al.*, 2000). It is thought that these DSB intermediates may be the result of

collapsed replication forks due to the torsional stress encountered close to an ICL, as DSBs are observed at greatest frequency in rapidly dividing exponential phase cells (Dardalhon and Averbeck, 1995; McHugh *et al.*, 2000). DSBs have also been observed in cisplatin treated cells using density gradients (Wilborn and Brendel, 1989). It remains to be determined whether DSBs occur on only one or both sides of the cross-link. However, the unidirectional gene conversion tracts associated with recombinational repair of a psoralen ICL primarily occur upstream of the cross-link, suggesting an asymmetric bias in the early incision and strand breakage events (Greenberg *et al.*, 2001).

In non-dividing haploid cells, where no sister chromatid or homologue is present, an alternative route for repair is provided by the PRR pathway. Cells deficient in PRR are sensitive to ICL-inducing agents, and this appears to be synergistic with both the NER and HR pathways (Chanet *et al.*, 1985; McHugh *et al.*, 2000). Most of the known PRR genes have a sensitive mutant phenotype to ICL agents, with the exception of *rad30* (Grossmann *et al.*, 2001; Wu *et al.*, 2004). The induction of DSBs occurs normally in these mutants, yet the reconstitution of higher molecular weight DNA is retarded (Chanet *et al.*, 1985; Dardalhon and Averbeck, 1995). Interestingly, some factors (*rad6*, *rad18*) seem to be required in both growing and stationary cells, whereas others are only essential in stationary phase (*rev3*) (Henriques and Moustacchi, 1981; McHugh *et al.*, 2000).

This ICL repair mechanism is less well defined than the NER/recombination system, but is believed to involve the activity of an error-prone DNA polymerase to fill in the gap resulting from incision (McHugh *et al.*, 2000). However, the reduced sensitivity to

ICL agents seen in the *rev3* mutant compared to the *rad6*, suggests that error-free sub-pathways of PRR are also utilised in ICL repair (Lawrence and Hinkle, 1996). It is not known whether translesion synthesis occurs in conjunction with sequential NER excision reactions, as suggested for *E. coli*. The fact that mutations associated with the repair of psoralen induced ICLs are found predominantly on the non-transcribed strand suggests a role for translesion synthesis after unhooking of the cross-link from the transcribed strand by NER. However, studies of psoralen ICL-associated mutagenesis have also revealed NER-independent roles of PRR in cross-link repair (Barre *et al.*, 1999 B; Greenberg RB *et al.*, 2001).

1.3.3 Mammals (Higher eukaryotes)

The mechanism of ICL repair in mammalian cells in largely unknown, and much of the available data have been determined from analyses of hamster cell lines sensitive to ICL agents, and comparisons of mammalian genes with their yeast homologues. It seems that, as in yeast and bacteria, the pathways of NER, recombination, and PRR are all involved in the response to ICL (reviewed in Dronkert and Kanaar, 2001). However, some significant differences have been observed. Unlike in yeast, where all NER mutants are equally sensitive to ICL inducing agents, most mammalian NER gene defects exhibit only a mild sensitivity, with the exception of mutations in either *XPF* or *ERCC1*, which result in a severe phenotype (Collins, 1993; De Silva *et al.*, 2000). This distinction is observed for most ICLs (HN2, cyclophosphamide, cisplatin, mitomycin C), but crucially not for UV-induced lesions. Interestingly, some studies have suggested that *XPF* and *ERCC1* mutants are not hypersensitive to psoralen-induced ICLs, suggesting a degree of substrate specificity (Kaye *et al.*, 1980; Vukannovic and Cleaver, 1987).

A comprehensive explanation for this phenomenon has not yet been achieved, although there are two plausible rationales. One is that the incision reaction at the ICL is more dependent upon XPF-ERCC1 than the other NER factors. The evidence for this hypothesis appears conflicting, yet this may result from variances in the repair of different types of ICL. For example, a direct correlation is observed between sensitivity to HN2 and the ability to uncouple the cross-link, and psoralen-induced ICLs can be incised *in vitro* by XPF-ERCC1 alone (De Silva *et al.*, 2000; Mu *et al.*, 2000; Kuraoka *et al.*, 2000). However, additional NER factors (including the XPG nuclease) are required to uncouple a cisplatin-induced ICL, despite not exhibiting a sensitive mutant phenotype (De Silva *et al.*, 2002). The other possibility is that the dual roles of *XPF* and *ERCC1* in NER and recombination may be more prominent in mammalian ICL repair, perhaps as a result of an increased preference for HR mechanisms involving XPF-ERCC1. Recent studies have suggested roles for XPF-ERCC1 in the recognition of ICL and initial incision reactions (5' and to a lesser extent 3' to the ICL), and also in the resolution of DSBs arising at cross-links, but not in the formation of the DSB (Kuraoka *et al.*, 2000; Kumaresan *et al.*, 2002; Rothfuss and Grompe, 2004; Niedernhofer *et al.*, 2004). Reports have also been made of dual incisions solely on the 5' side of a psoralen ICL *in vitro*, which require the full complement of NER factors, and appear to result in futile cycles of DNA synthesis across the gap, rather than acting as a recombinogenic signal (Bessho *et al.*, 1997; Bessho, 2003).

As in yeast, DSBs have been observed in mammalian cells following treatment with either HN2 or psoralen (De Silva *et al.*, 2000; Akkari *et al.*, 2000), but not cisplatin (De Silva *et al.*, 2002). Consistent with DSB formation as a result of replication fork collapse, these DSBs occurred in dividing but not confluent CHO (Chinese Hamster

Ovary) cells (De Silva *et al.*, 2000). Furthermore, passage through S-phase of the cell cycle was a prerequisite for chromosome breakage in human fibroblasts exposed to sub-lethal doses of psoralen (Akkari *et al.*, 2000). Indeed, the occurrence of DSBs at a single site-specific psoralen ICL has since been shown to correlate with the termination of DNA replication *in vitro* using a HeLa-cell extract (Bessho, 2003). Induction and repair of HN2-associated DSBs has been shown to be normal in all NER mutants, whilst cells deficient in the homologous recombination genes *XRCC2* and *XRCC3* are proficient in DSB induction, but severely impaired in DSB repair (De Silva *et al.*, 2000). Hence, as in yeast, DSBs are formed independently of ICL incision by NER factors. It has been suggested that DSBs may arise prior to unhooking of the cross-link, as the kinetics of DSB formation have been observed to be more rapid than incision in CHO cells (Damia *et al.*, 1996).

Analyses of sensitivity to cross-linking agents in hamster and human cell lines have suggested a particular requirement for *RAD51*-homologues such as *XRCC2* and *XRCC3* in ICL repair, but not genes associated with NHEJ (Jones *et al.*, 1987; De Silva *et al.*, 2000). Cells deficient in one of the *RAD51* paralogues are far more sensitive to ICLs than DSBs alone, implying that they may have an important role in the modulation of strand invasion for the complex intermediate DNA structures arising at an ICL (De Silva *et al.*, 2000; Dronkert and Kanaar, 2001). A plasmid-based system has provided further evidence for the involvement of homologous recombination, as ICL repair by mammalian cell extracts was significantly stimulated in the presence of a homologous substrate (Li *et al.*, 1999). This repair was dependent upon functional *XPF*, *ERCC1*, *XRCC2*, and *XRCC3*. An increase in sister chromatid exchange has been observed in

response to cross-linking agents, but not mono-functional compounds, suggesting an important role for recombination in mammalian ICL repair (Bodell, 1990).

Treatment of mammalian cells with ICL agents, as with ionizing radiation, results in the formation of nuclear foci consisting of a number of repair factors including Rad51 and Brca2 (Bishop *et al.*, 1998; Godthelp *et al.*, 2002; Kraakman-van der Zwet *et al.*, 2002). It is thought that these foci may represent centres of DNA repair, with proteins such as Brca1 and Brca2 providing coordinated regulation of the damage response and cell cycle checkpoints. Other repair foci containing the Rad50-Mre11-Nbs1 recombination complex are also observed after treatment with ICL agents, and the formation of these foci appears to occur independently of incision events (Pichierri *et al.*, 2002). Interestingly, the uncoupling of cisplatin-induced, but not HN2-induced ICLs, appears to require *XRCC2* and *XRCC3* in addition to *XPF-ERCC1* (De Silva *et al.*, 2000, 2002).

Even less is currently known about the role of PRR in the repair of ICLs. *RAD18* deficient chicken DT40 cells have been reported to be extremely sensitive to cisplatin, with an associated increase in the occurrence of sister chromatid exchange events, perhaps to compensate for the absence of PRR (Dronkert and Kanaar, 2001). Furthermore, mitomycin C sensitivity can be increased by the expression of a *RAD18* mutant, defective in the Rad6 binding domain, in human cells (Tateishi *et al.*, 2000). In contrast to yeast, human *RAD30* mutant cells exhibit hypersensitivity to psoralen ICLs and reduced replication bypass (Misra and Vos, 1993). One study has reported the requirement for a NER-dependent, but recombination-independent, pathway of repair for a site-specific psoralen ICL in mammalian cells, and that this repair correlates with an increased rate of mutagenesis (Wang *et al.*, 2001). This is strongly suggestive of a

role for PRR, particularly the error-prone subpathways, in mammalian ICL repair. The relative contribution of translesion synthesis to ICL repair may depend on the nature of the cross-link, as the degree of mutagenesis appears to be variable (Dronkert and Kanaar, 2001).

A number of other factors have also been implicated in the repair of ICLs in higher eukaryotes. Fractionation of nuclear extracts from HeLa cells revealed that RPA is required for incisions at a psoralen ICL *in vitro*, as well as during subsequent DNA synthesis (Zhang and Legerski, 2003). Furthermore, PCNA was shown to be necessary for DNA synthesis during ICL repair, and can enhance the incision reaction possibly through improved lesion recognition by MutSβ (Zhang N. *et al.*, 2002). Another group of genes that confer hypersensitivity to cross-linking agents are those associated with Fanconi anaemia (FA), an autosomal recessive cancer-prone syndrome (Grompe and D'Andrea, 2001). There are ten distinct FA complementation groups (*FANCA*, *FANCC*, *FANCD1/BRCA2*, *FANCD2*, *FANCE*, *FANCF*, *FANCG*, *FANCL*, *FANCI* and *FANCJ*), eight of which of these have now been cloned (all except *FANCI* and *FANCJ*). In addition to FA, somatic inactivation of the FA/BRCA pathway has been shown to account for the chromosomal instability of other cancers, and FANCF inactivation is associated with cisplatin sensitivity in ovarian cancer (Taniguchi *et al.*, 2003; D'Andrea and Grompe, 2003). A "core" complex of six FA proteins (A, C, E, F G and L) localises to the nucleus, where it regulates the activation of FANCD2 by monoubiquitylation (Garcia-Higuera *et al.*, 2001). The subunit responsible for the addition of ubiquitin moieties to substrate proteins, E3 ubiquitin ligase, has been shown to correspond to FANCL (Meetei *et al.*, 2003). Activated FANCD2 is then targeted to Rad51-BRCA1 nuclear foci, which are involved in the regulation of homologous

recombination repair and cell cycle checkpoints (Meetei *et al.*, 2003). FA cells are proficient in the incision reactions at an ICL, as well as the formation of DSBs (Rothfuss and Grompe, 2004). FANCC is required for the assembly of the RAD50-MRE11-NBS1 complex in response to DNA cross-links, and FANCD2 has also been shown to interact with NBS1 (Nakanishi *et al.*, 2002; Pichierri *et al.*, 2002).

1.4 *PSO2/SNM1*

1.4.1 Identification as a gene involved in ICL repair

The *S. cerevisiae PSO2* or *SNM1* gene was identified from two independent screens to isolate novel strains exhibiting sensitivity to ICLs produced by psoralen/UVA (Henriques and Moustacchi, 1980), and nitrogen mustard (mechlorethamine, HN2) (Ruhland *et al.*, 1981 A), respectively (*PSO2* = psoralen sensitive, *SNM1* = sensitivity to nitrogen mustard). Subsequent complementation studies and analysis of meiotic segregation proved the two genes to be allelic (Cassier-Chauvat and Moustacchi, 1988). *S. cerevisiae* cells defective for *pso2* are uniquely sensitive to all ICL-forming agents tested to date, irrespective of the type of bases involved in ICL formation. A representative sample illustrating the breadth of *pso2* sensitivity to ICL species comprises HN2 and derivatives such as chlorambucil, photoactivated psoralens, mitomycin C, triaziquone, diepoxyoctane, and platinum-based compounds including cisplatin (Fleer and Brendel, 1979; Pungartnik *et al.*, 2002). However, *pso2* strains demonstrate almost wild-type-like resistance to monofunctional alkylating agents and ionising radiation. Furthermore, *pso2* mutant cells exhibit only mild sensitivity to UVC, possibly as a result of the minor ICL lesions produced (Rahn and Patrick, 1976; Ruhland and Brendel, 1979; Ruhland *et al.*, 1981 B). This sensitivity results from a

DNA repair defect as *pso2* mutant cells are proficient in the uptake of drug (Ruhland *et al.*, 1981 B).

1.4.2 Homology

The *S. cerevisiae PSO2* gene is located on chromosome XIII, and encodes a 76kDa protein with 29% identity to both *Schizosaccharomyces pombe PSO2* and *Mus musculus SNM1A*, and 28% identity to the human gene *hSNM1A* (Fig. 1.12). However, a region of 327 amino acids in *hSNM1* exhibiting the greatest similarity to *ScPSO2* is 48% identical, and a further 14% of the residues are similar (Demuth and Digweed, 1998). Multiple paralogues are found in both mouse and humans, including *hELAC2*, which is associated with an inherited susceptibility to prostate cancer (Tavtigian *et al.*, 2001). It is possible that these paralogues may have evolved distinct functions, as the extent of complementation is not yet known. Sequence analysis has shown that *hSNM1B* may contain a mitochondrial localization sequence (P. McHugh, unpublished observations). Furthermore, the human paralogue Artemis/*hSNM1C* was identified as the mutant gene in RS-SCID (Radiation Sensitive Severe Combined Immune Deficiency), where the phenotype results from defects in V(D)J recombination and in the non-homologous end joining (NHEJ) of double strand breaks (DSBs) (Moshous *et al.*, 2001). In addition, a unique nonsense mutation in *Artemis* that results in a truncated protein has been implicated as the cause of the autosomal recessive trait Athabascan SCID (Li *et al.*, 2002). A further *PSO2* homologue, *MUS322*, which also confers mutant sensitivity to HN2, has recently been identified in Drosophila (Laurencon *et al.*, 2004).

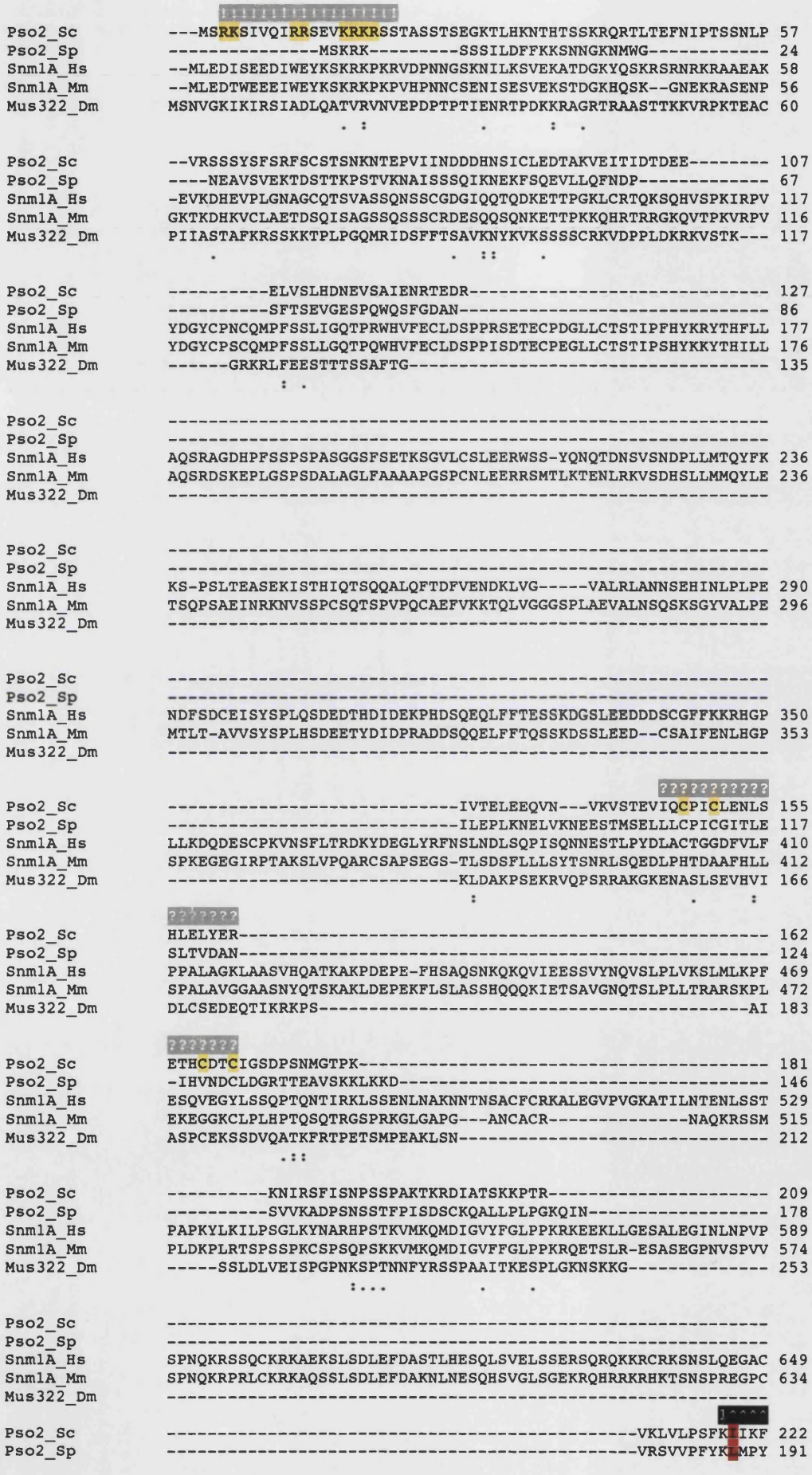
Pso2_Sc ---MSRKSIVQIRRSEVKRKRSSTASSTSEGKTLHKNTHTSSKRQRTLTEFNIPTSSNLP 57
Pso2_Sp ----------MSKRK---------SSSILDFFKKSNNGKNMWG---------- 24
Snm1A_Hs --MLEDISEEDIWEYKSKRKPKRVDPNNGSKNILKSVEKATDGKYQSKRSRNRKRAAEAK 58
Snm1A_Mm --MLEDTWEEEIWEYKSKRKPKPVHPNNCSENISESVEKSTDGKHQSK--GNEKRASENP 56
Mus322_Dm MSNVGKIKIRSIADLQATVRVNVEPDPTPTIENRTPDKKRAGRTRAASTTKKVRPKTEAC 60
Pso2_Sc --VRSSSYSFSRFSCSTSNKNTEPVIINDDDHNSICLEDTAKVEITIDTDEE-------- 107
Pso2_Sp ----NEAVSVEKTDSTTKPSTVKNAISSSQIKNEKFSQEVLLQFNDP------------- 67
Snm1A_Hs -EVKDHEVPLGNAGCQTSVASSQNSSCGDGIQQTQDKETTPGKLCRTQKSQHVSPKIRPV 117
Snm1A_Mm GKTKDHKVCLAETDSQISAGSSQSSSCRDESQQSQNKETTPKKQHRTRRGKQVTPKVRPV 116
Mus322_Dm PIIASTAFKRSSKKTPLPGQMRIDSFFTSAVKNYKVKSSSSCRKVDPPLDKRKVSTK--- 117
Pso2_Sc ----------ELVSLHDNEVSAIENRTEDR------------------------------ 127
Pso2_Sp ----------SFTSEVGESPQWQSFGDAN------------------------------- 86
Snm1A_Hs YDGYCPNCQMPFSSLIGQTPRWHVFECLDSPPRSETECPDGLLCTSTIPFHYKRYTHFLL 177
Snm1A_Mm YDGYCPSCQMPFSSLLGQTPQWHVFECLDSPPISDTECPEGLLCTSTIPSHYKKYTHILL 176
Mus322_Dm ------GRKRLFEESTTTSSAFTG---------------------------------- 135
Pso2_Sc --
Pso2_Sp --
Snm1A_Hs AQSRAGDHPFSSPSPASGGSFSETKSGVLCSLEERWSS-YQNQTDNSVSNDPLLMTQYFK 236
Snm1A_Mm AQSRDSKEPLGSPSDALAGLFAAAAPGSPCNLEERRSMTLKTENLRKVSDHSLLMMQYLE 236
Mus322_Dm --
Pso2_Sc --
Pso2_Sp --
Snm1A_Hs KS-PSLTEASEKISTHIQTSQQALQFTDFVENDKLVG-----VALRLANNSEHINLPLPE 290
Snm1A_Mm TSQPSAEINRKNVSSPCSQTSPVPQCAEFVKKTQLVGGGSPLAEVALNSQSKSGYVALPE 296
Mus322_Dm --
Pso2_Sc --
Pso2_Sp --
Snm1A_Hs NDFSDCEISYSPLQSDEDTHDIDEKPHDSQEQLFFTESSKDGSLEEDDDSCGFFKKRHGP 350
Snm1A_Mm MTLT-AVVSYSPLHSDEETYDIDPRADDSQQELFFTQSSKDSSLEED--CSAIFENLHGP 353
Mus322_Dm --
Pso2_Sc ----------IVTELEEQVN---VKVSTEVIQCPICLENLS 155
Pso2_Sp ----------ILEPLKNELVKNEESTMSELLLCPICGITLE 117
Snm1A_Hs LLKDQDESCPKVNSFLTRDKYDEGLYRFNSLNDLSQPISQNNESTLPYDLACTGGDFVLF 410
Snm1A_Mm SPKEGEGIRPTAKSLVPQARCSAPSEGS-TLSDSFLLLSYTSNRLSQEDLPHTDAAFHLL 412
Mus322_Dm ----------KLDAKPSEKRVQPSRRAKGKENASLSEVHVI 166
Pso2_Sc HLELYER---------- 162
Pso2_Sp SLTVDAN---------- 124
Snm1A_Hs PPALAGKLAASVHQATKAKPDEPE-FHSAQSNKQKQVIEESSVYNQVSLPLVKSLMLKPF 469
Snm1A_Mm SPALAVGGAASNYQTSKAKLDEPEKFLSLASSHQQQKIETSAVGNQTSLPLLTRARSKPL 472
Mus322_Dm DLCSEDEQTIKRKPS----------AI 183
Pso2_Sc ETHCDTCIGSDPSNMGTPK---------- 181
Pso2_Sp -IHVNDCLDGRTTEAVSKKLKKD---------- 146
Snm1A_Hs ESQVEGYLSSQPTQNTIRKLSSENLNAKNNTNSACFCRKALEGVPVGKATILNTENLSST 529
Snm1A_Mm EKEGGKCLPLHPTQSQTRGSPRKGLGAPG---ANCACR----------NAQKRSSM 515
Mus322_Dm ASPCEKSSDVQATKFRTPETSMPEAKLSN---------- 212
Pso2_Sc ----------KNIRSFISNPSSPAKTKRDIATSKKPTR---------- 209
Pso2_Sp ----------SVVKADPSNSSTFPISDSCKQALLPLPGKQIN---------- 178
Snm1A_Hs PAPKYLKILPSGLKYNARHPSTKVMKQMDIGVYFGLPPKRKEEKLLGESALEGINLNPVP 589
Snm1A_Mm PLDKPLRTSPSSPKCSPSQPSKKVMKQMDIGVFFGLPPKRQETSLR-ESASEGPNVSPVV 574
Mus322_Dm -----SSLDLVEISPGPNKSPTNNFYRSSPAAITKESPLGKNSKKG---------- 253
Pso2_Sc --
Pso2_Sp --
Snm1A_Hs SPNQKRSSQCKRKAEKSLSDLEFDASTLHESQLSVELSSERSQRQKKRCRKSNSLQEGAC 649
Snm1A_Mm SPNQKRPRLCKRKAQSSLSDLEFDAKNLNESQHSVGLSGEKRQHRRKRHKTSNSPREGPC 634
Mus322_Dm --
Pso2_Sc ----------VKLVLPSFKIIKF 222
Pso2_Sp ----------VRSVVPFYKLMPY 191

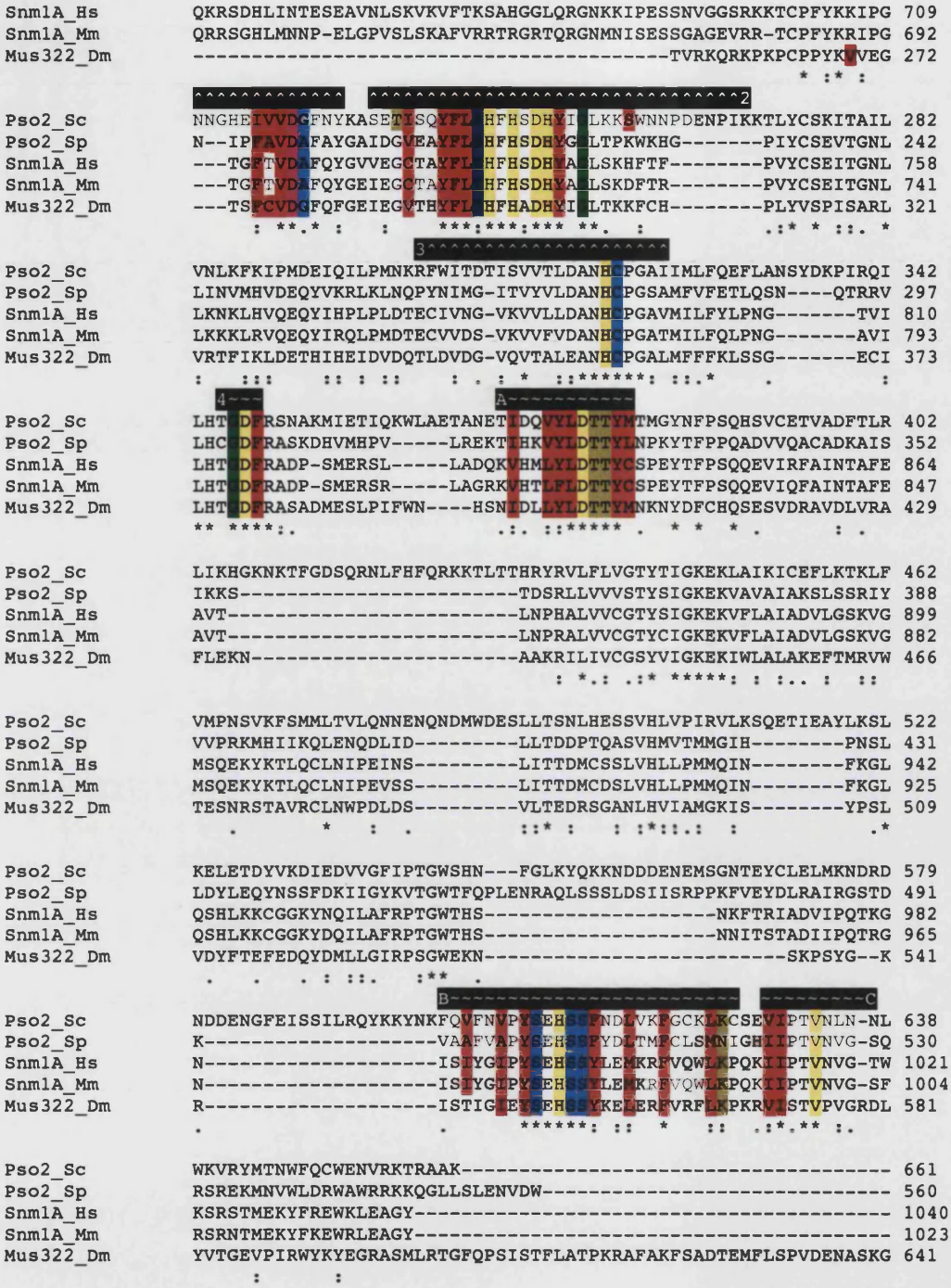

Figure 1.12 Multiple protein sequence alignment of members of the Pso2/Snm1 family, performed using ClustalW (www.ebi.ac.uk/clustalw) set to the default parameters. Protein sequences were obtained from the NCBI database, accession numbers: Pso2_Sc *NP_013857*, Pso2_Sp *Q10264*, Snm1A_Hs *AAT09762*, Snm1A_Mm *NP_061301*, Mus322_Dm *NP_061301*. Functional domains are highlighted above the sequence: putative bipartite nuclear localization signal ▮ (Prosite, www.expasy.org/prosite) putative zinc finger ▮ (SWISS-PROT, www.ebi.ac.uk/swissprot/), metallo-β-lactamase motifs 1-3 ▮ (L. Aravind, 1999), β-CASP motifs 4 and A-C ▮ (Callebaut *et al.*, 2002). Conserved residues in the metallo-β-lactamase/β-CASP motifs are highlighted as follows: catalytic *yellow*, hydrophobic *red*, small *turquoise*, hydroxylic *blue*, tiny *green*, polar *brown*. Extent of residue conservation is shown below the sequence: (*) identical residues, (:) conserved residue substitutions, (.) semiconserved residue substitutions (ClustalW).

In apparent contrast to the yeast gene, mouse embryonic stem cells with a null phenotype for *SNM1* solely demonstrate sensitivity to mitomycin C and not other ICL-inducing chemicals, although this may be explained by functional redundancy with the other murine homologue (Dronkert *et al.*, 2000). Complementation of mitomycin C sensitivity in *mSNM1*$^{-/-}$ cells was achieved by transfection with *hSNM1A* cDNA, implying a certain degree of functional conservation of this gene (Dronkert *et al.*, 2000). Furthermore, expression of *hSNM1A* from the galactose inducible vector pYES in *S. cerevisiae pso2* cells results in partial complementation of HN2 sensitivity (A. Hazrati and P. McHugh, unpublished observations). Hence it appears that Pso2 function is to some extent conserved from yeast to humans, and so detailed genetic studies in model organisms such as *S. cerevisiae* will be a powerful means to further elucidate the role of the *PSO2/SNM1* family in DNA metabolism.

1.4.3 Transcription and Inducibility

In *S. cerevisiae*, constitutive transcription of *PSO2* is maintained at a steady state of only 0.3 transcripts per cell as a consequence of an upstream silencer within the adjacent *GTP1* ORF (Richter *et al.*, 1992). A four-fold induction of transcription is seen within 4 hours following treatment with ICL-inducing drugs, but not by monofunctional agents or the UV-mimetic agent 4-nitroquinoline-1-oxide (Wolter *et al.*, 1996). Inducibility was shown to require a 15 bp motif with homology to the DRE2 box found in the promoter of the damage-inducible repair gene *RAD2*. Additionally, induction of *PSO2* is dependent upon the Dun1 kinase, known to be required for the transcription of a number of genes induced by DNA damage and replication checkpoint pathways (Wolter *et al.*, 1996). Interestingly, analysis of the promoter of the human *SNM1A* homologue KIAA0086 revealed consensus sequences for the transcription

activators NFκB and AP1, which respond to many factors including ionising radiation and mono/poly-functional alkylating agents (Demuth and Digweed, 1998). However, no change in either *hSNM1* transcript abundance or size has been observed in HeLa cells up to 22 hours after treatment with mitomycin C (Richie *et al.*, 2002).

A recent study has shown that the *hSNM1* transcript has a long 5' untranslated region and an internal ribosome entry site, which upregulates translation during mitosis, but maintains a suppressed state for the remainder of the cell cycle (Zhang X. *et al.*, 2002). Studies in murine ES cells intimate that Snm1 is strictly maintained at a low level, even when under the control of the strong PGK promoter, which is also suggestive of post-transcriptional regulation. Furthermore, human cells over-expressing *hSNM1* exhibit morphological changes consistent with apoptosis (Dronkert *et al.*, 2000). It is possible therefore, that Pso2/Snm1 may be toxic when present in large quantities.

1.4.4 Intracellular localisation

The Pso2 protein has a nuclear transport signal peptide and correspondingly, has been shown to localise to the nucleus by immunological staining (Henriques *et al.*, 1997; Dronkert *et al.*, 2000). Recent studies using human cell lines have observed that hSnm1 may be spread diffusely throughout the nucleus, sequestered in large nuclear bodies, or as multiple smaller foci (Richie *et al.*, 2002). These foci appear to co-localise with other repair proteins including Mre11, BRCA1, and 53BP1, and it has been suggested by Richie *et al.* that these smaller foci represent sites of recruitment to DNA double-strand breaks.

1.4.5 Metallo-β-lactamase superfamily

The Pso2 protein is a member of the metallo-β-lactamase superfamily of enzymes that share a hydrolytic domain (Aravind, 1999). The metallo-β-lactamase fold, first described for the *Bacillus cereus* β-lactamase, consists of a four layered β sandwich with two mixed β sheets flanked by helices, and metal co-ordination sites located at one edge of the β sandwich (Carfi *et al.*, 1995). Of the five conserved sequence motifs, the HxHxDH motif is the most characteristic feature of the superfamily, with the first histidine and aspartate conserved in all active members (Fig. 1.12). It has been inferred from the crystal structure of β-lactamases that the first two histidines are involved in zinc coordination, while the conserved aspartate projects close to the active site, participating in the hydrolysis reaction (Carfi *et al.*, 1995). Interestingly, a thermoconditional *pso2* mutant, deficient for ICL repair, results from a single amino acid change three residues downstream of the HxHxDH motif (Niegemann and Brendel, 1994). This modification replaces a small glycine residue with arginine, which has a large, charged polar side chain. Hence it is likely that the thermosensitive phenotype is due to disrupted binding at the active site. Indeed, a recent paper has demonstrated that this β-lactamase motif is essential for Pso2 function, as replacement of the highly conserved aspartate by site directed mutagenesis produces cells with a phenotype indistinguishable from the *pso2* null mutant (Li and Moses, 2003). Given the nuclear localisation of Pso2 and its role in DNA repair, the most likely substrate for hydrolysis is DNA. Indeed, one of the five human paralogues, Artemis, exhibits a single strand-specific 5' to 3' exonuclease activity *in vitro*, but when complexed with DNA-PKcs it becomes phosphorylated, acquiring 5' and 3' overhang and hairpin endonuclease activity (Ma *et al.*, 2002).

A further subdivision of the metallo-β-lactamase superfamily has led to the formation of the β-CASP group of proteins that act upon nucleic acid substrates. This group is named after the representative members: CPSF (a mRNA cleavage and polyadenylation specificity factor), Artemis, Snm1, and Pso2 (Aravind, 1999; Callebaut *et al.*, 2002). It had been noticed that the length between the fourth and fifth metallo-β-lactamase motifs could be extremely variable, to the extent that the catalytic histidine of motif 5 could not be convincingly identified in members of the β-CASP group (Aravind, 1999). However, the C-terminal region that encompasses motif 5 comprises a number of conserved sequences specific to this group, and constitutes a distinct globular domain, referred to as the β-CASP motif (Figs. 1.12, 1.13) (Callebaut *et al.*, 2002). Detailed analysis of this motif has resulted in the confirmation that DNA, rather than RNA, is the likely substrate for the *PSO2/SNM1* family, as they have a valine residue in place of the conserved histidine observed in RNA-specific proteins (Callebaut *et al.*, 2002).

In *S. cerevisiae* Pso2 and hSnm1, the C-terminal metallo-β-lactamase/β-CASP domain is preceded by a large N-terminal region, which includes a single putative zinc finger motif. Such motifs are characteristic of proteins that bind to DNA. However, deletion of this zinc finger by targeted mutagenesis established it to be dispensable for repair activity (Henriques *et al.*, 1997). Furthermore, a zinc finger motif has not been detected in other *PSO2* homologues, such as Artemis. In fact, the Artemis protein has a distinct configuration, with the metallo-β-lactamase/β-CASP domain at the N-terminus, followed by a large predominantly non-globular domain that does not share any detectable similarity with other proteins (Callebaut *et al.*, 2002) (Fig. 1.13). Interestingly, an Arabidopsis *SNM1* homologue also contains an additional domain, which is homologous to the eukaryotic DNA ligase I (Callebaut *et al.*, 2002).

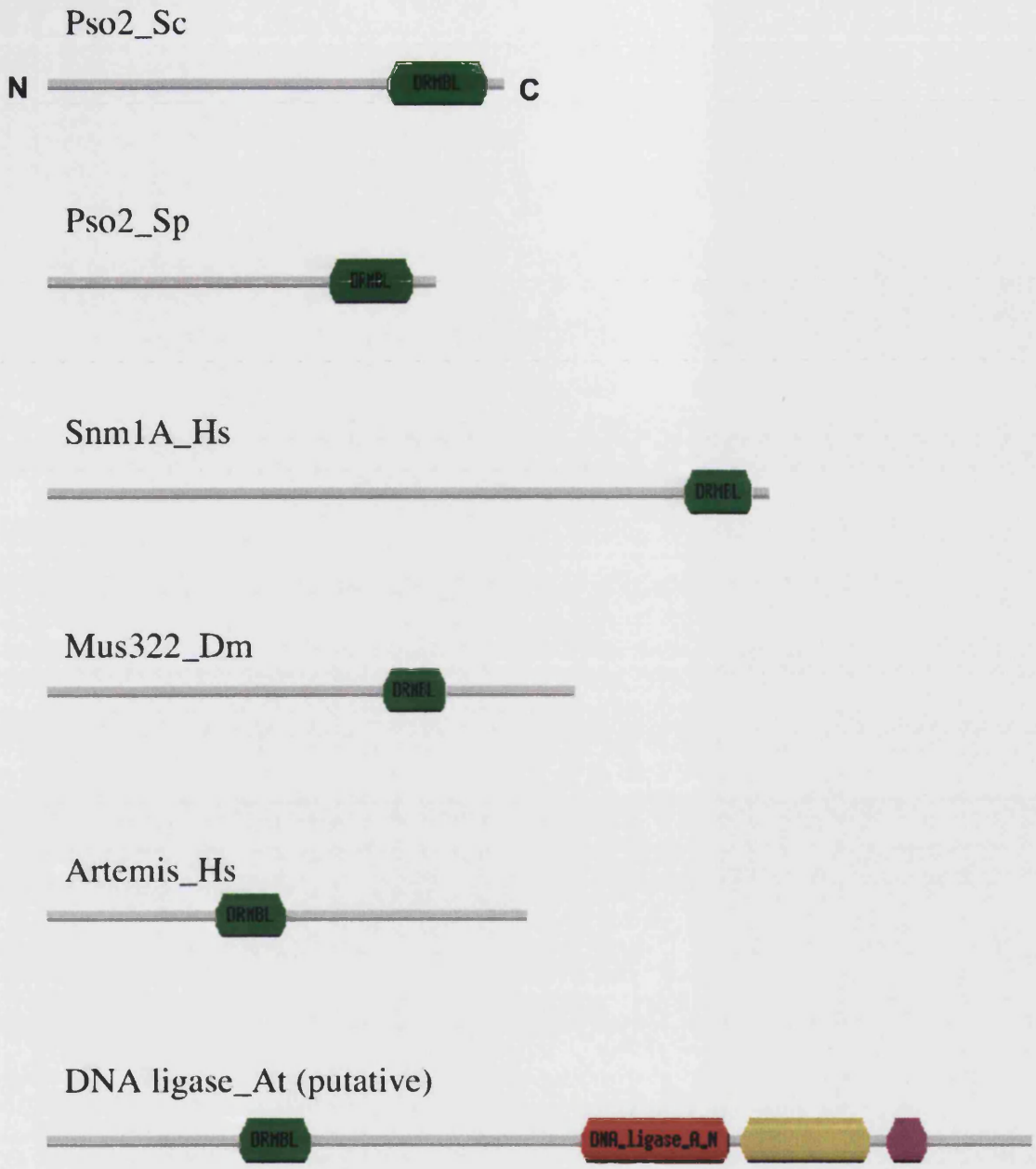

Figure 1.13 Graphical representation of proteins of the β-CASP family (reproduced from the Pfam database, www.sanger.ac.uk/Software/Pfam). The green DRMBL domain represents the metallo-β-lactamase motif 5/β-CASP motif, specific to the metallo-β-lactamase superfamily members predicted to interact with nucleic acids. This simple schematic highlights the broad similarities and differences in protein architecture: the highly conserved Pso2_Sc, Pso2_Sp and Snm1A_Hs all contain the DRMBL domain at the C terminus, whereas the Artemis_Hs DRMBL domain is located more centrally, with an additional non-conserved C-terminal region. Furthermore, the putative DNA ligase_At comprises DRMBL plus additional domains.

1.4.6 Epistasis and functional analysis

Although genetic studies in *S. cerevisiae* have assigned *PSO2* to the *RAD3*/NER epistasis group (Henriques and Moustacchi, 1981; Siede and Brendel, 1982), there are fundamental distinguishing features with respect to ICL repair. Density gradient centrifugation experiments, conducted by Magana-Schwencke *et al.* (1982), clearly demonstrated the formation and repair of single and double-strand DNA breaks in wild-type exponential phase yeast cells exposed to 8-methoxypsoralen photoaddition. In a *rad3* mutant (defective in NER) the incision step was almost completely abrogated, contrasting with *pso2* cells that produced both single and double strand breaks but were unable to subsequently reconstitute dsDNA. Hence *pso2* mutants are proficient in the incision step of ICL repair, but are defective at some downstream processing event. Nevertheless, investigations into the genetic relationships of *PSO2* with other key repair genes have shown no epistasis with the *RAD52*/homologous recombination group (Siede and Brendel, 1982), whilst data regarding the interaction with *RAD6*/PRR is inconsistent (Henriques and Moustacchi, 1981).

1.5 Objectives of this study

Despite more than 20 years of research since its identification from a mutant yeast strain exhibiting a specific sensitivity to DNA interstrand cross-links, little is known about the function of *PSO2*. However, such knowledge could be crucial in further elucidating the intricate eukaryotic system of ICL repair. Furthermore, given the unique specificity for ICLs, human Pso2 may prove to be a suitable target for new strategies in the treatment of cancer. A future prospect might be to develop an agent that could be used in combination with existing anticancer therapeutics, to overcome the acquired resistance that is so frequently observed.

DNA ICLs are complex lesions that require the co-operation of a number of different repair pathways to facilitate their removal. Hence, in addition to the clinical considerations regarding cytotoxicity and potential therapeutic applications, ICLs provide an interesting illustration of the co-ordination of DNA replication and repair processes within the cell. It is hoped that a detailed study of the *PSO2* gene will aid the elucidation of the complete mechanism by which ICLs are repaired. It is anticipated that the initial genetic approaches will clarify the probable role of *PSO2* at an intermediate stage of ICL repair, and hence facilitate a more targeted biochemical characterisation of Pso2 protein function.

CHAPTER 2 MATERIALS AND METHODS

2.1 Chemicals and enzymes

Analytical grade mechlorethamine (nitrogen mustard or HN2), 2-dimethyl-aminoethylchloride hydrochloride (half mustard, HN1), Benomyl, Hydroxyurea, Geneticin/G418 and L-canavanine were purchased from Sigma-Aldrich (Gillingham, UK). Vent DNA polymerase was purchased from New England Biolabs (NEB, Hertfordshire, UK), and Super Taq polymerase from HT Biotechnology (Cambridge, UK). All other enzymes were obtained from Promega (Southampton, UK).

2.2 Media and cell culture conditions

All media was sterilised by autoclaving, with the exception of galactose, which was filter sterilised to prevent isomerisation. Standard sterile techniques were employed.

2.2.1 *Saccharomyces cerevisiae*

Cells were grown on yeast extract-peptone-dextrose (1 %, 1 %, 2 % respectively) YEPD agar plates, or YEPD liquid media supplemented with adenine at 40 mg/l to give YPAD. YPG media consists of yeast extract and peptone, but utilises 3 % v/v glycerol as the carbon source. All media components were purchased from Sigma, with the exception of mycological peptone (Lab M, Lancashire, UK). For analysis of intrachromosomal recombination, identification of gene disruptants, and for plasmid retention, cells were grown on Synthetic Complete (SC) medium (0.67 % yeast nitrogen

base, 0.5 % ammonium sulphate and 2 % glucose) with appropriate amino acids omitted (BIO 101 supplied by Anachem, Luton, UK). Minimal media constituted SC media without amino acids. Induction media for the expression of genes from the *GAL1* promoter was SC medium with 2 % galactose and 1 % raffinose as the combined carbon source in place of glucose. All strains were grown at 28°C.

2.2.1.1 Alpha factor growth arrest

The yeast alpha mating factor was used to synchronise a culture of cells in the G1 phase of the cell cycle. 1 ml exponential phase cells at 2 x 10^7 cells/ml were treated with 10 μg alpha factor (Sigma) in pre-warmed YPAD for 1 h shaking at 28°C, and then a further 10 μg dose for a second 1 h incubation. Cells were sonicated for 30 s (Branson sonifier 250: output control 5, constant duty cycle) and observed microscopically to ensure that the culture had reached a 90 % proportion of shmooed and single cells.

2.2.2 *Schizosaccharomyces pombe*

Strains were maintained on standard YES (0.5 % yeast extract, 3 % glucose, 225 mg/l each of adenine, histidine, leucine, uracil, lysine hydrochloride) agar plates. Liquid cultures were sustained in YES media. All strains were grown at 28°C. Drug sensitivity assays were performed as for *S. cerevisiae* cells, with the exception that exponential phase cultures were sonicated for 1 min (Branson Sonifier 250: output control 5, constant duty cycle) prior to treatment.

2.2.3 *Escherichia coli*

E. coli cells were utilised for the amplification of plasmids. Luria-Bertani (LB) liquid medium consisted of 1x peptone, 0.5 x yeast extract, and 1 x NaCl. LB-agar plates were produced from pre-prepared pellets (Sigma), 10 per 500 ml as per manufacturers instructions. Plates and liquid media were supplemented with 100 mg/l, and 50 mg/l ampicillin (Sigma) respectively, to select for plasmid retention.

2.3 Production of yeast gene disruptants

The novel yeast strains used in this study are described in table 2.1, and were derived from B356-7C (a gift from Professor L. Symington, Columbia University, USA), DBY747 (a gift from Professor W. Xiao, University of Saskatchewan, Canada), or BY4741 (European *Saccharomyces cerevisiae* Archives for Functional Analysis (EUROSCARF) yeast deletion project) by Polymerase Chain Reaction (PCR)-based micro-homology targeted gene deletion (Manivasakam *et al.*, 1995; Longtine *et al.*, 1998; Goldstein and McCusker, 1999). This method entails the production of a DNA cassette bearing a selectable marker gene flanked by short regions of homology to the gene intended for disruption (Fig. 3.1 A). The cassette is transformed into an appropriate yeast strain where it recombines with the terminal regions of homology in the endogenous DNA. Hence any yeast gene, or any specific region of a gene can be permanently disrupted by replacement with the alternative cassette DNA, and modified cells can be readily identified by virtue of the selectable marker.

Table 2.1 ***S. cerevisiae* strains used in this study.**

Strain	Genotype	Source (ref.)
DBY747	*MATa his3-Δ1 leu2-3,-112 trp1-289 ura3-52*	Xiao *et al.*, 1996
WXY9387	*DBY747* with *rad52::LEU2*	Xiao *et al.*, 1996
WXY9382	*DBY747* with *rev3::LEU2*	Xiao *et al.*, 1996
WXY9394	*DBY747* with *rad4::hisG-URA3-hisG*	Xiao *et al.*, 1996
WXY9326	*DBY747* with *rad18::TRP1*	Xiao *et al.*, 1996
LBY1	*DBY747* with *pso2::kanMX4*	This study
LBY2	*DBY747* with *pso2::kanMX4 rad4::hisG-URA3-hisG*	This study
LBY5	*DBY747* with *pso2::kanMX4 rev3::LEU2*	This study
LBY7	*DBY747* with *pso2::kanMX4 rad18::TRP1*	This study
W303-1A	*MAT a his 3-11,15 leu2-3,112 ade2-1 trp1-1 ura3-1 can1-100*	Lab Stock
B356-7C	*W303-1A* with *ade2::hisG his3::ade2-5'Δ -TRP1-ade2-n*	Bai, Symington, 1996
B356-13D	*B356-7C* with *rad51::HIS3*	Bai, Symington, 1996
B356-11C	*B356-7C* with *rad52::TRP1*	Bai, Symington, 1996
LBY9	*B356-7C* with *pso2::kanMX4*	This study
LBY17	*B356-7C* with *rad4::kanMX4*	This study
LBY25	*B356-7C* with *pso2::his3 rad4::kanMX4*	This study
LBY28	*B356-7C* with *pso2::kanMX4 rad51::HIS3*	This study
LBY51	*B356-7C* with *pso2::kanMX4 rad52::HIS3*	This study
LBY13	*B356-7C* with *exo1::kanMX4*	This study
LBY11	*B356-7C* with *pso2::kanMX4 exo1::HIS3*	This study
LBY15	*B356-7C* with *mre11::kanMX4*	This study
LBY12	*B356-7C* with *pso2::kanMX4 mre11::HIS3*	This study
LBY26	*B356-7C* with *rad1::kanMX4*	This study
LBY50	*B356-7C* with *pso2::kanMX4 rad1::HIS3*	This study
LBY45	*B356-7C* with *rad27::HIS3*	This study
LBY47	*B356-7C* with *pso2::kanMX4 rad27::HIS3*	This study
LBY21	*B356-7C* with *rad4::kanMX4 exo1::HIS3*	This study
PJM37	*B356-7C* with *rad4::kanMX4 rad52::HIS3*	This study
LBY48	*B356-7C* with *msh2::kanMX4*	This study
LBY23	*B356-7C* with *pso2::kanMX4 msh2::HIS3*	This study
LBY29	*B356-7C* with *exo1::kanMX4 msh2::HIS3*	This study

Strain	Genotype	Source (ref.)
LBY73	*B356-7C* with *pso2::kanMX4 exo1::HIS3 msh2::URA3*	This study
LBY97	*B356-7C* with *msh3::kanMX4*	This study
LBY101	*B356-7C* with *pso2::kanMX4 msh3::HIS3*	This study
LBY93	*B356-7C* with *msh6::kanMX4*	This study
LBY95	*B356-7C* with *pso2::kanMX4 msh6::HIS3*	This study
LBY103	*B356-7C* with *mlh1::kanMX4*	This study
PJM39	*B356-7C* with *pso2::kanMX4 mlh1::HIS3*	This study
LBY34	LBY9 with pDB20	This study
LBY37	LBY9 with pDB-*EXO1*	This study
LBY109	LBY9 with pYES2	This study
LBY110	LBY9 with pYES-*EXO1*	This study
LBY107	LBY9 with pRS425	This study
LBY108	LBY9 with pRS-*MSH2*	This study
LBY116	LBY9 with pYES2 pRS425	This study
LBY115	LBY9 with pYES-*EXO1* pRS-*MSH2*	This study
LBY64	LBY13 with pYES2	This study
LBY67	LBY11 with pYES2	This study
LBY68	LBY11 with pYES-PSO2	This study
LBY69	LBY11 with pYES-EXO1	This study
LBY84	LBY48 with pYES2	This study
LBY89	LBY23 with pYES2	This study
LBY90	LBY23 with pYES-PSO2	This study
LBY92	LBY23 with pRS-*MSH2*	This study
LBY88	LBY9 with pGAL-c-FLAG-*PSO2*	This study
BY4741	*MAT a his3-1 leu2-0 met15-0 ura3-0*	EUROSCARF
Y06743	*BY4741* with *pso2::kanMX4*	EUROSCARF
Y01809	*BY4741* with *exo1::kanMX4*	EUROSCARF
Y06240	*BY4741* with *msh2::kanMX4*	EUROSCARF
Y01781	*BY4741* with *lig4::kanMX4*	EUROSCARF
LBY74	*BY4741* with *pso2::kanMX4 exo1::HIS3*	This study
LBY78	*BY4741* with *pso2::kanMX4 msh2::HIS3*	This study
LBY87	Y06743 with pGAL-c-FLAG-*PSO2*	This study
JEL1	*MATα leu2 trp1 ura3-52 nprb1-1122 pep4-3ΔHis3::pGAL10-GAL4*	Lindsley, Wang, 1993
LBY117	*JEL1* with pGAL-c-FLAG-*PSO2*	This study

2.3.1 PCR-based production of the disruption cassette

Specific deletion primers bearing 40 bp homology to the gene of interest and 20-25 bp of overlap with the selective marker (adapter sequence) were designed to generate each cassette (Appendix). In all cases, the regions of homology between the primer sequences and the endogenous gene lay at the 5' and 3' ends of the coding sequence, to ensure complete disruption. The F1 and R1 primer adapter sequences were used to amplify from either the KanMX4 or HIS3MX6 cassette templates (a gift from Professor M. Longtine, Universitat Basel, Switzerland) to give kanamycin or histidine selection, respectively. The URA5' and URA3' primer adapter sequences were designed to produce an *URA3*-based cassette from pYES2, providing an additional selective marker for the production of triple-disruptant yeast strains.

Reaction mixes were prepared in a total volume of 100 µl as follows: 100 ng (in 10 µl) of miniprepped plasmid template (prepared as described in Section 2.10.1.5); 1 x thermopol buffer (NEB); 100 mM magnesium sulphate; 2 mM dNTPs (Invitrogen, Paisley, UK); 250 pmol each primer (MWG Biotech., Milton Keynes, UK); and 2 units Vent polymerase. Vent polymerase was specifically used to reduce the incidence of replication errors. The optimised PCR conditions (regardless of gene or selective marker) were: 94°C 4 min; 94°C 1 min, 55°C 1 min, 72°C 2 min + 1 s/cycle, 30 cycles; 72°C 5 min. PCRs were performed on a MJ thermocycler machine.

PCR products were phenol-chloroform extracted and ethanol-precipitated using standard procedures, to provide a clean, concentrated cassette preparation for transformation. Briefly, four identical PCR reactions were combined, and a 1:1 volume of phenol-chloroform was added. This was vortexed, and spun in a microcentrifuge for

5 min at full speed. The upper aqueous layer was carefully transferred to a fresh eppendorf, and mixed with 2 volumes of 99 % ethanol and $^1/_{10}$ volume sodium acetate. This was then incubated on dry ice for 20 min, before centrifuging for 5 min at full speed. The supernatant was poured off, and the pellet was washed in cold 70 % ethanol. After further centrifugation and drying, the DNA pellet was resuspended in 10 µl sterile water. 0.5 µl was run in loading buffer (6 x bromophenol blue loading buffer, Sambrook *et al.*, 1989) on a 1 % agarose gel in 0.5 x Tris-Borate-EDTA (TBE, Sambrook *et al.*, 1989) buffer to confirm the quality of the cassette preparation. Cassettes were stored at – 20°C until required.

2.3.2 Transformation of *S. cerevisiae*

Exponential phase yeast cells were transformed with a single cassette using the BIO 101 Alkali-Cation Yeast Transformation Kit (Anachem), according to manufacturers instructions. Briefly, competent cells were produced from 2 x 10^7 Tris-EDTA (TE, Sambrook *et al.*, 1989) -washed exponential phase cells by incubating in 100 mM lithium acetate for 30 min at 30°C. Cells were then resuspended in TE, and a $^1/_{10}$ (100 µl) aliquot was mixed with 10 µl salmon sperm DNA (sheared and boiled) and 10 µl histidine solution. To this suspension was added the 10 µl preparation of cassette DNA, which was mixed well by pipetting and incubated at room temperature for 15 min. 1 ml of a PEG/cation mix was then added to the transformation reaction, and incubated at 30°C for 10 min. Reactions were heat-shocked in a water bath at 42°C for 10 min, resuspended in warm YEPD, and incubated for 3 h at 28°C to initiate expression of the selectable marker, before plating on selective media. Plates were incubated at 28°C for

3 days. Transformants were identified by resistance to G418/Geneticin (300 mg/l) or the capacity to grow in the absence of histidine or uracil, as appropriate.

2.3.3 Confirmation of gene disruption

Integration of the cassette at the correct locus was confirmed by PCR across the gene using specific gene primers designed to flank the disrupted region, and template DNA derived from a single transformant colony. Two approaches were used, depending on a number of factors, including the number of transformants to be tested and the ease of PCR across the disrupted region (especially with respect to size of the intended PCR product). Either DNA was extracted from cultured transformant cells for use in PCR (Section 2.3.3.1), or PCR was performed directly on cells picked from a single colony (Section 2.3.3.2). In most cases, the size of the PCR product could distinguish between disrupted genes and false positive transformants (a higher frequency was observed when using the histidine and uracil-based cassettes as regions of homology remained in the disrupted endogenous *HIS3* and *URA3* genes). However, further verification of the gene disruption was always obtained from restriction enzyme digests performed on the PCR product. Two restriction enzymes were chosen per gene that would each yield a characteristic array of fragments to distinguish between the normal and disrupted genes, as visualised by agarose gel electrophoresis. Restriction digests were performed directly on 10 µl of the PCR reaction in a total volume of 20 µl, for 1 h in a 37°C hotblock, and the entire reaction was subsequently run on a 1 % agarose gel in 0.5 x TBE buffer.

2.3.3.1 Isolation of yeast genomic DNA

Genomic DNA was isolated from exponential phase cells using the Nucleon Yeast DNA Mini-prep kit (Tepnel Life Sciences, Manchester, UK) but with a modified protocol. Briefly, 2 ml of an overnight culture were pelleted by centrifugation for 5 min at 2000 rpm, and resuspended in 540 µl solution A plus 60 µl solution B (Mini-prep kit). This cell suspension was vortexed for 30 s and incubated in a 70°C heat block for 20 min. A 1:1 volume of phenol-chloroform was then added instead of solution C, as this was found to result in an improved DNA yield. Samples were vortexed and spun for 5 min at full speed in a microcentrifuge. The upper aqueous layer was transferred by Gilson pipette to a fresh tube, and an equal volume of isopropanol was added. Samples were mixed by inversion and spun for a further 5 min. The supernatant was poured off, taking care not to dislodge the fragile pellet, which was then washed with 100 µl cold 70 % ethanol. Pellets were dried at 70°C and resuspended in 100 µl sterile water. Subsequent PCR reactions to check the disrupted gene were in a total volume of 30 µl as follows: 2 µl DNA preparation; 1 x Super Taq buffer (HT Biotech.); 2 mM dNTPs; 250 pmol each primer (MWG); and 2 units Super Taq polymerase. The PCR conditions were optimised to each gene, but in general resembled the following: 94°C 4 min; 94°C 1 min, 42-58°C (depending on primer specificity) 1 min, 72°C 2-10 min (depending on product size), 35 cycles; 72°C 5 min. PCRs were performed on a MJ thermocycler machine.

2.3.3.2 Yeast Colony PCR

A master mix for the total number of PCR reactions was prepared according to the following ratios, in order to give final reaction volumes of 30 µl: 1 x Super Taq buffer; 2 mM dNTPs; 250 pmol each primer (MWG); sterile water as appropriate. A small

quantity (equivalent in volume to 0.5 µl water) of a single transformant colony was transferred to a sterile PCR tube using a Gilsen pipette tip. Tubes were microwaved at full power for 90 s, and immediately placed on ice. The PCR reaction mix was added to each tube, and vortexed briefly. Super Taq polymerase (2 units) was added to each reaction after a hot start. PCR conditions were as described in Section 2.3.3.1.

2.4 Analysis of growth rate and cell cycle phase

Exponential phase cells were used to inoculate a fresh YPAD culture at 2 x 10^6 cells/ml, and 1 ml samples were taken at hour intervals for 10 h. A sample was also taken at 0 h (point of inoculation). Spectrophotometer analysis of absorption at 600 nm was performed immediately for each sample, diluting in media where appropriate to ensure readings were in the linear range, and using 1 ml YPAD for the zero reading. Results were normalised to the 0 h timepoint for each strain.

To investigate the proportion of cells in different stages of the cell cycle, cells were observed by light microscopy at 40 x objective, and counted using a haemocytometer slide. Populations were classified as either single unbudded cells (G1), small budded (S phase), or large budded (M phase), where the bud size constituted more than half of the volume of the mother cell.

2.5 Colony-based survival assays

In this study, colony-based survival assays were the routine approach for testing yeast sensitivity to various DNA damaging agents. This is a quantitative method, whereby

treated cells are grown on agar plates to yield countable colonies. Each colony therefore represents one cell that was able to withstand treatment at the tested dose. Results are expressed as percentages of the number of colonies arising from an untreated control, to enable comparison between different strains and experiments.

In all cases, liquid YPAD medium was inoculated with a single colony picked from a freshly streaked YEPD stock plate, and grown overnight at 28°C with vigorous shaking. Cultures were counted microscopically and only those in mid-exponential phase (2–5 x 10^7 cells/ml) were used.

2.5.1 Nitrogen mustard treatment

Exponential cells were resuspended in phosphate-buffered saline (PBS) at a density of 2 x 10^7 cells/ml. 2 ml aliquots were treated with 0, 1, 10, 100, or 1000 μM doses of HN2 (freshly dissolved in cold sterile water, and serially diluted to give appropriate stock solutions) for 60 min shaking at 28°C. The cells were harvested, washed twice with PBS, and plated onto YEPD in duplicate at appropriate dilutions giving rise to 200 colonies per plate in untreated controls. Plates were incubated at 28°C for 3 days, and then scored. Any experiments giving rise to more than 250 colonies per plate in untreated controls were discarded.

2.5.2 X-irradiation

Exponential cells were resuspended in sterile water at 2 x 10^5 cells/ml. 250 μl aliquots were exposed in microcentrifuge tubes to X-irradiation at a dose rate of 2.5 Gy/min (General Electric Corporation X-ray source). All treatments were performed on ice to

minimise repair activity. Exposure times were as follows: 0, 20, 40, 80, and 120 min (giving doses of 0, 50, 100, 200, and 300 Gy). Samples were plated in duplicate at appropriate dilutions to give rise to 200 colonies in untreated controls. Plates were incubated at 28°C for 3 days and then scored.

2.5.3 UVC

Exponential phase cells were serially diluted in sterile water to a final concentration of 2 x 10^3 cells/ml. 100 µl (~ 200 cells) of this suspension was plated onto 12 YEPD plates, to allow for 6 doses in duplicate. The UVC lamp used had been calibrated to emit radiation at a rate of 0.5 J/m^2/s when positioned at a height of 280 mm. A plate outline was made at the epicentre of the light falling on the surface below, to ensure that all treatments were irradiated equally. All normal light sources in the vicinity of the hood used for UVC exposure were switched off for the duration of the treatments. Plates (with the lid removed) were then individually exposed to UVC, and immediately placed in a dark incubator following treatment. Exposure times were as follows: 0, 10, 20, 50, 100, 200 s (giving doses of 0, 5, 10, 25, 50, and 100 J/m^2). Plates were incubated at 28°C for 3 days and then scored.

2.5.4 Colony spotting assay

For the qualitative screening of drug sensitivities, a colony spotting assay was employed. Exponential cells were resuspended in sterile water at a concentration of 5 x 10^7 cells/ml, and diluted in a ten-fold series to 500 cells/ml. 10 µl of each of the last four dilutions of the series were spotted onto square YEPD plates, using a grid layout: each line comprising a series of 'spots' of one strain, containing sequentially 5000, 500,

50, and 5 cells. Typically, 4 or 5 strains were spotted on any one plate, and plates were spotted in duplicate. Plates were incubated at 28°C for 3 days and then photographed.

Benomyl and hydroxyurea treatments were performed as above, using freshly prepared YEPD plates containing the drug. Drug doses were added in 2 ml aliquots per 200 ml media (4 plates), after autoclaving, and only once the media had cooled to 40-50°C. Benomyl was prepared in DMSO, and appropriate dilutions made to give final plate concentrations of 0, 10, 25, 50, and 100 μg/ml. DMSO was also added to YEPD plates in the same ratio (2ml per 200 ml), as a control for toxicity. Hydroxyurea (HU) was initially resuspended in sterile water, and appropriate dilutions were made to give final plate concentrations of 0, 2.5, 5, 10, 20 and 40 mM HU.

Colony spotting assays for the evaluation of sensitivity to 2-dimethyl-aminoethylchloride hydrochloride (half mustard, HN1) were performed slightly differently in that cells were treated in suspension, prior to serial dilution and spotting. Exponential phase cells were resuspended in PBS at a concentration of 2 x 10^7 cells/ml. 2 ml aliquots were treated with 0, 10, 100, 1000, or 10000 μM doses of HN1 (freshly dissolved in cold sterile water, and serially diluted to give appropriate stock solutions) for 60 min shaking at 28°C. The cells were harvested, washed twice with PBS, and then serially diluted for spotting onto YEPD plates as described above.

2.6 Analysis of mutagenesis

The yeast *CAN1* gene encodes arginine permease, a selective protein channel responsible for the transportation of both arginine and its toxic analogue canavanine,

into the cell. Canavanine resistance therefore corresponds with mutations in *CAN1* that abrogate protein function, hence providing a strong phenotypic selection for forward mutation. The incidence of forward mutations is a preferable approach to determining rates of mutation, as unlike systems based on specific reversion mutations, the measured phenotype can arise from a range of different types of mutation (e.g. frameshift, missense, deletion, insertion), and cannot be influenced by suppressor mutations in other genes. The *CAN1* system can reveal a wide spectrum of mutations that has proved useful in characterising deficiencies in both DNA replication and repair (Tishkoff *et al.*, 1997; Chen and Kolodner, 1999).

2.6.1 Spontaneous mutagenesis

Single yeast colonies were resuspended in sterile water at a concentration of 2×10^7 cells/ml. 100 µl was plated in duplicate on SC-arginine plates containing 60 mg/l L-canavanine (Sigma, added after autoclaving once media had cooled to ~50°C). Serial dilutions of the cell suspension were made to enable 200 cells to be plated on YEPD as controls for plating efficiency and to determine more accurately the number of cells in the original suspension. Plates were incubated at 28°C for 3 days and then scored. The rate of mutation was calculated as follows:

$$\frac{\text{mean arg-can colonies}}{(\text{mean YEPD colonies}) \times 10^4} \times 10^8 = \text{mutants}/10^8 \text{ survivors}$$

2.6.2 HN2-Induced mutagenesis

Exponential phase cells were treated with 0, 1, 10, 100, and 1000 μM doses of HN2 for 1 h as described in Section 2.5.1. Cells were washed with PBS, and serially diluted in order to plate 2 x 10^6 cells on SC-arg plus canavanine, and 200 cells on YEPD. All plates were made in duplicate, and incubated for 3 days at 28°C before scoring. Calculations were performed for each dose as described in 2.6.1, to give the mutation rate per 10^8 survivors at a specific HN2 dose.

2.6.3 PCR-based analysis of mutagenesis

The PCR-based screen for large insertion-deletion alterations in the *CAN1* gene was based that of Xie and co-workers (2001). Briefly, colony PCR (Section 2.3.3.2) was performed on 18 independent Can^R colonies per strain, which had been obtained by growth on SC-arg plus canavanine plates. The complete open reading frame of the *CAN1* gene (coordinates 50 to 1925 of the X03784 Genbank sequence) was amplified using the following primers: *CAN1-5'* 5'-GTT CTT CAG ACT TCT TAA CTC CTG-3', and CAN1-3' 5'-GAG AAT GCG AAA TGG CGT GG-3'. The optimised PCR conditions were: 94°C 4 min; 94°C 1 min, 54°C 1 min, 72°C 2.5 min, 35 cycles; 72°C 5 min. The PCR products were subsequently digested with 2.5 units *Hph* I for 2 h at 37°C, and visualised on a 2 % agarose gel. The full length *CAN1* gene, in the absence of large insertion-deletion mutations, yields the following characteristic set of *Hph* I digest fragments: 207, 249, 252, 271, 411, and 480 bp.

2.7 CHEF analysis of DSB repair

Pulsed-field gel electrophoresis (PFGE) was developed to facilitate the separation of larger DNA molecules than is possible by simple agarose electrophoresis. In PFGE, the direction of the electric field is altered at regular intervals, forcing DNA to reorient in the new field direction. Due to the resistance of the agarose matrix, smaller molecules are able to reorient more quickly than larger ones. Contour-clamped homogeneous field electrophoresis (CHEF) is one variation of PFGE in which the direction of the electrical field is changed electronically by altering the polarity of the electrode array (Chu and Gunderson, 1991). The practice of embedding cells in agarose plugs before enzymatic digestion to release the DNA is particularly appropriate for the study of DSB induction and repair, as it significantly reduces the incidence of background strand breaks arising from the handling of DNA. CHEF has been widely used in the study of DSBs, both in yeast and mammalian cells (Averbeck and Dardalhon, 1990; Averbeck *et al.*, 1992; Dardalhon and Averbeck, 1995; De Silva *et al.*, 2000).

2.7.1 HN2-induced DSBs

Cells were grown to exponential phase in YPAD, harvested, and resuspended in 20 ml PBS at a density of 2 x 10^7 cells/ml. This was split into two aliquots: 15 ml was treated with a dose of 50 or 100 μM HN2, and to the remaining 5 ml an equivalent volume of water was added as an untreated control. Cells were incubated at 28°C for 3 h with vigorous shaking, harvested, and resuspended in an equal volume of minimal media (MM). 5 ml samples were removed at 2, 4, and 24 h post-treatment at 28°C. The untreated control was incubated for 24 h. CHEF plugs were prepared from 3 x 10^7 cells for each sample using the Bio-Rad (Hemel Hempstead, UK) yeast CHEF genomic DNA

plug kit as instructed by the manufacturer. Briefly, cells were embedded in an agarose plug and sequentially treated with lyticase for 1 h at 37°C, and proteinase K overnight at 50°C. Plugs were washed thoroughly, and used whole. CHEF was performed with a 1% agarose gel (Biorad, pulse field certified) in 0.25 x TBE buffer using a Biometra Rotaphor type V apparatus, run for 24 h at 14°C under the following parameters: interval 100-10 s, log scale; angle 120-110°, linear scale; voltage 200-150 V, log scale. On completion, gels were stained with 2 μg/ml ethidium bromide for 30 min, destained for 1 h in distilled water, and photographed on a UV illuminator.

2.7.2 Irradiated cells

Exponential phase cells were exposed to 200 Gy X-rays (General Electric Corporation X-ray source, 2.5 Gy/min) in 4 x 1 ml aliquots of 6 x 10^7 cells/ml, on ice. After treatment, 3 of the aliquots were each resuspended in 3 ml MM and incubated, shaking at 28°C for 2, 4, and 24 h. The fourth treated aliquot was immediately washed in PBS, and maintained at 4°C as a cell pellet. An untreated aliquot of cells was also incubated in MM for 24 h as a control.

Exponential phase cells were exposed to 200 Gy γ-irradiation (^{60}Co source, 9.1 Gy/min) in 4 x 4 ml aliquots of 1.5 x 10^7 cells/ml, and immediately placed on ice. Aliquots were subsequently resuspended in MM for repair timepoints, as described above for X-irradiation.

The same procedure described in Section 2.7.1 was followed for the preparation of agarose plugs and subsequent CHEF analysis of X- and γ-irradiated cells.

2.7.3 Quantification of results

Two approaches were used in an attempt to quantify the extent of DSB induction and repair, as illustrated by CHEF analysis. Semi-quantitative analysis of the DNA bands revealed by UV-illumination of the ethidium bromide-stained gel was performed with the computer software Gel Pro Analyser (Media Cybergenetics). However, in contrast to the straightforward use of this software to quantify mammalian DSBs, where only broken chromosomes are released from the agarose plug, it was difficult to accurately distinguish between the intact yeast chromosome bands, and the smear of degraded DNA. The second approach involved Southern blotting of the CHEF agarose gel.

2.7.3.1 Gel Pro Analyser

The Gel Pro Analyser software has been used successfully to quantify CHEF gels of mammalian DSB samples. However, under the parameters used for mammalian CHEF only broken DNA is released from the plug, whereas yeast CHEF also produces a characteristic ladder of bands representing the intact chromosomes. This complicates the use of this software, which can be used to measure the optical density (OD) of any highlighted band on the gel image. Obviously, yeast DSBs cannot be quantified as percentage release from the plug if intact chromosomes are sufficiently small to migrate through the agarose gel. It is relatively easy to measure the intensity of the largest chromosome bands, but the smaller chromosomes overlap with the smear of degraded DNA, making it almost impossible to determine whether the ethidium bromide has intercalated with intact or broken DNA molecules. The approach used here was to measure the OD of the largest chromosome bands, and express each as a fraction (q) of the same chromosome band in the untreated control sample. This provides a

comparison of the number of intact chromosomes at different repair timepoints. It is only semi-quantitative as it assumes equal loading between the different plug samples, (which in practice is unlikely to be absolute). The number of DSBs (n) within a defined region can be determined by: $n = -\ln(q)$ (Geigl and Eckardt-Schupp, 1990). Using the Poisson distribution, the probability of at least one DSB occurring within that defined region can be calculated as $P = 1 - e^{-n}$.

2.7.3.2 Southern blotting

Southern blots were carried out according to standard protocols (Sambrook *et al.*, 1989; Hybond Protocol, Amersham Biosciences, Buckinghamshire, UK):

2.7.3.2.1 Preparation of probes

Primers were designed to produce two different probes to target a small and a large yeast chromosome, respectively: a 950 bp probe at the MATα locus on chromosome III, and a 1 kb probe at the *PHO80* gene on chromosome XV. Probe-specific template DNA was first prepared by PCR using the following reaction mix in a total volume of 100 µl: 2 µl yeast genomic DNA preparation (Section 2.3.3.1); 1 x thermopol buffer; 100 mM magnesium sulphate; 2 mM dNTPs; 250 pmol each primer, MATαtop/bottom or PHO80CHK5'/3', as appropriate (MWG); and 2 units Vent polymerase. The optimised PCR conditions (for either primer pair) were: 94°C 4 min; 94°C 1 min, 53°C 1 min, 72°C 4 min, 35 cycles; 72°C 5 min. PCRs were performed on a MJ thermocycler machine. PCR products were purified on a Qiaquick column (Qiagen), according to the manufacturers instructions, and eluted in 50 µl sterile water. Agarose

gel electrophoresis was performed on 5 µl each eluate to check the quality of the PCR products.

Radioactively-labelled probes were prepared from the above templates in a 50 µl reaction volume as follows: $^{1}/_{10}$ DNA eluate; 50 pmol primer, MATαtop or PHO80CHK5', as appropriate; 1 x Super Taq buffer (HT Biotech.); 2 mM dATP/dTTP/dGTP dinucleotide mix; 2 units Super Taq; 50 µCi ^{32}P dCTP (used with appropriate radioactivity precautions). The optimised PCR conditions (for either primer) were: 94°C 4 min; 94°C 1 min, 53°C 1 min, 72°C 1 min + 1 s/cycle, 35 cycles; 72°C 5 min. The radioactive probe was isolated using a Probe Quant G-50 microcolumn (Amersham) according to the manufacturers instructions, and stored at 4°C if necessary. Immediately before use, probes were denatured at 100°C for 5 min, and held on ice for 2 min.

2.7.3.2.2 Southern blotting of CHEF agarose gel

After a photograph had been taken, excess gel was removed to leave a minimal border around the DNA bands, taking care to limit UV exposure to prevent the induction of further DNA strand breaks. The trimmed gel was depurinated in 0.125 M HCl for 10 min, to aid the transfer of large (> 10 kb) DNA fragments, and then equilibrated in 0.4 M NaOH for 15 min. The blot apparatus was set up as follows: i) a glass plate was suspended over a tray containing 0.4 M NaOH; ii) a filter paper wick was soaked in 0.4 M NaOH and laid across the glass plate, with both ends immersed in the buffer below; iii) the equilibrated gel was laid on top of the filter paper; iv) a piece of Hybond membrane, cut exactly to the size of the gel, was laid over the gel and gently rolled with a sterile pipette to ensure absence of trapped air bubbles; v) saran wrap was carefully

laid around the edges of the membrane (creating a 5 mm border) and over the tray of buffer, to help prevent a short circuit from the upper filter paper coming into contact with either the wick or buffer; vi) 3 sheets of filter paper cut exactly to the size of the gel (to prevent a short circuit), and briefly wetted in 0.4 M NaOH, were overlaid on the membrane; vii) a tall stack of paper towels, cut exactly to the size of the gel, were placed on top; viii) finally, a weight was placed at the top to facilitate absorption through the stack. The blot was left at room temperature overnight. After blotting, the membrane was washed briefly in 2 x SSC (1 M sorbitol, 0.1 M sodium citrate, 10 mM EDTA, pH 7.5).

2.7.3.2.3 Hybridisation

Hybridisation was carried out in a specialised oven (Techne Hybridiser HB-1D), with a rotating cylinder. The membrane was pre-hybridised for 1 h at 65°C in a solution of 5 x SSPE (3 M sodium chloride, 0.2 M sodium phosphate, 20 mM EDTA, pH 7.0), 5 x Denhardts solution, and 0.5 % w/v SDS, containing 20 μg/ml salmon sperm DNA. The denatured probe was then added, and the hybridisation reaction was allowed to proceed overnight at 65°C. The membrane was washed with sequential buffers increasing in stringency as necessary, starting with 2 x SSPE, 0.1 % SDS at room temperature for 10 min, up to 0.1 x SSPE, 0.1 % SDS at 65°C. Once the membrane count had been reduced to about 80 cpm, the membrane was rinsed in 0.2 x SSC at room temperature, wrapped in Saran, and exposed to photographic film.

2.8 Recombination at an *ADE2* inverted repeat construct

The B356-7C yeast strain was engineered to contain an integrated (*HIS3* locus, chrom. XV) intrachromosomal inverted duplication of the *ade2* gene separated by the *TRP1* gene (Fig. 4.9 A), as a substrate for the analysis of mitotic recombination events (Rattray and Symington, 1994). Both *ade2* alleles are non-functional: one has a deletion of the 5' coding region and upstream DNA extending beyond the region of homology, and the other full-length allele bears a 3' frame-shift mutation at an *Nde* I site. The frequency of intrachromosomal recombination can be quantified by measuring reversion to *ADE*$^+$ prototrophy, in terms of the proportion of a population arising from a single cell that is able to grow in the absence of adenine. In addition, the nature of the recombination event (gene conversion and/or crossover) can be established through physical analysis of the *ADE2* construct orientation in a single prototroph.

2.8.1 Determination of spontaneous mitotic recombination frequency

Single pink colonies were picked from strains grown on YEPD for 3 days at 28°C (growth for longer gives artificially high recombination rates as Ade$^+$ cells continue to divide for longer than Ade$^-$ cells) and resuspended in 1 ml water. 200 cells were plated in duplicate on SC-trp medium to determine total cell number. Appropriate dilutions (typically 2 x 10^4 – 2 x 10^7 cells/ml) were plated in duplicate on SC-ade in order to determine the number of Ade$^+$ prototrophs. Plates were incubated for 3 days at 28°C and then scored. Mean mitotic recombination frequencies were determined from the ratio of Ade$^+$ prototrophs to the total cell number:

$$\frac{0.4343 \times (\text{ADE+ cells} / (\text{TRP+ cells} \times 100))}{\ln(N - N_0)}$$

where: N = TRP+ cells in colony

$N_0 = 1$

2.8.2 Analysis of HN2-induced mitotic recombination frequency

Single pink colonies were picked from strains grown on YEPD for 3 days at 28°C and resuspended in 1 ml water. 200 cells were plated in duplicate on SC-trp medium to determine total cell number and 2 x 10^4 cells on SC-ade to calculate the number of Ade^+ prototrophs in the inoculate. 25ml YPAD was inoculated with 2 x 10^6 cells, and grown overnight at 28°C with vigorous shaking. Cells were grown to mid-exponential phase, then resuspended at 2 x 10^7 cells/ml. 2 ml aliquots were treated with 0, 1, 10, 100, 1000 μM HN2 (freshly dissolved in cold sterile water) for 60 min at 28°C with vigorous shaking. The cells were harvested, washed twice with PBS and plated in duplicate at appropriate dilutions to determine total cell number (200 cells on SC-trp) and the number of Ade^+ prototrophs (2 x 10^4 -2 x 10^7 cells on SC-ade). Plates were incubated for 3 days at 28°C and then scored. Mean mitotic recombination frequencies were determined according to the formula:

$$\frac{0.4343 \times (\text{ADE+ cells} / (\text{TRP+ cells} \times 100))}{\ln(N - N_0)}$$

where: N = TRP+ cells in end culture

N_0 = TRP+ cells in inoculum

2.8.3 PCR-based analysis of recombination events

Investigation of the nature of the recombination events (cross-over, gene conversion, or both; Fig. 4.10 A) can be achieved through physical analysis of the *ADE2* construct, originally performed using Southern blot (Rattray and Symington, 1994). A novel PCR-based method is presented here, which allows the differentiation between the Class I, II, and III recombination events. This PCR-based protocol utilises the residual fragments of vector sequence arising from molecular cloning within the *ADE2* construct to provide unique primer sites (Rattray and Symington, 1994, and refs therein). The *ADE2* alleles are flanked on the outside by DNA from the pBluescript II KS(-) plasmid, containing the recognition sequences for the T7 and T3 standard primers, upstream of the *ade2-n* and *ade2-5'Δ* alleles, respectively (Fig. 4.10 B). A short region of the pBluescript II KS(-) multiple cloning site sequence remains between the *ade2-5'Δ* and *TRP1* genes, to which a novel primer, *int*, has been designed: 5'-GAT CTC GAA TTC CTG CAG CC-3'. PCR analysis of DNA extracted from single *ADE+* prototrophs was carried out using all 3 primers in the same reaction (in a total volume of 30 µl): 2 µl DNA preparation (Section 2.3.3.1); 1 x Super Taq buffer (HT Biotech.); 2 mM dNTPs (Invitrogen); 250 pmol each primer (MWG); and 2 units 'MOJO' polymerase (a blend of Super Taq (HT Biotech.) and Pfu (Promega) polymerases, optimised for long PCR products by Dr. F. Ghadessy, personal communication). In the original orientation of the *ADE2* construct, this *int* primer will only generate a DNA fragment with the T7 primer (Class I), whereas an inversion of the intervening DNA results in a product from the *int* and T3 primer pair (Class II and III). The conditions of the PCR reaction were optimised to exclude the longer T7-T3 product: 94°C 4 min; 94°C 1 min, 54°C 1 min, 72°C 10 min, 40 cycles; 72°C 5 min. Subsequent digestion of the PCR product with 20 units *Nde* I for 2 h at 37°C identifies colonies that have undergone gene conversion (and

hence restored the *Nde* I frameshift mutation). The entire digested PCR reaction was then visualised by ethidium bromide-agarose gel electrophoresis. The expected DNA fragment patterns were as follows: Class I, 2.1, 1.7 kb; Class II, 3.6 and 2.1 kb; Class III, 2.1, 1.2, and 1.0 kb.

2.9 NHEJ assay

The plasmid-based system used to investigate the efficiency of yeast NHEJ is based on the one developed by Professor S. Jackson using the plasmid pBTM116, which has been central to the discovery of many of the key factors involved in NHEJ (Boulton and Jackson, 1996). However, due to the restriction of available selectable markers an alternative plasmid, YEplac181 (*LEU2*-based), was utilised. This plasmid was chosen for its unique restriction sites, which enabled use of the same endonucleases to generate strand breaks as in the Jackson assay. Linearised plasmids can be used to detect the capacity of different yeast strains for NHEJ, as they can only be propagated in yeast if it is re-circularised – i.e. the DSB is repaired. Hence the number of colonies recovered on selective media corresponds with the proportion of plasmids that have been repaired. The assay can be conducted using restriction enzymes with different modes of action to investigate the repair of a variety of DSB termini. In this investigation, the repair of DSBs bearing 5' overhangs (*EcoR* I), 3' overhangs (*Pst* I), and incompatible ends (*EcoR* I and *Pst* I double digestion) were determined.

Miniprepped YEplac181 (prepared as described in Section 2.10.1.5) was digested with 1 unit restriction endonuclease per μg DNA (with appropriate buffer according to manufacturers instructions) in a 37°C hotblock for 24 h to ensure complete digestion.

Enzymes were then heat inactivated by incubating at 65°C for 20 min. 1 µl of each digest was checked for the absence of intact plasmid on a 1 % agarose gel in 0.5 x TBE buffer. 5 µg digested plasmid was used to transform 5 x 10^7 yeast cells, using the BIO 101 Alkali-Cation Yeast Transformation Kit (Anachem) as described for cassette DNA in Section 2.3.2, with the exception that cells were only incubated in YPAD for 1 h following heat shock. A control transformation was performed simultaneously using 5 µg supercoiled plasmid. Transformants were plated on SC-leu media, incubated for 3 days at 28°C and then scored. The NHEJ efficiency for each type of DSB was calculated as the number of transformants obtained using cut plasmid as a percentage of the control transformation.

2.10 Plasmids and Complementation Analysis

A number of different yeast expression vectors have been used in the course of this study. The *ADH1* promoter-based, *URA3* selective yeast expression vector pDB20 was used to provide high-level constitutive expression (Becker *et al.*, 1991; Ammerer, 1983). PDB-ScE (a gift from Professor B. Shen, City of Hope National Medical Center, California, USA) has an insertion of *S. cerevisiae EXO1* at the *Hind* III site of pDB20, and has been used successfully to complement yeast *exo1* and *rad27* mutants (Qiu *et al.*, 1999). To investigate overexpression in an inducible system, the *S. cerevisiae* genes *PSO2* and *EXO1* were cloned into the *GAL1* promoter-based, *URA3* selective yeast expression vector pYES2 (Invitrogen, Paisley, UK). The *GAL1-MSH2* expression vectors pEAE127 (*LEU2* based pRSY25 vector) and pAC12 (*URA3* based Yep195 vector) were obtained from Professor E. Alani (Cornell University, USA) (Sokolsky and Alani, 2000) and Professor T. Kunkel (National Institute of Environmental Health

Sciences, USA) (Clark *et al.*, 1999), respectively. The galactose-inducible *GAL1* promoter provides a simple system for the overexpression of tightly regulated cellular proteins, such as nucleases, as it allows transient increases in transcription from the plasmid-based gene upon a change in the media carbon source from glucose (which represses the *GAL1* promoter) to galactose.

Plasmids (1 μg of a miniprep, Section 2.10.1.5) were transformed into the appropriate yeast strain using the BIO 101 Alkali-Cation Yeast Transformation Kit (Anachem) as described for cassette DNA in Section 2.3.2, and selection was maintained using SC-ura or SC-leu media as appropriate.

2.10.1 Cloning of *PSO2* and *EXO1* into pYES2

The complete open reading frames (ORFs) of *S. cerevisiae PSO2* and *EXO1* were introduced into the yeast expression vector pYES2 using standard molecular cloning procedures (Sambrook *et al.*, 1989).

2.10.1.1 Gene amplification

Primers were designed to amplify the complete ORF from upstream of the 5' ATG to downstream of the 3' termination sequence: *PSO2* 131-2308 bp, *EXO1* 158-2720 bp (coordinates as per Genbank entries X64004 and U86134 respectively). The 5' end of the primers were modified with unique restriction sites to facilitate orientation-specific cloning into pYES, and 10 bp of random sequence was incorporated at the termini to aid enzyme recognition and cleavage (Table 2.2).

PCR reaction mixes were prepared in a total volume of 100 µl as follows: 2 µl yeast genomic DNA preparation (Section 2.3.3.1); 1 x thermopol buffer; 100 mM magnesium sulphate; 2 mM dNTPs; 250 pmol each primer (MWG); and 2 units Vent polymerase. Vent polymerase was utilised as its proofreading capacity would reduce the likelihood of incorporating a mutated form of the gene into the plasmid. The optimised PCR conditions (for both *PSO2* and *EXO1*) were: 94°C 4 min; 94°C 1 min, 55°C 1 min, 72°C 2 min, 35 cycles; 72°C 5 min. PCRs were performed on a MJ thermocycler machine. Products were phenol-chloroform extracted and ethanol precipitated as already described (Section 2.3.1). DNA pellets were resuspended in 18 µl sterile water, and 2 µl was electrophoresed on a 1 % agarose gel in 0.5 x TBE buffer to confirm that a clean, single fragment had been obtained from the PCR.

Table 2.2 **Primers used in the cloning of *PSO2* and *EXO1*.** Random bp are shown in black, restriction sites are in red upper case, and gene-specific sequences are in blue. RE denotes the restriction enzyme.

Primer	Sequence (5'-3')	RE
PSO2-O/E-5'	gct act gat cGG ATC Cac ctg cgt caa aac tca tgt	*BamH* I
PSO2-O/E-3'	gca ctt cga cGC GGC CGC gga ctc tga gta taa tac gat at	*Not* I
EXO1-O/E-5'	gct act gat cAA GCT Tgt tga cta cta cga gct ata cga	*Hind* III
EXO1-O/E-3'	gca ctt cga cGC GGC CGC aat tct tgt ctt gag gca tt	*Not* I

2.10.1.2 Restriction enzyme-based cloning of gene into pYES2

Double restriction digests (*PSO2*: *BamH* I, *Not* I; *EXO1*: *Hind* III, *Not* I) were performed for 2 h at 37°C on the remaining 16 µl of PCR product (as above) in a total reaction volume of 20 µl, using the appropriate buffer as recommended by the

manufacturer. Corresponding double restriction digests were performed on 2 µl of a pYES2 miniprep (prepared as described in Section 2.10.1.5). The digests were subsequently run on a 1 % agarose gel (0.5 x TBE) and the digested fragments were gel-extracted using the Qiaquick gel extraction kit (Qiagen), according to the manufacturers instructions. Bands were cut from the ethidium bromide-stained gel using a dark reader transilluminator (Clare Chemical Research Inc., Dolores, USA) to prevent incorporation of UV-induced mutations. The DNA was eluted in 30 µl EB, and 2 µl was checked on a 1 % agarose gel in order to determine the relative yields of gene:vector. Ligation reactions were performed with a 3:2 ratio of gene:vector (as the vector is considerably longer than the gene insert), 1 x T4 ligase buffer, and 400 units T4 DNA ligase (NEB), in a final volume of 20 µl for 20 min at room temperature.

2.10.1.3 Transformation of E. coli

A 50 µl aliquot of XL10-Gold ultracompetent *E. coli* cells (Stratagene, California, USA) was used per plasmid transformation. Cells were slowly thawed on ice and treated with β-mercaptoethanol, according to the manufacturers instructions. 5 µl of the ligation reaction (Section 2.10.1.2) was added, and mixed thoroughly by pipetting. The transformation mix was incubated on ice for 30 min, heat-shocked at 42°C for 30 s, and returned to ice for a further 2 min. 1 ml warm LB was then added, and the cells were incubated at 37°C for 1 hour. Subsequently, the cells were pelleted by pulsing in a microcentrifuge, and resuspended in 200 µl LB. A tenth of the transformant mix (20 µl) was plated on one LB-amp plate, and the remainder (180 µl) on another. Plated were incubated at 37°C overnight.

2.10.1.4 Confirmation of gene cloning into pYES2

E. coli transformants were checked by colony PCR, using primers specific to the inserted gene (identical sequences to the primers used in the initial amplification of the gene, but without the terminal restriction site/random bp modifications to improve PCR efficiency). A master mix for the total number of PCRs was prepared according to the following ratios, in order to give final reaction volumes of 30 µl: 1 x Super Taq buffer; 2 mM dNTPs; 250 pmol each primer (MWG); and 2 units Super Taq polymerase. A small quantity (equivalent in volume to 0.5 µl water) of a single transformant colony was transferred to a sterile PCR tube using a Gilson pipette tip, before the PCR mix was added and vortexed. The optimised PCR conditions were: 94°C 4 min; 94°C 1 min, 55°C 1 min, 72°C 2 min, 25 cycles; 72°C 5 min. PCRs were performed on a MJ thermocycler machine. Products were checked on a 1 % agarose gel (0.5 x TBE buffer) to confirm the presence of the insert.

2.10.1.5 Isolation of plasmid DNA

Single colonies isolated from an *E. coli* transformation were cultured in 1.5 ml liquid LB-amp media overnight. Plasmid DNA was isolated from pelleted cells using the Qiagen (Crawley, UK) miniprep kit according to the manufacturers instructions, and eluted in 50 µl sterile water. The integrity of the extracted DNA and the size of the plasmid (as an additional confirmation of gene insertion) was confirmed by running a 5 µl aliquot on a 1 % agarose gel in 0.5 x TBE buffer.

2.10.2 Complementation using a galactose-inducible system

For complementation analysis of genes regulated by the *GAL1* promoter, transformed cells were grown to exponential phase in SC-ura/SC-leu (as appropriate) with 2% glucose, then resuspended at an OD of 0.4 in induction media (SC-ura/SC-leu 2% galactose/1% raffinose) and incubated overnight at 28°C. Raffinose, which has no affect on expression from the *GAL1* promoter, was provided as an additional carbon source to reduce metabolic stress. Subsequent analysis of HN2 sensitivity was performed as already described (Section 2.5.1).

2.10.3 Complementation using a constitutive expression system

For complementation analysis of genes under the constitutive expression of the *ADH1* promoter, transformed cells were cultured overnight at 28°C in SC-ura (2 % glucose) media to select for plasmid retention. Subsequent analysis of HN2 sensitivity was performed as already described (Section 2.5.1).

2.10.4 Confirmation of gene overexpression by RT-PCR

Reverse transcriptase-PCR (RT-PCR) is a widely used method to evaluate levels of gene expression. Briefly, cellular RNA is extracted and the mRNA quotient specifically amplified by means of primers that target the poly-adenine tail, and the viral enzyme reverse transcriptase, which produces DNA from an RNA template. This cDNA is then used in a PCR reaction with primers specific to the gene of interest.

RNA was extracted from 4 x 10^7 cells using the Qiagen RNeasy kit, according to the manufacturers' instructions. The RNA was eluted in 50 µl DEPC-treated water, and

20 µl (in 3 ml DEPC water) was used to determine concentration by measurement of the absorbance at 260 nm using a spectrophotometer. 1 µg RNA was treated with 1 unit RQ1 RNase-free DNase (Promega) in 1 x RQ1 buffer and DEPC water, to a total volume of 10 µl. The digestion reaction was incubated at 37°C for 30 min before adding 1 µl of the provided stop solution and heating to 65°C for 10 min. The digested RNA was then diluted in DEPC water to give 1 µg/100 µl. Reverse transcription reactions were set up in a total volume of 20 µl as follows: 0.1 µg digested RNA; 1 x Sensiscript buffer (Qiagen); 0.5 mM dNTPs; 1 µM oligo dT (Invitrogen); 10 units RNasin (Promega); 1 µl Sensiscript RT (Qiagen); and DEPC water as necessary. RT was performed at 37°C for 60 min. The full RT reaction was subsequently used for PCR, in a total reaction volume of 100 µl: 20 µl RT reaction; 1x Taq buffer (Promega); 1.5 mM $MgCl_2$; 2.5 mM dNTPs; 100 pmol each primer (2 x gene specific, 2 x *ACT1* control primers). The primers for this PCR reaction were designed to lie within the coding region and generate short products (500 bp gene specific, 300 bp *ACT1* control) to maximise yield. Each PCR reaction contained 2 sets of primer pairs, one specific to the gene of interest, and another to the constitutively expressed *ACT1* gene, as a loading control. 5 units Taq polymerase (Promega) was added after a hot start. The PCR conditions were as follows: 94°C 2 min; 94°C 1 min, 51°C 1 min, 72°C 1.5 min, 40 cycles; 72°C 7 min. The entire PCR reaction was electrophoresed on a large 1.5 % agarose gel, in 0.5 x TBE buffer, and visualised by ethidium bromide staining and UV-exposure.

2.11 Protein analysis

A plasmid (pGAL-C-FLAG-*PSO2*) expressing a C-terminal FLAG-tagged Pso2 protein, under the control of the *GAL1* promoter was obtained from M. Tyers (Samuel Lunenfeld Research Institute, Toronto). The small FLAG-tag (DYKDDDDL) was the peptide of choice for this study, as it is not thought to interfere with fusion protein expression, proteolytic maturation, or activity (Molloy *et al.*, 1994; Lee and Altenberg, 2003; Terpe, 2003).

2.11.1 Protein extraction and quantification

The pGAL-C-FLAG-*PSO2* plasmid was transformed (as described in Section 2.3.2) into the protease-deficient *S. cerevisiae* strain, JEL1 (Lindsley and Wang, 1993; gift of Professor Ian Hickson, Weatherall Institute of Molecular Medicine, Oxford, UK), to prevent degradation of the Pso2 protein, and hence facilitate efficient extraction. Selection was maintained on SC-leu media.

Cells were cultured to exponential phase in SC-leu with 2% glucose, then resuspended at an OD of 0.4 in induction media (SC-leu 2% galactose/1% raffinose) and incubated at 28°C. A preliminary analysis was carried out to optimise the duration of galactose-induction for increased protein yield. Subsequent cultures for protein extraction were induced for 24 h, before washing in sterile water and freezing cell pellets at – 70°C, until required.

2.11.1.1 Whole-cell protein extraction

Cell pellets from 50 ml induced culture were resuspended in 1 ml RIPA buffer (50 mM Tris-HCl pH 7.5; 250 mM NaCl; 1 % deoxycholic acid; 1 % Triton-X100; 0.1 % SDS; protease inhibitor cocktail (1 complete EDTA-free tablet (Roche Diagnostics, Germany) per 50 ml buffer)) (P. Kaiser, University of California Irvine, USA: www.ucihs.uci.edu/biochem/faculty/Kaiser.html) and ground in liquid nitrogen, using a pestle and mortar. Disrupted cell solutions were microcentrifuged at top speed for 5 min at 4°C. The supernatant was carefully transferred to a sterile eppendorf, and maintained on ice. Protein concentrations were determined (Section 2.11.1.4).

2.11.1.2 Immunoprecipitation

Small-scale immunoprecipitations were performed on 200 μg crude protein extract, made up to a final volume of 500 μl in RIPA buffer. 4 μg anti-FLAG polyclonal antibody (Sigma) was added to each sample, and incubated overnight at 4°C on a rotary wheel.

Protein A-sepharose (Sigma, 10 μl stock per immunoprecipitation reaction) was prepared by washing in PBS and resuspending in RIPA buffer as a 50 % suspension. This was then added to the antibody-protein samples, and incubated for 1 h at 4°C on the rotary wheel. Subsequently, the conjugates were washed 3 times in RIPA buffer (microcentrifuging for 2 min at 3000 rpm at 4°C) and resuspended in a final volume of 30 μl RIPA buffer to enable loading of the entire sample on a PAGE gel. Samples were boiled in SDS-loading buffer prior to PAGE.

2.11.1.3 Large scale Pso2 protein extraction

Cell pellets from 1-2 litres induced culture were resuspended in 5 ml CelLytic-Y buffer (Sigma) per gram of cells, and ground in liquid nitrogen, using a mortar and pestle. The CelLytic-Y buffer was freshly supplemented with a cocktail of protease inhibitors (1 complete EDTA-free tablet (Roche Diagnostics, Germany) per 50 ml buffer). Disrupted cell samples were then spun in an ultracentrifuge at 30 000 rpm for 1.5 h at 4°C. After checking the protein concentration (Section 2.11.1.4), the supernatant was recentrifuged for a further 45 min. A second calculation of the protein concentration was made. Extracts were maintained on ice at all times, and stored at – 70°C until required.

1 ml aliquots of the extract supernatant were added to Anti-FLAG M2-agarose affinity gel (Sigma, murine IgG_1 monoclonal antibody), prepared from 20 µl packed gel according to the manufacturers instructions. This immunoprecipitation reaction was incubated overnight on a rotary wheel at 4°C. Samples were then washed 3 times in 1 x TBS (50 mM Tris HCl, 150 mM NaCl, pH 7.4), spinning for 10 s in a microcentrifuge at 10 000 rpm, 4°C. FLAG-Pso2 was eluted from the washed resin by resuspending in 100 µl 1 x TBS containing 150 µg 3 x FLAG peptide and 1 x protease inhibitors (Roche Diagnostics), and incubating for 1 h shaking at 4°C. The unbound agarose resin was then compacted by centrifuging for 10 s at 10 000 rpm, and the supernatant was transferred to a sterile eppendorf. The protein concentration of the supernatant was determined as described in Section 2.11.1.4.

Aliquots of the FLAG-Pso2 extract were further purified by centrifugation in a Vivascience Vivaspin 6 ml column (5- 50 000 MWCO) for 3 h at 4000 rpm, at 4°C.

The concentrated fraction remaining in the column was transferred to a sterile eppendorf for storage at –70°C.

2.11.1.4 Quantification of protein concentration

Protein concentrations were determined by spectrophotometer analysis using the Biorad DC Protein Assay reagents. Briefly, 2 µl of protein sample was diluted in 18 µl sterile water and combined with 100 µl of a 100:2 mix of Reagents A and S, respectively. 800 µl reagent B was added and vortexed. Samples were incubated at room temperature for 15 min before measuring absorption at 750 nm. Protein concentration (µg/µl) was calculated as A750 x 25.

2.11.2 Analysis of post-translation modifications

2.11.2.1 Phosphorylation

To determine whether Pso2 is modified by phosphorylated residues, extracted protein was treated with calf intestinal alkaline phosphatase (CIAP, NEB). Briefly, the eluate from an immunoprecipitation reaction (Section 2.11.1.2) was treated with 20 units CIAP or 20 units heat-inactivated CIAP (15 min, 80°C) in 1 x CIAP buffer for 1.5 h at 37°C. Reactions were performed in the manufacturer's buffer (100 mM NaCl, 50 mM Tris-HCl, 10 mM $MgCl_2$, 1 mM dithiothreitol, pH 7.9). Samples were subsequently prepared by boiling in Laemmli buffer for loading on a PAGE gel (Section 2.11.3).

2.11.2.2 Glycosylation

To determine whether Pso2 is modified by glycosylation, extracted protein was treated with the glycosidase EndoH (NEB). Briefly, the eluate from an immunoprecipitation

reaction (Section 2.11.1.2) was pre-treated in 1 x glycoprotein denaturing buffer (NEB) for 10 min at 100°C. 2500 units EndoH was then added in 1 x G5 buffer (NEB) and incubated for 1.5 h at 37°C. Samples were subsequently prepared by boiling in Laemmli buffer for loading on a PAGE gel (Section 2.11.3).

2.11.3 Polyacrylamide Gel Electrophoresis (PAGE)

Protein extracts were separated by Tris-glycine SDS-PAGE, according to standard protocols (Sambrook *et al.*, 1989). The expected size of the FLAG-Pso2 fusion protein is 80 kDa, so PAGE was performed with an 8 % resolving gel topped with a 5 % stacking gel, prepared in single-use cassettes (Invitrogen). About 30 ng whole cell extract (or a single IP reaction) was prepared in 5 x Laemmli SDS sample buffer (Laemmli, 1970), boiled for 3 min at 100°C, and pulsed in a microcentrifuge. Standard protein suspensions (Biorad kaleidoscope) were loaded on each gel for reference purposes. The composition of the 1 x running buffer was as follows: 25 mM Tris-HCl pH 8.3, 200 mM glycine. Electrophoresis was carried out using the XCell SureLock Mini-Cell apparatus (Invitrogen), at 60 V until the samples had passed to the boundary of the stacking and resolving gels, followed by 100 V for a further 2 h. Gels were carefully removed from the cassette, and subsequently stained with Coomassie blue in methanol-acetic acid (Sambrook *et al.*, 1989), or transferred by Western blotting, as appropriate.

2.11.4 Western blotting

The membrane (Millipore Immobilon-P) was prepared by cutting to the size of the PAGE gel, soaking in methanol for 15 min, rinsing in sterile water for 2 min, and

finally soaking in transblot buffer (1 x PAGE running buffer, 2 x methanol) for 5 min. The transfer apparatus (XCell II Blot Modul, Invitrogen) was arranged from the bottom of the tray upwards, as follows: two pre-soaked sponges; pre-soaked filter paper; PAGE gel; membrane; pre-soaked filter paper; and two further pre-soaked sponges. The transfer was carried out in transblot buffer for 1 h at 30 V.

2.11.5 Immunoblotting

Immunoblotting of western membranes was performed using one of two primary antibodies, both of which are polyclonal IgG raised in rabbit: anti-FLAG (Sigma), or anti-Sumo1 (Abcam, Cambridge, UK). Anti-FLAG antibody was prepared at a concentration of 2.5 μg/ml in PBS with 1 % bovine serum albumin (BSA, Sigma). Anti-Sumo1 was used at a working dilution of 1:1000 in PBS with 1 % BSA. Antibodies were found to be effective at the manufacturers recommended concentration, and could be re-used 3-4 times without loss of activity (if stored at –20°C).

Membranes were blocked overnight at 4°C in a filtered solution of 5 % low-fat milk in PBS. The membrane was subsequently washed 3 times in PBS/0.05 % Tween. Membranes were incubated in the appropriate primary antibody on a roller for 3 h at room temperature, and then washed three times in PSB/0.05 % Tween. The secondary antibody, peroxidase-conjugated anti-rabbit IgG raised in goat (Rockland Inc., USA), was diluted to 1:12000 in PBS/0.05 % Tween, and incubated with the membrane at room temperature on a roller for 1 h. Membranes were washed a further 3 times in PBS/0.05 % Tween, and blot-dried. Chemilluminescent detection of the peroxidase-conjugated antibody-protein complexes was performed using ECL (Amersham),

according to the manufacturers instructions. Briefly, the ECL solutions were mixed in a 1:1 ratio, and incubated with the membrane at room temperature for 1 min. The membrane was then blot-dried, wrapped in Saran, and exposed to photographic film over a range of time points, typically 10 s, 30 s, 1 min, 3 min, and 5 min.

Membranes to be re-blotted were first stripped for 30 min at 50°C, in stripping buffer (100 mM 2-Mercaptoethanol, 2 % SDS, 62.5 mM Tris-HCl pH 6.7), and washed twice in PBS/0.05 % Tween at room temperature. Complete removal of the bound antibody complexes was confirmed by performing ECL detection, as above. The membranes were rinsed in PBS, and then blocked overnight at 4°C in a filtered solution of 5 % low-fat milk in PBS, ready for immunoblotting.

CHAPTER 3 CHARACTERISATION OF YEAST STRAINS DEFICIENT FOR *PSO2*

The genetic characterisation of mutant *S. cerevisiae* strains is one of the few areas of research into the *PSO2* gene that has been actively pursued in the past. In particular, their specific sensitivity to a wide range of cross-linking agents, including the nitrogen mustards (Fleer and Brendel, 1979), psoralens (Henriques and Moustacchi, 1980), platinum-based compounds (Wilborn and Brendel, 1989), and mitomycin C (Pungartnik *et al.*, 2002), but not other forms of DNA damage, is well established. However, the genetic characterisation of *pso2* strains is incomplete, and the results are in some cases ambiguous and contradictory. It is therefore desirable to revisit the fundamental aspects of this phenotype in order to present a definitive study.

The extent to which *PSO2* is involved in either the normal function of the cell cycle, or the response to DNA damage is not yet fully determined. It has been reported that loss of *PSO2* results in the induction of a G2 arrest after treatment with cisplatin, but a normal S-phase was observed (Grossmann *et al.*, 2000). The question of whether *PSO2* acts to repair ICL at a particular stage of the cell cycle is an important one as it holds many clues as to the mechanism of ICL repair in general. The DSBs that have been observed after treatment with ICL-inducing agents are believed to result from replication fork collapse and as such are obviously a cell cycle-dependent aspect of the repair of DNA cross-links.

Another paradox still to be resolved is the involvement of *PSO2* with the major yeast repair pathways and how this relates to the current model of ICL repair. By analogy

with the well-characterised pathway in *E. coli* (Section 1.3.1), the repair of cross-links in yeast is believed to involve three key stages. Firstly, incision at the site of an ICL by the NER apparatus, leading to the 'unhooking' of the cross-link from one strand of DNA. This is followed by resection in order for recombination to proceed into the gapped DNA. Previous studies of epistasis between *pso2* disruptant cells and strains deficient in the main repair groups suggest that *PSO2* is involved with NER but not homologous recombination during the repair of ICLs (Henriques and Moustacchi, 1981; Siede and Brendel, 1982). This apparent contradiction between the activity of a cross-link repair specific gene and the currently proposed mechanism of ICL repair remains to be resolved.

3.1 Disruption of the *PSO2* gene

The *pso2* mutant strains used in this study were derived from the B356-7C (parent W303-1A) or DBY747 haploid parent strains by PCR based micro-homology targeted deletion, using the template plasmids derived by Longtine *et al.* (1998). This method involves PCR synthesis of a DNA cassette with terminal regions of homology to *PSO2*, from a plasmid bearing a selectable marker gene (Fig. 3.1 A). Two primers, each comprising 40 bp of homology to the *PSO2* gene and 20 bp of overlap with the *KanMX4* cassette were used: 5'AGC ATA CGC ACT AGT GAC TAA TTT GGG TGG TCG GTT GAT Tcg gat ccc cgg gtt aat taa3' (forward) and TCA TAC ATT CAT ATA ATA TCC ATT ACG TAC GTA CAT CTT Aga att cga gct cgt tta aac3' (reverse), where the region homologous to *PSO2* is in uppercase and to *Kan MX4* in lowercase. In order to ensure complete disruption of the *PSO2* gene, these primers were designed to allow deletion of the coding sequence from upstream of the 5' ATG, to downstream

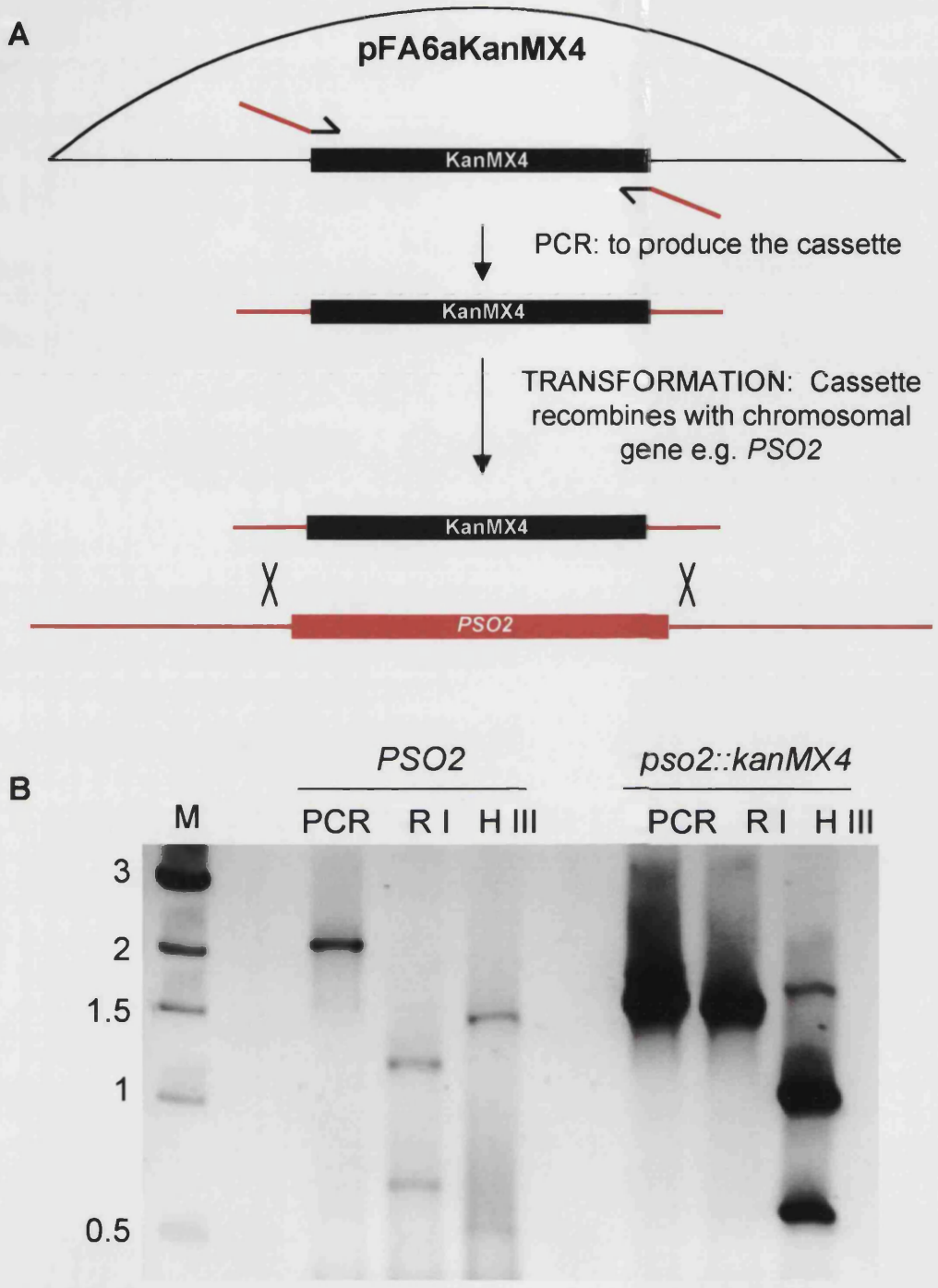

Figure 3.1 PSO2 gene disruption. **A**. Schematic of PCR based microhomology-targeted deletion. Plasmid DNA is depicted in black, and yeast DNA in red. **B**. Agarose gel comparing PCR products from a wild-type *PSO2* strain and an *pso2::kanMX4* disruptant. *PSO2* gives a 2.2 kb PCR product, which when digested with *EcoR* I (RI) gives two fragments of 1.25 and 0.7 kb, and digested with *Hind* III (H III) gives two fragments of 1.5 and 0.5 kb. The *pso2::kanMX4* PCR product is 1.6 kb, reduced to 1.5 kb by *EcoR* I digestion, and fragmented to give 1.0 and 0.6 kb bands after *Hind* III digestion. M = 1 kb DNA marker.

of the 3' termination site (primer locations as coordinates of the X64004 GenBank *PSO2* sequence: forward 156-195, reverse 2270-2231, CDS 196-2181). The resulting DNA fragment was transformed into the parent yeast strain by the lithium acetate method, and kanomycin resistant colonies were isolated by growth on YEPD-G418 plates. Disruption of the *PSO2* gene was confirmed by PCR across the insertion region using two primers flanking the 5' and 3' deletion cassette primers, respectively (X64004 coordinates: forward 131-150, reverse 2308-2286), producing a DNA fragment of 1.6 kb in the *pso2* disruptant, compared to 2.2 kb in the *PSO2* wild-type. Subsequent *EcoR* I and *Hind* III restriction enzyme analysis of the PCR product yields different patterns of DNA fragments in the wild-type and disrupted gene, hence providing conclusive evidence that *PSO2* was fully disrupted (Fig. 3.1 B).

3.2 *PSO2* is not required for normal growth and cell cycle kinetics

3.2.1 Loss of *PSO2* does not disrupt the normal pattern of cell division

One of the first avenues of research was to confirm that mutant *pso2* cells are able to grow in the normal fashion. Simple analysis of the growth pattern was achieved by inoculating a fresh culture with exponential phase cells at 2 x 10^6 cells/ml, and observing the change in culture density at hourly intervals using a spectrophotometer. It is clear from figure 3.2 that the growth profile of the *pso2* strain is indistinguishable from the wild-type parent B356-7C. The culture density was also analysed microscopically at 0 and 10 h, by performing cell counts using the haemocytometer method. Consistent with the spectrophotometer analysis, no significant difference was

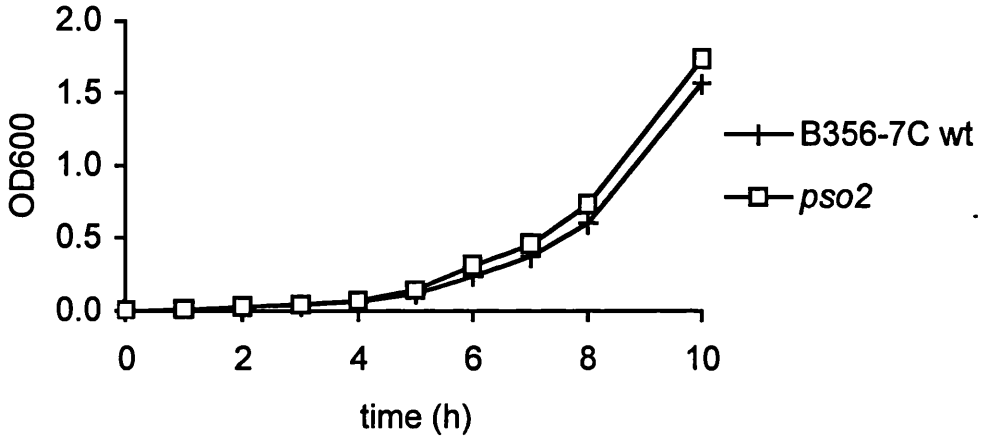

Figure 3.2 Analysis of the growth profile of pso2 deficient cells, relative to the wild-type parent B356-7C. Samples of a freshly inoculated YEPD culture (0 h) were taken at hour intervals to determine cell density by spectrophotometer measurement at OD600. The analysis was repeated 3 times, and a typical result is shown.

observed between the wild-type and *pso2* strains (culture density at 10 h was 6.7 x 10^7 and 6.4 x 10^7 cells/ml, respectively, relative to 0 h).

Exponential phase cells (cultured for 10 h) were also examined microscopically to ascertain the relative populations in each cell cycle phase: G1 (unbudded), S (small budded), and M (large budded, where the bud size is greater than 50 % of the volume of the mother cell). About 200 cells from each strain were counted. No significant difference was observed between the wild-type and *pso2* defective strains, with both exhibiting equal proportions of cells in S and M phase (Table 3.1). As would be expected from an exponential phase culture, the majority of cells (70-80 %) have entered the replication and division phases of the cell cycle.

Table 3.1 **Microscopic analysis of cell cycle phase.**

Strain	G1 (unbudded)	S (small bud)	M (large bud)
B356-7C	19.1 %	51.9 %	29.0 %
pso2	28.1 %	47.7 %	24.2 %

3.2.2 Loss of *PSO2* does not prevent or render cells sensitive to cell cycle arrest

In order to further discount a role for *PSO2* in the normal operation of the cell cycle, mutant *pso2* strains were tested for sensitivity to a number of checkpoint-specific inhibitors. Hydroxyurea (HU) is a potent inhibitor of the enzyme ribonucleotide reductase, and blocks DNA synthesis by causing elongation arrest (Slater, 1973). Colony spotting assays were employed, in which defined numbers of cells are grown on

YEPD plates supplemented with different concentrations of HU. It can be seen from figure 3.3 A that *pso2* cells were as competent as the wild-type B356-7C strain to grow on YEPD supplemented with 40 mM HU. This contrasts with an *mre11* strain, which fails to survive even a concentration of 5 mM HU (data not shown). The anti-mitotic systemic benzimidazole fungicide, Benomyl, prevents spindle assembly by causing depolymerisation of microtubules. Colony spotting assays were again utilised to test the response to a range of different concentrations of Benomyl. As for HU, loss of *PSO2* does not lead to either a sensitive or a resistant phenotype to Benomyl, compared to the wild-type strain (Fig. 3.3 B). The *pso2* and B356-7C strains are equally able to survive in the presence of Benomyl at a concentration of 25 μg/ml (Fig. 3.3 B), but fail to grow at all upon plates supplemented with 50 μg/ml (data not shown).

A further indication of proficiency in cell cycle progression is the ability to initiate G1 arrest in the presence of alpha mating factor. Cells from an actively growing culture were transferred to YPAD containing 10 μM alpha mating factor, and incubated at 28 °C. In the original exponential phase cultures, single unbudded cells were observed at a frequency of 13.1 % (27/206) and 20.9 % (49/235), for the wild-type and *pso2* strains, respectively. However, after a 3 h incubation the presence of alpha mating factor, 92.3 % (203/220) of *pso2* deficient cells were observed microscopically as unbudded or "shmooed" (cells with a characteristic mating projection). This compares favourably with the parent DBY747 strain where 96.7 % (172/178) of cells were unbudded/shmooed after 3 h incubation. Hence it would seem that *PSO2* does not play a significant role in normal cell cycle kinetics, as cells are able to arrest normally in G1 phase.

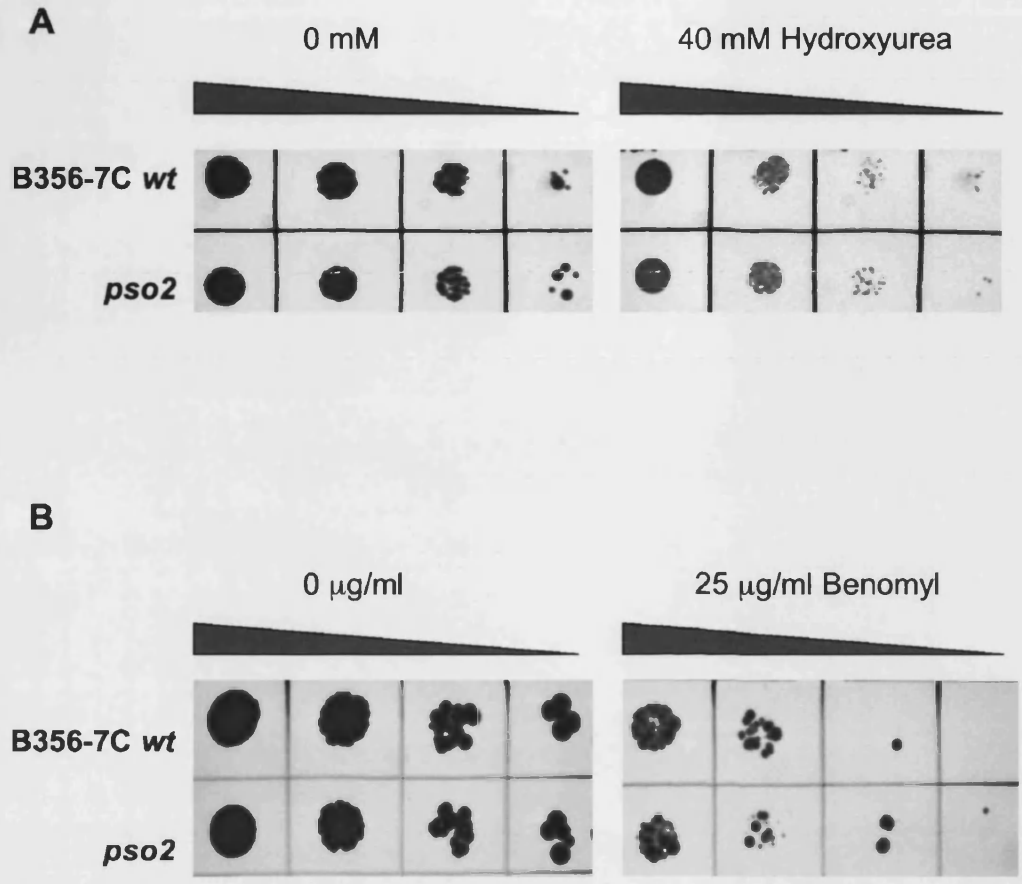

Figure 3.3 Sensitivity to HU and Benomyl. A 10 fold serial dilution series (represented by the tapered grey bar) of B356-7C wild-type and *pso2* deficient cells were spotted on YEPD containing **A**. 0 or 40 mM Hydroxyurea, **B.** 0 or 25 μg/ml Benomyl. Plates were spotted in duplicate, and incubated at 28°C for 3 days.

3.2.3 *PSO2* is not essential for mitochondrial function

In addition to the observed nuclear localisation of the Pso2 protein (Henriques *et al.*, 1997; Dronkert *et al.*, 2000; Richie *et al.*, 2002), a systematic mass spectrometry screen of protein complexes identified using 10 % of the yeast genome as tagged bait, has suggested an interaction between FLAG-tagged-Pso2 and the mitochondrial proteins Mgm101 and YHR076W (Ho *et al.*, 2002). Mgm101 has been shown to bind mitochondrial DNA as part of the nucleoid involved in the repair of oxidative damage (Meeusen *et al.*, 1999). The biological function of YHR076W is as yet unknown, although it is known to exhibit protein phosphatase activity (Jiang *et al.*, 2002).

Analysis of the Pso2 protein sequence using PSORTII (http://psort.nibb.ac.jp, Gavel and von Heijne, 1990) reveals a potential mitochondrial targeting R-2 motif at residue 77. The predictive software assigns a 34.8 % likelihood that the Pso2 protein will localise to the mitochondria, which, although a lesser probability than nuclear localisation (56.5 %), is significant, and contrasts with the negligible prospect of localisation to other cellular compartments (cytoplasm 4.3 %, endoplasmic reticulum 4.3 %). Hence it was important to determine whether functional *PSO2* was essential for normal mitochondrial metabolism. *pso2* deficient cells were grown on YPG media, which contains the non-fermentable carbon sources glycerol and ethanol. Figure 3.4 clearly shows a similar level of growth on YPG in the *pso2* strain as for the parent B356-7C, which is indistinguishable from the capacity to grow on YEPD. It follows that *PSO2* is not essential for normal mitochondrial function, yet this does not preclude a role in some redundant mtDNA repair process.

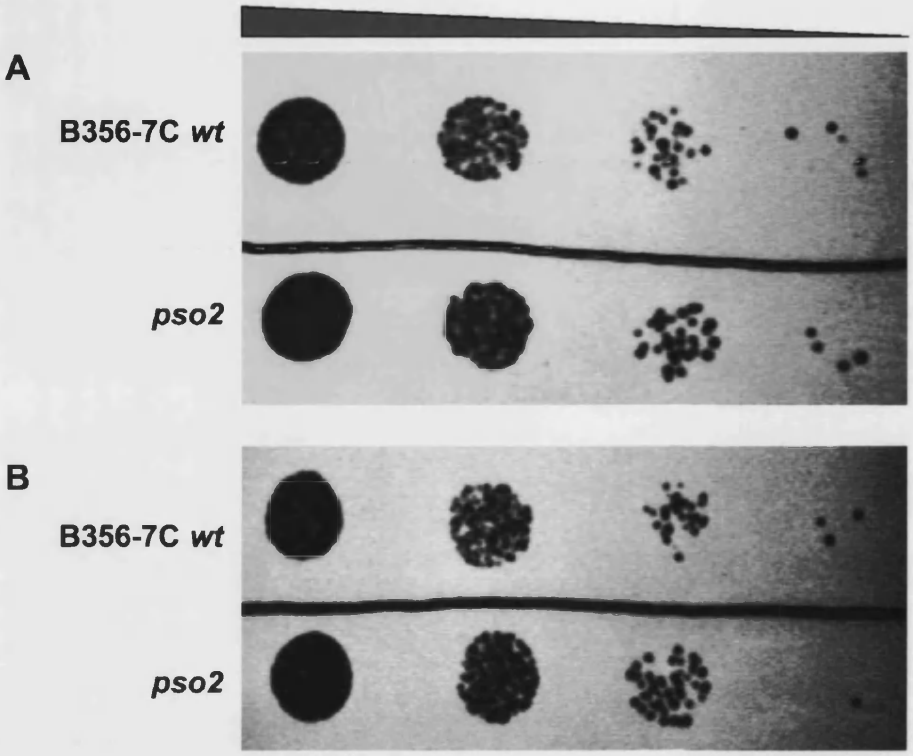

Figure 3.4 Analysis of growth on non-fermentable media. A 10 fold serial dilution series (represented by the tapered grey bar) of B356-7C wild-type and *pso2* deficient cells were spotted on either **A**. YEPD or **B**. YPG (non-fermentable) agar plates, and incubated for 3 days at 28°C.

3.3 Confirmation that loss of *PSO2* results in specific sensitivity to DNA ICL, but not other forms of DNA damage

One of the considerations of previous research into *PSO2* has been the sensitivity of *pso2* mutants to different DNA damaging agents. As already discussed (Section 1.4.1), initial interest in the *PSO2* gene was aroused following its identification from an unusual mutant strain sensitive to bifunctional, but not monofunctional, alkylating agents. To date, *pso2* disruptant cells have been screened for sensitivity to many ICL-inducing agents, and this original observation stands unchallenged. It would not, therefore, be beneficial to conduct further examination of the *pso2* mutant phenotype with regards to drug sensitivity. However, it was felt reasonable to utilise this knowledge to check the validity of the new *pso2* disruptants produced by PCR-based micro-homology targeted gene deletion. The sensitivity to nitrogen mustard (HN2) resulting from a complete loss of the *PSO2* gene was investigated in three commonly used genetic backgrounds. A *pso2* mutant in either the B356-7C (W303-IA) or DBY747 strains led to a 10,000-fold increase in sensitivity at the highest dose, compared to the respective parent (Fig. 3.5 A and B). Interestingly, the BY4741-derived *pso2* strain from the EUROSCARF Yeast Deletion Project is considerably more sensitive to HN2 (100-fold more than the DBY747 and B356-7C *pso2* mutants at 1000 μM HN2), and this is not reflected in an increased susceptibility of the parent strain (Fig. 3.5 C).

These *pso2* mutants were also tested for sensitivity to UVC and X-irradiation. Figure 3.6 A shows a mild increase (about 5-fold over the parent strain) in sensitivity to UV for

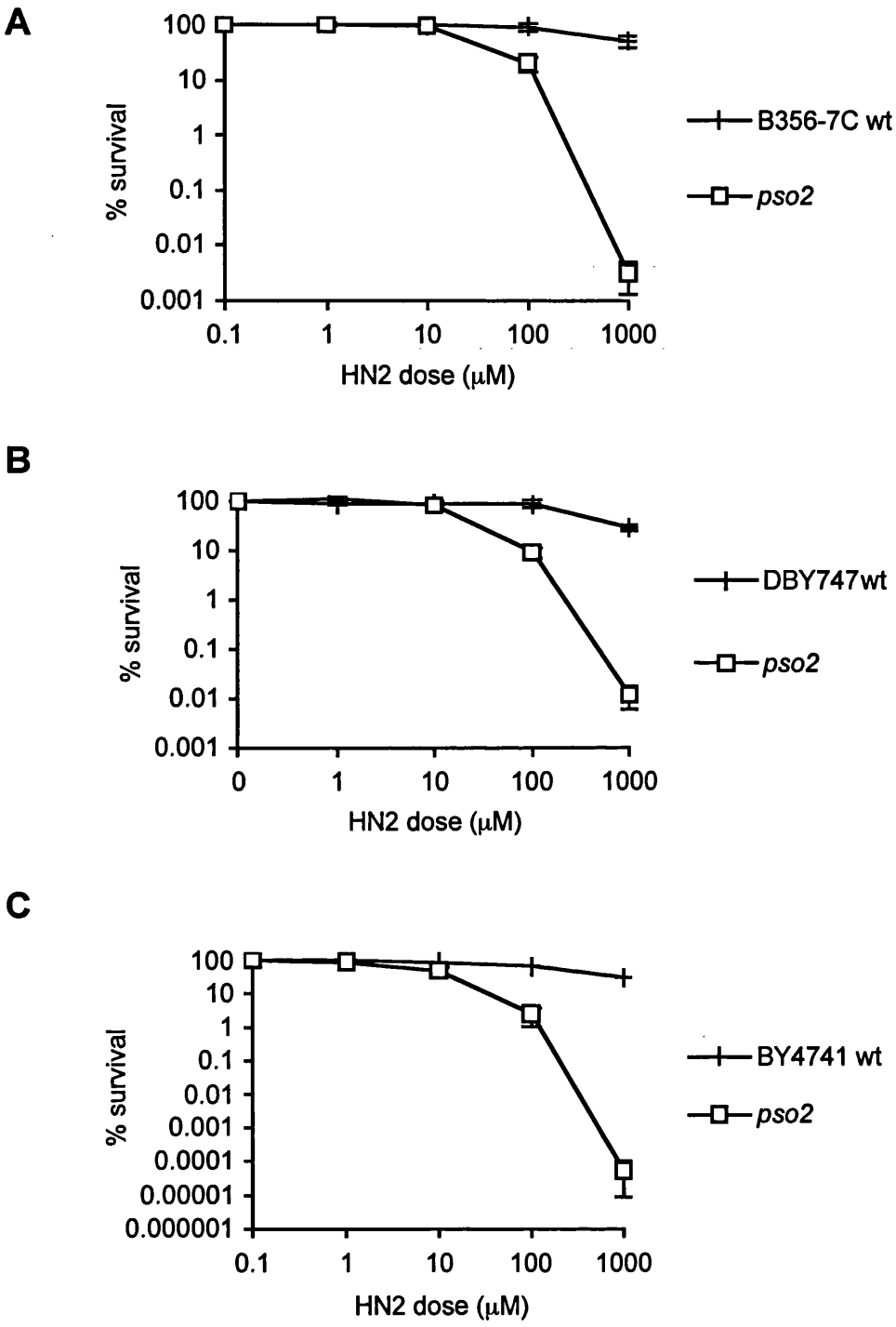

Figure 3.5 Sensitivity to HN2. Exponential phase parental and *pso2* cells were treated with 0 to 1000 μM HN2 for 1 h, and survival monitored by plating on YEPD. **A.** B356-7C background. **B.** DBY747 background. **C.** BY4741 background. All results are the mean of at least three independent

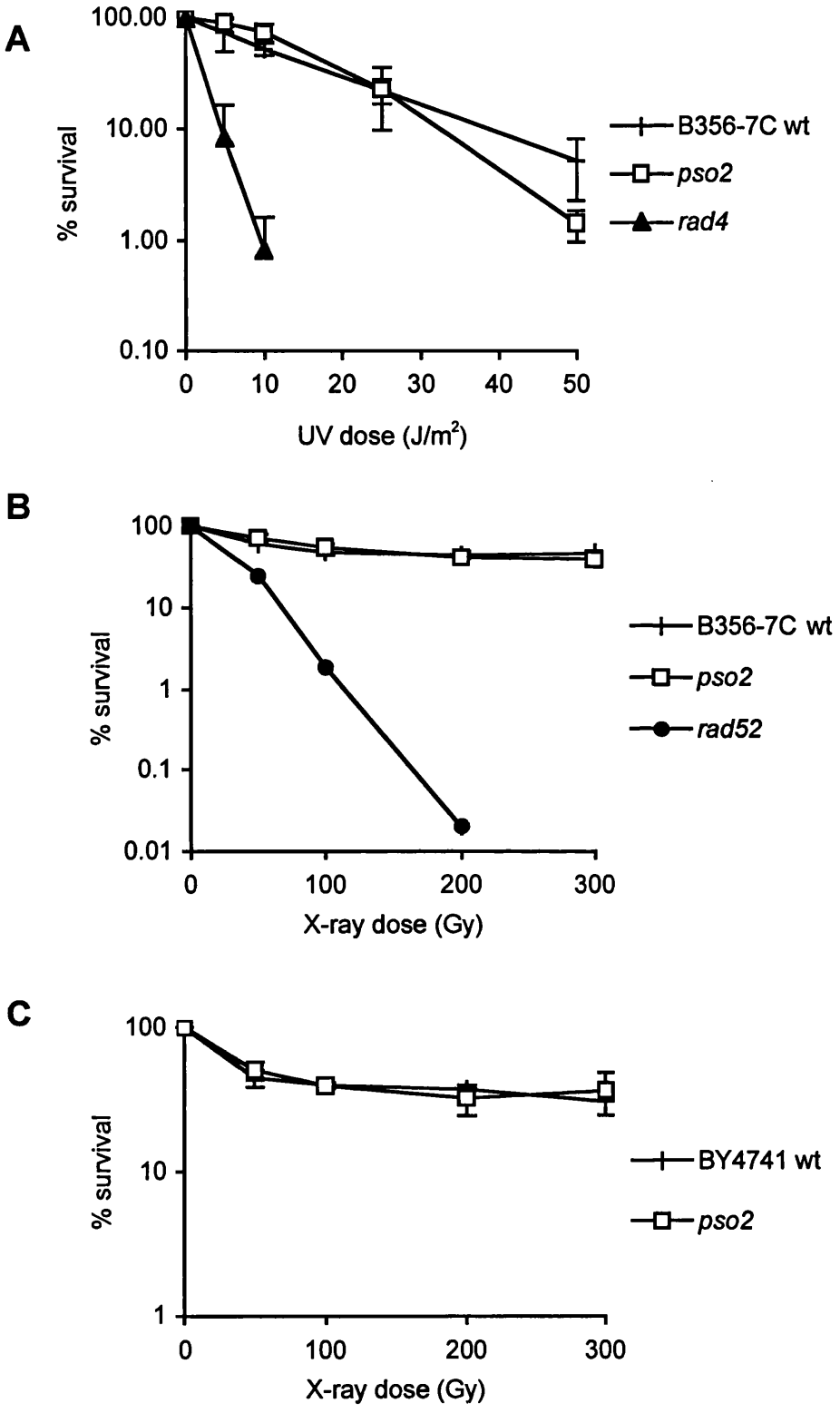

Figure 3.6 Sensitivity to UVC and X-irradiation. Survival of parental and *pso2* deficient cells following treatment with **A** UVC, or **B** and **C** X-irradiation, at the doses shown. Comparisons are made with mutants known to be highly sensitive to these treatments. All results are the mean of at least three independent experiments, and the error bars show the SEM.

pso2, but only at the highest dose (50 J). This is extremely modest compared with the *rad4* (NER) mutant, where survival could not be detected at doses greater than 10 J (Fig. 3.6 A). Additionally, it can be clearly seen from figure 3.6 B that loss of *PSO2* does not lead to any sensitivity to X-irradiation, where a *rad52* (homologous recombination mutant) strain is shown as a positive control. It is interesting to note that the BY4741 *pso2* mutant also demonstrates a wild-type resistance to X-irradiation (Fig. 3.6 C), suggesting that should there be any other disrupted genes in this strain, they are not directly involved in the repair of DNA double-strand breaks.

3.4 The *Schizosaccharomyces pombe pso2* mutant phenotype reflects that of *S. cerevisiae pso2*

Schizosaccharomyces pombe (fission yeast) is evolutionarily distinct from *S. cerevisiae*. A putative *S. pombe PSO2* gene was isolated by sequence analysis and the entire ORF was disrupted by *KanMX6* insertion in collaboration with Professor Tony Carr (Genome Stability Centre, University of Sussex). This candidate gene gives rise to a protein with 42 and 55 % similarity and 27 and 37 % identity across the complete protein sequence with *S. cerevisiae* Pso2 and human Pso2, respectively (Fig. 1.12; Lambert *et al.*, 2003). The newly isolated *pso2* mutant was tested for sensitivity to both HN2 and its monofunctional derivative mono-nitrogen mustard (2-dimethylaminoethylchloride hydrochloride, HN1) to determine whether this homologue is also involved in the specific processing of DNA ICL. It can be seen from figure 3.7 A that in *S. pombe*, loss of *pso2* results in a moderate sensitivity to HN2 - approximately six-fold compared to the 501 parent strain at the highest dose used (1000 μM). Furthermore, in a serial dilution colony spotting assay the *pso2* deficient strain demonstrates wild-type

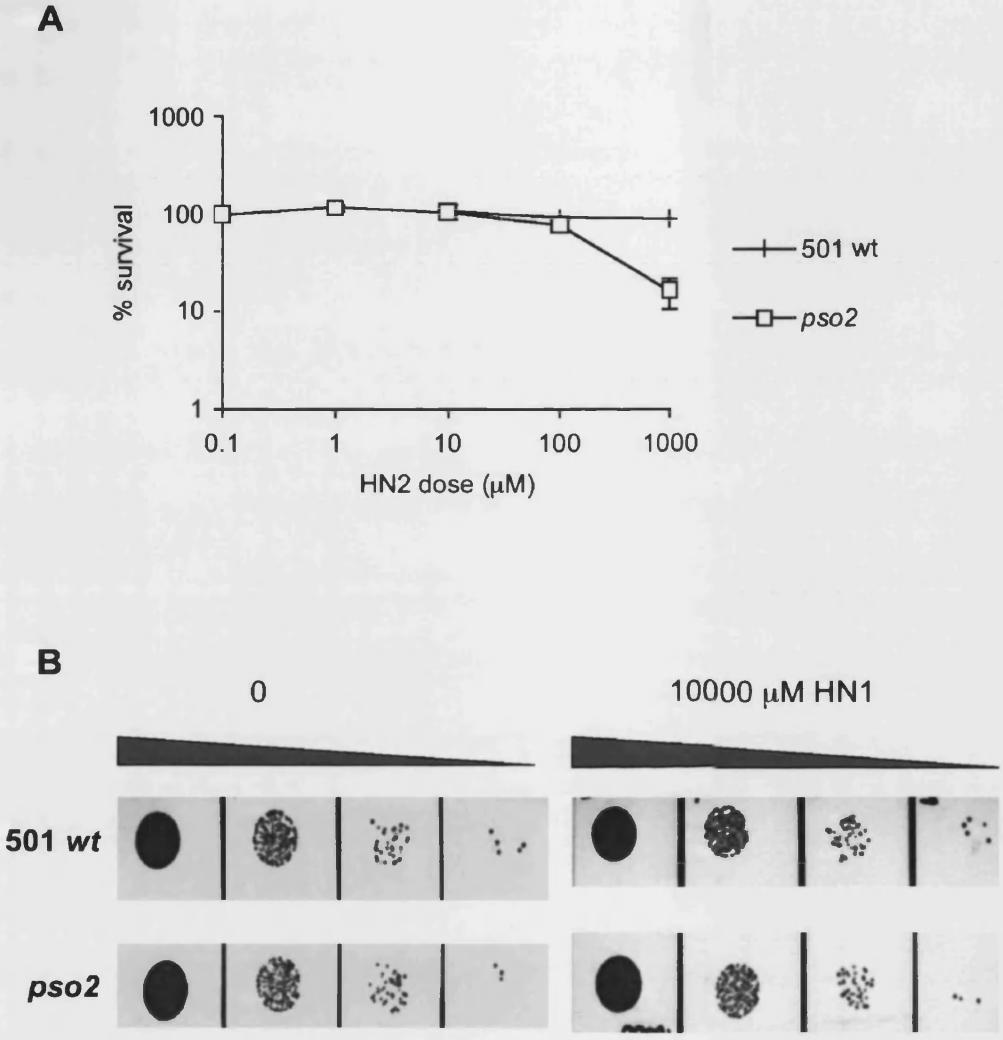

Figure 3.7 S. pombe pso2 sensitivity to HN2 and HN1. **A.** Survival following a 1 h treatment with 0 to 1000 μM HN2 in PBS. Results are the mean of at least three independent experiments, and the error bars show the SEM. **B.** Colony spotting assay in which 10 fold serial dilutions of cells (represented by the tapered grey bar) are spotted onto YEPD plates containing 0 to 10000 μM HN1. All plates were incubated for 3 days at 28°C before scoring.

resistance to HN1, even at a dose of 10000 μM, 10 fold higher than the maximum HN2 treatment applied (Fig. 3.7 B). It would therefore appear that although the degree of sensitivity of the *S. pombe pso2* mutant to HN2 is less than in *S. cerevisiae*, the specificity of Pso2 activity does extend only to ICL-inducing agents and not monoadducts. Such a difference in the magnitude of drug sensitivity between these yeasts is not unusual, with *S. pombe* cells often demonstrating a far greater resistance to DNA damage.

3.5 Creation of a panel of single and multiple gene disruption strains in a defined isogenic background in *S. cerevisiae*

As discussed in section 1.4.6, previous research has been conducted regarding the genetic interactions of *PSO2* with the three key epistasis groups for DNA repair in yeast – *RAD3* (NER), *RAD52* (homologous recombination), and *RAD6* (post-replication repair/translesion synthesis). However, these investigations have involved the use of a spectrum of gene mutations, some of which may have retained hypomorphic (leaky) phenotypes. Furthermore, these studies have been carried out in non-isogenic genetic backgrounds. In the main part of this study, epistasis relationships for *PSO2* have been established using HN2 in the isogenic background B356-7C (Bai and Symington, 1996). However, it has been necessary to use other strains for certain experimental techniques where B356-7C cannot be used, such as the *CAN1* forward mutation assay. For the first time, a comprehensive panel of haploid single and multiple gene disruptant strains encompassing genes from the key yeast DNA repair pathways has been isolated in a defined genetic background (Table 2.1). In the creation of these strains, PCR-based micro-homology targeted deletion has been used employing combinations of selectable

marker genes for kanamycin resistance, and histidine (*HIS5*) and uracil (*URA3*) metabolism. All gene deletions have been systematically checked by PCR across the insertion region, and by subsequent characteristic dual restriction enzyme analysis, as already described for the disruption of *PSO2* (Section 3.1).

3.5.1 *PSO2* is epistatic to the NER pathway for ICL repair

To elucidate any association of *PSO2* with established yeast epistasis groups for DNA repair, the sensitivity of haploid double disruptant strains to HN2 relative to their respective single mutants was determined using exponentially growing cultures. Previous studies have focussed on the use of *RAD1*, *RAD2*, and *RAD3* as markers for the NER epistasis group. In this study, the genetic interaction of *PSO2* with *RAD4*, an NER factor involved in damage recognition (Section 1.2.1), has been determined. Figure 3.8 shows the sensitivity of *pso2, rad4* and *rad4 pso2* strains to HN2 in two different parental backgrounds, DBY747 and B356-7C. Two defined genetic backgrounds were investigated as the sensitivity of this assay (survivors per 2 x 10^7 cells) proved insufficient at the 1000μM HN2 dose in the *rad4 pso2* double mutant. In the case of DBY747 *rad4 pso2*, no colonies were obtained in any of 4 repeats, whereas in the B356-7C background, colonies were observed only once in 7 assays. By comparison, *rad4* survivors were found at the highest dose in 1 in 4 (DBY747) and 4 in 7 repeats (B356-7C), plating at the same concentration as for *rad4 pso2*. This reflects the fact that the DBY747 *rad4* strain demonstrates greater sensitivity to HN2 at the lower doses than in B356-7C (Fig. 3.8). In conclusion, the double mutant *pso2 rad4* does not exhibit significantly increased sensitivity to HN2 compared to the most sensitive corresponding single mutant (rad4), inferring an epistatic interaction of *pso2* with genes of the NER pathway.

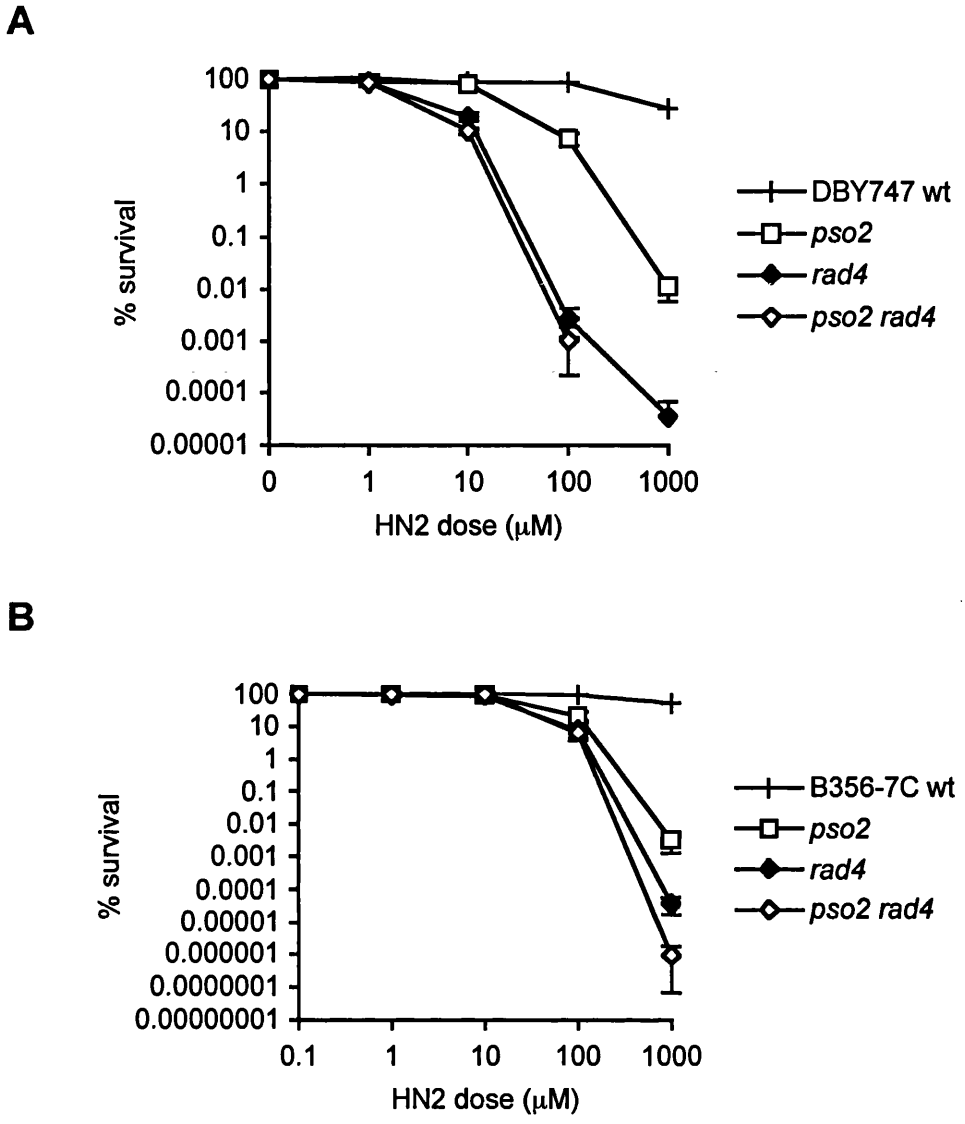

Figure 3.8 Comparison of HN2 sensitivity in pso2 and rad4 (NER) deficient cells. **A.** DBY747 background. **B.** B356-7C background. Exponential phase cells were treated with 0 to 1000 μM HN2 for 1 h, and survival monitored by plating on YEPD. All results are the mean of at least three independent experiments, and the error bars show the SEM.

3.5.2 Both *PSO2* and NER exhibit a non-epistatic relationship with homologous recombination for the repair of cross-links

The original examination of *PSO2* interaction with the homologous recombination epistasis group concentrated on *RAD52* (Siede and Brendel, 1982). *RAD52* is central to all pathways of homologous recombination, both conservative (involving gene conversion, cross-overs) and non-conservative (SSA, BIR and ectopic) (Symington, 2002). Hence if *PSO2* was directly involved in one of these sub-pathways, but not others also relevant to ICL repair, it is possible that use of such a ubiquitous marker as *RAD52* would prevent detection. In contrast, *RAD51* is crucial only to conservative homologous recombination events (Symington, 2002). Therefore an epistatic association might be expected if *PSO2* interacted with *RAD51*, or a synergistic relationship should *PSO2* be involved in *RAD51*-independent sub-pathways. The HN2 sensitivity of *pso2 rad51* and *pso2 rad52*, compared to the respective single mutants and B356-7C parental strain, is shown in figure 3.9. Consistent with a requirement for homologous recombination in ICL repair, both *rad51* and *rad52* cells demonstrate increased sensitivity to HN2 compared to the isogenic parent B356-7C, and this sensitivity is comparable to that of the *pso2* single mutant strain. Interestingly, *rad52* deficient cells are only fractionally more sensitive to HN2 than *rad51*, suggesting that *RAD51*-dependent homologous recombination is the preferred repair mechanism for ICLs. Both *pso2 rad51* and *pso2 rad52* double disruptants are more sensitive to HN2 than either single mutant alone. Loss of both *rad51* and *pso2* does not lead to as severe a phenotype as for the absence of *rad52* and *pso2*. Certainly, it was never possible to

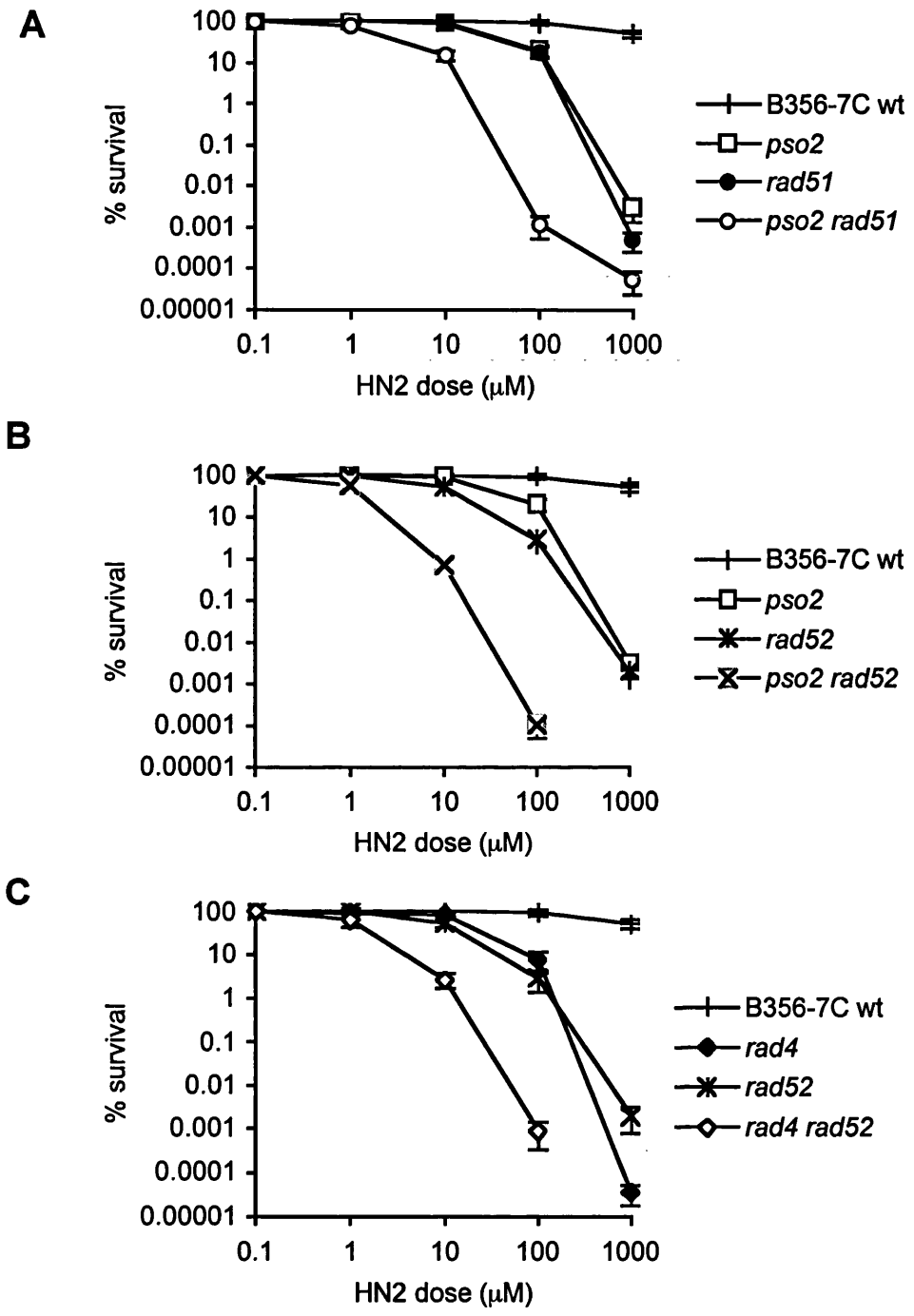

Figure 3.9 Comparison of HN2 sensitivity in pso2 and HR mutants. **A.** Comparison of *pso2* with *rad51* deficient cells. **B.** Comparison of *pso2* with *rad52* deficient cells. **C.** Comparison of *rad4* and *rad52* mutants. Exponential phase cells were treated with 0 to 1000 μM HN2 for 1 h, and survival monitored by plating on YEPD. All results are the mean of at least three independent experiments, and the error bars show the SEM.

detect *pso2 rad52* survivors at the highest dose of 1000 μM HN2 (0/3 assays versus 3/5 for *pso2 rad51*) and *pso2 rad52* double disruptants are at least 10 fold more sensitive at the lower doses of 10 and 100 μM HN2. It would seem that *PSO2* acts synergistically with *RAD51*-dependent pathways of recombination. Furthermore, an epistatic relationship with non-conservative pathways of recombination is unlikely, as a greater synergism is seen with *RAD52* than with *RAD51*, presumably reflecting the spectrum of *RAD52* activity. Hence it appears that *pso2* does not exhibit any involvement with the homologous recombination pathways of DNA repair.

However, a synergistic relationship between *PSO2* and *RAD51/RAD52* could also result from the additional occurrence of ICL-associated homologous recombination events that are totally independent of the epistatic NER-*PSO2* pathway. To address this hypothesis, the relationship between NER (*rad4*) and recombination (*rad52*) for ICL repair was determined. If prior processing of a cross-link by the NER apparatus is required for all ICL-associated recombination events, then *rad4* should be epistatic to *rad52* for sensitivity to HN2. It is clear from figure 3.9 C however, that the *rad4 rad52* double mutant is significantly more sensitive to HN2 than either *rad4* or *rad52* alone. The magnitude of the sensitivity of the *rad4 rad52* double mutant is identical to that for *pso2 rad52*, and again no colonies were recovered at the highest dose (cf. 3.9 B and C). It is clear therefore, that neither *pso2* nor NER is epistatic to homologous recombination for the repair of ICLs, but that this does not exclude the possibility that downstream recombination events may be required to reconstitute dsDNA from an ICL intermediates generated by the combined actions of NER factors and Pso2.

3.5.3 *PSO2* acts synergistically with the *RAD6*/post-replication repair pathway

It has been suggested that the PRR pathway is predominantly involved in the repair of ICLs in stationary phase cells where homologous DNA regions are not available for recombination (McHugh *et al.*, 2000). Hence it is feasible that *pso2* may be epistatic to the *RAD6* pathway in stationary phase cells but not those that are exponentially growing. Figure 3.10 A and B contrast the genetic interactions between *pso2* and *rev3* for HN2 treatment in exponential phase cells and after G1-arrest induced by α-mating factor, respectively. The *rev3* mutant is sensitive to HN2 but only in stationary (G1-arrested) cells. However, *pso2 rev3* double disruptants exhibit greater HN2 sensitivity than the single mutants in either growth phase. This would suggest a role for *PSO2* in the repair of ICLs in stationary phase yeast that is distinct from the post-replication repair pathway.

Interestingly, *pso2* appears to show epistasis with *rad18* (Fig. 3.10 C) in exponential cells. This is not necessarily contradictory with the observation of synergism with *REV3*, as *RAD18* acts upstream at the initial recognition phase of post-replication repair, before the pathway diverges into the mutagenic (*REV3*) and error-free (*MMS2/RAD5*) branches. It is entirely feasible that Pso2 may act in conjunction with Rad18 for the recognition and repair of ICL by the error free pathway.

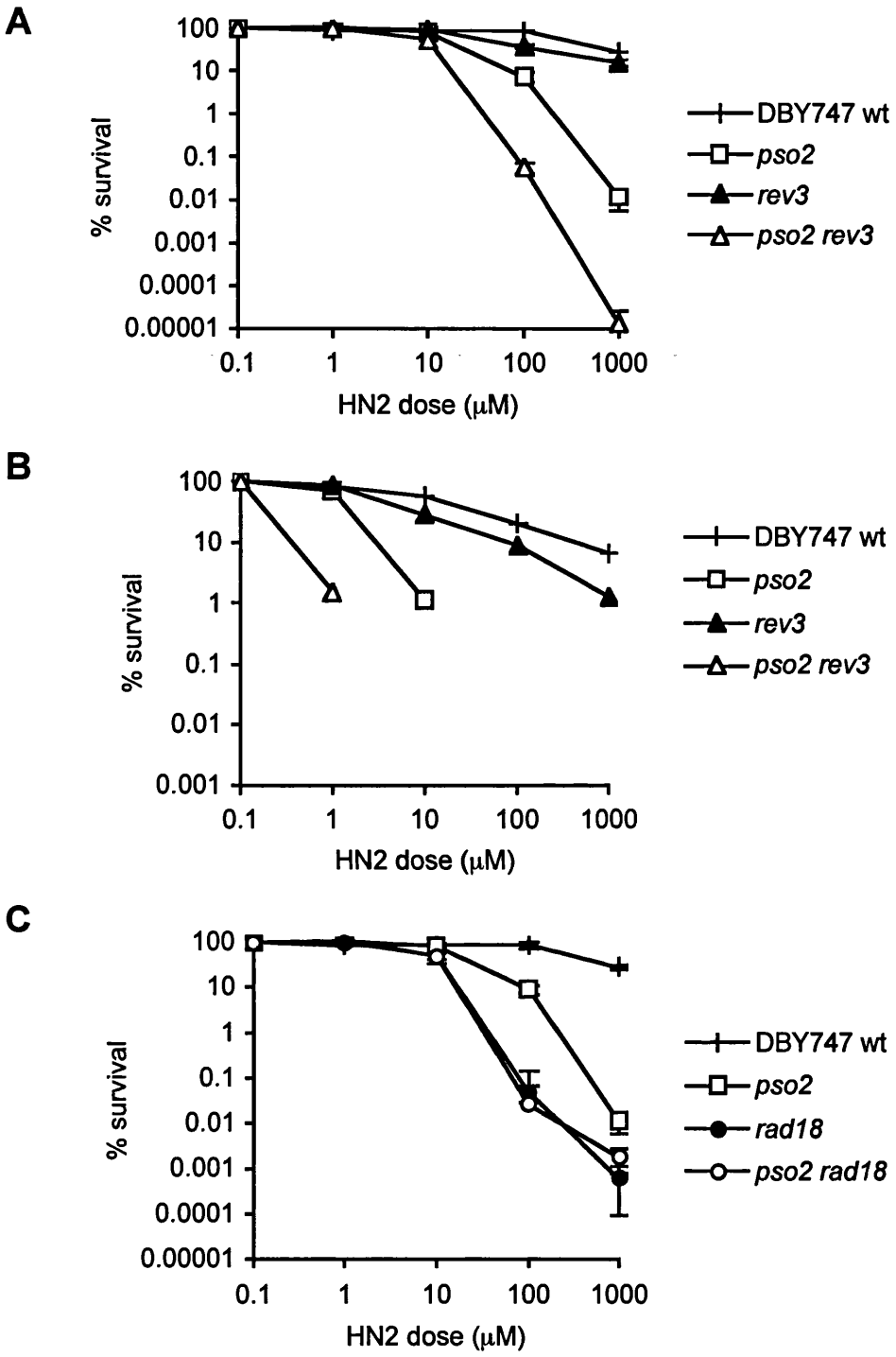

Figure 3.10 Comparison of HN2 sensitivity in pso2 and rev3, or rad18 (PRR) deficient cells. **A** and **C.** Exponential phase, **B.** G1-arrested cells were treated with 0 to 1000 μM HN2 for 1 h, and survival monitored by plating on YEPD. All results are the mean of at least three independent experiments, and the error bars show the SEM.

3.5.4 Loss of *PSO2* leads to increased mutagenesis, dependent on *REV3*

The *RAD6*/post-replication repair pathway is known to be important for the efficient processing of ICLs, as already discussed (Section 1.3.2). If *PSO2* were involved in mechanisms of ICL repair distinct from the *REV3*/error-prone sub-pathway, then in the absence of *PSO2*, mutagenic repair would be expected to predominate. The *CAN1* forward mutation assay is a convenient method for the analysis of mutagenicity, as it measures the frequency of gain of function mutations (Grenson et al., 1966; Crouse, 2000). This contrasts with other assays of mutagenesis such as *hom3-10* and *lys2ΔBgl*, which look for the reversal of an existing mutation, and as such can be compromised by the detection of suppressor mutations in addition to those in the original gene (Crouse, 2000). Briefly, *CAN1* encodes an arginine permease that is equally able to transport the toxic arginine-analogue L-canavanine. It follows that to survive in the presence of L-canavanine, cells must acquire mutations in the *CAN1* gene that prevent permease activity. It was necessary to conduct these experiments in the DBY747 genetic background that carries the *CAN1* wild-type allele, as the B356-7C/W303-1A background is *can1-100* and as such is already resistant to L-canavanine.

The frequency of *CAN1* forward mutation after treatment with increasing doses of HN2 was calculated as mutants per 10^8 survivors (Fig. 3.11). The *pso2* deficient strain shows a spontaneous mutation frequency around 2-fold higher than in the wild type DBY747. After treatment with HN2, *pso2* cells are hyper-mutagenic, with 4-times more mutations detected at 100 μM HN2 than for the parent strain. As expected, loss of *REV3* results in

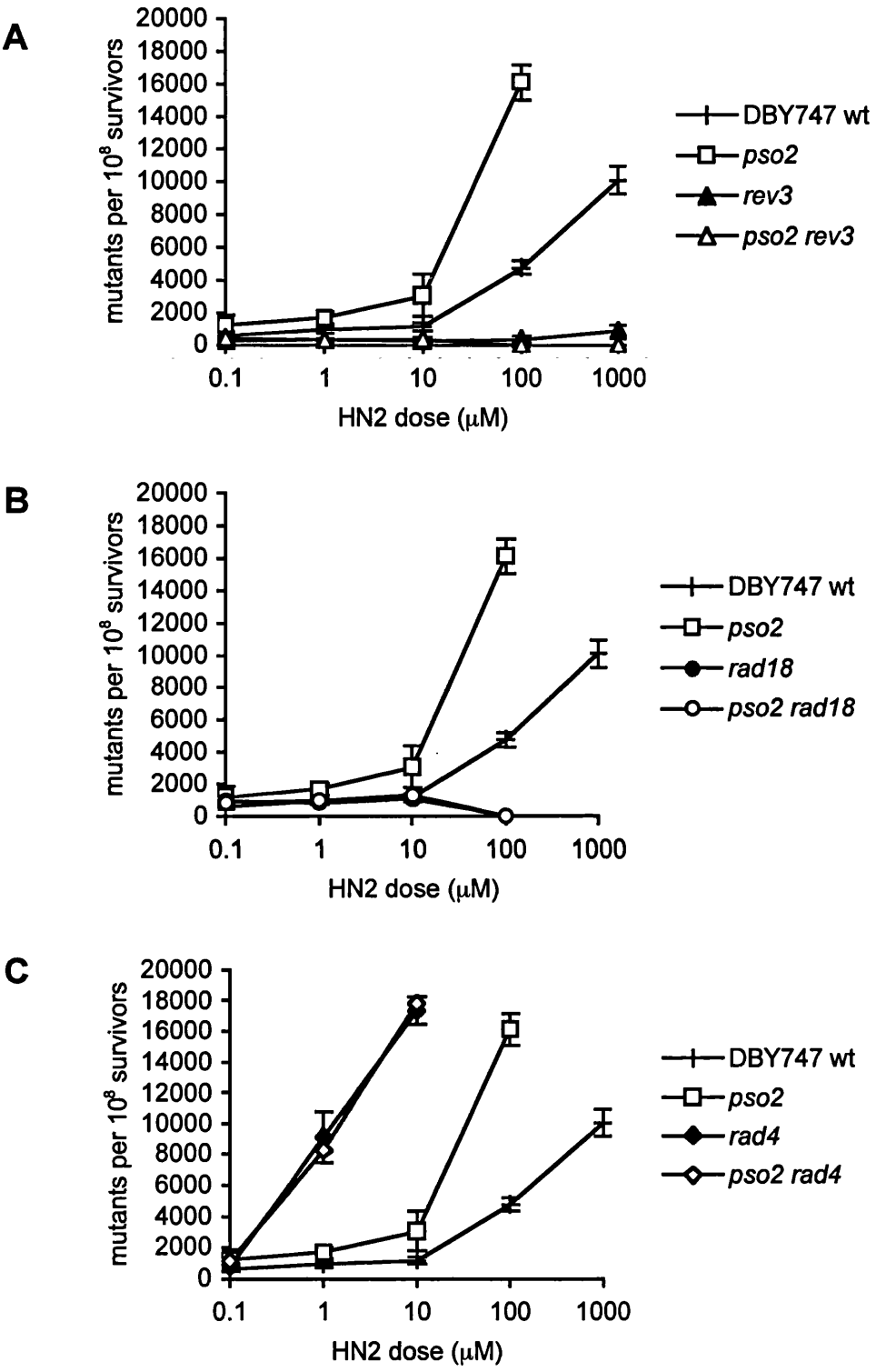

Figure 3.11 Mutagenesis in pso2, PRR, and NER mutants. Analysis of HN2-induced Can^R forward mutagenesis in *pso2* cells, compared with **A.** *rev3*, **B.** *rad18*, **C.** *rad4*, in the DBY747 background. Due to the logarithmic scale, spontaneous mutagenesis is plotted as 0.1 μM HN2. All results are the mean of at least 3 independent experiments, and the error bars represent the SEM.

a significantly lower mutation frequency, and no HN2-inducibile mutagenesis is seen (Fig. 3.11 A). The *pso2 rev3* double mutant exhibits an equally low rate of mutagenesis (Fig. 3.11 A) indicating that the elevated mutation frequency seen in *pso2* cells is entirely due to the activity of *REV3*. This implies that the *REV3*/error-prone repair pathway is an important compensation mechanism in the absence of *PSO2*.

Interestingly, mutation frequency in the *rad18* mutant strain does not fall below the wild-type level until 100 μM HN2 (Fig. 3.11 B), at which dose survival is negligible (Fig. 3.10 C). This confirms the observations published by Liefshitz *et al.* where hypomutagenesis was only observed in the absence of both *rad18* and *rad5* (Liefshitz *et al.*, 1998). A similar mutation frequency is observed in the *pso2 rad18* double disruptant (Fig. 3.11 B), confirming the role of the post replication repair pathway in the HN2-induced mutagenic phenotype of the *pso2* strain.

Mutation frequency was also analysed in a *rad4 pso2* double disruptant to observe whether the hyper-mutagenic phenotype was *PSO2*-specific. The *rad4* single mutant elicits a greater frequency of mutation at the *CAN1* locus than for *pso2*, even at a low dose of 1 μM HN2 where a 10-fold increase over the wild type mutation rate is seen (Fig. 3.11 C). This corresponds with the *CAN1* forward mutation frequency observed previously for another NER factor, *rad14* (McHugh *et al.*, 1999). It is clear from figure 3.11 C that the epistatic relationship between *PSO2* and *RAD4* for HN2 extends to induced mutagenesis, as no further increase in mutation frequency is seen in the double mutant compared to the *rad4* single. This implies that a deficiency in NER/*PSO2*-dependent ICL repair causes a diversion into the alternative *RAD6*/post-replication repair pathway, and in particular, the *REV3*/error-prone mechanism.

3.6 DSB repair is deficient in the absence of *PSO2*

The occurrence of DSBs has frequently been observed in eukaryotic cells following treatment with ICL-forming drugs, particularly HN2 (Akkari *et al.*, 2000; De Silva *et al.*, 2000; McHugh *et al.*, 2000). Furthermore, density gradient centrifugation experiments have suggested that repair of these breaks is deficient in the absence of *pso2* (Magana-Schwencke *et al.*, 1982; Wilborn and Brendel, 1989). A convenient technique for the visualisation of DSBs is contour-clamped homogeneous electric field (CHEF) pulsed field gel electrophoresis. In CHEF, yeast chromosomes appear as a distinct ladder of bands that are replaced by a smear of lower molecular weight material if DSBs are present. This procedure has been successfully used to study the occurrence of DSBs during the repair of ICLs (Averbeck and Dardalhon, 1990; Averbeck *et al.*, 1992; Dardalhon and Averbeck, 1995).

Here, CHEF is used to evaluate the formation and repair of DSBs after treatment with 100 μM HN2 in cells deficient in the major pathway of ICL repair, namely *pso2*, *rad4*, and *rad52*. Exponentially growing cells were treated with HN2 and subsequently allowed to repair for 2, 4, or 24 h in drug-free minimal nutrient medium (MM) that prevents DNA replication (Dardalhon and Averbeck, 1995), before analysing the chromosomal preparations on CHEF gels. Samples were not investigated at 0 h repair, as DSBs have not been detected immediately after treatment (P. McHugh, unpublished observations). In the repair competent wild-type strain, DSBs are observed 2 h after HN2 treatment with initiation of repair by 4 h and completion after a 24 h period (Fig. 3.12 A). In contrast, an increased yield of DSBs is apparent in the absence of *PSO2*, and very little repair is evident after 24 h (Fig. 3.12 A).

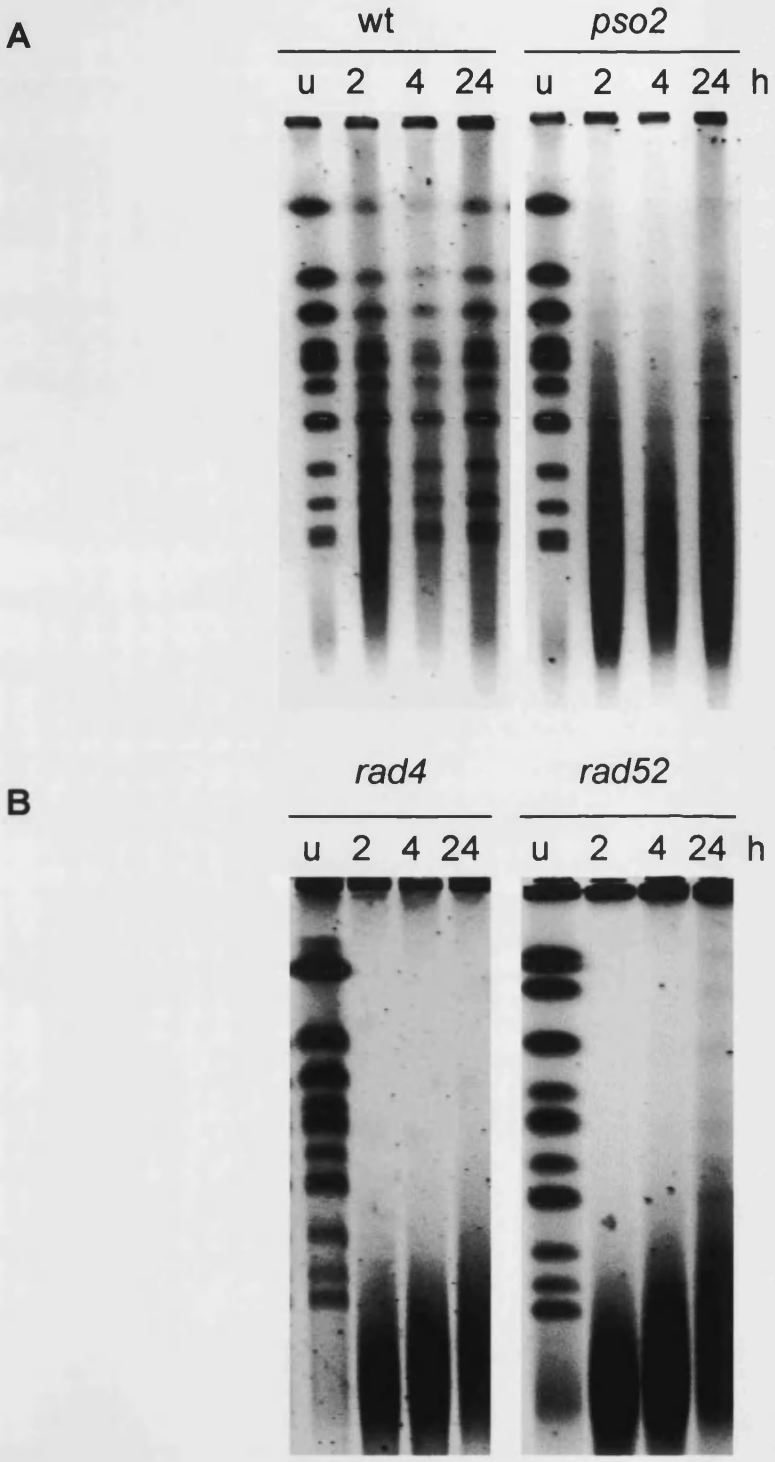

Figure 3.12 HN2-induced DSB repair in pso2, NER, and HR mutants. Exponential phase cells were treated with 100 μM HN2 for 3 h, and subsequently allowed to repair in minimal media for 2, 4, or 24 h. Mock treated (u) cells were allowed to repair for 24 h. Chromosomal preparations were analysed by CHEF, and typical gels are shown. **A**. DBY747 wt and *pso2* strains. **B**. *rad4* and *rad52* deficient cells.

The appearance and subsequent repair of DSB arising from ICLs has previously been investigated to some extent in cells deficient in the major repair pathways (McHugh *et al.*, 2000; Dardalhon and Averbeck, 1995). However, for completion, *rad4* and *rad52* disruptant strains representing NER and homologous recombination repair, respectively, were also considered here. It is clear from figure 3.12 B that the *rad4* and *rad52* strains are deficient in DSB repair. Strikingly, the *rad4* mutant appears less able to repair ICL-associated DSBs than the recombination-defective *rad52*, as a small proportion of intact chromosomes have been recovered by 24 h in *rad52* cells, whereas the *rad4* chromosomes remain completely degraded. Furthermore, the *rad4* strain exhibits a greater accumulation of DSBs and a reduced capability for repair than *pso2* (cf. Fig. 3.12 A).

3.7 Discussion

After decades of inconclusive investigation into the precise role of *PSO2*, it was prudent to revisit some of the published data using defined isogenic disruption strains and techniques, in order to unambiguously define the *pso2* mutant phenotype. It is clear from the data accumulated from microscopy, culture density, and drug-induced arrest assays (Section 3.2) that loss of *pso2* does not affect the normal progression of the cell cycle, compared to the wild-type parent strain. However, it was beyond the scope of this thesis to conduct a detailed study of the cell cycle response to ICL damage. Such an investigation has been performed concurrently in Oxford, using confocal microscopy and FACS (fluorescent activated cell sorting) analysis, with the conclusion that a deficiency in *pso2* does not lead to irregular cell division or cell cycle arrest (S. Sarkar, J. Sidebotham and P. McHugh, personal communication). Hence the response to

nitrogen mustard appears to differ to some extent from that observed with cisplatin, where cells have been reported to arrest in G2 (Grossmann *et al.*, 2000).

Despite the putative interaction between Pso2 and Mgm101 identified in large-scale proteomic screens (Ho *et al.*, 2002), the activity of Pso2 appears to be primarily nuclear rather than within the mitochondria (Section 3.2.3). This correlates with the PSORTII prediction of 56.5 % that Pso2 is localised to the nucleus, compared to a 34.8 % likelihood of localisation to the mitochondria. Furthermore, although assigned to the mitochondrion, the high-throughput mass spectrometry screen also detected an association of YHR076W with the nuclear factors Rad26 (DNA repair) and Drc1 (a replication fork progression factor) (Ho *et al.*, 2002). Likewise for Mgm101, which was discovered in complexes with Mus81 (DNA repair) and Rfa2 (a subunit of replication factor A involved in replication, recombination, and repair) (Ho *et al.*, 2002), and in a similar independent screen with Msh6 (DNA repair) (Gavin *et al.*, 2002). Interestingly, some of these protein complexes were only detected after treatment of the cells with DNA damaging agents. The association of Pso2 with YHR076W was observed after exposure to 4-nitroquinoline 1-oxide, a UV radiation-like drug that produces bulky base damage and significant DNA strand breakage (Ho *et al.*, 2002). Similarly, the interactions of Mgm101 with Mus81 and Rfa2, and YHR076W with Drc1, were found after treatment with the alkylating agent MMS (Ho *et al.*, 2002). Hence it is equally possible that the involvement of Pso2 with Mgm101 and YHR076W occurs within the nucleus, or that a number of nuclear factors have as yet undefined additional roles within the mitochondrion. It is appreciated that such high-throughput screens are susceptible to spurious results, and that further research is necessary to elucidate any involvement of *PSO2* with these mitochondrial genes.

Nevertheless, this research has concentrated on the known requirement for *PSO2* in the repair of cross-linked nuclear DNA.

As discussed in Chapter 1, the *PSO2* gene was originally isolated as a result of its novel mutant phenotype, namely a specific sensitivity to agents that induce DNA ICL, but no susceptibility to any other form of DNA damage. In the course of this work, new *pso2* deletion strains have been produced in 3 different yeast genetic backgrounds. Some variability was observed in the degree to which these strains are sensitive to HN2 (Section 0), however, considerable strain differences have been reported previously for other gene deletants, such as *rad26* strains irradiated with UVC (Gregory and Sweder, 2001). Furthermore, aneuploidy has been detected in a number of BY4743 (diploid) strains arising from the EUROSCARF project, not all of which could be explained as a result of the known gene deletion (Hughes et al., 2000). Hence the augmented HN2 sensitivity of the BY4741 *pso2* strain may be due to inappropriate expression of other genes responsible for repair of DNA ICL. As an additional confirmation of the reliability of these gene disruptants, a brief study was undertaken to determine sensitivity to the cross-linking drug HN2, as well as X-rays and UVC-irradiation. Consistent with published data, these *pso2* mutants solely exhibited a significantly diminished degree of survival following treatment with HN2 (Section 3.2.4). The mild (5-fold) increase in sensitivity to high doses of UV in the *pso2* mutant is comparable to that observed by Ruhland and co-workers (Ruhland *et al.*, 1981 A).

PSO2 has previously been assigned to the NER epistasis group on the basis of sensitivity to ICL-forming agents in strains disrupted for *pso2* and *rad1/rad2/rad3*. Early HN2-sensitivity analysis of the original *pso2* isolates had shown that a *pso2 rad1*

rad2 triple mutant strain is epistatic to a *rad1 rad2* double disruptant (Siede and Brendel, 1982). Concurrent studies relating to the ICL-inducing agent psoralen demonstrated an epistatic relationship between *PSO2* and the NER gene *RAD3* (Henriques, 1981). This relationship has been confirmed here for an additional NER factor, *rad4* (Section 3.3.1). Furthermore, it has been shown that both *PSO2* and NER factors are required for the efficient repair of DSBs associated with cross-links (Section 3.4). Hence *PSO2* and NER must act in a single pathway for the repair of ICL. However, Pso2 must act downstream of NER as *pso2* mutants are proficient in the incision of ICL, whereas components of the NER apparatus are essential (Grossmann *et al.*, 2000; Magana-Schwencke et al., 1982; Wilborn and Brendel, 1989; Meniel *et al.*, 1995). The prevailing theory for the mechanism of ICL repair in yeast, and indeed all eukaryotes, has been derived from the well-established system in *E. coli*, in which cross-links are incised by the NER apparatus (potentially a specialised XPF-ERCC1 dependent reaction in mammals) and resected, with the subsequent intermediate targeted by recombination. It would seem that *PSO2* acts in concert with NER in the early stages of this pathway. However, if as proposed, the downstream events were accomplished by homologous recombination, an epistatic relationship would be expected between *PSO2* and key genes in this pathway. This is clearly not the case (Section 3.3.2; Siede and Brendel, 1982), and suggests that, in contrast to bacteria, the NER-*PSO2* system of ICL repair must be independent of recombination in yeast (Grossmann *et al.*, 2001).

An alternative explanation for the increased sensitivity of *pso2*-recombination double deficient cells to ICL-forming agents could be that some recombination events occur at cross-links independently of NER-*PSO2*. It is possible that such a mechanism may only

act to tolerate lesions and hence salvage cells in the absence of an effective NER-*PSO2* pathway. The observation that the NER genes *rad4* (Section 3.3.2) and *rad14* (P. McHugh, personal communication) also fail to exhibit an epistatic relationship with recombination for ICL repair supports this revised model. Furthermore, like *rad52* strains, both *pso2* and NER defective cells have been shown to accumulate DSBs after treatment with HN2, and these fail to be repaired (Section 3.4). This corresponds with the findings of a recent report by Li and Moses (2003), and also corroborates the evidence from density gradient centrifugation experiments (Magana-Schwencke *et al.*, 1982; Wilborn and Brendel, 1989) for the persistence of ICL-associated DSBs in *pso2* mutant cells. The DSB repair deficiency in *rad4* cells has been confirmed in a further NER mutant, *rad14* (P. McHugh, unpublished data) that is also required for recognition and binding to damaged DNA. DSBs are known to be a potent trigger for recombination events. It is hard to imagine how NER factors and *PSO2* alone would be able to resolve these DSBs if recombination acted in a totally independent pathway of ICL repair. It is unlikely that ICL-associated DSBs are repaired by non-homologous mechanisms, as mutations in genes of the NHEJ pathway do not render cells sensitive to cross-links (McHugh *et al.*, 2000).

There is yet further evidence to support the involvement of recombination with NER-*PSO2* in ICL repair. In repair proficient yeast cells, diploids exhibit an increased resistance to ICL compared to haploid cells. This ploidy-related resistance to cross-links is believed to result from the greater potential for homologous recombination utilising the homologous chromosome. A loss of *pso2* corresponds with a loss of ploidy-related resistance to 8-methoxypsoralen plus UVA, and an absence of the normal resistant fraction in G2 relative to stationary phase cells (Cassier *et al.*, 1980; Henriques

and Moustacchi, 1980). Given that no reduction in sporulation efficiency was observed, the authors concluded that *PSO2* was likely to be involved in a specific step in mitotic DNA repair. These characteristics reflect those seen in recombination-defective mutants in response to ionising radiation, where both diploid and haploid G2-associated resistance is absent (Bressan *et al.*, 1990; Mortimer, 1958; Saeki *et al.*, 1980). Together with the DSB repair deficiency observed here, this is strongly indicative of a requirement for homologous recombination in the *PSO2*-dependent pathway of ICL repair.

Previous investigations into the relationship between *PSO2* and the *RAD6*/post-replication repair system have produced conflicting data. Siede and Brendel (1982) demonstrated a synergistic interaction between two independent *pso2* mutant alleles and either *rad6*, or *rad18*, in stationary phase yeast cells treated with HN2. Henriques and Moustacchi (1981) also found *pso2* and *rad6* to be synergistic for 8-methoxypsoralen (8-MOP) photoaddition in stationary phase cells, yet they observed an epistatic relationship between *pso2* and *rev3*. More recently, Grossmann and co-workers have shown synergism for exponentially growing *pso2* and *rev3* cells exposed to cisplatin or 8-MOP (Grossmann *et al.*, 2001). Post-replication repair is believed to play a greater role in the response to ICL damage in stationary phase haploid cells, as no substrate is available for homologous recombination (McHugh *et al.*, 2000). Hence, the genetic interaction between *PSO2* and *REV3* was considered in both exponential and stationary growth conditions. A synergistic relationship was observed in both cases, indicating that *PSO2*-dependent repair of ICL is distinct from DNA polymerase ζ mediated post-replication repair (Section 3.3.3). Further evidence to support this observation was obtained from the analysis of HN2-induced mutagenesis. If these two pathways were

indeed distinct, then it would be assumed that in the absence of *PSO2*, repair would be channelled into the post-replication pathway, leading to increased mutagenesis. This phenomenon was clearly observed (3.3.4), and suggests that the *REV3*-dependent error-prone repair branch of post-replication repair is required for *PSO2*-independent repair of ICLs.

The novel observation that *PSO2* is epistatic to *RAD18* in exponentially growing cells is particularly interesting with regards to published work suggesting an interaction between *RAD18* and NER in the repair of minor groove adducts that prevent efficient DNA strand separation (Kiakos *et al.*, 2002). It was proposed by the authors that Rad6-Rad18 and Rad5 might be required to target repair factors to lesions that are poorly displayed or prevent effective strand separation. Cross-links by definition prevent the separation of DNA strands, and so it is entirely conceivable that *RAD18* may be required in the initial stages of ICL recognition and repair. One possibility is that as the cross-link is bound to both strands of DNA, ICL repair may require a combined recombination/bypass pathway, which is dependent upon both Rad18 and Rad52, in addition to initial processing by NER-Pso2 (discussed in more detail in Chapter 6).

Homologues of *PSO2* have been identified throughout the eukaryotic kingdom from yeast to humans. However, complementation between these homologues has yet to be fully determined. Indeed, mouse embryonic stem cells null for the paralogue *PSO2* only appear to be sensitive to mitomycin C (of the cross-linking agents tested) (Dronkert *et al.*, 2000). It is possible that this may result from a functional redundancy between the multiple murine *PSO2* homologues, however this theory remains to be verified. Here, a *pso2* deficient *Schizosaccharomyces pombe* strain is presented that is

sensitive to HN2, but not the monofunctional derivative HN1. This study was performed in collaboration with Professor Tony Carr, who further confirmed the extent to which these two yeasts share an identical *pso2* phenotype. In *S. pombe*, as for *S. cerevisiae*, *pso2* defective cells were shown to be sensitive to the ICL-inducing agents cisplatin and MMC, but not UVC, gamma radiation, HU, and camptothecin (Lambert *et al.*, 2003). This represents the first identification of an evolutionarily distinct *PSO2* homologue with the same mutant phenotype as in *S. cerevisiae*, and provides an additional model organism through which the role of *PSO2/SNM1* in DNA repair may be elucidated.

CHAPTER 4 INTERACTIONS OF *PSO2* WITH YEAST REPAIR NUCLEASES

As discussed in Chapter 3, the nature of interaction of *PSO2* with genes of the NER and homologous recombination pathways suggests that Pso2 acts at some intermediate stage of repair, downstream of the initial incision event, but prior to reconstitution of high molecular weight DNA. It is plausible that the DNA product resulting from incision is unsuitable as a substrate for recombination, and so requires further processing before strand invasion can occur. Indeed, it is already established that the 5' to 3' exonuclease activity of DNA polymerase I is required to resect the incised strand during ICL repair in *E. coli* (Sladek *et al.* 1989), and that this is a prerequisite for subsequent strand-invasion mediated by RecA (van Houten *et al.*, 1986). The classification of *PSO2* as a β-CASP metallo-β-lactamase also supports the hypothesis that Pso2 may be involved in resection of the incised cross-link as to date, all other eukaryotic members of this family have been shown to act nucleolytically (Callebaut *et al.*, 2002).

The relationship of *PSO2* with the known yeast repair nucleases *EXO1*, *MRE11*, *RAD27*, and *RAD1* was therefore investigated. Exo1 is a 5'-3' exonuclease implicated in DNA replication, homologous recombination, and mismatch repair (Tishkoff *et al.*, 1997 A). Mre11 has been shown to possess 3' to 5' exonuclease and an endonuclease activity, and is involved in DSB resection and the S-phase checkpoint as a complex with Rad50 and Xrs2 (Usui *et al.*, 1998; Haber, 1998). Rad27, the yeast homologue of mammalian *FEN1* (Greene *et al.*, 1999), has 5'-3' exonuclease and flap endonuclease activity required for Okazaki fragment processing in DNA replication and also in BER

(Reagan *et al.*, 1995; Sommers *et al.*, 1995). Rad1 forms a complex with Rad10 to form a structure specific endonuclease that cuts 5' to the lesion in NER (Bardwell *et al.*, 1992), and is also involved in cleavage of 3' non-homologous tail structures during the single strand annealing recombination pathway (Fishmann-Lobell and Haber, 1992; Schiestl and Prakash, 1988; Tomkinson *et al.*, 1993). A panel of single and multiple gene deletions encompassing these factors and *PSO2* was established in the isogenic background B356-7C, as described in Section 3.5.

4.1 Repair of nitrogen mustard-induced DNA ICL

4.1.1 *PSO2* exhibits significant synergism with *EXO1*

In the first instance, *S. cerevisiae* strains deficient for nuclease activities and *PSO2* were treated with HN2, and sensitivity was compared to their respective single mutant parents (Fig. 4.1). Given that *RAD1* belongs to the NER repair group, an epistatic relationship with *PSO2* would be expected, as has already been established for *RAD4* (Section 3.5.1). As can be seen from figure 4.1 A, *rad1* cells are more sensitive to HN2 than *pso2* mutants, and the double disruptant exhibits a moderate (less than 10 fold) increase in sensitivity. The magnitude of this increase is not sufficiently large to indicate additivity, but presumably reflects the involvement of *RAD1* in a minor, recombination-dependent repair pathway, that acts on ICL lesions in the absence of *PSO2*. It is noteworthy, however, that *rad1* is equally sensitive to HN2 as *rad4* (Fig. 4.1 A, E), exhibiting 2.1 and 3.5 x 10^5 % survival, respectively, at 1000 μM HN2. This

A

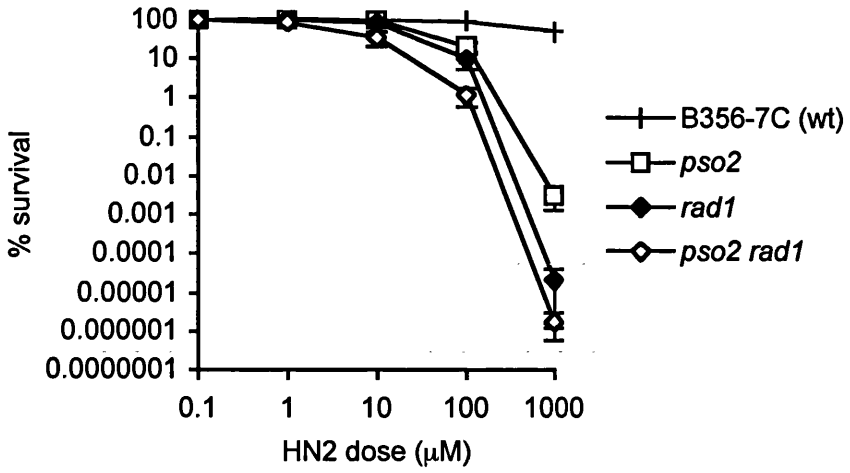
100
10
1
0.1
0.01
0.001
0.0001
0.00001
0.000001
0.0000001
% survival
0.1
1
10
100
1000
HN2 dose (μM)
B356-7C (wt)
pso2
rad1
pso2 rad1

B

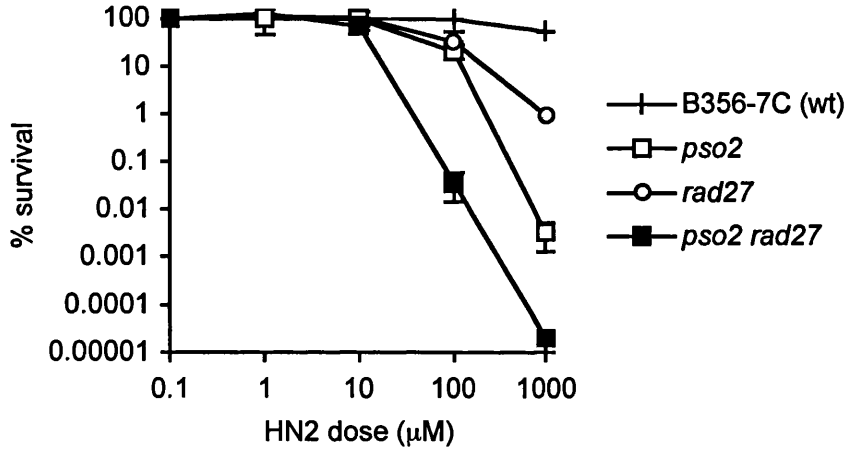
100
10
1
0.1
0.01
0.001
0.0001
0.00001
% survival
0.1
1
10
100
1000
HN2 dose (μM)
B356-7C (wt)
pso2
rad27
pso2 rad27

C

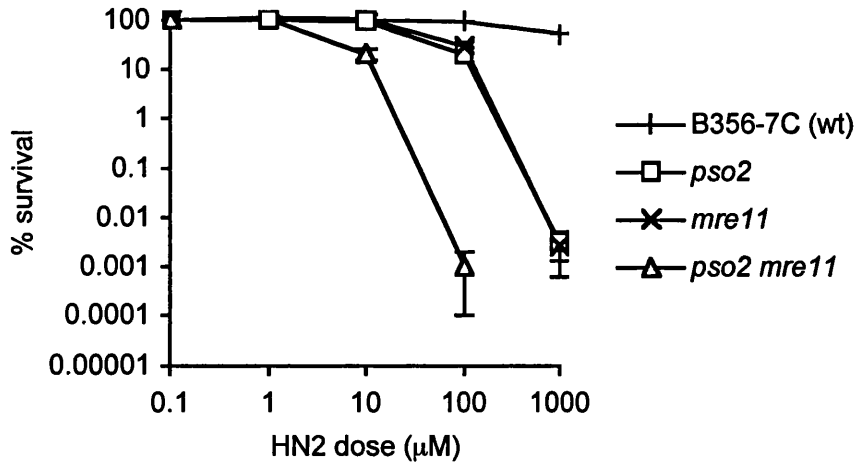
100
10
1
0.1
0.01
0.001
0.0001
0.00001
% survival
0.1
1
10
100
1000
HN2 dose (μM)
B356-7C (wt)
pso2
mre11
pso2 mre11

D

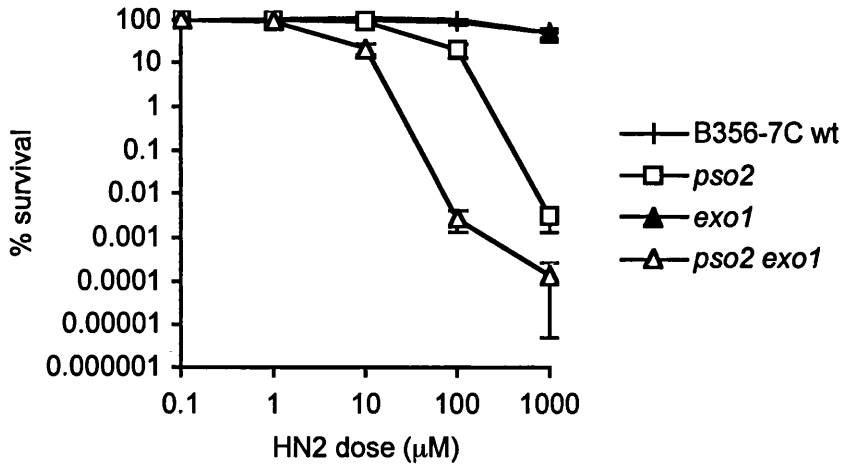

E

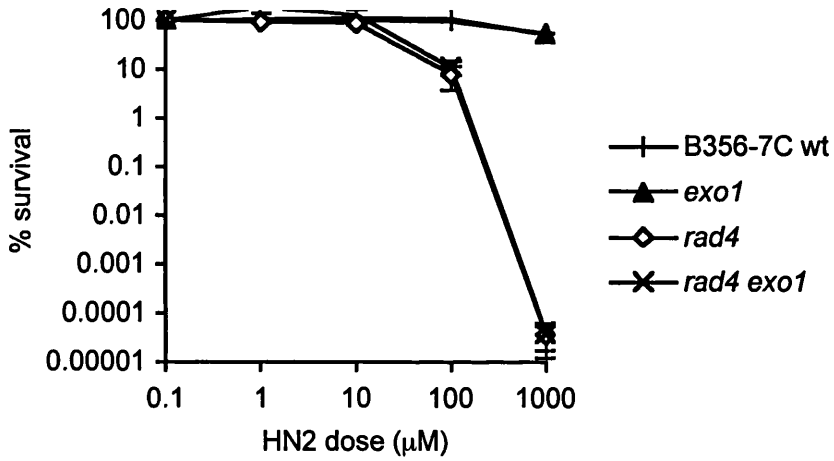

Figure 4.1 Comparison of HN2 sensitivity in pso2 and nuclease mutants. Exponential phase parental B356-7C, single and double mutant cells were treated with 0 to 1000 μM HN2 for 1 h, and survival monitored by plating on YEPD. Comparisons of *pso2* with: **A.** *rad1*, **B.** *rad27*, **C.** *mre11*, **D.** *exo1*. **E.** *exo1* with *rad4*. All results are the mean of at least three independent experiments, and the error bars show the standard error of the mean (SEM).

suggests that *RAD1*-dependent recombination is not significant for ICL repair in the presence of functional *PSO2*. A loss of *RAD27* leads to a mild sensitivity to HN2 (Fig. 4.1 B), indicating some involvement in ICL repair, as has been reported previously (McHugh *et al.*, 2000). The sensitivity of the *pso2 rad27* double mutant to HN2 is approximately equivalent to the sum of the individual mutant sensitivities, particularly at the highest dose (Fig. 4.1 B). Hence, *PSO2* shows an additive association with *RAD27*, as would be expected for genes operating in different repair capacities.

In contrast, *PSO2* acts synergistically with both *MRE11* and *EXO1* for HN2 sensitivity (Fig. 4.1 C, D). At 100 μM HN2, the *pso2 exo1* and *pso2 mre11* double mutants exhibit 10,000-fold greater sensitivity than the *pso2* strain alone, and no survivors were obtained from 2 x 10^7 double-disruptant cells treated with 1000 μM HN2. This relationship is most striking for *EXO1*, as unlike *mre11*, the *exo1* single mutant demonstrates wild-type resistance to HN2 (Fig. 4.1 D). Indeed, the *mre11* strain is as sensitive to HN2 as other recombination defective mutants such as *rad51* and *rad52*, and the corresponding double disruptants with *pso2* give similar phenotypes for HN2 sensitivity (cf. Fig. 3.9 A, B). It follows that the synergism existing between *PSO2* and *MRE11* is more likely to reflect the involvement of Mre11 in recombination events, rather than specifically its nuclease activity. The synergism with *EXO1* is interesting as it intimates that, although Exo1 does not play an essential role in the repair of ICL, as some degree of sensitivity would be expected for *exo1*, it may be able to compensate for the loss of Pso2 to some extent, and therefore may have a similar mode of activity, potentially a nuclease function.

As *PSO2* is generally assigned to the NER epistasis group, the relationship between *EXO1* and *RAD4* was investigated to determine whether the overlap of activity with Exo1 is specific to Pso2 rather than NER as a whole. It is clear from figure 4.1 E that the *rad4 exo1* double disruptant does not exhibit increased sensitivity to HN2, and hence synergism with *EXO1* is not observed with the NER repair group in general. Hence, for the first time, separation of function is presented genetically for *PSO2* and genes of the NER pathway during ICL repair.

4.1.2 *PSO2* also acts synergistically with *MSH2*

Exo1 has been shown to interact physically with Msh2 and Mlh1 by co-immunoprecipitation and two-hybrid analysis (Tishkoff *et al.*, 1997 A; Tran *et al.*, 2001). A recent study has shown that Msh2, as part of the MutSα complex, acts to regulate the 5'-3' exonucleolytic activity of Exo1 during mismatch repair (Genschel and Modrich, 2003). Exo1 is known to be required for the processing of DSBs (Tsubouchi and Ogawa, 2000), and it has also been suggested that the Msh2-Msh3 (MutSβ) heterodimer is recruited to DSBs and branched DNA structures, with a possible role in the promotion of cleavage by the Rad1-Rad10 endonuclease (Sugawara *et al.*, 1997; Evans *et al.*, 2000). Consequently, the relationship of *PSO2* with *MSH2* was investigated, to determine whether a *pso2 msh2* double mutant would phenocopy *pso2 exo1* cells for sensitivity to HN2. Figure 4.2 A shows a similar pattern of interaction between *PSO2* and *MSH2* as with *EXO1*. The single *msh2* mutant demonstrates an almost wild-type level of resistance to HN2, similar to the *exo1* mutant (Fig. 4.1 D). The double disruptant *pso2 msh2* is significantly more sensitive than the *pso2* strain

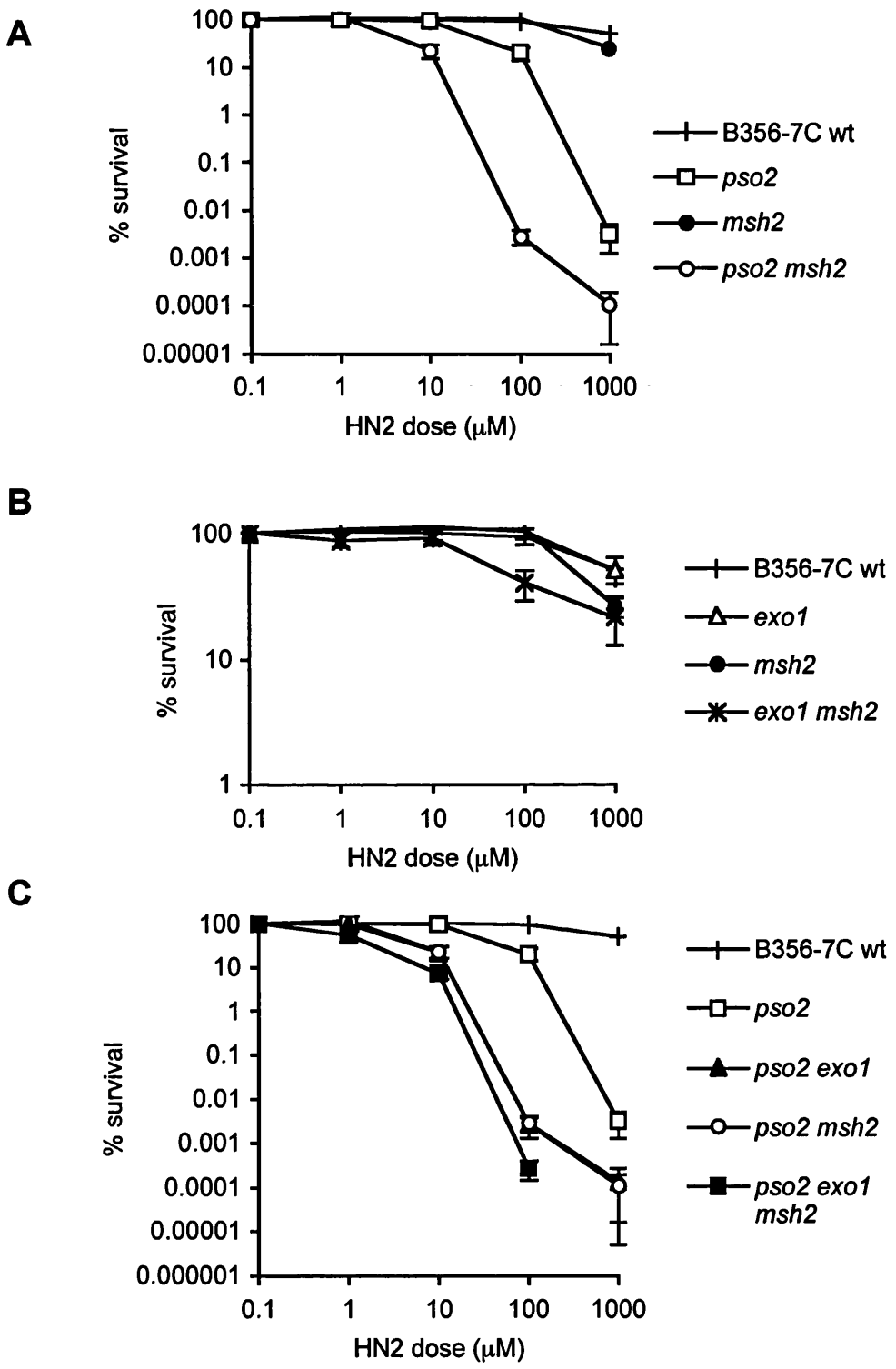

Figure 4.2 Comparison of HN2 sensitivity in pso2 and msh2 mutants. Exponential phase cells were treated with 0 to 1000 μM HN2 for 1 h, and survival monitored by plating on YEPD. Comparisons of : **A.** *pso2* with *msh2*, **B.** *exo1* with *msh2*, **C.** double and triple disruptants. All results are the mean of at least three independent experiments, and the error bars show the SEM.

(Fig. 4.2 A), exhibiting a 10,000-fold increase in sensitivity at 100 μM HN2, equal to that observed for *pso2 exo1* cells.

An *exo1 msh2* double mutant demonstrates near wild-type resistance to HN2 (Fig. 4.2 B), consistent with epistasis amongst these genes in the response to ICLs. A triple mutant, *pso2 exo1 msh2* was also tested for sensitivity to HN2 (Fig. 4.2 C). Although a very slight increase in sensitivity was seen, this probably only reflects the variability in this experimental system, especially given the moderate differences between the *pso2 exo1* and *pso2 msh2* sensitivities to HN2 at the intermediate doses. Furthermore, this increase is not significant enough to be considered as non-epistatic. Hence, it would seem that Exo1 and Msh2 are jointly involved in the repair of DNA cross-links in a mode that overlaps with the activity of Pso2.

4.2 Sensitivity to other DNA damaging agents

Given the well-established *pso2* mutant phenotype of specific sensitivity to DNA cross-links, yet the apparent non-essential role of Exo1-Msh2 in ICL repair, it was important to establish whether the observed overlap of activity between *PSO2* and *EXO1/MSH2* was exclusive to the repair of ICL. A range of cytotoxic agents was considered, including other DNA damaging agents (X-irradiation and UVC) and also inhibitors of cell cycle progression (Hydroxyurea and Benomyl).

4.2.1 Loss of both *PSO2* and *EXO1/MSH2* causes increased sensitivity to ionising radiation

The *pso2 exo1* and *pso2 msh2* double disruptants, and corresponding single gene mutants, were exposed to X-irradiation. As demonstrated in Section 3.3 for *pso2* mutants, the phenotypes of *exo1* and *msh2* deficient cells also resemble that of the wild-type parent strain (Fig. 4.3 A, B). Hence, neither gene is required for the repair of DNA lesions arising from ionising radiation. Yet it is clear from figure 4.3 A and B that both the *pso2 exo1* and *pso2 msh2* double mutants are sensitive to X-irradiation. This increased sensitivity is more pronounced in the case of *pso2 msh2* than *pso2 exo1* (5 x and 2 x more sensitive, respectively). It is clear that, although significant, these increases in sensitivity are mild compared to the extreme sensitivity of the recombination-defective *rad52* strain (Fig. 4.3 C). Interestingly, *PSO2* appears epistatic to *RAD52* for the repair of ionising radiation, as a *pso2 rad52* double mutant does not further impair the *rad52* strain. Therefore, any involvement of *PSO2* in the repair of X-irradiation-induced DNA damage must be co-operative with homologous recombination.

It is well established that the cytotoxicity of ionising radiation primarily results from the induction of DSBs, and that homologous recombination is the principal DSB repair pathway in yeast (van Gent *et al.*, 2001). To confirm the important finding that the overlap of activity between *PSO2* and *EXO1/MSH2* extends to the repair of lesions arising from ionising radiation, the analyses of sensitivity to X-irradiation were repeated in a different *S. cerevisiae* genetic background, BY4741. It can be seen from figure 4.3

A

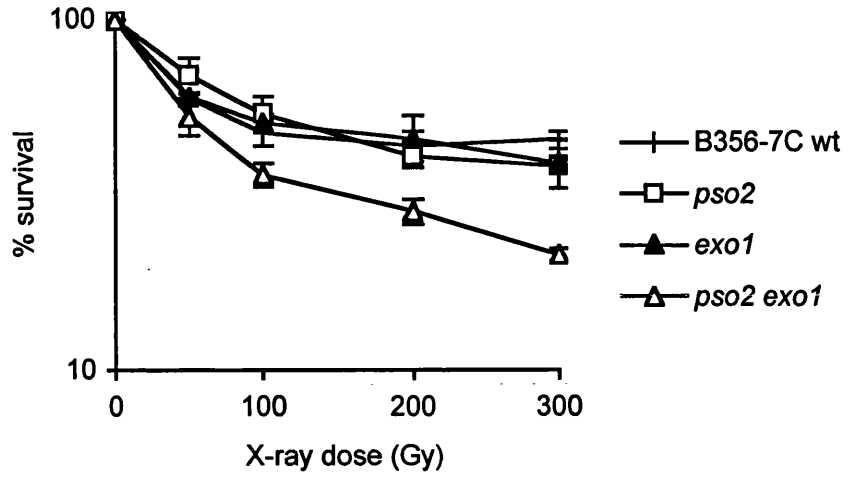
100
10
% survival
0
100
200
300
X-ray dose (Gy)
B356-7C wt
pso2
exo1
pso2 exo1

B

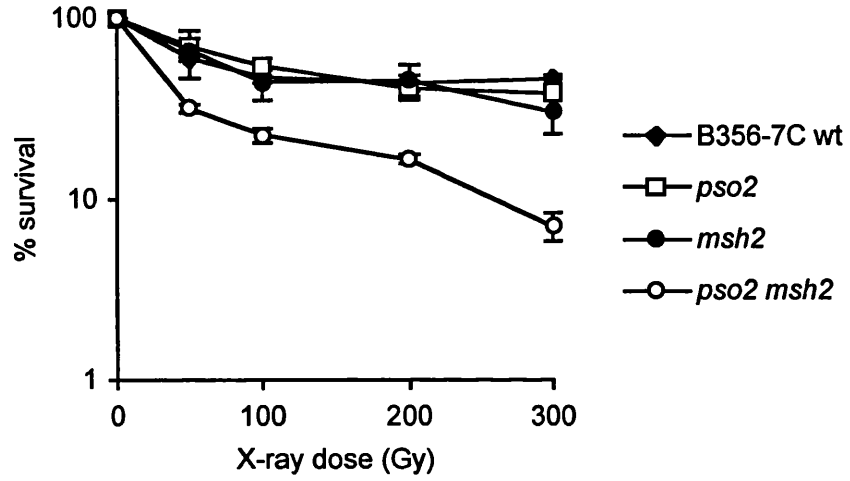
100
10
1
% survival
0
100
200
300
X-ray dose (Gy)
B356-7C wt
pso2
msh2
pso2 msh2

C

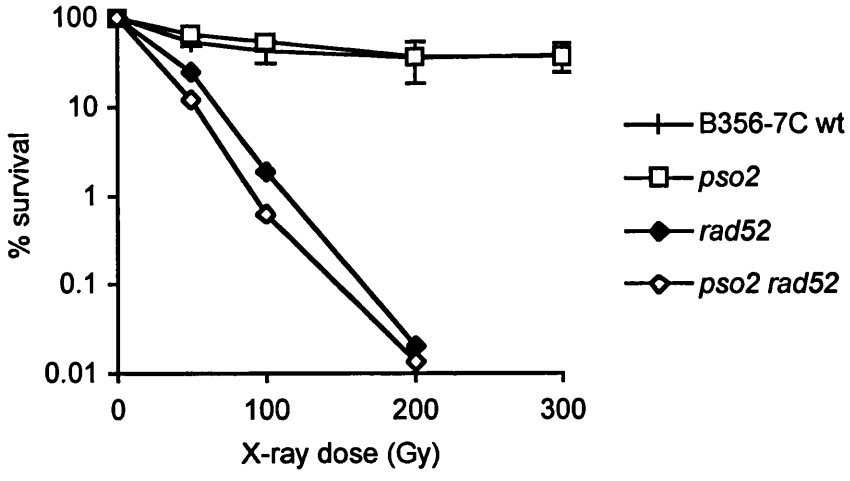
100
10
1
0.1
0.01
% survival
0
100
200
300
X-ray dose (Gy)
B356-7C wt
pso2
rad52
pso2 rad52

D

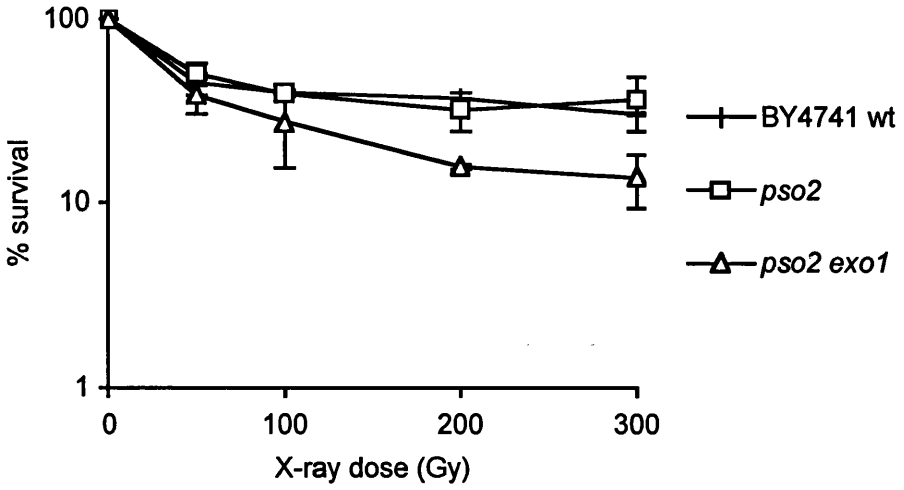

E

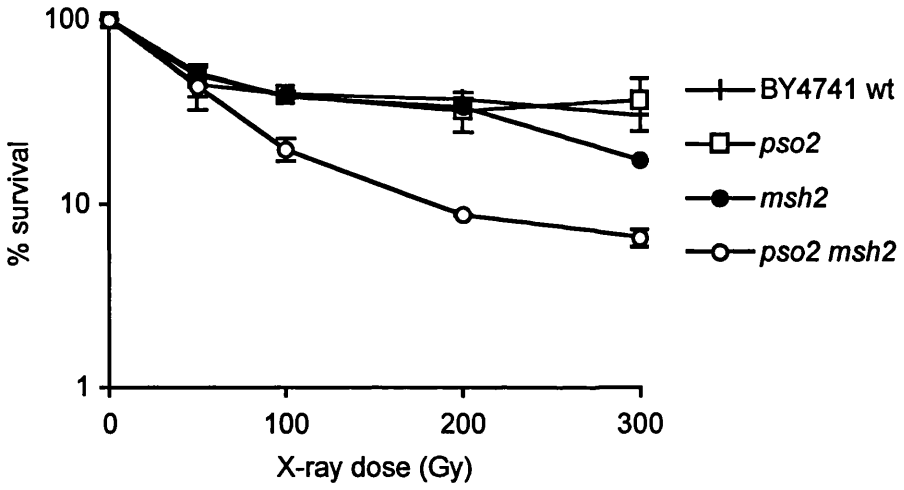

Figure 4.3 Comparison of X-irradiation sensitivity in pso2, exo1, msh2, and rad52 mutants. Exponential phase parental, single and double mutant cells were treated on ice with 0 to 300 Gy X-irradiation at a dose rate of 2.5 Gy/min, with survival monitored by plating on YEPD. Comparisons of *pso2* with: **A.** *exo1*, **B.** *msh2*, **C.** *rad52*, **D.** *exo1* (BY4741), **E.** *msh2* (BY4741). All results are the mean of at least three independent experiments, and the error bars show the SEM.

D and E that an identical result was obtained in this strain, implying that the increased sensitivity observed in the *pso2 exo1* and *pso2 msh2* double mutants is solely related to these genetic factors. The discovery that *PSO2* appears to have an overlap of activity with *EXO1/MSH2* for the repair of ionising radiation-induced DNA damage is suggestive of a more fundamental, possibly DSB-associated, repair defect in the absence of both pathways.

4.2.2 *PSO2* and *EXO1/MSH2* are not synergistic for the repair of DNA damage associated with UVC

It has already been ascertained that loss of *PSO2* results in a mild sensitivity to high doses of UVC (Fig. 3.6 A). It was therefore prudent to determine whether a further deficiency in *EXO1/MSH2* would exacerbate this condition. The double disruptants *pso2 exo1* and *pso2 msh2* were exposed to UVC and the resulting sensitivities were compared to those of the respective single mutants. It is clear from figure 4.4 that neither *exo1* nor *msh2* single mutants are sensitive to UVC. The *exo1* strain appears indistinguishable from the wild-type, whereas *msh2* cells show a slight resistance over this UVC dose range. This result is contrary to the report published by Qiu and co-workers (1998) in which *exo1* and *msh2* deficient yeast strains exhibited a mild sensitivity to UV, however, this was primarily observed at high doses (in excess of 100 J/m^2), and not in the range presented here. No increase in sensitivity to UVC is observed in either the *pso2 exo1* or *pso2 msh2* double disruptant strains, compared to the respective single mutants (Fig. 4.4). Hence neither *PSO2* nor *EXO1/MSH2* play a role in the repair of UVC-induced DNA damage. Although it remains possible that a

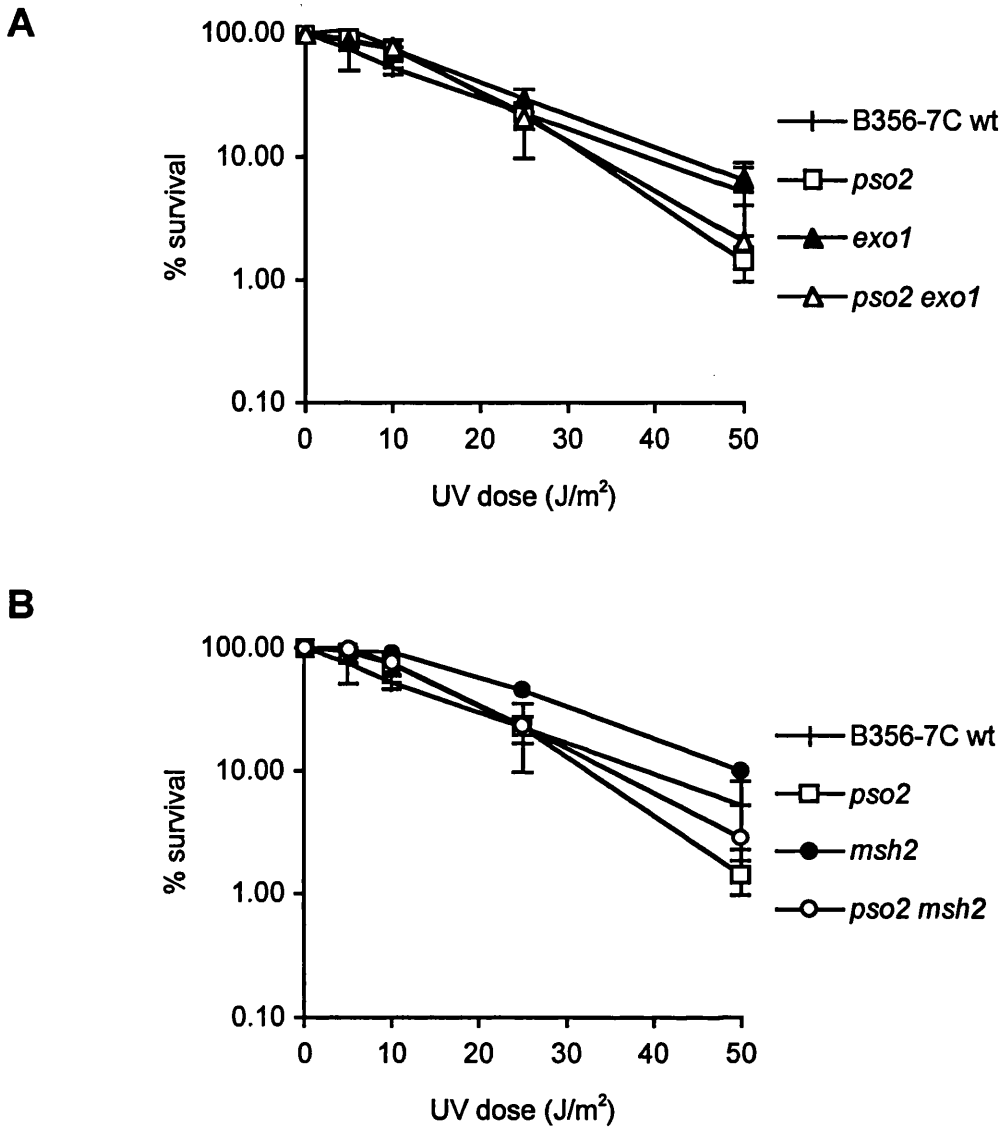

Figure 4.4 Comparison of UVC sensitivity in pso2, exo1, and msh2 mutants. Exponential phase parental B356-7C, single and double mutant cells were treated with 0 to 50 J/m^2 UV light at a dose rate of 0.5 J/s/m^2, with survival monitored by plating on YEPD. Comparisons of *pso2* with: **A.** *exo1*, **B.** *msh2*. All results are the mean of at least three independent experiments, and the error bars show the SEM.

non-epistatic interaction may be manifest at doses of UV greater than 50 J/m^2, it is debatable whether this would represent a true physiological relationship, given the loss of viability of NER deficient yeast exposed to UVC in excess of 10 J/m^2 (Fig. 3.6 A).

4.2.3 *PSO2* and *EXO1/MSH2* do not function in the S-phase or mitotic checkpoints

As already discussed (Section 3.2.2), HU and benomyl are potent inhibitors of cell cycle progression, affecting DNA synthesis and mitosis, respectively. Single and double mutant combinations of *pso2*, *exo1*, and *msh2* were grown on YAPD plates supplemented with HU (0, 2.5, 5, 10, 20, 40 mM) or benomyl (0, 10, 25, 50 μg/ml). An *mre11* mutant was used as a positive control for HU sensitivity, as previous studies have shown it to be hypersensitive to replicative stress, with no viability detected on YPAD supplemented with 10 mM HU (D'Amours and Jackson, 2001). In the case of HU, viability of the *pso2*, *exo1*, *msh2*, and *pso2 exo1*, *pso2 msh2* double disruptants was indistinguishable from the wild-type parent B356-7C in that all were able to grow unhindered at the maximum dose of 40 mM HU (Fig. 4.5 A). This contrasts with the *mre11* strain, which exhibited negligible growth when treated with 10 mM HU, and not at all at doses above 20 mM HU (data not shown).

A similar result was achieved upon treatment with benomyl (Fig. 4.5 B). Both the *pso2 exo1* and *pso2 msh2* double mutants were able to survive as competently as the wild-type and *pso2* strains, exhibiting good growth at a dose of 25 μg/ml (Fig. 4.5 B), but negligible survival at 50 μg/ml benomyl (data not shown). The *exo1* and *msh2* strains appeared to be slightly more sensitive at 25 μg/ml, but not to any significant degree, and

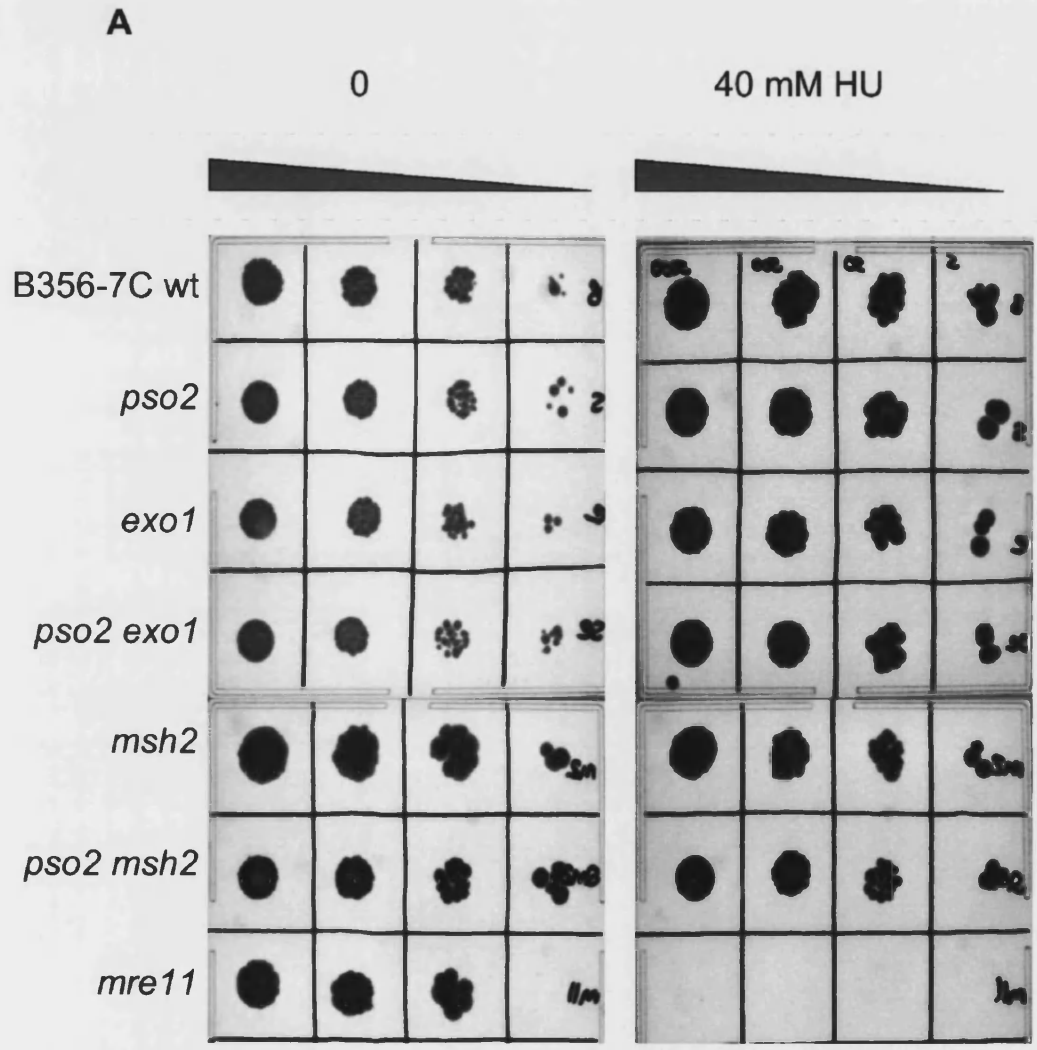
A
0
40 mM HU
B356-7C wt
pso2
exo1
pso2 exo1
msh2
pso2 msh2
mre11

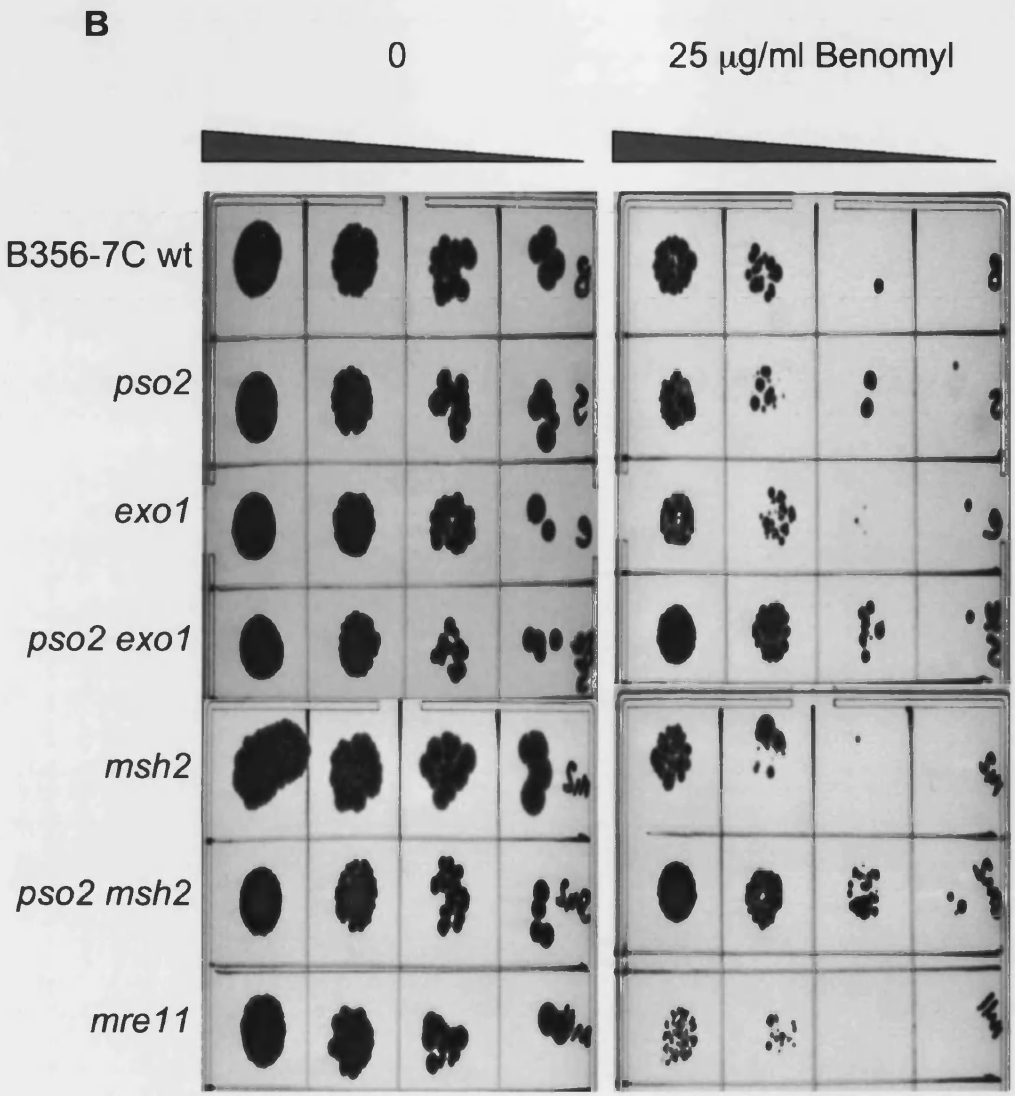

Figure 4.5 Comparison of HU and Benomyl sensitivity in pso2, exo1, and msh2 mutants. A 10 fold serial dilution series (represented by the tapered grey bar) of B356-7C wild-type, single and double mutant cells were spotted on: **A.** YEPD containing 0 or 40 mM Hydroxyurea. **B.** YEPD containing 0 or 25 μg/ml Benomyl. Plates were spotted in duplicate incubated at 28°C for 3 days.

their growth in the presence of benomyl was not as affected as the *mre11* deficient cells (Fig. 4.5 B). Together this suggests that *PSO2* and *EXO1/MSH2* do not play a major role in either the maintenance of replication forks stalled by dNTP depletion, or the S-phase or mitotic checkpoints.

4.3 Analysis of DSB repair by CHEF

The discovery of sensitivity to ionising radiation in cells doubly disrupted for *pso2* and *exo1/msh2* (Section 4.2.1), suggests the possibility of a more general defect in DSB repair in the absence of both of these factors, than just ICL-associated DSBs. The application of CHEF for the study of DSB repair has already been introduced in Chapter 3. Here it has been utilised to further investigate the role of *PSO2* and *EXO1-MSH2* in DSB repair, following treatment with HN2 and also after ionising radiation. Given the observed sensitivity to X-irradiation, it was expected that *pso2 exo1/msh2* gene disruptants would demonstrate a reduced capacity to repair DSBs. However, the precise sequence of events surrounding the formation of a DSB at a cross-link has not yet been determined. One intriguing possibility is that if Pso2 and Exo1-Msh2 were redundantly involved in incision events at a cross-link that resulted in the formation of a DSB, then loss of both activities may manifest as a failure to produce DSBs. If the DSB was an important stimulus for recombination, then the overall efficiency of the repair pathway would be reduced, and sensitivity would increase, as observed.

4.3.1 DSB repair intermediates fail to be repaired and accumulate after HN2 treatment

Exponentially growing cells were treated with HN2 and subsequently allowed to repair for 2, 4, or 24 h in drug-free minimal nutrient medium that permits efficient repair but prohibits cell division before analysing the chromosomal preparations on CHEF gels. Figure 4.6 shows typical CHEF gels obtained from B356-7C (wild type), *pso2*, *exo1*, *pso2 exo1*, *msh2*, *pso2 msh2*, and *pso2 exo1 msh2* mutant cells, treated with 50 μM HN2. Consistent with the results obtained using 100 μM HN2 (3.4), repair is evident by 2 h, and intact chromosomes are significantly restored by 24 h in the wild-type strain (Fig. 4.6 A). Also, *pso2* mutant cells are proficient in the formation of DSB, but these fail to be repaired to the same extent as in the parental strain, as degraded chromosomes (smear) are still observed after 24 h (Fig. 4.6). The *exo1* strain has a repair profile indistinguishable from the wild-type (Fig. 4.6 A), as expected from the lack of sensitivity to HN2 (Fig. 4.1 D). Although the *msh2* mutant exhibits significant DSBs at 2 h, the proportion of the chromosomes recovered by 24 h is comparable to the wild-type and *exo1* strains (Fig. 4.6 B, Table 4.1). In contrast, the double disruptants, *pso2 exo1* and *pso2 msh2*, accumulate a higher proportion of DSBs than the *pso2* strain, as can be seen from the complete degradation of the largest yeast chromosomes in the double disruptants (Fig. 4.6 A, B). Despite the large differences in cell survival between the strains at 50 μM HN2 (Fig. 4.2), the considerable chromosomal degradation observed in the double mutants is not thought to be due to cell death.

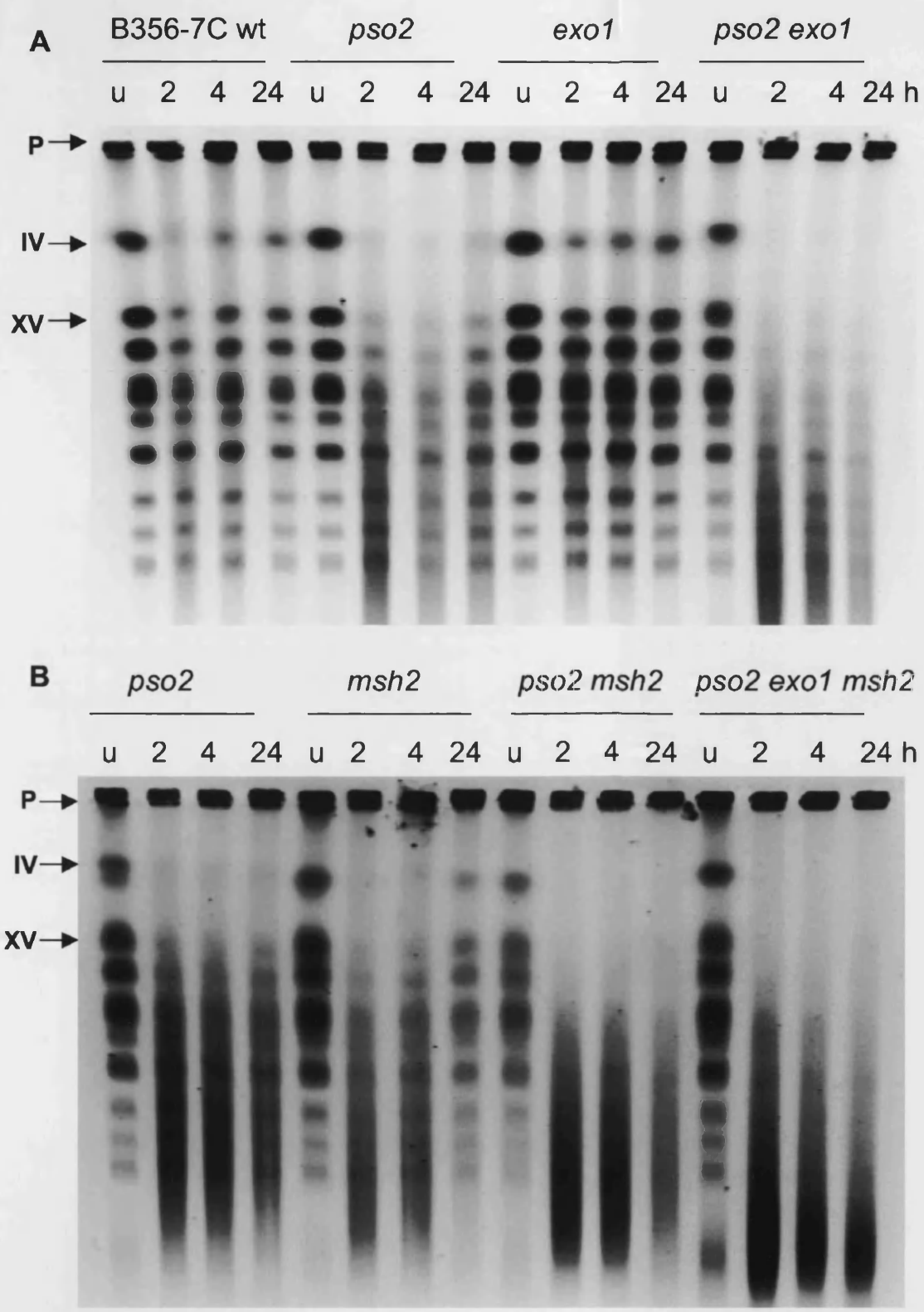

Figure 4.6 HN2-induced DSB repair in pso2, exo1, and msh2 mutants. Exponential phase cells were treated with 50 μM HN2 for 3 h with subsequent repair in MM for 2, 4, or 24 h. Mock treated cells = (u). Position of the plugs (P), chromosomes IV and XV are marked with arrows. Typical CHEF gels comparing **A**. B356-7C, *pso2*, *exo1*, and *pso2 exo1*, and **B**. *pso2* and *msh2*.

Indeed, little smearing is observed in *rad52* cells treated with 200 Gy ionising radiation (Figs. 4.7, 4.8), even though the surviving cell population is just 0.01 % (Fig. 4.3 C). Furthermore, the double mutants show an even greater deficiency in DSB repair, as indicated by the persistence of a smear rather than recovery of clear defined chromosomal bands. This is most clearly observed in the larger yeast chromosomes, such as chromosome IV, which by virtue of their size will receive more cross-links and therefore DSBs. The triple gene disruptant, *pso2 exo1 msh2*, demonstrates a complete deficiency in DSB repair (Fig. 4.6 B). It is apparent from figure 4.6, that partial recovery of chromosome IV is achieved in the absence of *PSO2*, but that an additional deficiency in *EXO1* and *MSH2* renders cells unable to reconstitute any detectable high molecular weight DNA. Hence disruption of both *PSO2* and *EXO1/MSH2* amplifies the deficiency in repair of ICL-induced DSB.

Attempts were made to quantify this deficiency by Southern blotting of the CHEF gels and subsequent probing with a radioactive marker for chromosome XV, which exhibits the second slowest migration (Fig. 4.6). A good level of detection was achieved in the untreated samples of all strains. However, this technique did not prove sensitive enough to differentiate between the repair capacities of the *pso2*, *pso2 exo1*, and *pso2 msh2* strains (data not shown). An indication of the repair capacities of each strain was instead obtained by computational Gel-Pro analysis (Media Cybergenetics) of the images of the ethidium bromide-stained CHEF gels taken under UV light. As a result of the highly stained smear of fragmented DNA, it was impossible to quantify the extent to which the smaller chromosomes could be reconstituted. Therefore it was decided to base the quantification of repair solely upon the largest chromosome, IV, which runs considerably slower than the smear in any of the strains investigated. Using Gel-Pro,

the maximum optical density (OD) was calculated for this chromosome band in the untreated and 24 h repair lanes. From this data, the DSB repair capacity of each strain could be estimated from the percentage of untreated chromosome IV recovered at 24 h (Table 4.1).

Table 4.1 **DSB repair efficiencies.** The maximum OD was calculated by Gel-Pro analysis of chromosome IV in the untreated (u) and 24 h repair samples. The extent of DSB repair at 24 h is expressed as a percentage of the untreated chromosomal preparation for each strain, and this figure is also given relative to the wild-type strain.

Strain	Repair after 24 h (% of u)	Repair after 24 h (rel. to wt)
B356-7C wt	44.9	100
pso2	14.8	33.0
exo1	38.1	84.9
pso2 exo1	1.7	3.9
msh2	30.2	67.3
pso2 msh2	3.4	7.6
pso2 exo1 msh2	0.3	0.7

These semi-quantitative results confirm the observations already made by visual inspection of the gels. The wild-type strain is able to repair 45 % of the DSBs in the largest chromosome population after 24 h. Both the *exo1* and *msh2* strains exhibit a slight deficiency in repair, reconstituting chromosome IV to 70-80 % of the wild-type level. In contrast, repair in *pso2* deficient cells is significantly reduced, to only 30 % of the wild-type capacity. This deficiency in DSB repair is further reduced in both the *pso2 exo1* and *pso2 msh2* double mutants, which recover just 4-8 % of the largest chromosomes, relative to the wild-type. Less than 1 % of the parental capacity for DSB repair is observed in the absence of all three genes.

4.3.2 CHEF analysis of X- and γ-irradiated cells

The moderate sensitivity of *pso2 exo1/msh2* double mutant cells to X-irradiation suggests an underlying deficiency in the general repair of DSBs, rather than specifically those associated with ICL. Hence CHEF was also used to investigate the repair of DSBs arising from ionising radiation. Cells were irradiated with 200 Gy X-rays, and then allowed to repair for 2, 4, or 24 hours in minimal media, as for HN2 treatments. Samples were also taken immediately following the irradiation, as contrary to HN2, where DSBs occur as an intermediate of repair, ionising radiation-induced DSBs are a direct DNA lesion. Figure 4.7 shows a typical set of CHEF gels. It is apparent that 200 Gy X-irradiation does not induce the same extent of detectable DSBs, compared to HN2 (Fig. 4.6). This is surprising, as at 200 Gy, ionising radiation might be expected to produce a significant number of DSBs. Nevertheless, some DSBs are observed, most clearly at the level of the largest chromosome (Fig. 4.7).

It has been suggested that the frequency of DSB induction is proportional to the dose rate (Dardalhon *et al.*, 1994). Therefore, in order to obtain a higher yield of DSBs, and to facilitate greater strain comparison, yeast cells were irradiated using a Co-60 γ-ray source with a higher dose rate of 9 Gy/min. Figure 4.8 shows a typical CHEF gel of chromosome preparations from cells irradiated at 200 Gy γ-rays. A smear of degraded DNA is not apparent for any of the strains at any of the time-points. Hence, despite an almost four-fold increase in dose rate, fewer DSBs were observed than for X-irradiation. Detectable levels of DSBs have been observed in yeast using the CHEF method after treatment at 200 Gy γ-ray from comparable Co-60 sources (Geigl and Eckardt-Schupp, 1990; Dardalhon *et al.*, 1994; Moore *et al.*, 2000). However the dose rates used in these published studies were greater than 20 Gy/min, and experiments

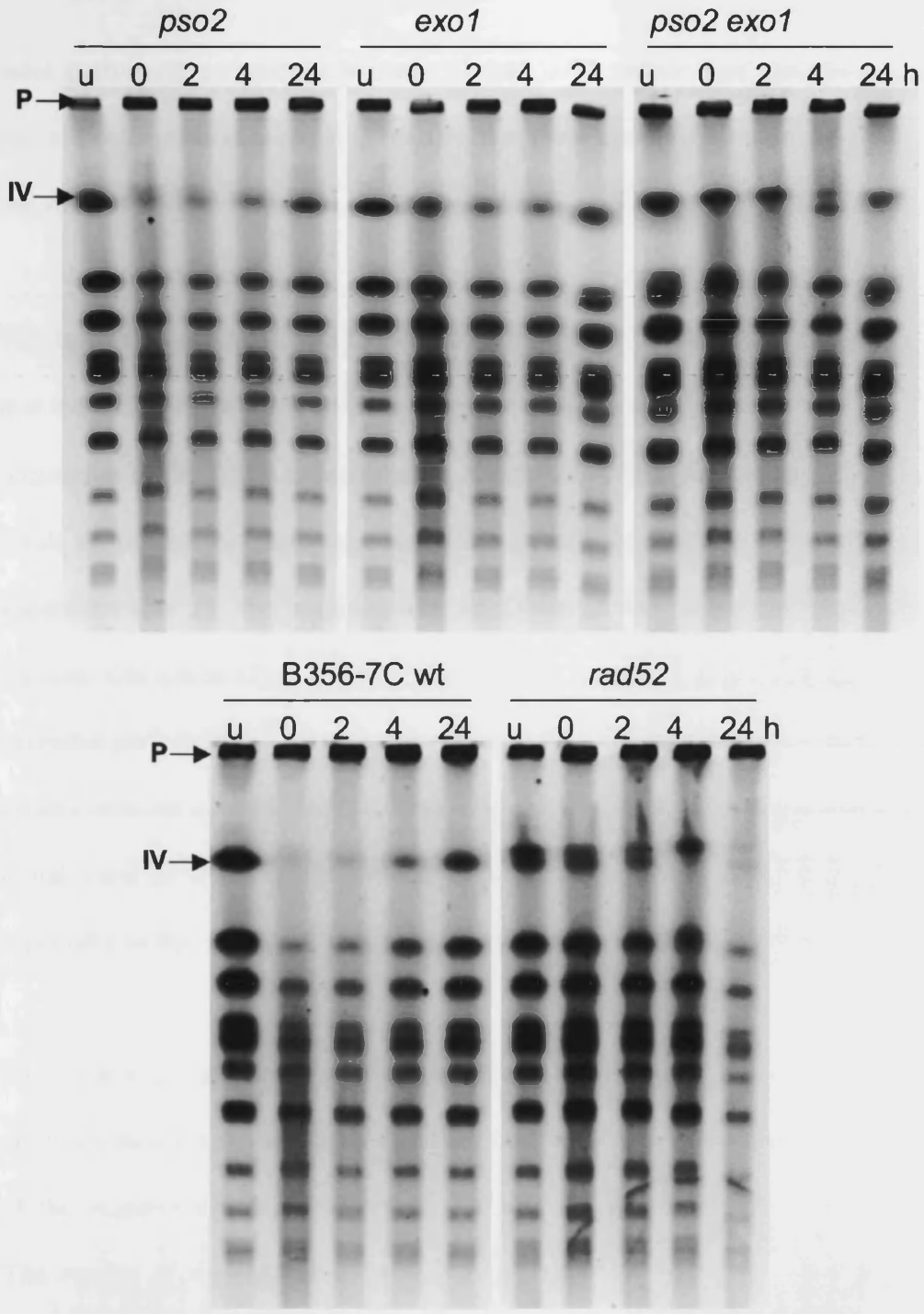

Figure 4.7 X-irradiation-induced DSB repair. Exponential phase cells were treated with 200 Gy X-rays with repair in MM for 0, 2, 4, or 24 h. Mock treated cells (u) were allowed to repair for 24 h. Typical CHEF gels comparing B356-7C parental, *pso2*, *exo1*, *pso2 exo1*, and *rad52* strains. The plug, P, and largest chromosome, IV, are marked with arrows.

were performed on stationary phase diploid cells, rather than the exponential phase haploid cells utilised here. It is feasible that these conditions could significantly affect the yield of DSBs.

The lack of detectable DSBs induced by γ-irradiation, as compared to X-rays, suggests that the incidence of frank DSBs is very rare under these conditions. It is possible that a proportion of the DSBs observed after X-irradiation may have occurred indirectly, as a result of replication forks meeting SSBs caused by reactive oxygen species. The apparent delay in the accumulation of DSBs in the repair-defective *rad52* strain supports this notion (Fig. 4.7), as these cells are extremely slow growing, and arrest for extended periods in G2. Hence, the potential for DSB formation at a replication fork is greatly reduced in *rad52* cells, compared to the wild-type. It is conceivable that the low initial yield of DSBs in the *pso2 exo1* strain (Fig. 4.7) is also due to growth arrest, especially as this strain exhibits a mild sensitivity to ionising radiation (Fig. 4.3).

By calculating the ratio of chromosomal band intensities between treated and untreated cells (q), an estimate can be made of the number of DSB breaks per molecule, in terms of the negative natural logarithm of q (Table 4.2) (Geigl and Eckardt-Schupp, 1990). The results of this analysis are within the range of 0.23–0.65 DSB per Mb DNA, presented by Geigl and Eckardt-Schupp for wild-type cells irradiated with Co-60 γ-radiation (1990). Evaluation of this data using a Poisson distribution, gives an estimation that the likelihood of at least one DSB within a region of DNA comparable to the largest yeast chromosome (Ch. IV, 1531 kb) is 37 %, whereas for the smallest chromosome (Ch. I, 230 kb), the probability is only 7 %. It is therefore likely that the level of DSBs detected here represents the limits of detection using CHEF, and as such,

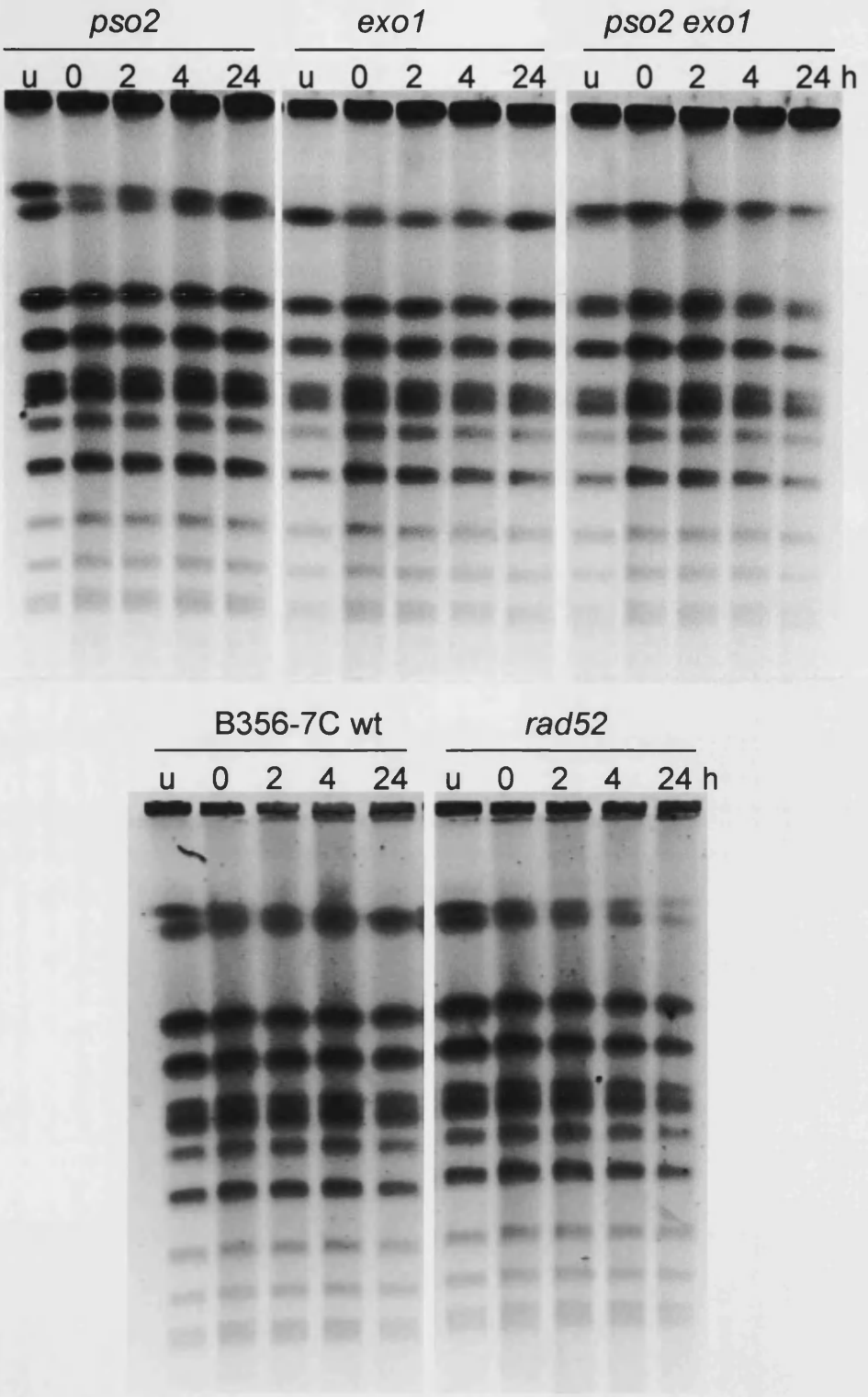

Figure 4.8 γ-irradiation-induced DSB repair. Exponential phase cells were treated 200 Gy γ-irradiation with subsequent repair in MM for 0, 2, 4, or 24 h. Mock treated cells = (u). Typical CHEF gels comparing B356-7C parental, *pso2*, *exo1*, *pso2 exo1*, and *rad52* strains.

Table 4.2 **Number of DSBs per 1 Mb DNA induced by 200 Gy X-irradiation,** as given by n=-ln(q), where q has been determined experimentally using Gel-Pro analysis of the CHEF gel image. The intensity of each band in treated (0, 24 h) lanes was calculated as a fraction of the equivalent band in the untreated lane, to give a value of q for each chromosome. Data is presented as the mean DSBs observed for the 7 largest chromosomes (giving an average length of ~1 Mb), and standard deviations are stated.

Strain	DSB /Mb at 0 h (+/- SD)	DSB /Mb at 24 h (+/- SD)
B356-7C wt	0.47 (+/- 0.32)	0.26 (+/- 0.08)
pso2	0.24 (+/- 0.21)	0.22 (+/- 0.08)
exo1	0.20 (+/- 0.22)	0.20 (+/- 0.15)
pso2 exo1	0.02 (+/- 0.08)	0.17 (+/- 0.12)
rad52	0.07 (+/- 0.11)	0.57 (+/- 0.18)

the variation in DSB yield observed in the wild-type and *pso2/exo1* single mutants is probably not significant. Hence an alternative procedure will be required to reliably determine whether the sensitivity of the *pso2 exo1* and *pso2 msh2* double mutant strains is due to a deficiency in DSB repair.

4.4 Recombination at an inverted repeat substrate

Homologous recombination is known to be the major pathway by which DSBs generated at ICLs are repaired (McHugh *et al.*, 2000). The parent strain selected for this study was developed by L. Symington to contain a novel construct for the analysis of mitotic recombination events, integrated at the *HIS3* locus on chromosome XV (Rattray and Symington, 1994). This well-characterised recombination substrate is comprised of an intrachromosomal inverted duplication of the *ade2* gene, separated by *TRP1* (Fig. 4.9 A). Both *ade2* alleles are non-functional: one has a deletion of the 5' coding region and

upstream DNA extending beyond the region of homology (hence may only act as the donor), and the other full-length allele bears a 3' frame-shift mutation at an *Nde* I site. It follows that, in haploid cells, it is possible to compare the frequency of intrachromosomal recombination in different genetic backgrounds by measuring reversion to *ADE*$^+$ prototrophy, quantified in terms of the proportion of a population arising from a single cell that is able to grow in the absence of adenine. Furthermore, this system has the additional benefit that the nature of the recombination event (gene conversion and/or crossover) can be established through physical analysis of the resultant orientation of the *ADE2* construct.

4.4.1 Spontaneous intrachromosomal recombination

Rates of spontaneous mitotic intrachromosomal recombination at the *ade2* inverted repeat construct were determined for the same panel of repair-defective strains as considered for HN2 sensitivity (Section 4.1). The results presented here represent the mean of at least 10 independent analyses of *ADE2*$^+$ prototrophs arising spontaneously from a founder *ade2-* cell, upon a switch to solid SC media lacking adenine. Rates (events per cell per generation) were calculated from the recombination frequency (ADE$^+$ cells/TRP$^+$ cells), according to the formula first described by Drake (1970) to account for fluctuations in the population size (Section 2.8.1).

In the parental, recombination-proficient strain, the rate of Ade$^+$ recombination was observed as 564 (+/- 133) x 10^{-6} events/cell/generation (Fig. 4.9 B). Spontaneous recombination was reduced to 23 % of the wild-type rate in a recombination defective *rad51* strain, and 0.01 % in a *rad52* strain (Table 4.3). These relative rates correspond with the original results published by Rattray and Symington for these strains (1994). A

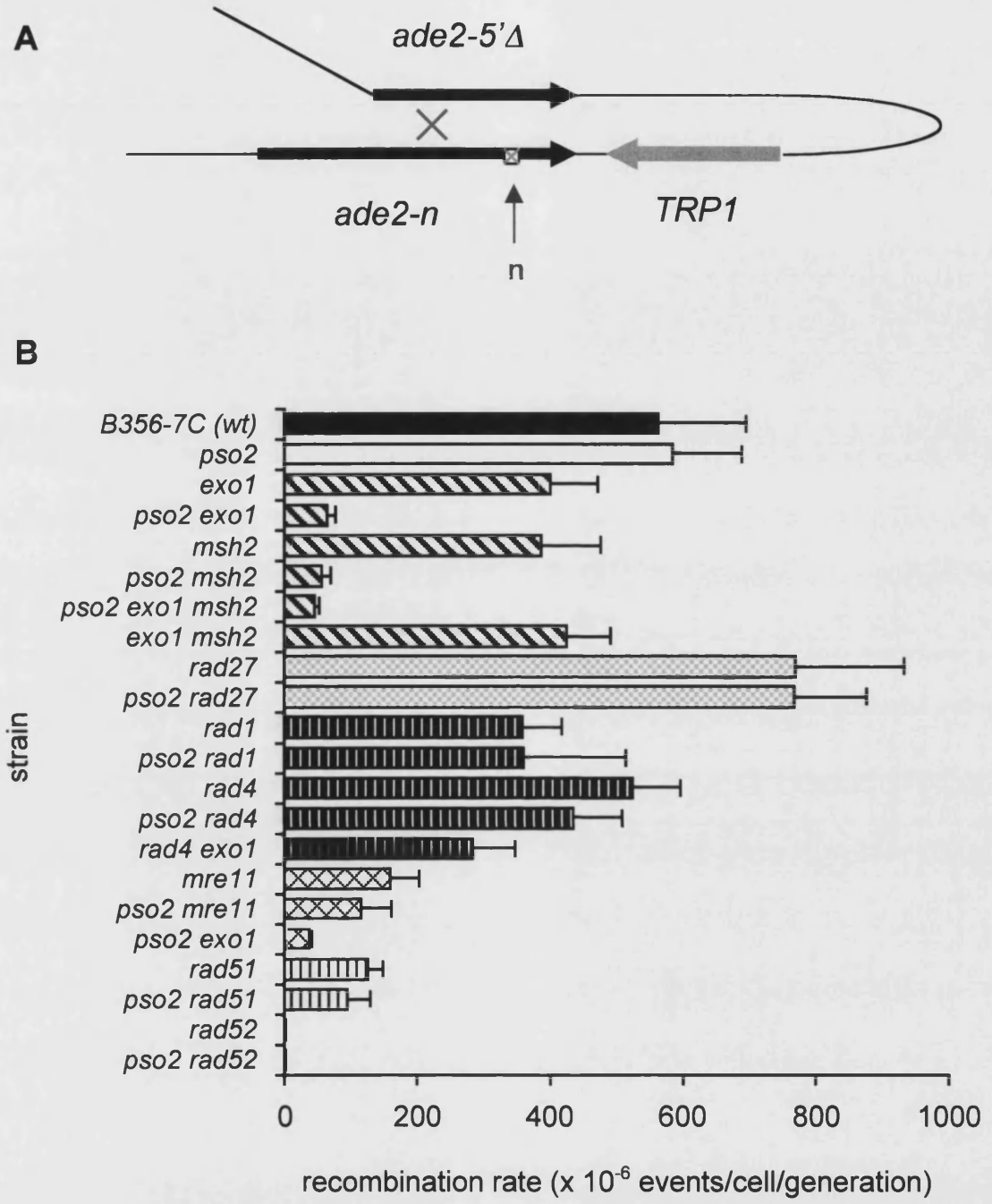

Figure 4.9 Spontaneous recombination at an inverted repeat substrate. **A.** Representation of the mutant *ade2* alleles arranged in an inverted repeat about the *TRP1* gene. One *ade2* allele has a 5' deletion, the other has a 3' frameshift at an *Nde* I site (marked n with a blue arrow). **B.** Comparison of spontaneous recombination rates in various single and multiple gene disruptants. Rates are the mean of 10-20 independent assays, and error bars represent the SEM.

Table 4.3 **Spontaneous recombination rates at an inverted repeat substrate.** Mean rates are calculated as events/cell/generation from 10-20 independent analyses (SEM as represented in Fig. 4.9 B), and relative rates are expressed as a percentage of the wild-type.

Strain	Mean rates (x 10^{-6})	Relative rates (% wt)
B356-7C wt	564	100.0
pso2	585	103.6
exo1	400	70.9
pso2 exo1	64	11.3
msh2	386	68.4
pso2 msh2	55	9.8
pso2 exo1 msh2	45	7.9
exo1 msh2	425	75.4
rad27	771	136.7
pso2 rad27	769	136.4
rad1	358	63.5
pso2 rad1	361	64.0
rad4	525	93.0
pso2 rad4	435	77.1
rad4 exo1	283	50.1
mre11	160	28.3
pso2 mre11	116	20.6
pso2 exo1 mre11	36	6.4
rad51	126	22.3
pso2 rad51	94	16.7
rad52	0.030	0.0052
pso2 rad52	0.020	0.0036

wild-type level of spontaneous recombination was observed in the *pso2* mutant cells (Fig. 4.9 B), whereas both *exo1* and *msh2* single disruptants exhibit a moderate reduction in recombination rate (70 % of the wild type rate, Table 4.3). In contrast,

spontaneous recombination was reduced 9 fold in the *pso2 exo1* double disruptant, comparative to the 10 fold decrease in recombination seen in a *pso2 msh2* defective strain (11 and 10 % of the wild type rate, respectively, Fig. 4.9 B, Table 4.3). Each of these results was confirmed in two independently obtained *pso2 exo1* or *pso2 msh2* double disruptants.

The reduced rates of spontaneous recombination in the absence of both *PSO2* and *EXO1* or *MSH2* are greater than in the *rad51* strain, suggesting that these factors play a considerable role. Furthermore, control studies were performed in a *rad4 exo1* double mutant to determine whether the reduced capacity for spontaneous recombination is unique to *pso2 exo1* and *pso2 msh2*. It can be seen from figure 4.9 B that an additive relationship, rather than a significant reduction in recombination rate is observed for *rad4 exo1*. This is indicative of independent roles for Rad4 and Exo1 in spontaneous recombination events. In addition, *EXO1* and *MSH2* appear epistatic as the capacity for spontaneous recombination was not diminished further in either the *exo1 msh2* (compared to the respective single mutants) or *pso2 exo1 msh2* disruptants (relative to the *pso2 exo1* and *pso2 msh2* strains) (Fig. 4.9 B). In contrast to the *pso2 exo1* and *pso2 msh2* double disruptants, no significant differences were observed for the frequency of spontaneous recombination in the *pso2 mre11*, *pso2 rad1*, *pso2 rad27*, or *pso2 rad51* strains compared to their respective single mutants (Fig. 4.9 B).

4.4.2 Analysis of spontaneous recombination events in the absence of *PSO2*

Further investigation of the nature of the recombination events occurring in the absence of *PSO2*, *EXO1*, and *MSH2* can be achieved through physical analysis of the *ADE2* construct. The primary advantage of using this inverted-repeat substrate rather than a direct-repeat system is that only DNA crossovers occurring via a fully reciprocal mechanism are viable, as incomplete exchanges result in fragmentation of the chromosome, which is obviously lethal in a haploid cell. Such reciprocal crossovers can be identified as a consequence of the inversion of the DNA between the two *ADE2* alleles (Class II, Fig. 4.10). In contrast, if recombination has occurred by gene conversion, the intervening DNA remains in its original orientation, but the unique *Nde* I restriction site in the full-length allele is restored (Class I, Fig. 4.10). Further, if a crossover has been accompanied by a gene conversion event, then both inversion of the connecting DNA and recovery of the *Nde* I site are observed (Class III, Fig. 4.10). It would be expected that a double crossover event would result in the transfer of the *Nde* I mutation to the *ade2-5'Δ* allele (Class IV, Fig. 4.10), yet this class of event has not been recovered to date (Rattray and Symington, 1995).

The original approach, adopted by Rattray and Symington (1994), was to use Southern blot for the physical analysis of the *ADE2* construct arrangement. A combination of probes homologous to the *ADE2* and *TRP1* genes, and restriction digest by *Nde* I and *Pst* I, enabled the four classes of recombination events to be distinguished. A new PCR-based method is presented here, which can differentiate between the first three classes of recombination event, but not between Class I/ gene conversion and Class IV/

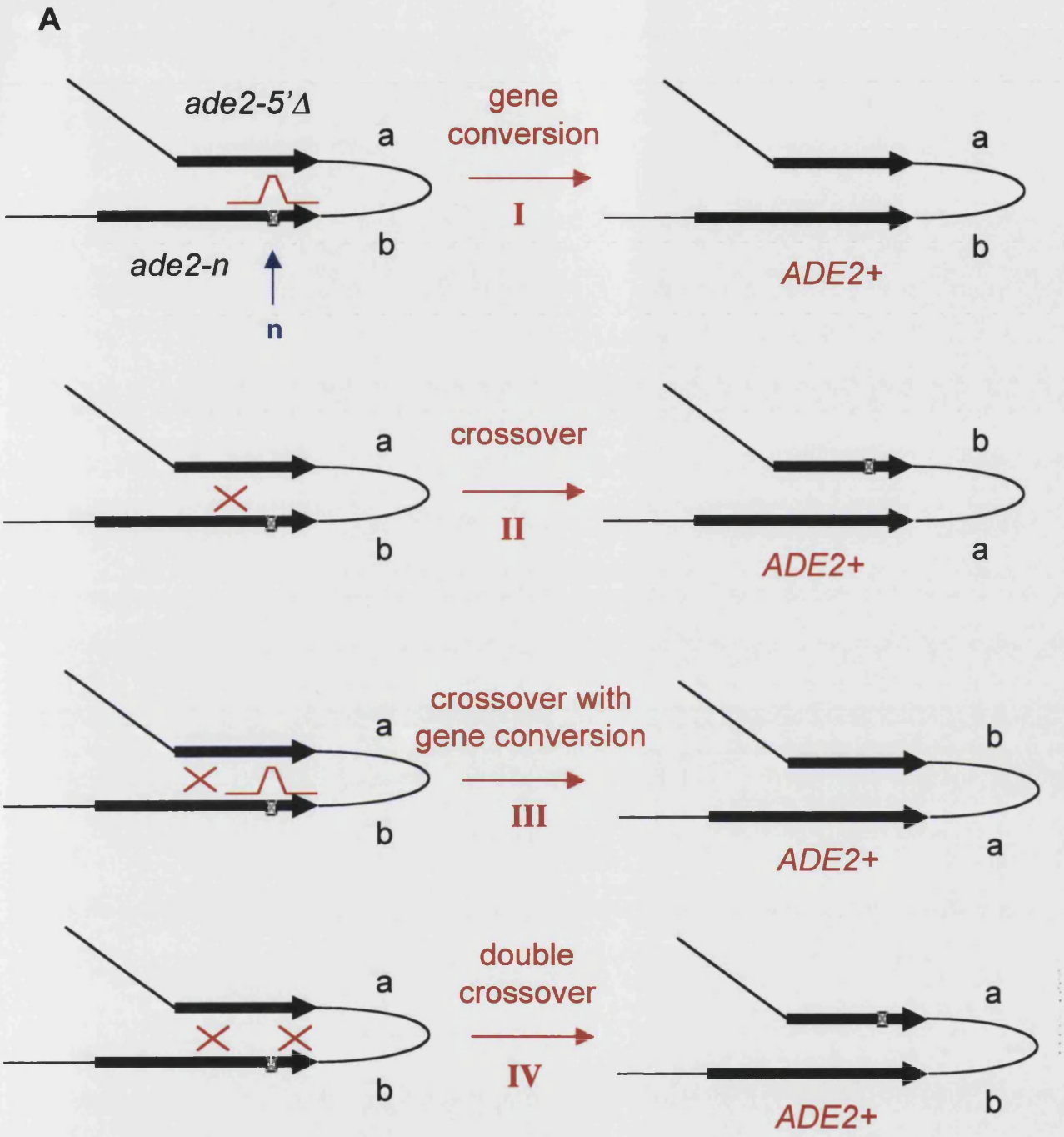

Figure 4.10 Representation of the classes of recombination event at the *ADE2* inverted repeat construct. The *Nde* I frameshift is marked n with a blue arrow and boxed cross. a and b show the orientation of the intervening TRP1 gene.

double crossover. Given the lack of detectable Class IV/ double crossover events in previous analyses, it was deemed satisfactory to use this approach. This PCR-based protocol takes advantage of the fragments of vector sequence arising from molecular cloning that have been retained within the *ADE2* construct after integration into the host genome (Rattray and Symington, 1994, and refs therein). The *ADE2* alleles are flanked on the outside by DNA from the pBluescript II KS(-) plasmid, containing the recognition sequences for the T7 and T3 standard primers, upstream of the *ade2-n* and *ade2-5'Δ* alleles, respectively (Fig. 4.11 A). A short region of the pBluescript II KS(-) multiple cloning site sequence remains between the *ade2-5'Δ* and *TRP1* genes, to which a novel primer, *int*, has been designed: 5'-GAT CTC GAA TTC CTG CAG CC-3'. PCR analysis of DNA extracted from individual *ADE+* prototrophs was carried out using all 3 primers in the same reaction. In the original orientation of the *ADE2* construct, this *int* primer will only generate a DNA fragment with the T7 primer, whereas an inversion of the intervening DNA results in a product from the *int* and T3 primer pair. The conditions of the PCR reaction were optimised to exclude the longer T7-T3 product. Products were digested with *Nde* 1 and visualised by agarose gel electrophoresis (Fig. 4.11 B).

Confirmation of the reliability of this new PCR-based analysis of spontaneous recombination events can be achieved through comparison of the data for the B356-7C recombination-proficient strain with that obtained by Rattray and Symington using Southern blots. A spectrum of 75 % Class I/ gene conversions, 16.7 % Class II/ crossovers, and 8.3 % Class III/ crossovers associated with gene conversions, was identified by PCR (Table 4.4). This compares favourably with the previously published event ratios: 50, 35, 15 % Class I, II, III, respectively (Rattray and Symington, 1994).

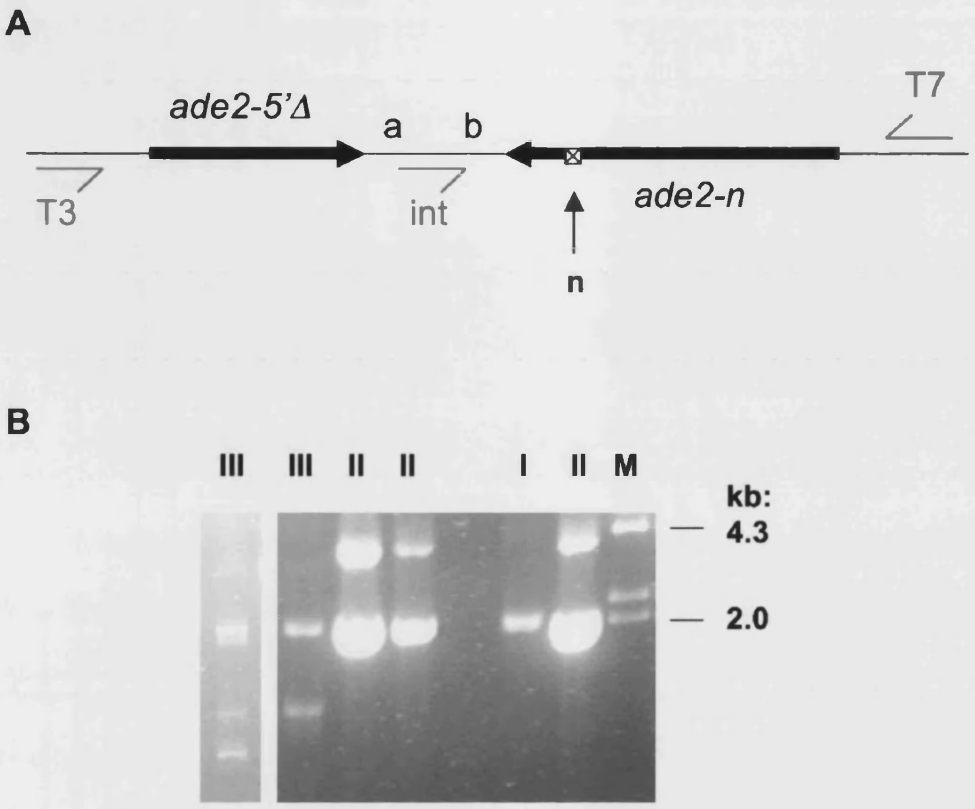

Figure 4.11 Analysis of spontaneous recombination events occurring at the *ADE2* inverted repeat construct. **A**. Schematic to show the location and orientation of the primers (T3, int, T7) used in the PCR-based analysis of the classes of recombination event. Only two primers (T3-int or T7-int) are compatible with each substrate, depending on the DNA orientation between the *ade2* alleles (a, b), as the longer T3-T7 product is largely excluded by the PCR conditions. The *Nde* I frameshift is marked n with a blue arrow and boxed cross. **B**. Typical agarose gel showing *Nde* I digested PCR products from independent recombinants. The expected band sizes for each recombination class are approximately: I - 2.1 and 1.7 kb, II - 3.6 and 2.1 kb, III - 2.1, 1.2, and 1.0 kb. The recombination class is marked above each lane as I, II, or III. M = DNA ladder (λ*Hind* III digest).

The wild-type predominance of gene conversion events over crossovers is also observed in the *pso2* mutant (Table 4.4). This contrasts greatly with the significantly increased preference for crossovers in the absence of *exo1* or *msh2* (70 % crossovers versus 20 % gene conversion). In both the *pso2 exo1* and *pso2 msh2* double mutants, crossover events predominate to a similar degree as in the *exo1* and *msh2* strains (Table 4.4). Hence, it would appear that the influence of *PSO2* on the outcome of recombination reactions is epistatic to *EXO1-MSH2*.

Table 4.4 **Classification of recombination events.** Percentage of recombinant colonies exhibiting a Class I, II, or III recombination event at the *ADE2* inverted repeat construct, as detected by PCR and subsequent *Nde* I digestion. A total of 10-25 colonies were examined per strain.

Strain	Recombination Class (% events)		
	I	II	III
B356-7C	75.0	16.7	8.3
pso2	50.0	25.0	25.0
exo1	20.0	70.0	10.0
pso2 exo1	19.2	61.5	19.2
msh2	20.0	70.0	10.0
pso2 msh2	11.1	77.8	11.1

4.4.3 HN2-induced recombination at the inverted repeat construct

It is apparent that *PSO2*, *EXO1*, and *MSH2* act synergistically in both the repair of HN2-induced ICL and spontaneous homologous recombination. However, the question remains as to whether these factors are involved in the processing of recombination

intermediates at the ICL. Intrachromosomal recombination rates at the inverted repeat construct were determined following HN2 treatment of the B356-7C-derived strains. Individual pink colonies were cultured overnight in adenine-rich (YPAD) media in order to provide sufficient cells to be tested against a range of HN2 doses. The recombination rate calculation was adjusted to account for this culture step, with an estimation of the number of cells in the inoculum determined from samples plated on media lacking tryptophan. Cultured cells were resuspended in PBS and treated with 0, 1, 10 or 100 μM HN2 for 1 hour, before plating at appropriate dilutions on solid media lacking adenine or tryptophan. Recombination rates were calculated as events per cell per generation, with due consideration given to variations in the number of cells produced in the overnight culture (Section 2.8.2).

Overall, a similar pattern was observed as for spontaneous recombination (Fig. 4.12). The untreated B356-7C wild-type cells exhibit a mean recombination rate of 410 x 10^6 events/cell/generation, comparable to that observed in the absence of a culture step (Fig. 4.9). This suggests that growth in liquid culture does not adversely affect the rate of spontaneous recombination. Neither the *pso2* and *exo1* single mutants, nor the *exo1 msh2* strain, showed any deficiency in recombination rate at the inverted repeat construct (Fig. 4.12). In contrast, both the *pso2 exo1* and *pso2 msh2* double disruptant strains are as defective as the *rad51* recombination-deficient strain (Fig. 4.12). The extent of this deficiency does not appear to be as severe as observed for spontaneous recombination, as all three strains have a recombination capacity at 40 % of the wild-type rate. The reduced recombination rates in *pso2 exo1* and *pso2 msh2* strains at the highest dose of 100 μM HN2 are due to the severely limited cell survival at this dose (Fig. 4.1 E, 4.2 A). It is interesting to note that even the rate of recombination in the

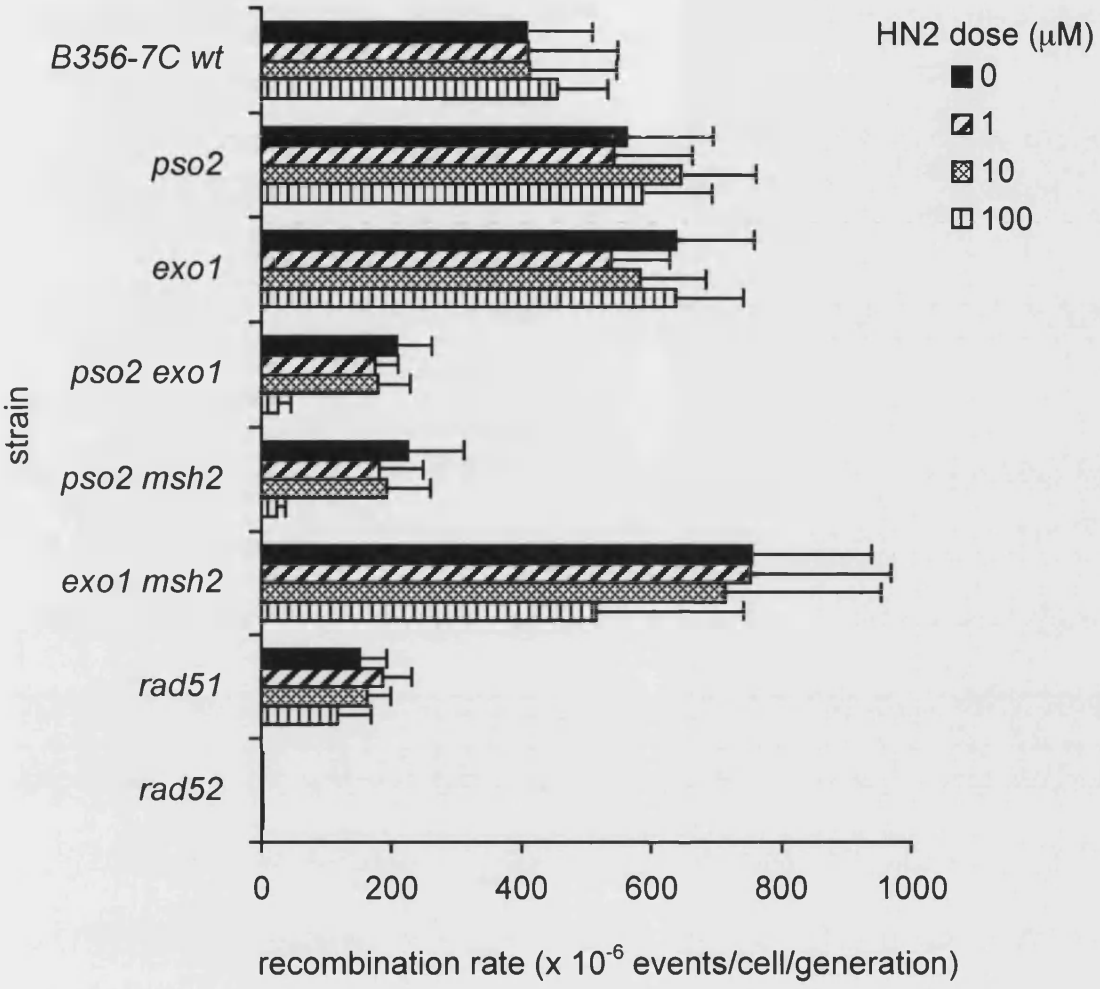

Figure 4.12 HN2-induced recombination at an ADE2 inverted repeat construct. Exponential phase cells were treated with 0, 1, 10, or 100 μM HN2 prior to plating on SC-ade and SC-trp media to determine recombination rate. All results are the mean of 5-10 independent experiments, and error bars represent the SEM.

rad52 strain is 10 fold higher after growth in liquid culture (0.26 x 10^6 events/cell/generation in the untreated cells), compared to the conditions of the spontaneous recombination assay. Hence it is possible that although recombination in the wild-type parent does not appear to be affected by the overnight culture step, these conditions are biased where recombination events are limited, likely as a result of the increased capacity for cell division in ADE^+ prototrophs (Rattray and Symington, 1994). The observation that neither the *exo1* nor *exo1 msh2* strains show the mild recombination deficiency seen in the spontaneous recombination assay also supports this hypothesis. Nevertheless, it is clear that induction of intrachromosomal recombination above the spontaneous rate was not observed in any strain following treatment with HN2.

4.5 Non-homologous End Joining

Non-homologous end joining (NHEJ) is not believed to play an important role in the repair of ICL in yeast, as no significant sensitivity to agents such as HN2 and psoralen has been observed in cells deficient for the key genes in this repair pathway, such as *KU70* (McHugh *et al.*, 2000). Nevertheless, one of the human *PSO2* homologues, Artemis (*hPSO2C*), has been identified as a component of the V(D)J recombination apparatus, which is a specific NHEJ event at the immunoglobulin loci. Furthermore, in mice, both *EXO1* and *MSH2* seem to be required for immunoglobulin class-switch recombination, in addition to the role of MMR in somatic hypermutation of the V region (Bardwell *et al.*, 2004). Consequently, a plasmid-based assay in which cell survival depends upon NHEJ competence was used to determine whether the yeast *PSO2* is involved in this pathway. Comparison is made between the transformation

efficiency of cut versus supercoiled plasmid DNA to provide a simple quantitation of NHEJ incidence. This assay has been widely utilised, and was key in establishing the roles of the NHEJ factors Yku70, Yku80, and Lig4 (Boulton and Jackson, 1996; Teo and Jackson, 1997).

Strains were transformed with YEplac181 plasmid DNA that had been linearised with restriction enzymes to give 5' (*Eco*R I), 3' (*Pst* I) overhang, or incompatible ends (*Eco*R I and *Pst* I) in a region that bears no homology to the yeast genome. Preliminary titration experiments were conducted to ensure that DNA quantity was in the linear range of transformation efficiency per μg to facilitate comparisons across strains. The wild-type BY4741 strain demonstrates good recovery of plasmids digested with either *Eco*R I or *Pst* I, but a reduced efficiency to rejoin fragments with non-homologous ends (Fig. 4.13). In contrast, the NHEJ-deficient strain *lig4* is only able to recircularise up to 20 % of DNA fragments, regardless of the nature of the ends. The *pso2* mutant demonstrates a wild-type pattern of transformant recovery (Fig. 4.13), and loss of *EXO1* does not significantly affect the efficiency of NHEJ (Fig. 4.13), consistent with published reports (Wu and Lieber, 1999). The *pso2 exo1* double disruptant strain also shows no quantitative defect in joining of compatible or incompatible substrates relative to the wild-type, and especially compared to the considerably greater reduction in transformant recovery in the *lig4* strain (Fig. 4.13). Similarly, neither *msh2* nor *pso2 msh2* are defective in NHEJ of the range of substrates considered here (Fig. 4.13). In conclusion, *PSO2* does not appear to be required for NHEJ, even in the absence of either *EXO1* or *MSH2*.

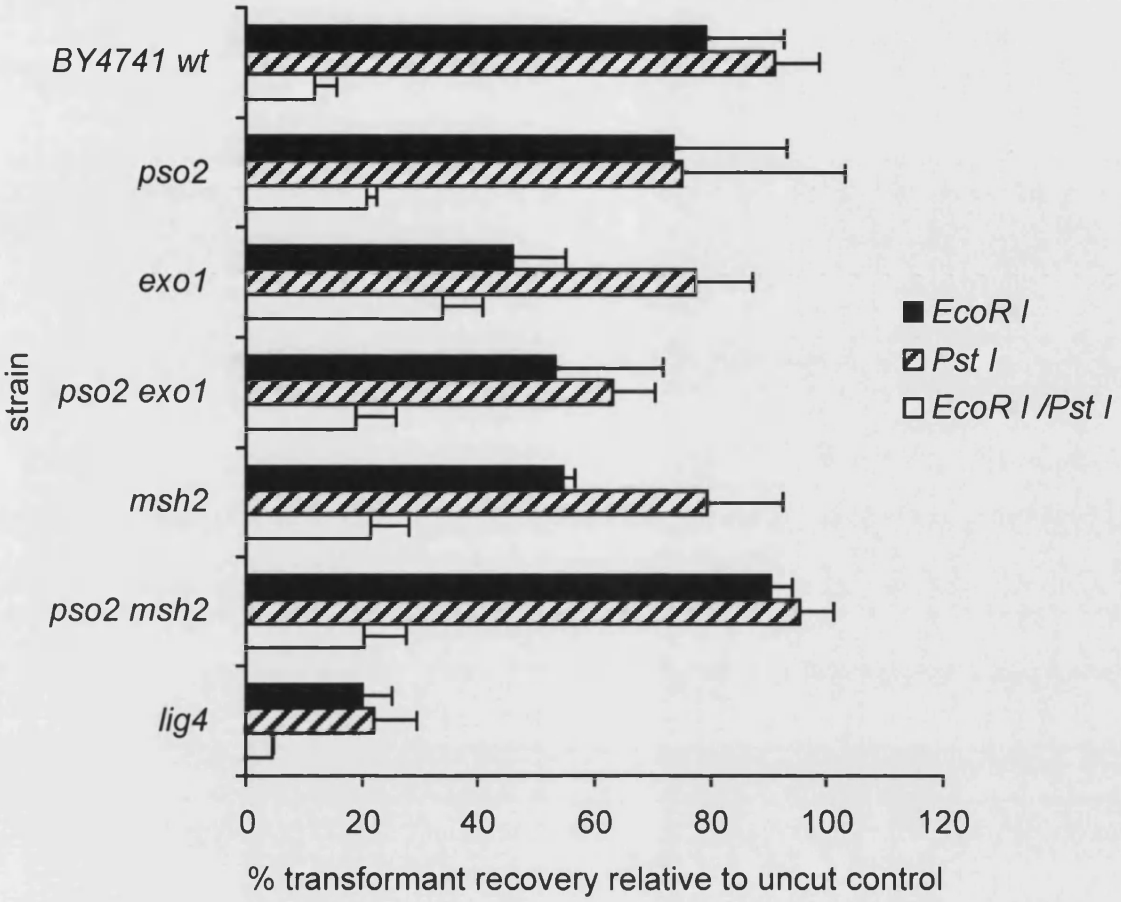

Figure 4.13 Non-homologous end joining assay. The plasmid YEplac181 was digested with *EcoR* I, *Pst* I, or both enzymes, and transformed into *S. cerevisiae* strains defective for one or more repair genes, as shown. The percentage transformant recovery relative to a parallel transformation with uncut plasmid was used as a determinant of the cells ability to rejoin DNA in the absence of a homologous template. Assays were repeated at least 3 times, and error bars represent the SEM.

4.6 Complementation studies

In cases of genetic redundancy where a cellular process can be carried out by more than one gene product, overexpression of one gene can often compensate for the phenotype associated with loss of another. There are several examples of complementation involving the nucleolytic function of *EXO1*. For example, overexpression of *EXO1* has been shown to suppress a number of *rad27* mutation phenotypes, including temperature sensitivity, Okazaki fragment accumulation, elevated mutation frequency, and the rate of minichromosome loss (Sun *et al.*, 2003). Similarly, *EXO1* overexpression has been found to complement other phenotypes associated with *rad50*, *mre11*, *msh2*, and *mlh1* mutants (Sokolsky and Alani, 2000; Lewis *et al.*, 2002; Argueso *et al.*, 2002). If the activity of Pso2 is truly redundant with that of Exo1 and Msh2 for ICL and DSB repair, it is possible that overexpression of *EXO1* or *MSH2* would rescue the HN2-sensitivity of the *pso2* deficient strain.

4.6.1 Overexpression of *EXO1* or *MSH2* does not compensate for loss of *PSO2*

EXO1 was constitutively expressed under the control of the *ADC1* (*ADH1*) promoter from the 2μ plasmid pDB20 (here designated *pDB-EXO1*; Qiu *et al.*, 1999, published as PDB-ScE). It is clear from figure 4.14 A that constitutive expression of *EXO1* in *pso2* defective cells could not reverse the increased HN2 sensitivity to any extent. However, it is known that the *ADC1* promoter drives high levels of expression in yeast and it is possible that the constitutive upregulation of such a fundamental cellular nuclease as Exo1 may be toxic to general metabolic processes such as replication.

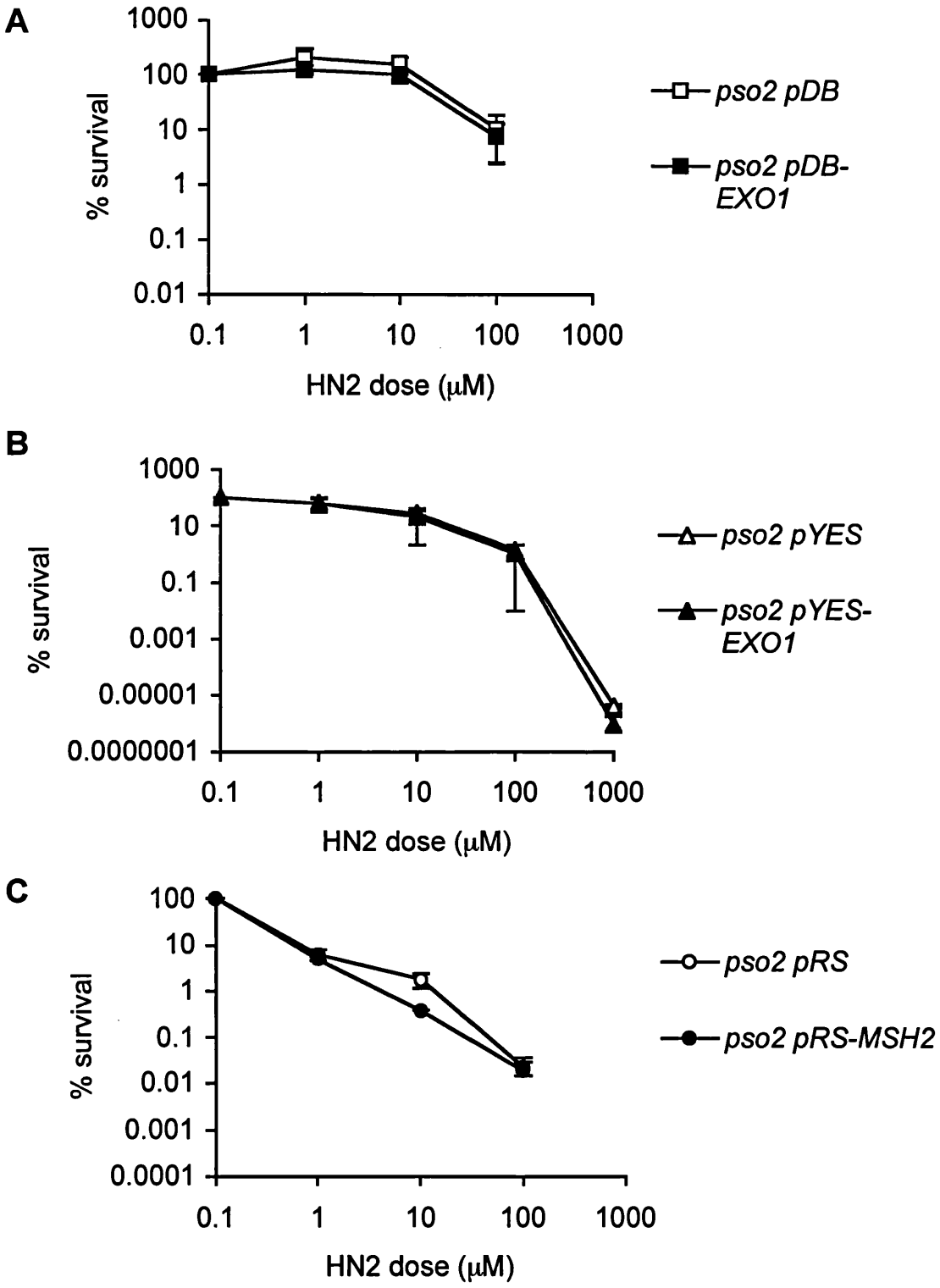

Figure 4.14 Complementation analysis of a pso2 mutant. **A.** Constitutive expression of *EXO1*. **B.** Galactose-induced (overnight) expression of *EXO1*. **C.** Galactose-induced expression of *MSH2*. Cells were treated with 0 to 1000 μM HN2, and survival determined by plating on YEPD. Comparisons are made with empty vector controls. Error bars show SEM.

In order to account for possible interference with other cellular processes, *EXO1* was also expressed in an inducible fashion using the *GAL1* promoter (pYES2-*EXO1*). The plasmid pYES2-*EXO1* was cloned for the purposes of this study using standard molecular techniques. Briefly, a 2.6 kb fragment incorporating the complete CDS of *S. cerevisiae EXO1* was amplified by PCR using primers designed to incorporate a unique *Hind* III restriction site at the 5' end, and a *Not* I site at the 3' end. This facilitated cloning of the fragment into pYES2 in an orientation-specific manner, and this was subsequently confirmed by sequencing across the insert. The effect of *EXO1* upregulation on the HN2 sensitivity of *pso2* disruptant cells was investigated across a range of induction periods using galactose and raffinose (which neither activates nor represses the *GAL1* promoter) as carbon source. Cells were found to be more viable if treatment with HN2 followed an overnight incubation in the induction media, although the experimental outcome was no different after 2 to 5 hours induction. In all cases, the overexpression of *EXO1* did not suppress the HN2 sensitivity of the *pso2* mutant, as compared to the native vector (Fig. 4.14 B). Similarly, upregulation of *MSH2* from the galactose-inducible episomal plasmid pRS425 (here designated pRS-*MSH2*; Sokolsky and Alani, 2000, published as pEAE127) did not complement the *pso2* mutant (Fig. 4.14 C).

The lack of an observable phenotype for sensitivity to HN2 in either the *exo1* or *msh2* mutant strains prevents additional control experiments for the efficiency of complementation from these plasmids. However, both pDB-*EXO1* and pRS-*MSH2* have been used to successfully express the cloned gene according to published reports, and the integrity of the *EXO1* coding sequence was confirmed for pYES-*EXO1*. Furthermore, RT-PCR was carried out to investigate the extent of overexpression above

the level of the endogenous gene. Figure 4.15 compares *MSH2* expression (520 bp fragment) in a *pso2* deficient cell line carrying either the empty vector pRS425, or pRS-*MSH2*. It is clear that in cells carrying the pRS-*MSH2* plasmid, *MSH2* is expressed at a considerably greater extent than the endogenous background, particularly after 24 h galactose induction but even in the uninduced state. The PCR reactions also contained a control primer pair for *ACT1* expression (300 bp fragment). Other appropriate controls included: an *msh2* deficient strain, omission of the reverse transcriptase enzyme (designated '-'), and an RT-PCR reaction containing no RNA/DNA template. Unfortunately, the *EXO1* transcript has not yet been successfully identified by RT-PCR, despite the use of a range of different primers.

One possible explanation for the lack of complementation by *EXO1* or *MSH2* for *pso2* sensitivity to HN2 could be that both components of the Exo1-Msh2 complex need to be overexpressed, otherwise one factor will be limiting. This was investigated by co-transforming *pso2* deficient cells with both the pYES-*EXO1* and pRS-*MSH2* plasmids (facilitated by the different selectable marker genes *URA3* and *LEU2*, respectively). The HN2 sensitivity of *pso2* strains bearing both empty vectors or pYES-*EXO1* and pRS-*MSH2* was assessed following an overnight induction in galactose-raffinose media. No rescue of the *pso2* mutant phenotype was observed after the combined overexpression of both genes (Fig. 4.16). It is unlikely that this is a result of the effective drug concentration being diminished by the significantly increased DNA content of the cells (pYES-*EXO1* is 8.5 kb, pRS-*MSH2* is 10.6 kb) as in all cases, the *pso2* cells are more sensitive to HN2 than in the absence of any vector (Fig. 4.1 A). Given that this increase is more substantial for the larger pRS vector, it is plausible that the reduced tolerance of HN2 is due to the extra replicative stress imposed in

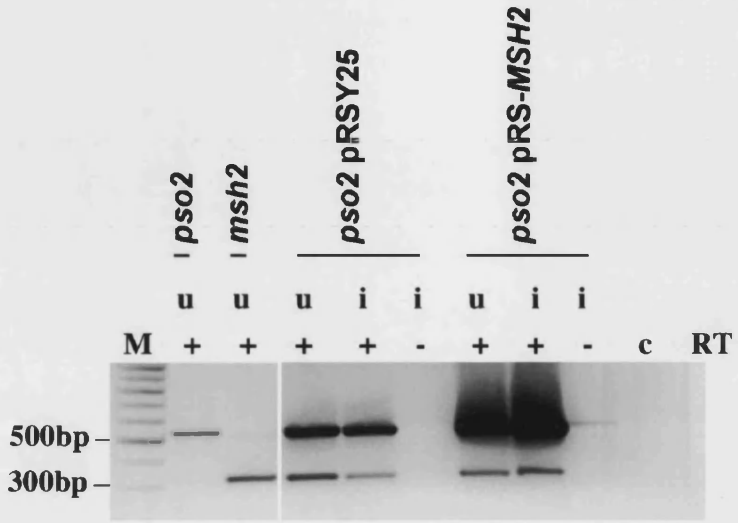

Figure 4.15 Confirmation of MSH2 gene expression by RT-PCR. The extent of *MSH2* expression is compared across four different strains: *pso2*, *msh2*, and *pso2* bearing either the empty vector pRSY25, or pRS-*MSH2*. RNA was extracted from uninduced cells (u), or after 24 h galactose induction (i). RNA preparations were treated with RNase-free DNase before RT-PCR, to prevent contamination by cellular DNA, and this is confirmed by the omission of reverse transcriptase enzyme in the RT reaction (+/- RT). The 520 bp fragment is *MSH2*, and the 300 bp fragment is the *ACT1* loading control. c = water control (no template). M = 100 bp marker.

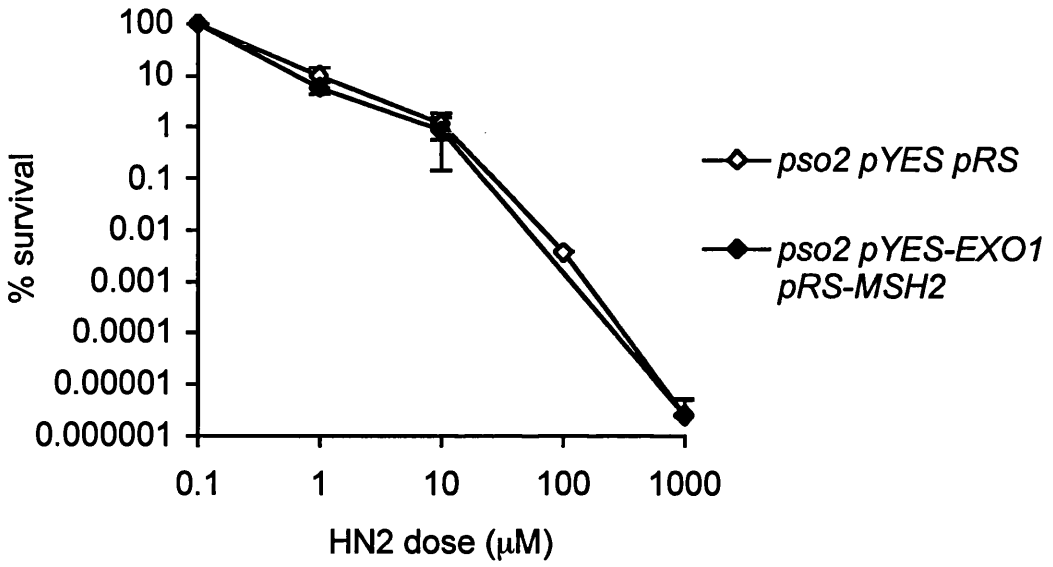

Figure 4.16 Simultaneous complementation analysis of a pso2 mutant by EXO1 and MSH2. Cells were incubated in galactose media overnight to induce expression of *EXO1* and *MSH2*, then treated with 0 to 1000 μM HN2, and survival determined by plating on YEPD. A comparison is made with the empty vector controls. Results are the mean of two independent experiments, and error bars show the SEM.

maintaining the plasmid. Indeed, subsequent replica plating to selective media revealed that few cells retain either plasmid after treatment with HN2 (data not shown).

4.6.2 The HN2 sensitivity of *pso2 exo1* and *pso2 msh2* can be rescued by plasmid expression of the disrupted genes

Given the lack of complementation of *pso2* mutants by *EXO1* or *MSH2*, it was crucial to confirm that the HN2 sensitivity observed in the *pso2 exo1* and *pso2 msh2* double mutants is solely due to the loss of these genes. The *pso2 exo1* and *pso2 msh2* strains were transformed with plasmids expressing wild type copies of one of the disrupted genes (pYES-*PSO2*, pYES-*EXO1*, and pRS-*MSH2*, respectively). If the phenotype of the double disruptant were true, it would be expected that *pso2 exo1* pYES-*PSO2* should resemble a single *exo1* mutant, and *pso2 exo1* pYES-*EXO1* should resemble the *pso2* single mutant. Likewise for *pso2 msh2*: replacing the *PSO2* gene should recover the phenotype back to that of the *msh2* mutant, and overexpression of *MSH2* should give a phenotype resembling *pso2*. As has been already observed, strains carrying a plasmid are sometimes more sensitive to HN2, and so comparisons were made with empty vector controls. It is clear from the graphs in figure 4.17 that both double mutants can be rescued as predicted by the respective wild type genes. Although it appears that expression of *MSH2* in the *pso2 msh2* double disruptant strain provides more resistance to HN2 than is expected from the vector control *pso2* pYES, the observed cell survival is identical to that of the *pso2* strain without a plasmid (Fig. 4.1). Hence, it is the *pso2* pYES strain that is hyper-sensitive to HN2 rather than an increased resistance in *pso2 msh2* pRS-*MSH2*. Conclusively, the significant sensitivity to HN2

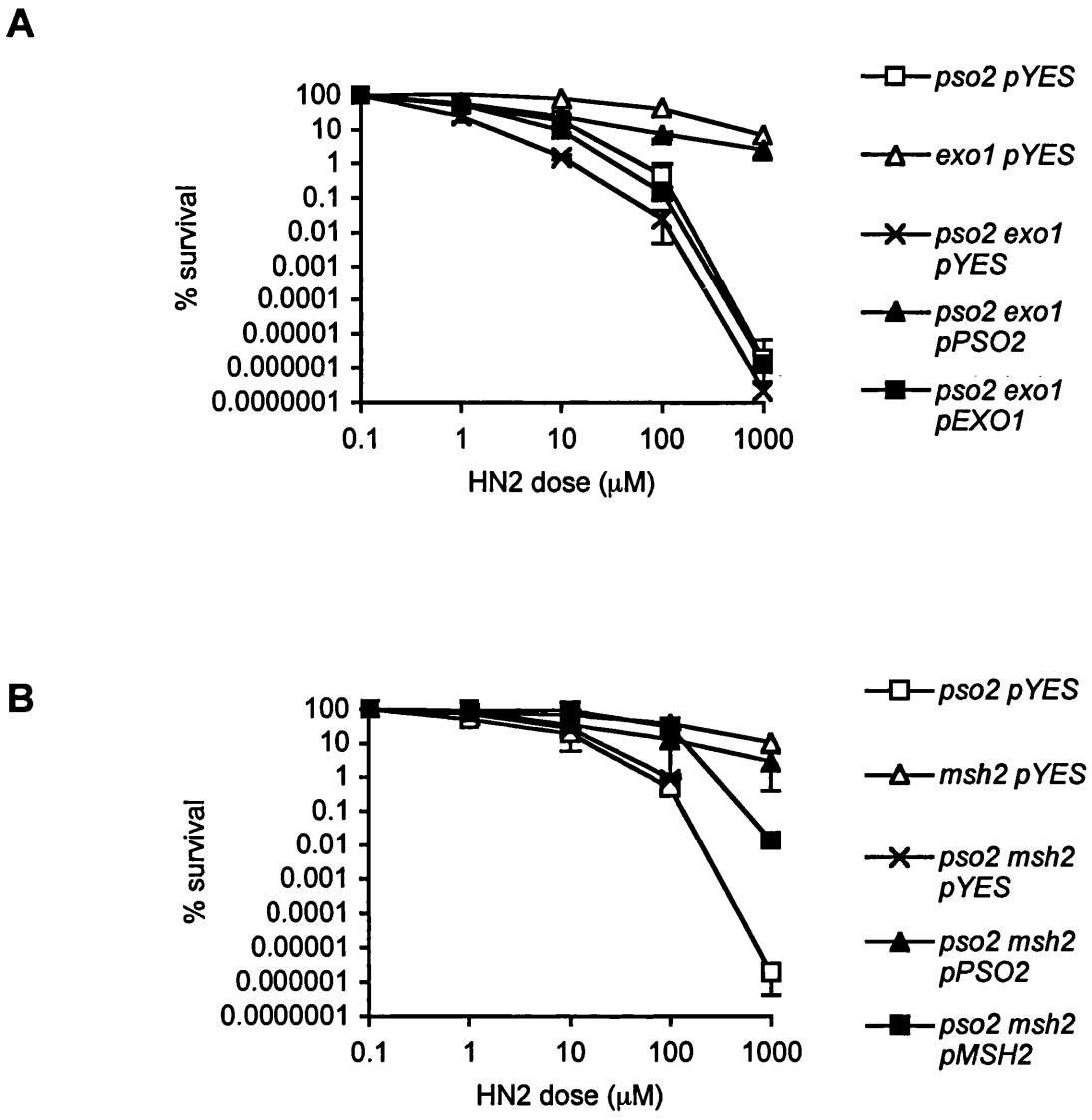

Figure 4.17 Complementation analysis in the pso2 exo1 and pso2 msh2 double disruptants. Cells were incubated in galactose media overnight to induce expression of *PSO2*, *EXO1* or *MSH2*, then treated with 0 to 1000 μM HN2, and survival determined by plating on YEPD. **A.** *pso2 exo1* and **B.** *pso2 msh2*. Comparisons are made with the double disruptants and respective single mutant strains bearing empty vector controls. Results are the mean of two independent experiments, and error bars show the SEM.

observed in the *pso2 exo1* and *pso2 msh2* double disruptants is exclusively due to the synergism between these genes.

4.7 Further analysis of the relationship between *PSO2* and Mismatch Repair

One of the possible explanations for the absence of complementation of the *pso2* phenotype by *EXO1* and *MSH2* could be a requirement for the entire MMR pathway in ICL and DSB repair. Indeed, it is possible that in the absence of Pso2, the role played by Exo1 and Msh2 is not specific for their nuclease and DNA recognition activity, but simply part of a compensatory mechanism provided by the combined activity of MMR. It is well established that MMR is not a predominant mechanism in ICL repair, as the disruption of genes involved in MMR does not render a cell sensitive to interstrand cross-linking agents (Fig. 4.1.2; McHugh *et al.*, 2000). However, the observations of synergism between *PSO2* and *MSH2* suggest that MMR may act in some reserve capacity in the absence of *PSO2*. Previous research into the involvement of MMR proteins in recombination have shown that in some pathways, Msh2 may act without the cooperation of the full MMR family. Msh2 acts in a complex with Msh3 in the removal of 3' non-homologous tails in *RAD1*-dependent single-strand annealing reactions, yet Msh6, Mlh1, and Pms1 are not required (Sugawara *et al.*, 1997). It is therefore important to elucidate whether it is MMR in general, or specific activities attributed to Exo1 and Msh2 that are able to compensate for Pso2, as this will clarify the function of Pso2 in ICL repair.

4.7.1 Other MMR factors show an intermediate phenotype for the modification of *pso2* sensitivity to HN2

A panel of single and double (with *pso2*) disruptant strains encompassing the major MMR factors *MSH3*, *MSH6*, and *MLH1* were created in the B356-7C *S. cerevisiae* background. All known examples of DNA repair involving Msh2 have been found to require interaction with either Msh3 or Msh6. Hence a role for either of these factors is plausible in the *EXO1*/*MSH2*-dependent ICL repair mechanism. Mlh1 acts downstream of Msh2 in MMR, but has also been found to interact with Exo1, and so is another candidate factor for this reserve ICL repair pathway. *PMS1* was not investigated, as it is not required in all MMR reactions. The disruptant strains were examined for sensitivity to nitrogen mustard, as for *exo1* and *msh2* (Section 4.1).

Consistent with the accepted view that MMR is not involved in the repair of ICL and the results already presented here for *msh2*, loss of *msh3*, *msh6*, or *mlh1* alone did not significantly increase sensitivity to HN2 compared to the wild-type parent strain (Fig. 4.18 A-C). However, disruption of any of these MMR factors combined with a deficiency in *pso2* results in a synergistic increase in HN2 sensitivity (Fig. 4.18). The response to HN2 in the *pso2 msh3*, *msh6*, and *mlh1* double mutants varies slightly from that observed for either *pso2 exo1* or *pso2 msh2*. The latter strains demonstrated a very severe reduction (10,000-fold) in cell survival after treatment at 100 μM HN2, whereas the *pso2 msh3*, *msh6*, and *mlh1* double disruptants all exhibit a normal shoulder of resistance at this dose, with only 100-fold lower survival than the wild-type strain. At the highest dose, all double mutant strains are equally sensitive to HN2. Hence it would seem that while loss of any of the major MMR repair genes in conjunction with *pso2* leads to a synergistic increase in sensitivity to HN2, only a deficiency in *msh2*

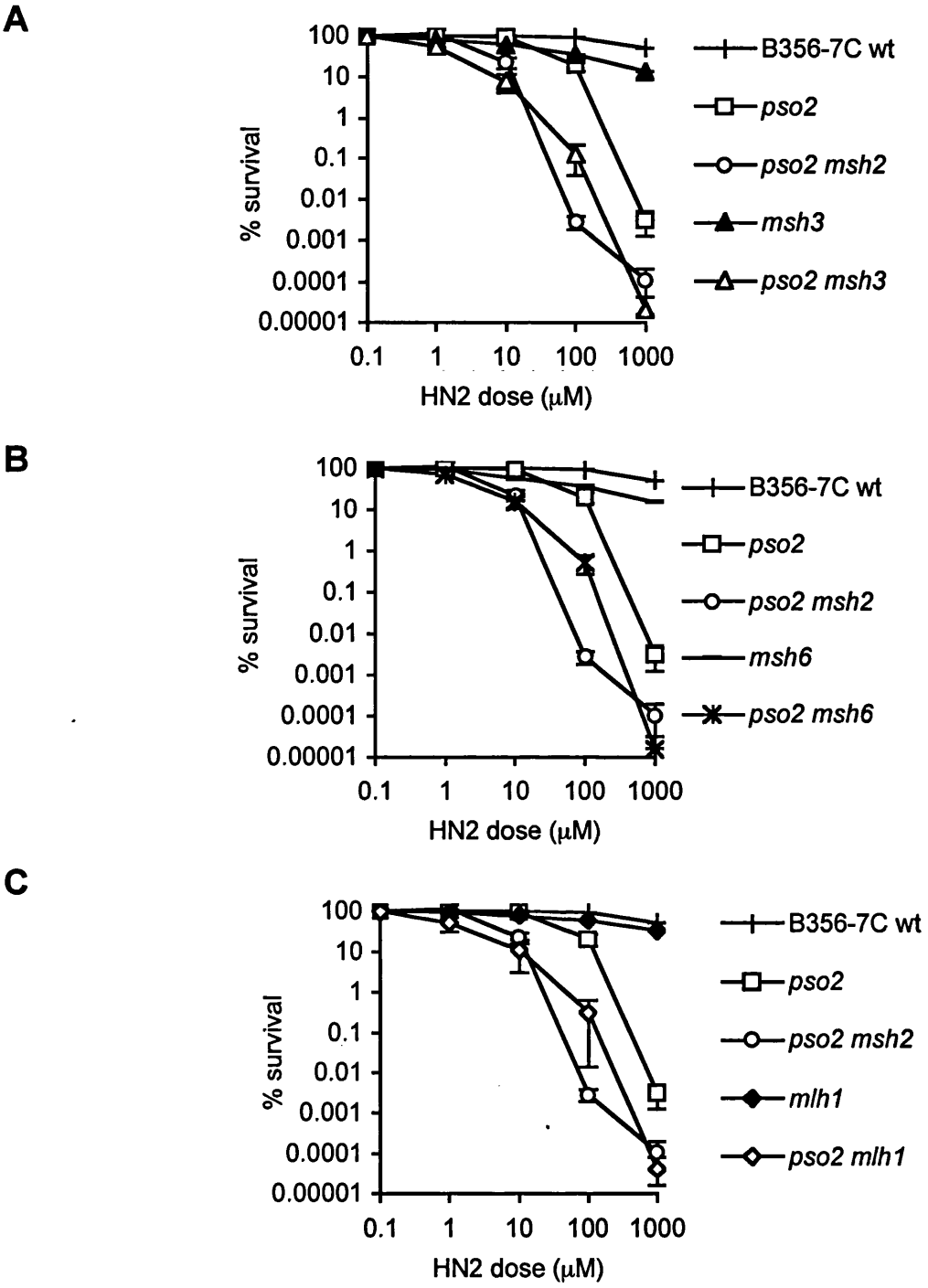

Figure 4.18 Comparison of HN2 sensitivity in pso2 and MMR mutants. Exponential phase cells were treated with 0 to 1000 μM HN2 for 1 h, and survival monitored by plating on YEPD. Comparisons of *pso2* with: **A.** *msh3*, **B.** *msh6*, **C.** *mlh1*. All results are the mean of at least three independent experiments, and the error bars show the SEM.

resembles the phenotype of an *pso2 exo1* strain, with the other strains (*pso2 msh3*, *pso2 msh6*, *pso2 mlh1*) exhibiting an intermediate response. However, this notion is dependent upon the set of data at one single dose, and should be more thoroughly investigated using a range of doses between 50 and 500 μM HN2.

4.7.2 An intermediate phenotype is also observed for sensitivity to ionising radiation in *pso2*-MMR double disruptants

The same panel of MMR-deficient strains (*msh3*, *msh6*, *mlh1*) was subjected to X-irradiation, as already described for *exo1* and *msh2* (Section 4.2.1). As anticipated, none of the single MMR mutants responded differently to ionising radiation, compared to the wild-type parent strain (Fig. 4.19 A-C). The three double disruptant strains *pso2 msh3*, *pso2 msh6*, and *pso2 mlh1* display a range of sensitivity to X-irradiation (Fig. 4.19), yet none are as susceptible as the *pso2 msh2* strain (Fig. 4.3 B). The response to X-rays in *pso2 msh3* and *pso2 msh6* cells is of a similar magnitude as in *pso2 exo1* cells, being approximately 2-fold more sensitive than the wild-type at 300 Gy (Fig. 4.19 A, B). In contrast, *pso2 mlh1* double disruptants are only negligibly more sensitive (1.3-fold) than the respective single mutants (Fig. 4.19 C). Hence it would seem that loss of the MMR factors *MSH3*, *MSH6*, and *MLH1* in a *pso2* deficient background leads to an intermediate sensitivity to X-irradiation.

4.7.3 No deficiency in recombination is observed for other MMR factors in combination with *pso2*

Further investigation of the effects of incomplete MMR in cells deficient for *PSO2* activity utilised the inverted repeat recombination substrate introduced into the B356-

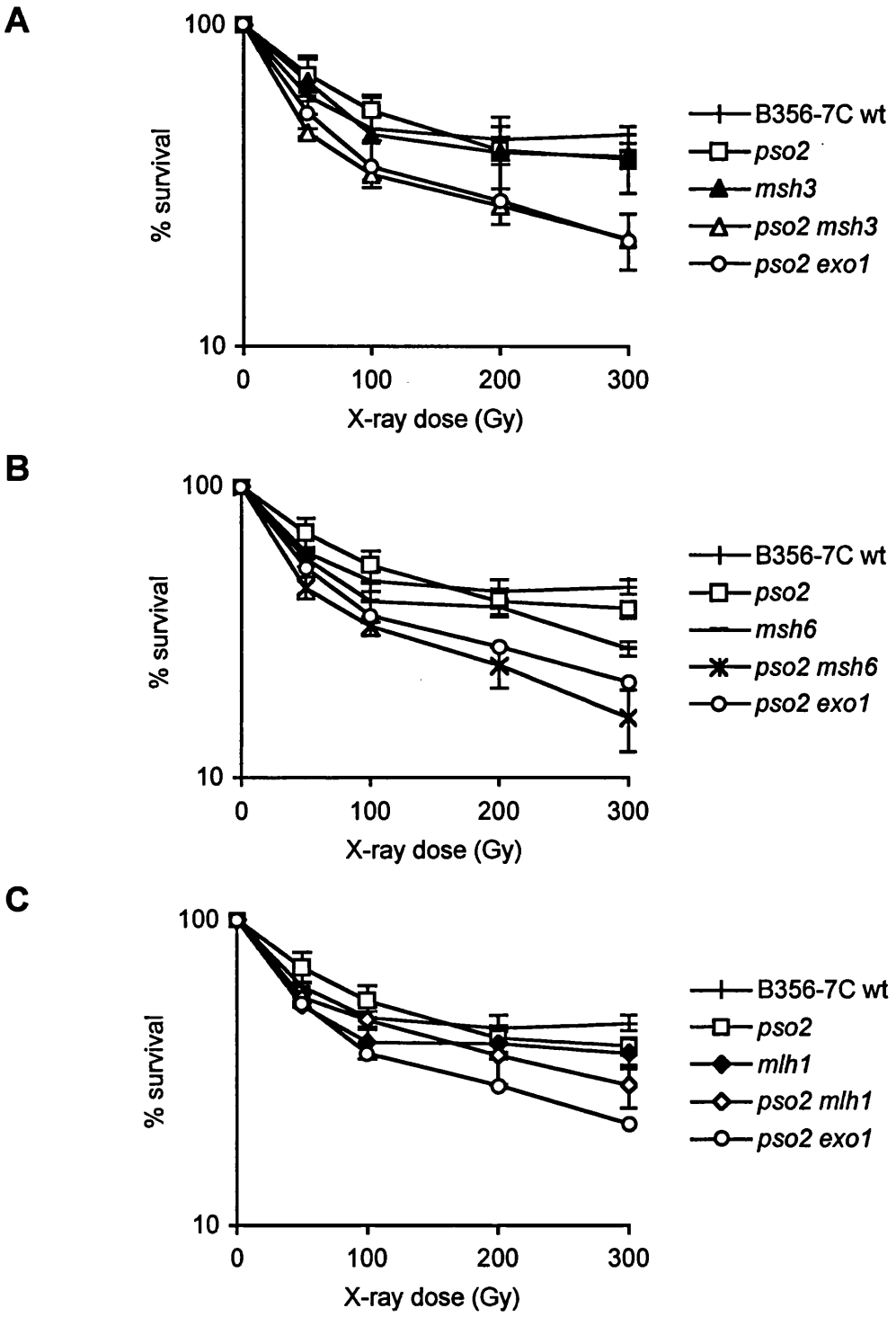

Figure 4.19 Comparison of X-irradiation sensitivity in pso2 and MMR mutants. Exponential phase cells were treated with 0 to 300 Gy X-irradiation, and survival monitored by plating on YEPD. Comparisons of *pso2* with : **A.** *msh3*, **B.** *msh6*, **C.** *mlh1*. All results are the mean of at least three independent experiments, and the error bars show the SEM.

7C strain background. As can be seen from figure 4.20, the *msh3* and *mlh1* single mutants exhibit a 50 % reduction in recombination at the inverted repeat substrate, compared to the wild-type parent, B356-7C. This represents a slightly more recombination-deficient phenotype than observed for *msh2* cells. However, the most significant difference between these MMR mutants and *msh2* is that there is no synergism with *pso2* for recombination. It is clear that *pso2 msh3* and *pso2 mlh1* demonstrate no further reduction in recombination capacity compared to the respective single mutants (Fig. 4.20, Table 4.5). Recombination rates were not calculated for the MMR factor *MSH6*, as to date, only white (ADE^+) *pso2 msh6* colonies have been isolated.

Table 4.5 **Spontaneous recombination rates in *pso2*-MMR defective strains.** Mean rates at the *ADE2* inverted repeat construct are calculated as events/cell/generation from 10-20 independent analyses (SEM as represented in Fig. 4.20), and relative rates are expressed as a percentage of the wild-type.

Strain	Mean rates (x 10^{-6})	Relative rate (% wt)
B356-7C wt	564	100.0
msh2	386	68.4
pso2 msh2	55	9.8
msh3	261	46.3
pso2 msh3	258	45.7
mlh1	306	54.2
pso2 mlh1	328	58.1

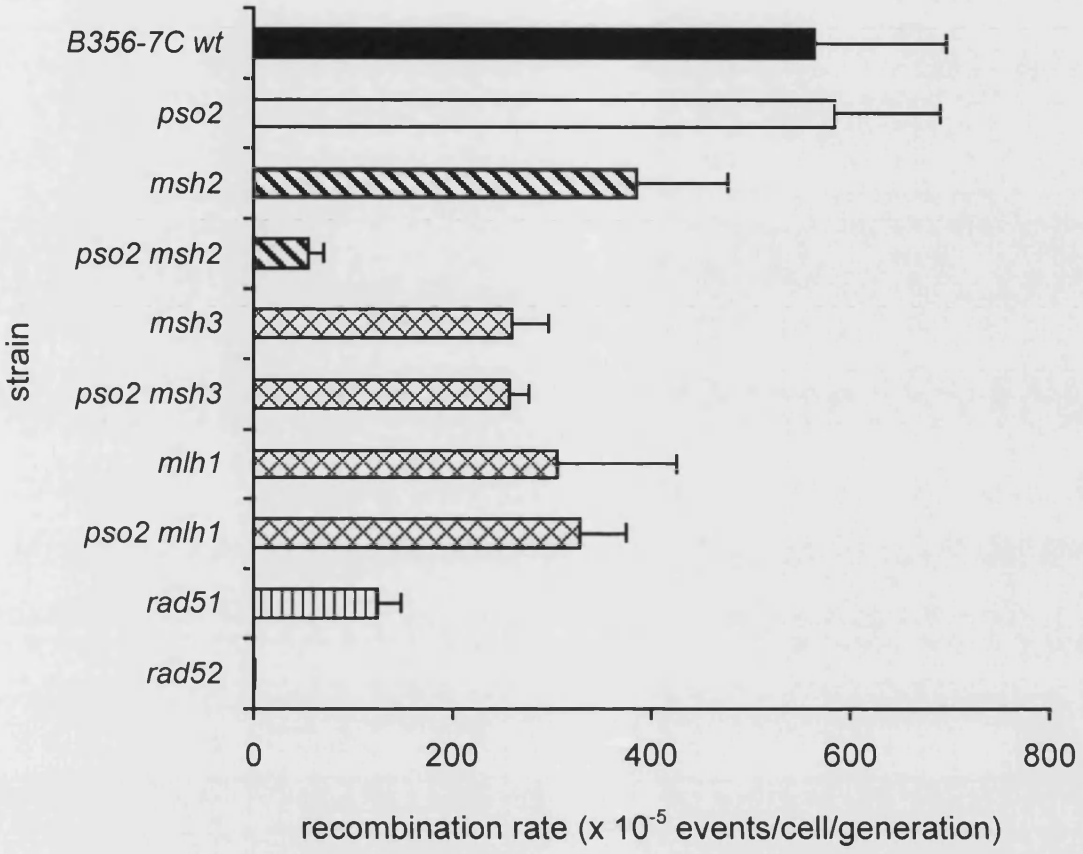

Figure 4.20 Comparison of spontaneous recombination in pso2 and MMR mutants, at the *ADE2* inverted repeat construct. Rates are the mean of 10-20 independent assays, and error bars represent the SEM.

4.7.4 Increased spontaneous mutation is not further affected in *exo1* and *msh2* mutants by the loss of *PSO2*

Both *exo1* and *msh2* disruptant cells are deficient in mismatch repair, and have been shown to cause an increased rate of mutation in the *CAN1* gene, particularly frameshifts, after growth in the presence of canavanine (Marsischky *et al.*, 1996). Consequently, the *CAN1* forward mutation assay was used to determine whether the overlap of activity between *PSO2* and *EXO1-MSH2* extends to MMR as well as recombination. Given that neither *exo1* nor *msh2* deficient cells are sensitive to HN2, and that HN2-induced mutagenesis is not observed in either strain (data not shown), the relationship between *PSO2* and *EXO1-MSH2* was investigated for spontaneous mutagenesis at the *CAN1* locus. As already discussed in Chapter 3, the B356-7C parental strain is derived from the W303 background which is CAN^R, and hence not compatible with this assay. In the wild-type strain, forward mutation to canavanine resistance was observed at a rate of 126 mean mutants per 10^8 survivors, and loss of *PSO2* did not result in any significant deviation from the wild-type (Fig. 4.21 A). Both the *exo1* and *msh2* mutants demonstrate an elevated rate of spontaneous mutation, 14 and 22 fold higher than the wild-type, respectively. It is clear from figure 4.21 A that *PSO2* behaves epistatically with both *EXO1* and *MSH2* for forward mutation at the *CAN1* locus, as the mutator phenotypes of the *pso2 exo1* and *pso2 msh2* double disruptants are no more pronounced than in the *exo1* or *msh2* single mutants.

To examine whether the additional deletion of *PSO2* altered the type of mutagenic event occurring in the *exo1* or *msh2* background, the PCR-based screen designed by Xie and co-workers (2001) for the investigation of *rad27* mutagenesis was employed. This strategy involves PCR amplification of the *CAN1* gene and subsequent *Hph* I

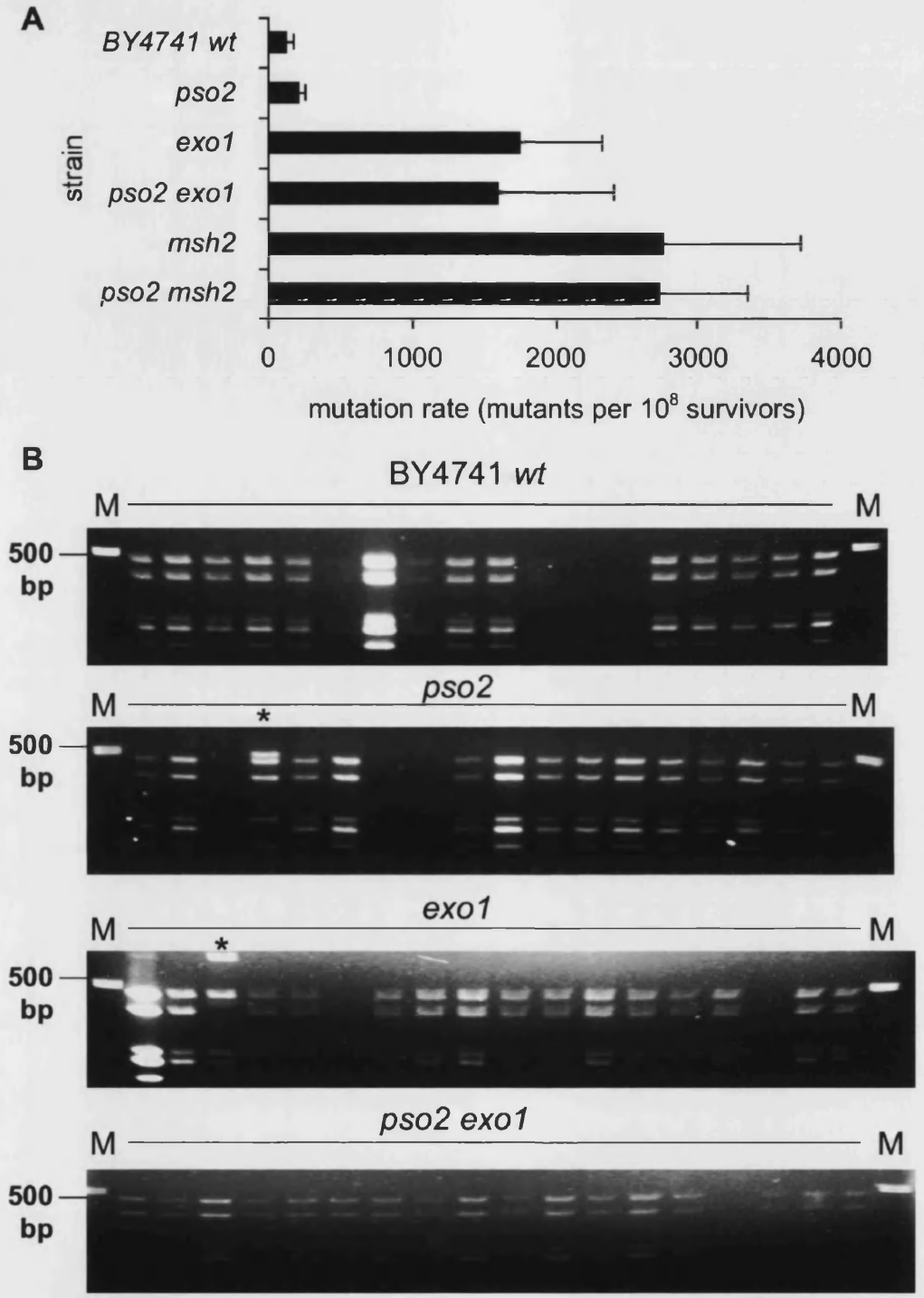

Figure 4.21 Analysis of mutagenesis in pso2, exo1 and msh2 mutants. **A.** Mean spontaneous forward mutation rate at the *CAN1* locus, determined from the relative ability to grow on SC–arg plates supplemented with canavanine (mutants) compared to YEPD (survivors). Results are the mean of three independent experiments and error bars show the SEM. **B.** Agarose gel electrophoresis showing the *Hph* I digested PCR products obtained from Can^R colonies. M = 100 bp marker. * = variant *Hph* I restriction fragments.

restriction, with the products visualised by agarose gel electrophoresis. It is possible to distinguish between the single nucleotide deletions and small frameshifts or base substitutions that are characteristic of mismatch repair mutants, and gross rearrangements such as large duplications that predominate in the absence of *rad27* (Tishkoff *et al.*, 1997 B). Examination of the *Hph* I digestion pattern indicated that there is no difference between the wild-type, and *pso2*, *exo1*, *msh2* single and double disruptant strains (Fig. 4.21 B). Hence *PSO2* behaves epistatically to both *EXO1* and *MSH2* for spontaneous mutagenesis, and a loss of *PSO2* does not further influence the spectrum of mutation events. No insertion-deletion mutations were observed, and the low frequency occurrence of variant *Hph* I fragments (starred lanes, Fig. 4.21 B) can be explained by the loss of an *Hph* I restriction site in all cases. The absence of frequentgross alterations of the *CAN1* gene in these mutants is consistent with a defect in single base and small-tract MMR (Xie *et al.*, 2001; Tran *et al.*, 2001).

4.8 Discussion

Conclusions drawn from the studies presented in Chapter 3 endorsed a model of ICL repair requiring initial processing of the cross-link by both NER and Pso2, and subsequent repair of the resulting DSB by homologous recombination. In this chapter, consideration was given to elucidating the role of Pso2 at this early-intermediate stage of ICL repair. On the basis of its metallo-β-lactamase hydrolytic domain and putative events expected to coincide with the period of Pso2 activity in ICL repair, a hypothesis was drawn that Pso2 is involved in the nucleolytic processing of repair intermediates. The preliminary approach was to evaluate whether *PSO2* interacts genetically with any of the known DNA repair nucleases. Synergism was identified between *PSO2* and

EXO1 in the repair of HN2-induced cross-links, which is particularly significant considering that a loss of *EXO1* alone does not affect a cells capacity to repair ICL (Section 4.1.1). This appears to represent a novel relationship for *PSO2* that is not shared with other NER factors, and is specific for *EXO1* of the yeast repair nucleases tested. Exo1 is a member of the Rad2 nuclease family, of which the nuclear members are Rad2, Exo1 and Rad27 in yeast. These nucleases appear to be redundant in some processes, such as DNA replication where Rad27, and Exo1 collaborate in Okazaki fragment maturation (Tishkoff *et al.*, 1997; Qiu *et al.*, 1999; Sun *et al.*, 2003). However, it is clear that the overlap of activity between Pso2 and Exo1 in ICL repair does not extend to the other members of this family. An additive relationship is observed for *RAD27* and *PSO2* (Section 4.1.1), suggesting independent roles in the repair of cross-linked DNA, and consistent with the involvement of Rad27 in the BER of mono-alkylation damage produced by nitrogen mustards (McHugh *et al.*, 1999, 2000). Furthermore, *PSO2* consistently exhibits an epistatic relationship with NER, even for factors such as *RAD1*, which have additional nucleolytic roles in recombination (Section 4.1.1).

In contrast to the other repair nucleases, an identical synergistic effect to that seen with *EXO1* was observed upon the disruption of *MSH2* in a *pso2* deficient background (Section 4.1.2). Given that the Exo1 and Msh2 proteins are known to associate (Tishkoff *et al.*, 1997 A; Sokolsky and Alani, 2000) and the observation that *exo1* and *msh2* are epistatic, it would seem that their combined activity compensates for a loss of Pso2 in the repair of ICL.

Further to the overlapping role for *PSO2* with *MSH2* and *EXO1* in the repair of DNA interstrand cross-links, a synergistic relationship was also observed for spontaneous homologous recombination and DSB repair. It has already been observed that loss of *pso2* is associated with a deficiency in the repair ICL-associated DSBs (Section 3.6). This has been further investigated using CHEF-PFGE for the *pso2 exo1* and *pso2 msh2* double mutants, with the discovery that DSBs accumulate to a greater extent and fail to be repaired (Section 4.3.1). The apparent requirement for Pso2, Exo1, and Msh2 in the repair of DSBs associated with ICL also extends to the lesions arising from ionising radiation, although only to a modest degree (Section 4.2.1). None of these factors were required in the repair of UVC-induced DNA damage, nor were they involved in the response to cell cycle inhibition by benomyl and hydroxyurea. However, the combination of a *pso2* mutation with the disruption of *msh2* or *exo1* leads to a significant defect in spontaneous inverted repeat homologous recombination (Section 4.4.1). The recombination defect observed in the *exo1* and *msh2* single mutants correlates with published data, although a greater degree of deficiency has been observed using alternative direct repeat recombination substrates (Saparbaev *et al.*, 1996; Fiorentini *et al.*, 1997; P. McHugh, unpublished data).

It was appropriate to investigate the complete panel of B356-7C gene disruptants in the analysis of spontaneous recombination as each is known to affect recombination to some extent. *RAD51*, *RAD52*, and *MRE11* are all key factors in homologous recombination. However, this inverted repeat substrate highlights differences in the relative involvement of these genes in recombination, with *RAD52* having a more fundamental role in multiple pathways (Section 4.4.1; Rattray and Symington, 1994). The extent of the recombination deficiency observed in the absence of both *PSO2* and

EXO1/MSH2 is not as severe as the complete abrogation of recombination in the *rad52* mutant, yet it is more pronounced than that seen in the *rad51* or *mre11* strains. *RAD1* removes 3' flaps and heterologies during single strand annealing and DSB repair pathways (Ivanov and Haber, 1995). Loss of *RAD1* has resulted in variable effects on spontaneous recombination in direct repeat substrates (Thomas and Rothstein, 1989; Klein, 1998; Schiestl and Prakash, 1998), but none at an inverted repeat (Rattray and Symington, 1995), although a mild defect is observed here (Section 4.4.1). Furthermore, mutations in the *RAD27* gene have previously been associated with a hyper-recombinant phenotype (Vallen and Cross, 1995; Tishkoff et al., 1997; Symington, 1998; Debrauwere *et al.*, 2001), which is confirmed by this study (Section 4.4.1). The observation that deletion of *PSO2* in these backgrounds does not further affect the recombination phenotype (Section 4.4.1), indicates that *PSO2* either behaves epistatically or does not affect the pathways of spontaneous recombination represented by these genes. However, the interaction with *RAD52* is less easily defined, as accurate and quantifiable detection of recombination events in the absence of *RAD52* is beyond the scope of this assay. Unfortunately, the *ADE2* inverted repeat construct also proved unsuitable for the investigation of HN2-induced recombination events, probably as a result of the infrequent occurrence of a cross-link within the substrate DNA (Section 4.4.3).

In the *pso2 exo1* and *pso2 msh2* double mutants the defect in spontaneous recombination is associated with a reduction in gene conversion and compensatory increase in the occurrence of cross-overs (Section 4.4.2). That only a subset of recombination events are blocked in *pso2 exo1* and *pso2 msh2* cells likely explains their only moderate sensitivity to ionising radiation and partial defect in spontaneous

recombination. Presumably some intermediate structure arising from the repair of both endogenous and ionising radiation-induced damage needs to be processed by Pso2 and/or Exo1-Msh2 prior to recombinational repair. It is possible that these factors are recruited in the presence of an irreversibly collapsed replication fork, such as that occurring in the presence of an ICL. Indeed, the current models of fork restart are based upon the replication machinery encountering an adduct that afflicts a single DNA strand, and so it is plausible that additional factors or alternative mechanisms may be required in cases where both strands are affected (McGlynn and Lloyd, 2002).

The diverse nature of DSBs arising from different genotoxic agents is highlighted by the fact that mammalian cells often repair radiation-induced DSBs by NHEJ (Lieber *et al.*, 2003), whereas ICL-associated DSBs are almost exclusively processed by homologous recombination (De Silva *et al.*, 2000; Caldecott and Jeggo, 1991). For example CHO cells deficient in XRCC5 (ku80) show a near wild-type sensitivity to cross-linking drugs but are highly sensitive to ionising radiation. This contrasts with cells lacking XRCC2 and XRCC3 (Rad51-paralogs), which are sensitive to both ionising radiation and cross-linking drugs, and also show a profound defect in the repair of ICL-associated DSBs (De Silva *et al.*, 2000). A greater understanding of the structures of replication forks inhibited by ICLs and other DSBs would help in elucidating the DNA structures acted upon by Pso2 and Exo1-Msh2.

Several mechanisms have been proposed to account for the spectrum of recombination events that can contribute to the recovery of *ADE* prototrophs following recombination events at the inverted repeat construct used here. The original models of simple intrachromatid gene conversions, with or without associated crossovers (Rattray and

Symington, 1994, 1995) have more recently been extended to include mis-aligned sister chromatid exchanges mediated by long conversion tracts, and break-induced recombination followed by single-strand annealing (Symington, 2002). An increased frequency of crossovers during spontaneous recombination has been observed previously for an *exo1* strain, although with a different substrate, used to determine plasmid gap repair (Symington *et al.*, 2000). It was suggested that the increase in crossovers may result from the elimination of MMR-mediated constraints on the recombination process, which would be consistent with increased occurrence of crossovers seen in the *msh2* mutant in this study (Section 4.4.2). However, the absence of an associated rise in the Class III events (gene conversions associated with cross-overs) is unexpected. This may reflect a general loss of cells attempting gene conversion in the *exo1/msh2* defective strains, due to a defect in the processing of an intermediate structure, such as the removal of ssDNA tails generated during recombination. As the spectrum of recombination events is not further modified by the loss of *PSO2* in either an *exo1* or *msh2* background despite the decreased incidence of recombination, it would seem that the activities of Pso2 and Exo1-Msh2 are redundant in the initial processing of spontaneous lesions, but Pso2 does not directly influence the final recombination outcome. It is likely that Exo1 and Msh2 have two roles: one that overlaps with Pso2 for the recognition and processing of damaged sites prior to commitment to a recombination-based repair pathway, and a second role during the recombination reaction that is involved with the suppression of crossovers, probably due to rejection of pairing in homeologous regions of DNA (Evans *et al.* 2000).

Unlike the human homologue Artemis, *PSO2* does not appear to play a role in NHEJ. This is not surprising, as of the three known human homologues of *PSO2*, Artemis is

the least conserved (30 % identity by Blast, but only within 132 residues of the metallo-β-lactamase and β-CASP motifs; Fig. 1.13). Also, it is well known that gene duplications enable the evolution of proteins with novel functions. Normal frequencies of plasmid rejoining have been observed in *pso2* cells regardless of the nature of the DNA ends, and this was not affected by the further deletion of *exo1* or *msh2* (Section 4.5). The absolute values are slightly higher than those observed by Teo and Jackson for the BY4741 wild-type and *lig4* strains (1997), however, the trend is the same, and the variance probably reflects the use of a different *S. cerevisiae* strain and plasmid. A minor, qualitative role for Pso2 in the fidelity of NHEJ cannot be excluded, as this can only be examined by sequencing the rejoined plasmids recovered from this assay. Nevertheless, a recent report by Yu and co-workers (Yu J. *et al.*, 2004) also failed to detect any deficiency in the NHEJ of restriction endonuclease-linearised plasmids or HO endonuclease-cleaved chromosomal DNA, in the absence of *PSO2*. This suggests that Pso2 induces a homologous recombination-based pathway of DSB repair, especially given that NHEJ does not play a significant role in ICL repair in yeast (McHugh et al., 2000).

Although Artemis has been associated with the NHEJ pathway of repair, its function is primarily involved with the opening of DNA hairpin structures, such as those formed during vertebrate immunoglobulin gene (V(D)J) rearrangement (Ma *et al.*, 2002). The study by Yu and co-workers (Yu J. *et al.*, 2004) also investigated the involvement of yeast *PSO2* in the transposition and repair of maize Ac/Ds transposon excision sites introduced into *S. cerevisiae* (thought to be similar to V(D)J rearrangement: Kunze and Weil, 2002). In contrast to the major NHEJ factors (which are completely deficient in this assay), *pso2* mutants retained 10 % of the wild-type capacity for reversion of the

ade2::Ac-1 allele, and this was associated with an increased incidence of transposase mis-cutting. The authors suggest that Pso2 may act in the recognition of the DNA hairpin structures that arise during transposition, and subsequently assist binding of the transposase. It is plausible that the DNA confirmation adopted following the excision of the first transposon end resembles that of a partially incised ICL-repair intermediate. Indeed, where suitable DNA regions are accessible in the absence of the transposition complex, this structure will be resolved by homologous recombination. Furthermore, it has been suggested that Msh2 recognises and binds sites of DNA damage, and that human MutSα activates mismatch excision by Exo1 (Genschel and Modrich, 2003), which would seem to resemble the profile of Pso2 and transposase. If this were the case, it may explain the nominal increase in sensitivity to HN2 seen in the triple gene disruptant, *pso2 exo1 msh2* (Section 4.1.2), as there may be alternative, less efficient nucleolytic partners that can be recruited by Msh2. High throughput proteomic screens have as yet failed to detect any association of nuclear proteins with Pso2 (Ho *et al.*, 2002). However, it is entirely possible that Pso2 may only interact with its relevant partner after binding to ICLs, especially given the variations in protein complexes identified after treatment with other DNA damaging agents (Ho *et al.*, 2002), and this scenario has not yet been investigated. Alternatively, Pso2 may act independently to process some DNA lesions by means of its hydrolytic metallo-β-lactamase domain.

The synergism between *PSO2* and *EXO1* or *MSH2* for sensitivity to HN2, DSB repair, and spontaneous recombination suggests that these factors act in independent pathways that can perform the same function. In the case of cross-link repair, the lack of HN2 sensitivity in the *exo1* and *msh2* single mutants strains indicates that these factors do not make a significant contribution in the presence of functional Pso2. Hence, any

involvement of Exo1 and Msh2 in ICL repair transpires purely as a backup mechanism in the absence of Pso2. This may partially explain the inability of Exo1 and Msh2 to complement the *pso2* mutant, as it is possible that the obtained level of overexpression was not sufficient to allow for further repair activity. It is possible that Exo1 and Msh2 are only able to recognise and process certain types of intermediate structures that occur during ICL repair. There may even exist other factors that can substitute to some extent for Pso2. Alternatively, the population of these proteins may be so tightly regulated that no significant increase in enzymatic activity was achieved despite the apparent increase in mRNA. Although overexpression of Exo1 has been reported to complement a number of other nuclease deficiencies, closer inspection of the data shows that often only partial complementation was achieved (Sokolsky and Alani, 2000; Lee S.E. *et al.*, 2002), and others have been unable to overexpress Exo1 in *S. cerevisiae* for protein purification (Tran *et al.*, 2001; P. McHugh, personal communication). Interestingly, sufficient expression is achieved from the pYES-*EXO1* vector to restore the phenotype of the *pso2 exo1* double disruptant back to that of the *pso2* single mutant (Section 4.6.2), although this would obviously be achievable within any post-transcriptional regulation existing for the endogenous gene. A further explanation for the absence of complementation between *PSO2* and *EXO1*/*MSH2* may be that the full complement of MutS genes (i.e. *MSH3* and *MSH6* as well), are required to facilitate the function of Msh2. Investigation of such a requirement for these Msh2-dimerisation partners in the complementation of a *pso2* mutant strain is obviously beyond the scope of this plasmid-based assay.

Given the overlap in activity of *PSO2* and *MSH2-EXO1* it was also clearly important to determine if this extended to mismatch repair itself. The predominant phenotypes

associated with this relationship, namely, hypersensitivity to HN2, moderate sensitivity to ionising radiation, and a deficiency in spontaneous recombination, were considered. It is clear from the results presented in section 4.7 that *PSO2* does not interact with all MMR factors to the same extent. In the case of ICL repair, it would seem that at lower doses of HN2, Msh3, Msh6, and Mlh1 cannot compensate for a loss of Pso2 activity to quite the same extent as Msh2 and Exo1 (Section 4.7.1). However, at the maximum dose, all *pso2*-MMR double mutants are equally sensitive to HN2, regardless of which MMR factor is absent. This suggests that either the Exo1-Msh2 complex recruits other MMR factors as part of the repair process, perhaps with redundancy between Msh3 and Msh6, or that the function of Pso2 in ICL repair can only be substituted by the complete MMR pathway. If the data for HN2 survival is considered alongside that of the ionising radiation and recombination assays, the former hypothesis seems more tenable. Clearly the overlap of activity of *PSO2* with *EXO1* and *MSH2* is not related to the role of MMR in the maintenance of genetic fidelity, as an epistatic relationship is observed for mutagenesis at the *CAN1* locus (Section 4.7.4). The elevated rates of mutagenesis observed in the *exo1* and *msh2* strains are consistent with previously published data (Reenan and Kolodner, 1992; Tran *et al.*, 2001), however, these are not modified by the additional loss of *PSO2*. Most strikingly, none of these other MMR factors are absolutely required for spontaneous recombination in the absence of *PSO2* (Section 4.7.3). Furthermore, neither *MSH6* nor *MLH1* has any significant effect on cell survival after treatment with ionising radiation, yet *MSH3* exhibits a moderate effect, comparable to *EXO1* (Section 4.7.2). It is possible that a preference for Msh3 as the binding partner for Msh2 reflects the type of lesion arising from ionising radiation damage that can be acted on by Pso2, Exo1, and Msh2. In MMR, Msh2 preferentially complexes with Msh3 for the repair of heteroduplex DNA loops, rather than Msh6.

Additionally, it has been suggested that the Msh2-Msh3 complex may be involved in the recognition of branched DNA structures incorporating a free 3' tail (Sugawara *et al.*, 1997). Hence, in the absence of Pso2, Msh2 may recognise and bind some of the intermediate DNA structures arising from the repair of ICL and other DSBs, subsequently recruiting Exo1 and other MMR factors as required to resume repair. Recent analysis of the HN2 sensitivity of a *pso2 msh3 msh6* triple disruptant strain has shown that it phenocopies the *pso2 msh2* strain (T. Ward and P. McHugh, personal communication). This indicates that the intermediate phenotypes seen in the *pso2 msh3* and *pso2 msh6* double deficient cells are due to redundancy between the MutS complexes. Furthermore, it is clear that Msh2 must be associated with either Msh3 or Msh6 in order to function in ICL repair.

In conclusion, it appears that Pso2 plays an overlapping role specifically with Exo1 and Msh2 (MutS) in the processing of ICL repair intermediates, as well as some spontaneous and ionising radiation-induced damage. In the presence of *EXO1* and *MSH2* the recombination defective phenotype of *pso2* cells is not apparent, except during interstrand cross-link repair. This presumably reflects the unusual nature of the intermediates produced at this form of damage, which are preferentially acted upon by Pso2, with Exo1-MutS acting in reserve. In contrast, both *PSO2* and *EXO1/MSH2* are redundantly important during the repair of spontaneous and ionising radiation-induced damage, since no single disruptant demonstrates any reduction in repair efficiency, yet in combination, a significant increase in ionising radiation sensitivity and a reduction in homologous recombination events were observed.

CHAPTER 5 BIOCHEMICAL ANALYSIS

To further elucidate the role of Pso2 in ICL repair, it is necessary to employ biochemical techniques. The genetic studies in yeast that have been described in Chapters 3 and 4 have given a good insight into the relationship between *PSO2* and the DNA repair epistasis groups of NER, homologous recombination, and MMR. However, conclusive evidence relating to the putative nucleolytic activity of Pso2 is only likely to be resolved by producing purified protein for use in *in vitro* assays. This chapter details the procedures used in the first purification of the ScPso2 protein direct from *S. cerevisiae*. Preliminary analysis of the Pso2 protein has been made, providing the foundations for a comprehensive *in vitro* investigation of the function of Pso2 in ICL repair.

A yeast expression vector bearing *S. cerevisiae PSO2* modified with the small antigenic FLAG® epitope at the C-terminus (pGAL-c-FLAG *PSO2*, here abbreviated to pFLAG-*PSO2*) was obtained from Dr M. Tyers (Samuel Lunenfeld Research Institute, Toronto, Canada) (Ho *et al.*, 2002). It was deemed preferable to use a C-terminal tag to investigate the function of Pso2, as although the valine belonging to the final β-CASP motif C has been predicted to lie close to the C-terminal, it remains separated from the FLAG tag by a buffer of 29 residues (Fig. 1.12). Furthermore, the critical HXHXDX motif of the putative catalytic site is positioned more than 200 residues from the C-terminus. It was felt that the application of an N-terminal tag would be more likely to interfere with the nuclear localisation of the Pso2 protein. The FLAG tag is an octapeptide (N-Asp-Tyr-Lys-Asp-Asp-Asp-Asp-Leu-C), which has been designed to be hydrophilic in nature in order to increase the probability of localisation to the surface of

the fusion protein (Sigma product information; Einhauer and Jungbauer, 2001). This is obviously a prerequisite for affinity purification and immunogenic identification of the tagged protein, as the epitope must be accessible to its specific antibody. Previous research suggests that modification with FLAG rarely affects the original conformation and function of the native protein (Molloy *et al.*, 1994; Lee and Altenberg, 2003; Terpe, 2003).

Given the existence of a yeast expression vector bearing the *PSO2* gene, it seemed prudent to attempt to purify Pso2 direct from yeast, rather than using an alternative host organism such as *E. coli.* Considerable effort has recently been made in the use of *E. coli* for the production of yeast Pso2 protein, but without success (P. McHugh, personal communication). Purification of proteins from *S. cerevisiae* is not without limitations, particularly related to complications arising from the need to break down the cell wall. However, extraction from bacterial cells can also prove difficult as a result of the lack of relevant, targeted post-translational modification processes such as phosphorylation and glycosylation, and the frequent production of denatured or inappropriately folded proteins.

5.1 Verification of FLAG-Pso2 activity

The pFLAG-*PSO2* plasmid was initially transformed into *pso2* deficient cells in two different genetic backgrounds (B356-7C and BY4741) to confirm the complete functionality of the FLAG-Pso2 protein in ICL repair. Expression of FLAG-*PSO2* from the *GAL1* promoter was induced by incubation for 5 h in galactose-raffinose media. It was found that cell viability was improved by the inclusion of a pre-induction step, in

which cells were grown to exponential phase in the presence of glucose. Induced cells were subsequently treated with 1, 10, 100, and 1000 μM doses of HN2 (as in previous chapters), and plated to determine the extent of survival. Unfortunately, the empty parent plasmid, pMT2250 was not available as a control. Parallel control experiments were performed instead, in which the *pso2* pFLAG-*PSO2* strains were treated with HN2 in the absence of galactose induction.

It is clear from figures 5.1 A and B that expression of FLAG-*PSO2* completely complements the HN2 sensitivity of the *pso2* disruptant strain. A very slight increase in survival is observed in the uninduced cells carrying the FLAG-*PSO2* plasmid, compared to the parent *pso2* strain. This may result from a residual level of expression from the GAL1 promoter, even in the absence of galactose, as in some cases this promoter has been reported to be leaky.

Therefore, the presence of the FLAG epitope at the C-terminus of Pso2 does not appear to affect the activity of the Pso2 protein in the repair of ICL. It is notable that analogous results are obtained in both genetic backgrounds, despite the variance in HN2 sensitivity of the two independent *pso2* strains.

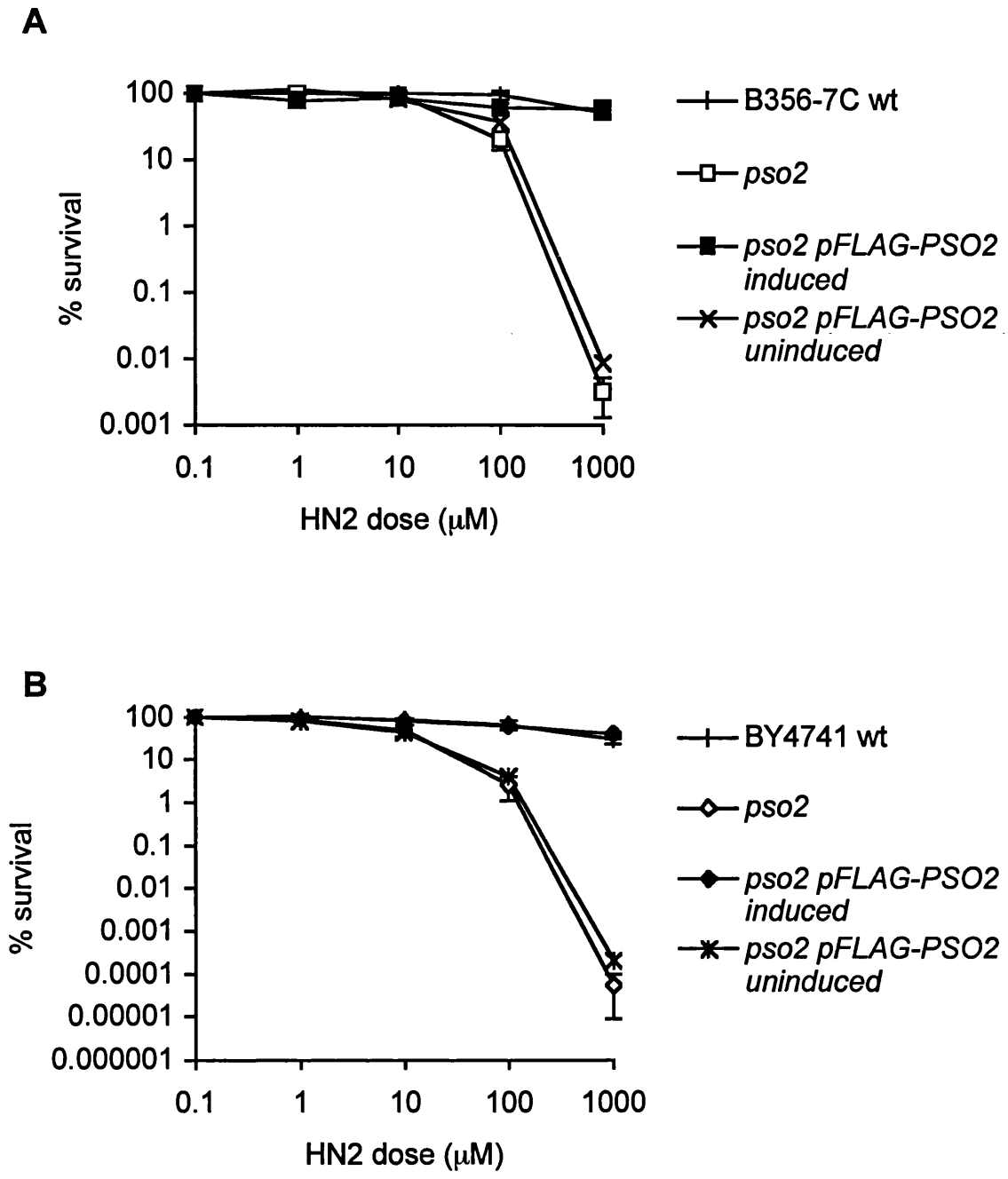

Figure 5.1 Complementation of a pso2 mutant by FLAG-PSO2 expression. *pso2* deficient cells carrying the pFLAG-*PSO2* vector were treated with 0, 1, 10, 100, or 1000 μM HN2, either after a 5 h induction in galactose media (induced) or directly following normal culture in glucose media (uninduced). Survival was monitored by plating on YEPD. **A.** B356-7C genetic background. **B.** BY7471 background. Error bars show the SEM.

5.2 Optimisation of protein extraction

Having established that FLAG-Pso2 is fully active in the repair of HN2-induced DNA ICL, it was necessary to optimise both the galactose induction conditions and the protocol for protein extraction, in order to maximise the protein yield. Initially these extractions were performed on a small scale. A protease-deficient yeast strain, JEL1 (Lindsley and Wang, 1993, gift of Professor Ian Hickson), was exploited for the expression and extraction of Pso2, in order to overcome the normal processes of protein degradation once the cell is disrupted. This is an important consideration for the overall protein yield, as yeast contains a large number of different proteases located within various cellular compartments and membranes. Two of the most problematic proteases for protein purification, the luminal vacuolar endoproteinases PrA and PrB (encoded by *PEP4* and *PRB1* respectively), have been disrupted in the JEL1 strain. PrB in particular is activated by the typical extraction conditions of neutral pH and SDS, and gene disruption has been shown to be far more effective than the use of pepstatin as an inhibitor (Guthrie and Fink, 1991). A further advantage of using the JEL1 strain is that *GAL4* expression has been modified to be under the control of the galactose-inducible *GAL1* promoter (Lindsley and Wang, 1993). As the Gal4 protein is also a transcriptional activator of the *GAL1* promoter, a positive feedback loop is initiated upon exposure to galactose, ensuring a greater efficiency of expression of the target gene from the *GAL1* promoter, in this case *PSO2*.

5.2.1 Protein extraction techniques

To determine the most favourable conditions for extraction of the total cellular protein content, a number of different buffers and cell disruption methods were tested. These

procedures were rated by the resulting protein yield, as determined spectrophotometrically using the Biorad DC reagents.

Three buffers were investigated: *Breaking buffer* (Invitrogen pYES2 manual) consisting of 50 mM sodium phosphate pH7.4, 1 mM EDTA, 5 % glycerol, 1 mM PMSF, plus protease inhibitor cocktail; *RIPA buffer* (widely used for extraction and immunoprecipitation; P. Kaiser, University of California, USA) consisting of 50 mM Tris-HCl, 250 mM NaCl, 1 % deoxycholic acid, 1 % Triton X-100, 0.1% SDS, plus protease inhibitors; and the commercial buffer, *CelLytic-Y* (Sigma), which has been optimised for efficient yeast protein extraction with minimal interference with protein immunoreactivity and biological function. An EDTA-free cocktail of broad-spectrum serine and cysteine protease inhibitors (Roche Diagnostics) was used in conjunction with all three buffers. These buffers were chosen for their diverse spectrum of components, and as they have been used successfully in, or are marketed for, the extraction of proteins from yeast. Both the RIPA and CelLytic buffers were found have a superior performance (3 to 4-fold greater protein yield) compared to the Breaking buffer (Table 5.1).

Two different methods for mechanical disruption of the yeast cell wall were analysed: vortexing in the presence of glass beads, and grinding cells frozen in liquid nitrogen. Both of these procedures are widely used (Ausubel *et al.*, 1993), with glass beads perhaps being the more popular, although usually only where there is access to a bead beater machine. A bead beater was not available during this study, and consequently, the grinding of cells in liquid nitrogen using a pestle and mortar, was found to be twice as efficient than regular vortexing with glass beads (Table 5.1).

Table 5.1 **Comparison of protein yields obtained using different extraction techniques.** Different combinations of extraction buffer and mechanical disruption mechanisms were investigated. Data are the means of at least 6 independent protein extractions.

Method of protein extraction	Mean protein yield (+/- SEM) μg/μl
RIPA buffer/ Liquid Nitrogen	3.88 (+/- 0.72)
Breaking buffer/ Liquid Nitrogen	1.32 (+/- 0.19)
CelLytic-Y/ Liquid Nitrogen	4.63 (+/- 0.34)
CelLytic-Y/Glass beads	2.40 (+/- 1.02)

5.2.2 Galactose inducibility

Given that expression of the endogenous *PSO2* gene appears to be strictly regulated in yeast, and that it is maintained at a low constitutive expression in the absence of DNA damage (Richter *et al.*, 1992), it is likely that an excess of the Pso2 protein could be toxic to the cell. Indeed, overexpression of *hSNM1* has been shown to correlate with the symptoms of apoptosis (Dronkert 2000). Therefore, it could not be assumed that an increase in the period of exposure to galactose would result in a higher concentration of Pso2 protein within the cell. It was therefore possible that excessive induction of *PSO2* expression would either result in cell death, or that the protein would be subject to stringent regulation by proteolytic degradation.

Exponentially growing cells were transferred to a fresh culture containing galactose (plus the neutral carbon source, raffinose), and 50 ml samples were taken at the following time points: 0, 2, 3, 4, 6, and 24 h. Cells were pelleted and washed, before immediately freezing at –80°C. Protein was subsequently extracted from each of these samples by resuspending in RIPA buffer and grinding in liquid nitrogen. 30 μg of each

whole cell extract was separated by SDS-Polyacrylamide gel electrophoresis, and subjected to Western blotting using the optimised conditions described in Chapter 2. The primary antibody utilised was a rabbit polyclonal IgG αFLAG (Sigma), recommended by the manufacturer for the recognition of C-terminal FLAG-tagged proteins. A horseradish peroxidase-conjugated secondary antibody was selected to facilitate analysis of the blot by commercial ECL detection reagents. It is clear from figure 5.2 that a band representing a protein of about 100 kDa (estimated from the standard size markers) is first detected after 4 h galactose induction, and is maximal at the longest incubation time of 24 h. This band is not seen in either the JEL1 parent strain, or the uninduced cells carrying the pFLAG-*PSO2* vector. Although this protein migrates at a slower rate than would be expected for Pso2 (sequence-based prediction of Pso2 size is 76 kDa, plus 3 kDa FLAG epitope), it is the only band that does not appear in the control extracts. There is a band at 85 kDa, which is closer to the expected size, but this is seen in all extracts, including the vector-free control (Fig. 5.2). Even though the JEL1 strain is wild-type for *PSO2*, this cannot account for the presence of the 85 kDa band, as the immunodetection is for the FLAG epitope, and not Pso2 directly. Furthermore, repetition of the Western blot analysis using a number of independent extracts has shown that this 85 kDa protein is consistently expressed (data not shown). This protein is likely to display a naturally occurring FLAG-like epitope that is recognised under the immunoblotting conditions used here.

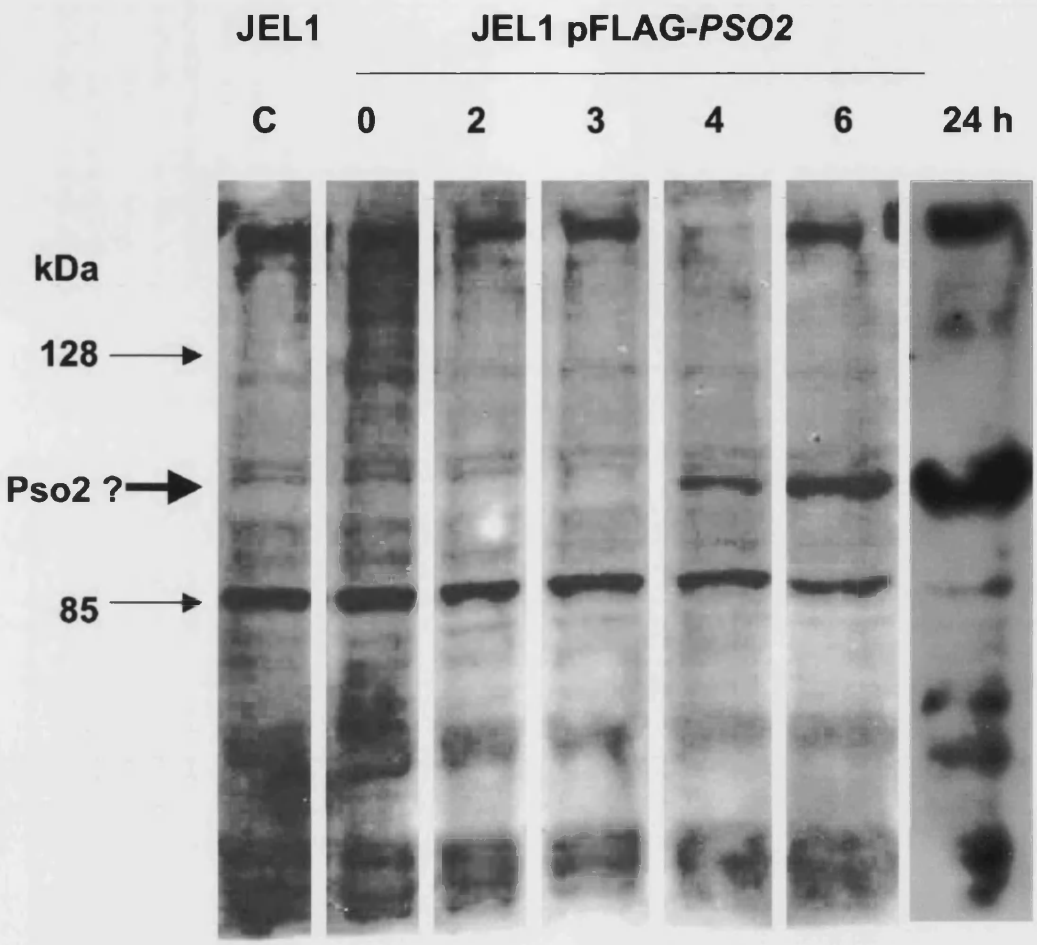

Figure 5.2 Analysis of galactose-inducible FLAG-PSO2 expression. Western blot of whole cell extracts (30 μg) from JEL1 cells carrying the pFLAG-*PSO2* vector , with anti-FLAG primary antibody. Cells were cultured in galctose induction media for 0, 2, 3, 4, 6, or 24 h. The JEL1 control (c, no vector) was incubated for 24 h. The probable location of the Pso2 protein band is marked with an arrow (~ 100 kDa).

5.3 Isolation of FLAG-Pso2 by immunoprecipitation

To further enrich the putative FLAG-Pso2 from the whole cell protein extract, immunoprecipitation reactions were implemented. The basic principle is that the desired protein is recognised by a specific antibody, which in turn is bound by a protein-agarose conjugate, forming large complexes that can be precipitated by centrifugation. Standard procedures (such as those described in the Sigma *Procedures* publication) were tested under different conditions in order to find an optimal method. The variable conditions that were considered included the period and temperature of incubation with the anti-FLAG antibody, and the order of mixing the antibody, protein A sepharose, and total cell lysate. The efficiency of any one system was determined by calculation of protein concentration. The optimal conditions for isolation of FLAG-Pso2 using the polyclonal anti-FLAG antibody were deemed to involve sequential incubations in RIPA buffer: firstly, the total protein extract and anti-FLAG antibody were mixed on a rotary wheel overnight at 4°C, with subsequent addition of the protein A sepharose and a further 1 h incubation prior to thorough washing. Both the antibody and protein A sepharose were found to be effective at the manufacturers recommended concentration.

A set of immunoprecipitations prepared from JEL1 pFLAG-*PSO2* cells, either induced in galactose for 5 or 24 h, or uninduced, were analysed by Western blotting (Fig. 5.3). Compared to the respective total cell protein extracts, the immunoprecipitations are relatively clean, with only one dominant protein band of about 100 kDa, detected in the galactose-induced samples. This protein is the same as that observed previously, appearing only after 4 h galactose induction, and not in the control sample that lacks the

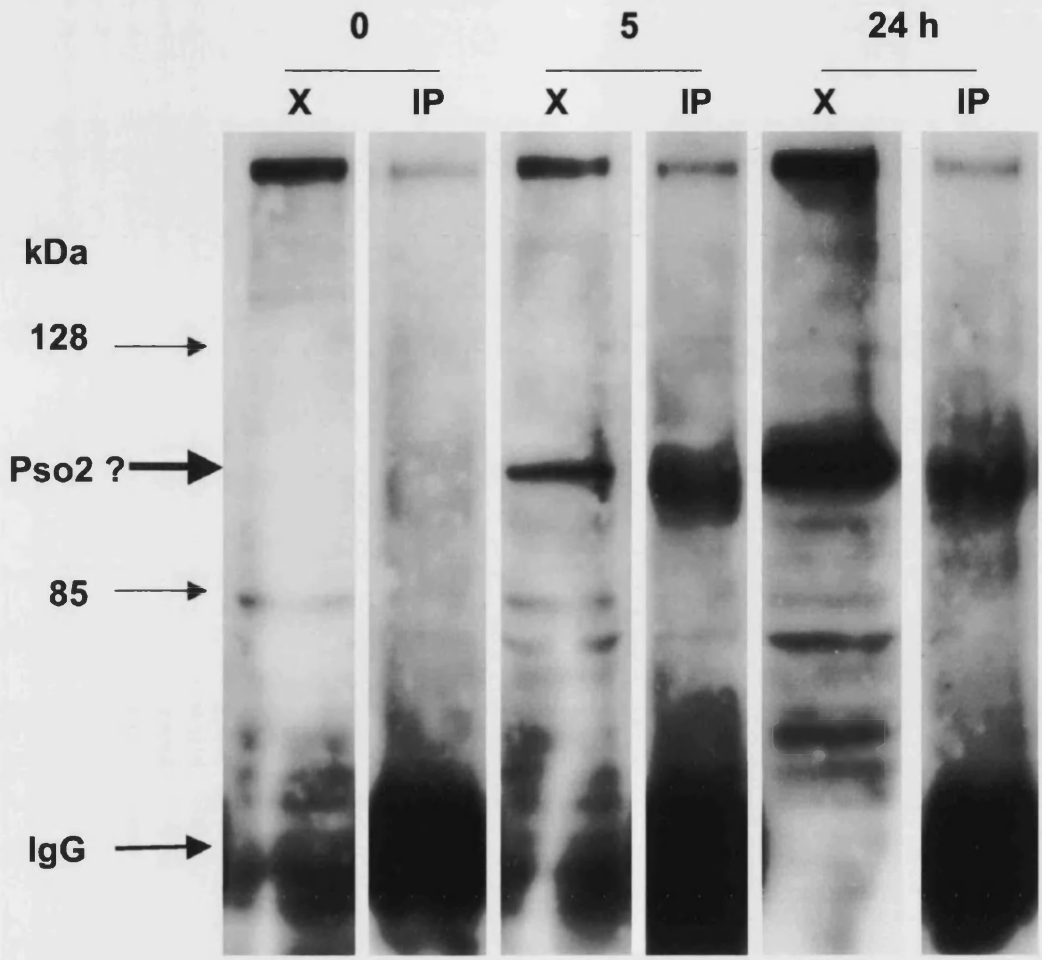

Figure 5.3 FLAG-PSO2 immunoprecipitation. Western blot of whole cell extracts (X, 100 μg) and αFLAG immunoprecipitates (IP, each from 200 μg crude extract) from JEL1 cells carrying the pFLAG-*PSO2* vector, with anti-FLAG as the primary immunoblot antibody. Cells were cultured in galactose induction media for 0, 5, or 24 h. The location of the putative Pso2 protein band and the IgG (released from the sepharose due to the pre-PAGE preparative step of boiling in SDS) band is marked with an arrow.

pFLAG-*PSO2* vector (Figs. 5.2, 5.3). Hence, if this protein proves to be FLAG-tagged Pso2, it appears that it can be isolated from the other cellular proteins by immunological means. However, further optimisation is necessary, as the resulting yield of putative FLAG-Pso2 is low. It is apparent from figure 5.3 that considerably less 100 kDa protein is present in the immunoprecipitate, compared to the whole cell extract, despite the use of twice as much crude extract in the immunoprecipitation reaction.

5.4 Large-scale purification of Pso2

Suitable conditions for FLAG-*PSO2* expression and subsequent protein extraction have been determined from the small-scale reactions. The experience of these analyses has also highlighted aspects for improvement. In particular, in order to scale up these reactions by at least 40-fold, it would be preferable to use a commercially prepared agarose-conjugated anti-FLAG antibody, rather than using the sequential antibody and protein A sepharose method. This should ensure a greater yield as the protein A sepharose is particularly difficult to prepare accurately and manipulate efficiently. Furthermore, antibody-agarose conjugates can be more easily recycled for repeated use.

One-litre galactose induction cultures of JEL1 pFLAG-*PSO2* were initiated from exponentially growing cells and incubated for 24 hours, before washing and freezing the resultant cell pellet at –70°C. Crude cellular protein extracts were performed using a combination of CelLytic-Y buffer and grinding in liquid nitrogen to fully disrupt the cell walls. To account for the larger volumes of extract (on average 5 ml per litre of culture), the protein fraction was separated from cellular debris by two ultracentrifugation steps at 30,000 rpm, initially for 1.5 h, and subsequently for 45 min.

The yield of total cellular protein (as determined spectrophotometrically using Biorad DC reagents) was usually in the region of 50 mg per litre of cell culture.

Two methods were tested for the isolation of FLAG-Pso2 from the total cellular protein complement, both utilising anti-FLAG-M2 affinity gel agarose (Sigma). This gel consists of a murine IgG monoclonal antibody (with specificity for C-terminal FLAG epitopes) covalently attached to agarose by hydrazide linkage. The use of a monoclonal antibody should also assist in reducing the cross-reactivity with endogenous proteins, as observed with the polyclonal antibody. One of the reasons for opting to use the CelLytic-Y buffer for the crude cellular extracts, rather than the equally well performing RIPA buffer, is that the M2 affinity gel is sensitive to the detergent components of the RIPA buffer. SDS causes denaturation of the M2 antibody on the resin, and deoxycholate inhibits the interaction between the M2 antibody and the FLAG fusion protein (Sigma technical bulletin).

The total cellular protein extract was either introduced to the freshly prepared M2 affinity gel by column chromatography, or incubated in smaller aliquots on a rotary wheel (akin to the small scale immunoprecipitations). In both cases, samples were agitated at 4°C overnight, to ensure complete formation of the protein-antibody/resin conjugates. Subsequent washing was performed by gravity flow (column) or centrifugation (eppendorf aliquots), as appropriate. Despite the extra care needed to avoid disrupting the resin after centrifugation, this method was found to be more satisfactory, both in terms of time and protein yield (3-fold greater yield from centrifugation compared to column chromatography). The conjugated protein was eluted from the affinity gel by competition with 3 x FLAG peptide for 1 h at 4°C. After

centrifugation, the FLAG-Pso2 supernatant fraction (X1) was removed and stored at –70°C (with protease inhibitors). The yield was typically in the region of 200 μg protein per litre of original culture (aliquot/centrifuge method).

It can be seen from the PAGE analysis in figure 5.4 that the X1 fraction exhibits a number of protein components additional to the suspected FLAG-Pso2 (100 kDa) band, although this is the predominant constituent. Further purification of the extract was achieved by centrifugation in a Vivascience Vivaspin column with a molecular weight cut-off of 5- 50 000 kDa. Clearly, the resulting fraction (X2) contains just two major proteins (at 80 and 100 kDa), the larger of which is prevalent (Fig. 5.4). These two proteins were excised from the PAGE gel, and sent for analysis by peptide mass fingerprint (Cancer Research UK Protein Analysis Laboratory, London Research Centre). This analysis involves in-gel protease digestion of the protein band, and measurement of the peptide masses using an ABI 4700 TOF-TOF machine (Applied Biosystems), which uses high-energy fragmentation to generate characteristic patterns for accurate protein identification through comparison with an extensive database. The 100 kDa protein was indeed found to correspond to Pso2, whereas the 80 kDa contaminant is the yeast metabolic protein Leu1.

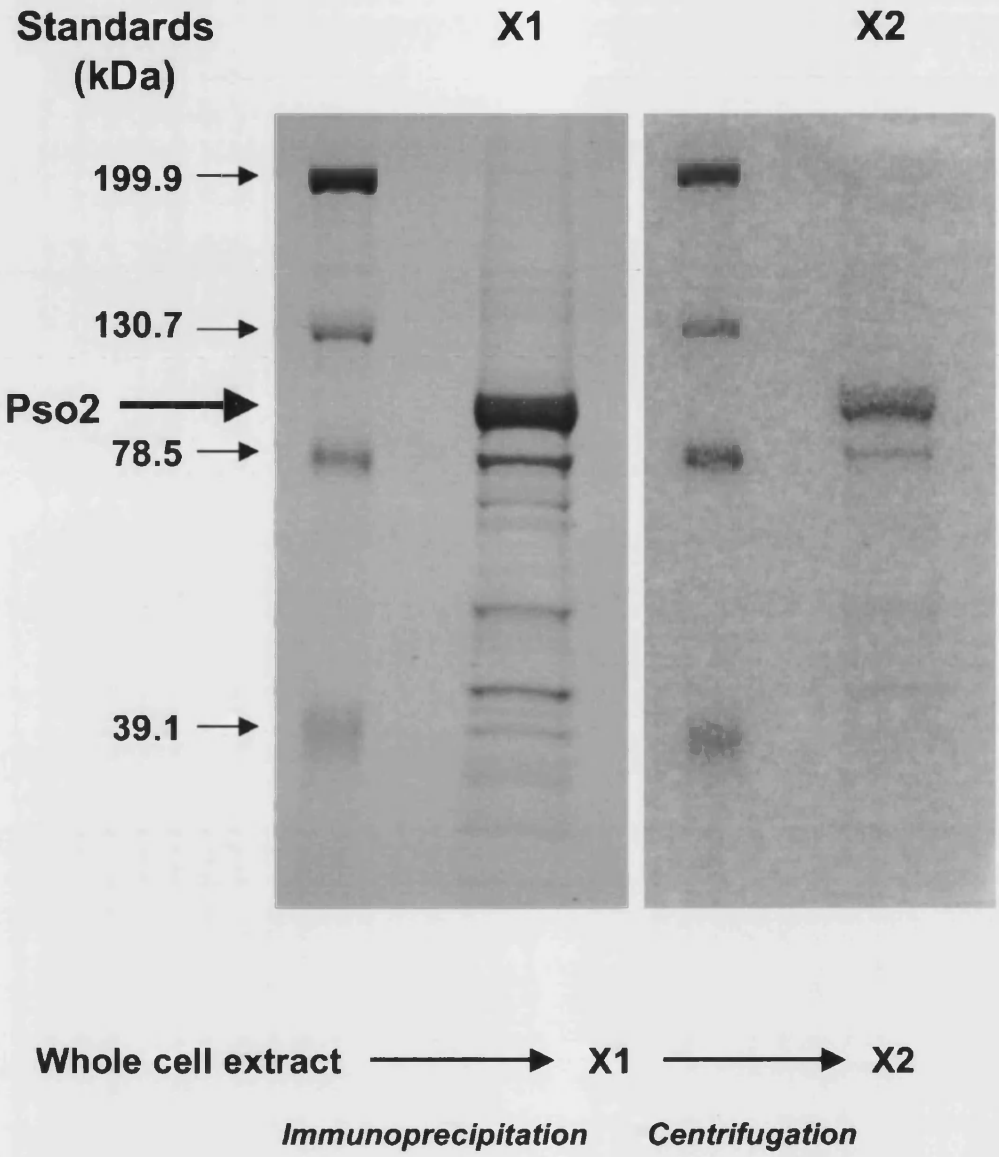

Figure 5.4 Purification of FLAG-PSO2. PAGE gel resolution of the large scale Pso2 extracts, visualised by Coomassie Blue staining. X1 is the protein fraction resulting from immunopurification with anti-FLAG M2 agarose affinity gel. X2 is the protein fraction after further purification of X1 by centrifugation in a Vivascience Vivaspin column for 3 h at 4000 rpm. Gel one contains 20 μg X1, whereas gel two contains a third of the purified X2 fraction resulting from a total of 40 μg X1. The location of the Pso2 protein band is marked with an arrow (~ 100 kDa).

5.5 Analysis of post-translational modifications of the Pso2 protein

After translation of the mRNA, nascent proteins are often modified by the addition of small groups to the amino acid side chains (phosphorylation, glycosylation, methylation, acetylation), and by the binding of small proteins (ubiquitin, SUMO/small ubiquitin-like modifier). These reversible modifications are crucial for protein regulation, and enable rapid alterations in protein function, complex specificity, and subcellular localisation. Post-translational modification is an important mechanism that enables the cell to respond to changes in both its internal and external environment. Observations have already been made of transcriptional upregulation of *PSO2* in response to DNA damage (Wolter R *et al.*, 1996), however this is a relatively slow mechanism of protein regulation. Hence it is quite possible that the cell employs post-translational mechanisms as well, perhaps to ensure the rapid mobilisation of Pso2 to the sites of damage, or to facilitate interactions with other repair and signal transduction proteins. Given that purified FLAG-Pso2 migrates significantly more slowly during SDS-PAGE than would be expected for a protein of 79 kDa (Fig. 5.4), it is reasonable to hypothesize that the protein is modified in some way. The magnitude of this migration retardation corresponds to a modification of around 20 kDa. This could be consistent with multiple phosphorylated sites (as each corresponds with a shift of 1-5 kDa, depending on the nature of the protein and of the PAGE gel), multiple glycosylation events (for example, the N-linked oligosaccharide $Man_8GlcNAc_2$ contributes about 2 kDa to the molecular weight; Guthrie and Fink, 1991) or the addition of at least one ubiquitin/SUMO moiety (8.5 and 12 kDa respectively; *Saccharomyces Genome Database* www.yeastgenome.org).

5.5.1 Phosphorylation

The phosphorylation of proteins, most often at serine, threonine, tyrosine and histidine residues, is an important regulatory mechanism that can have a variety of effects, including activation, repression or altered function/substrate specificity. Phosphorylation of the human Pso2 paralogue, Artemis, by DNA-PKcs has been shown to change the substrate specificity of Artemis to include the endonucleolytic cleavage of ssDNA overhangs and hairpins (Ma *et al.*, 2002). Furthermore, the phosphorylation of tyrosine residues is a key aspect of signal transduction pathways. For example, the DNA damage checkpoint consists of a cascade of protein kinase events to amplify the signal arising from the detection of the damaged DNA in order to stimulate the numerous effector pathways (Toh and Lowndes, 2003). It has been suggested that the induction of *PSO2* expression in response to DNA damage is dependent upon the Dun1 kinase, which is one of the substrates for the Rad53 checkpoint kinase (Wolter R *et al.*, 1996; de la Torre Ruiz and Lowndes, 2000). It is not known whether the involvement of Pso2 in ICL repair extends to a role in the detection and signalling of DNA damage.

The Pso2 protein sequence was screened for the existence of potential phosphorylation sites using two freely available internet databases: Prosite (www.expasy.org/prosite), a general database of biologically significant sites and protein motifs, and NetPhos 2.0 (www.cbs.dtu.dk/services/NetPhos), which specifically produces neural network predictions for serine, threonine and tyrosine phosphorylation sites in eukaryotic proteins Blom *et al.*, 1999). The Prosite database returned a number of putative phosphorylation sites, such as those recognised by protein kinase C and tyrosine kinase. However, it should be noted that these predictions are subject to a high frequency of false positive associations. Nevertheless, the more refined NetPhos database

highlighted a total of 28 serine, 13 threonine, and 9 tyrosine residues that could represent potential phosphorylation sites (score above a 50 % likelihood threshold). Five of these residues (4 serine and 1 tyrosine) correlated with sites specified in the Prosite scan, as well as returning a NetPhos prediction score of 99 % (only 88 % for the tyrosine residue) (Fig. 5.5, Table 5.2).

Table 5.2 **Putative Pso2 phosphorylation sites.** The NetPhos predictive scores (probabilities) are presented for the Pso2 serine and tyrosine residues that are most likely to be targeted by phosphorylation.

Residue	S19	S26	S38	S204	Y529
Predictive Score	0.988	0.991	0.996	0.997	0.875

These sequence-based predictive screens, although purely speculative, provided reasonable justification to investigate the phosphorylation status of the purified FLAG-Pso2 protein. The alkaline phosphatase, CIAP (extracted from calf intestinal mucosa), is known to dephosphorylate serine, threonine and tyrosine residues in proteins, in addition to its activities on nucleic acids. Immunoprecipitated Pso2 was treated with 20 units of CIAP for 1.5 h at 37°C, with subsequent electrophoretic mobility shift analysis performed by PAGE. Two control reactions were also performed, namely, a mock-treatment, and incubation with 20 units of heat-inactivated CIAP enzyme. It is clear from figure 5.6 that no change is observed in the migration of the Pso2 protein after

```
  1 msrksivqir rsevkrkrSs tasstSegkt lhknthtSsk rqrtltefni ptssnlpvrs
 61 ssysfsrfsc stsnkntepv iindddhnsi cledtaKvei tidtdeeelv slhdnevsai
121 eNrtedrivt eleeqvnvkv steviqcpic leNlshlely erethcdtci gsdpsnmgtp
181 kknirsfisn psspaktkrd iatSkkptrv klvlpsfkii kfnngheivv dgfnykaset
241 isqyflshfh sdhyiglkks wnnpdenpik ktlycskita ilvnlkfKip mdeiqilpmn
301 krfwitdtis vvtldanhcp gaiimlfqef lansydkpir qilhtgdfrs nakmietiqk
361 wlaetaNeti dqvyldttym tmgynfpsqh svcetvadft lrliKhgkNk tfgdsqrnlf
421 hfqrkktltt hryrvlflvg tytigkekla ikiceflktk lfvmpnsvkf smmltvlqnn
481 enqndmwdes lltsnlhess vhlvpirvlk sqetieaylk slkeletdYv kdiedvvgfi
541 ptgwshnfgl kyqkknddde nemsgnteyc lelmKndrdn ddengfeiss ilrqykkynk
601 fqvfnvpyse hssfndlvKf gcklkcsevi ptvnlnnlwk vrymtnwfqc wenvrktraa
661 k
```

Figure 5.5 Sequence-based prediction of post-translational modifications. Predictive analysis of three types of post-translational modification in the Pso2 protein (Genbank sequence NP_013857). Putative phosphorylation sites identified by both the NetPhos and Prosite databases are highlighted in red. Putative glycosylation sites identified in the Prosite screen are hihglighted in green. Putative Sumoylation motifs, as predicted by SUMOplot, are highlighted in blue.

treatment with CIAP, suggesting that phosphorylation of the FLAG-Pso2 protein does not account for the mobility shift observed. The CIAP used in this assay was a fresh stock, and so its activity is not in question. However, it is possible that the conditions used were not optimal for protein dephosphorylation, and so it would be good practise to confirm the activity of CIAP for a protein known to be in a phosphorylated state.

5.5.2 Glycosylation

Yeast proteins can be modified by the addition of carbohydrate moieties, either attached to asparagine (N-linked) or to serine/threonine (O-linked) residues. N-linked structures consist predominantly of mannose sugars, whereas O-linked mono- or oligosaccharides are more varied (Guthrie and Fink, 1991). Glycosylation used to be considered as a specific adaptation of extracellular proteins, particularly those destined for the cell wall. However, glycosylation (particularly O-linked N-acetylglucosamine, O-GlcNAc) has been found to play an important role in the regulation of intracellular (nuclear and cytoplasmic) proteins in higher eukaryotic cells, sometimes even acting antagonistically with phosphorylation (Vosseller *et al.*, 2002; Kamemura *et al.*, 2002).

Analysis of the Pso2 protein sequence using the Prosite database identifies four asparagine residues as potential N-glycosylation sites, although these are motifs with a disproportionately high probability of occurrence (Fig. 5.5). A simple assay for the presence of N-glycosylation is to treat the protein with Endoglycosidase H (Endo H), and determine whether there is a reduction in protein size by electrophoretic mobility shift analysis. Endo H is a recombinant glycosidase that cleaves high mannose structures and some hybrid oligosaccharides (such as mannose combined with AcNeu-

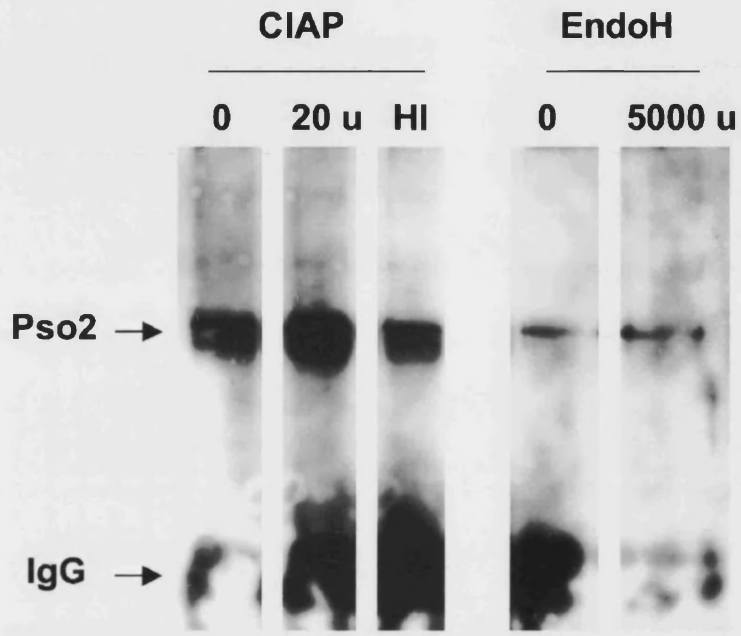

Fig. 5.6 Biochemical analysis of post-translational modifications. Western blot of αFLAG immunoprecipitates (performed on 200 μg crude extract), subsequently treated with either calf intestinal alkaline phosphatase (CIAP, 0, 20 units, or heat inactivated, HI) or EndoH (0 or 5000 units) for 1.5 h at 37 °C. Due to volume restrictions, only half of the EndoH reactions were electrophoresed. The position of bands corresponding to Pso2 and IgG are marked with an arrow.

Gal-GlcNAc) (Maley *et al.*, 1989). The Western blot in figure 5.6 shows that a shift in the mobility of immunoprecipitated FLAG-Pso2 is not observed following exposure to Endo H (5000 units, 1.5 h at 37°C). Hence it is doubtful that the post-translational modification of Pso2 by N-glycosylation accounts for its decreased mobility.

5.5.3 Sumoylation

SUMO (small, **u**biquitin-like **mo**difier) is a small polypeptide that can be covalently, yet reversibly attached by specific cellular machinery to the lysine residues of other proteins, in order to regulate their function. As the name suggests, it is related to the well-characterised modifier, ubiquitin, which is essential for the targeting and correct degradation of proteins by the proteasome, as well as regulating other processes such as endocytosis and meiosis. It is thought that sumoylation is required for protein transport into the nucleus (Muller *et al.*, 2001, Schwartz and Hochstrasser, 2003), and accordingly, protein modification by Smt3 in *S. cerevisiae* (homologue of human Sumo1) is thought to regulate a number of nuclear processes G2-M cell cycle progression (Meluh and Koshland, 1995; Li and Hochstrasser, 1999). Crucially, sumoylation also appears to regulate some DNA repair pathways, such as *RAD6*/PRR (Hoege *et al.*, 2002).

Many sumoylated proteins exhibit the tetrapeptide motif Ψ-K-x-D/E, where Ψ is a hydrophobic residue, K is the conjugated lysine, and D/E is an acidic residue (Rodriguez *et al.*, 2001). SUMOplot (www.abgent.com/sumoplot.html) is an internet database designed to determine the probability that sequences matching this consensus motif are likely to be sumoylated. Analysis of the ScPso2 sequence highlights 5

potential motifs (at K97, K288, K405, K575, and K619), all of which are assigned a likelihood probability between 75 and 80 % (Fig. 5.5, Table 5.3).

Table 5.3 **Putative Pso2 sumoylation sites.** The SUMOplot predictive scores (probabilities) are presented for the lysine residues in Pso2 that could potentially be sumoylated.

Residue	K97	K288	K405	K575	K619
Predictive Score	0.794	0.744	0.772	0.800	0.756

Consequently, a Western blot of 20 μg purified (X2) Pso2 protein was sequentially immunoblotted with the polyclonal anti-FLAG antibody, stripped, and reprobed with a polyclonal anti-hSumo1 antibody (anti-Smt3 is not yet available). It is clear from figure 5.7 that both antibodies identify a band of equal magnitude. Given that the Pso2 protein fraction is relatively pure, it seems likely that Pso2 may be modified by the covalent attachment of one or more SUMO polypeptides.

5.6 Discussion

Attaching a FLAG epitope to Pso2 provides a very convenient way of extracting the protein directly from yeast, without having to identify Pso2 directly. Both monoclonal and polyclonal antibodies to the FLAG peptide are readily available, which provide the means to specifically isolate FLAG-tagged proteins from the total cellular extract. These antibodies have been well characterised, with respect to both their immunoprecipitation capabilities and spectrum of cross-reactivity with non-specific

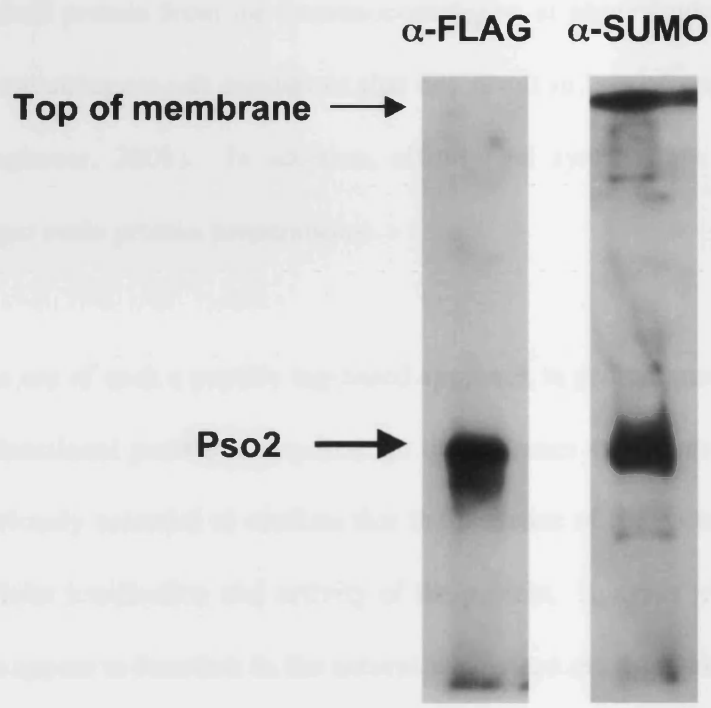

Fig. 5.7 Putative sumoylation of FLAG-Pso2. Further analysis of post-translational modifications. Western blot of large scale Pso2 preparation (20 μg). The membrane was first immunoblotted with anti-FLAG primary antibody, and subsequently stripped and reblotted with anti-SUMO primary antibody.

proteins. Subsequent incubation with excess FLAG peptide facilitates elution of the desired protein from the immunocomplexes, at physiological pH, and without the need to use stringent salt conditions that can result in loss of protein integrity (Einhauer and Jungbauer, 2001). In addition, affinity gel systems are commercially available for larger scale protein preparations.

The use of such a peptide tag-based approach to protein purification can cause problems if functional protein is required for downstream assays, as is the case with Pso2. It is obviously essential to confirm that the presence of the epitope does not alter the normal cellular localisation and activity of the protein. In cases where the tagged protein does not appear to function in the natural way, steps must be taken to incorporate a cleavage site between the protein and the epitope, so that it can be efficiently removed after the extraction procedure. In the case of Pso2, it can be assumed that cellular localization and activity is normal if Pso2-FLAG is proficient in the repair of HN2-induced ICL, as this is the identifying feature of this protein. Since the expression vector utilised here is for yeast, the most straightforward means to test functionality is to assay for complementation in a *S. cerevisiae pso2* defective strain. It is evident from the data presented in figure 5.1 that expression of the Pso2-FLAG protein can completely compensate for the absence of the endogenous gene, as the extent of HN2 survival is indistinguishable from the wild-type strain. Having established that the Pso2-FLAG protein is completely functional in the repair of HN2-induced DNA damage, it was not deemed necessary to check the extent of activity in other processes such as recombination and DSB repair.

Once the use of a FLAG epitope was confirmed as suitable for the identification of Pso2, the next phase was to optimise the procedure for small-scale protein extractions. One of the advantages of the FLAG system is that the available anti-FLAG antibodies are sufficiently specific to produce a relatively homogeneous preparation of the fusion protein direct from the whole-cell protein extract (Einhauer and Jungbauer, 2001). Exploitation of either the polyclonal anti-FLAG antibody in small-scale immunoprecipitations, or the monoclonal anti-FLAG-M2 affinity gel in larger preparations, has proved successful in isolating the FLAG-Pso2 protein from the crude cell extract (Sections 5.3 and 5.4). The yield of Pso2 protein was higher under the conditions of the larger preparations, probably as a consequence of the reduced handling inaccuracies achievable with the antibody-conjugated affinity gel. It is also possible that the interaction of the monoclonal M2 antibody with the FLAG epitope is more efficient than the polyclonal antibody, in the case of FLAG-tagged Pso2. Subsequent purification through a size exclusion column was found to significantly improve the quality of the FLAG-Pso2 immunoprecipitate fraction (Fig. 5.4).

The conditions of protein extraction have been optimised, in terms of incubation times, buffer compositions, and the mechanism employed to disrupt the yeast cell wall (Sections 0 and 5.4). The final preference for the commercial CelLytic-Y buffer resulted predominantly from consideration of the need for efficient downstream immunopurification (inhibited by some detergent constituents of other extraction buffers), and also for the maintenance of Pso2 biological activity. For example, the presence of high levels of EDTA in the Breaking buffer may have affected the stability of Pso2 zinc coordination at the metallo-β-lactamase site, possibly to the extent where the purified protein is rendered inactive. Significantly, a relatively pure fraction of

ScPso2 protein has been isolated, directly from yeast, for the first time (Section 5.4). There now exists a sufficient stock (approximately 0.5 mg) of Pso2 protein for biochemical analysis, and a simple protocol has been elucidated for its replenishment.

Attempts have been made to start to characterise the purified Pso2 protein, initially in terms of post-translational modifications that could be responsible for the observed retardation of about 20 kDa in the migration of FLAG-Pso2. Multiple phosphorylation was considered to be one of the most likely putative modifications, especially considering the number of candidate residues (Section 5.5.1). However, incubation with the phosphatase CIAP failed to induce a change in the pattern of FLAG-Pso2 migration, at least under the conditions employed here (Fig. 5.7). Furthermore, a detailed analysis of the phosphorylation status of Pso2, perhaps considering various stages during the repair of ICLs, should be performed in the future, even if only to confirm that it is not a regulatory mechanism. Modification by multiple glycosylation was also investigated, as this could account for the considerable size difference between the sequence-based prediction and that observed by PAGE (Section 5.5.2). However, this was a less likely hypothesis, given that glycosylation has not yet been observed for any yeast nuclear protein (Guthrie and Fink, 1991; Vosseller *et al.*, 2002). Accordingly, no change in protein size was identified after exposure to Endoglycosidase H (Fig. 5.6).

Nevertheless, these speculative analyses of the state of the Pso2 protein have resulted in a novel and significant discovery. A polyclonal antibody raised against a prokaryotic recombinant protein corresponding to human Sumo1 appears to cross-react with the purified FLAG-Pso2 protein (Fig. 5.7). The 101 amino acid yeast homologue, Smt3, exhibits 48 % identity (as determined by BLAST, NCBI) with the human Sumo1

protein, and so it is entirely feasible that the polyclonal antibody could recognise a common epitope. Furthermore, the size of Smt3 is predicted to be 12 kDa, which (singularly, or at two sites) could well account for the retarded migration of FLAG-Pso2. Analysis of the sequence of Pso2 suggests five different lysine residues that lie within putative sumoylation motifs (Section 5.5.3). Nevertheless, it should be noted that the SUMOplot predictive database also identifies a number of suitable lysine residues (7 with a probability of greater than 70 %) in the sequence of Leu1, the major contaminant found in the Pso2 preparation. Whether the cytosolic protein Leu1 is a likely substrate for sumoylation is debatable, as in higher eukaryotes at least, the majority of the modified proteins are nuclear (Muller *et al.*, 2001). Correspondingly, most of the known functions of Sumo are related to the regulation of nuclear processes, including transcription, chromosome segregation, and DNA repair (Muller *et al.*, 2001; Schwartz and Hochstrasser, 2003).

Interestingly, a recent report has shown that the enzyme responsible for conjugation of SUMO to its target proteins, Ubc9, is required for damage induced homologous recombination in yeast, and that loss of this gene renders cell sensitive to a range of genotoxic agents, including the ICL-inducing compounds mitomycin C and cisplatin (Maeda *et al.*, 2004). Hence, the observation that the Pso2 protein may be sumoylated is an important one, and warrants detailed investigation, including an analysis of protein extracted from cells exposed to ICL-inducing agents. In particular, Pso2 protein should be purified from a *ubc9* deficient strain, to conclusively demonstrate whether the protein is sumoylated.

It is notable that none of the Pso2 preparation migrates at the expected, lower molecular weight of 76 kDa. One possibility is that the unmodified form is less stable, and is more difficult to purify. By analogy with other sumoylated proteins, it is unlikely that all Pso2 is quantitatively modified by SUMO (Hoege *et al.*, 2002). However, recent studies have suggested that proteins involved in DNA repair, such as PCNA, can be alternately regulated by mono/poly-ubiquitination and sumoylation of the same residue (Hoege *et al.*, 2002). Such a phenomenon should be investigated for Pso2, as if Pso2 always existed in some kind of a modified state, it could explain the homogeneous preparation of higher molecular weight protein. Nevertheless, the migration of FLAG-tagged Pso2 protein as a single band precludes the existence of a range of differently sized modifications, unless the presence of the FLAG epitope causes aberrant post-translational modification. It has already been shown that Pso2 functions normally with respect to the repair of ICLs (Section 5.1), but for clarification, future studies of post-translational modification could be performed after the removal of the FLAG tag from the purified protein.

It is tempting to speculate upon the possible role of SUMO modification in the function of Pso2. Perhaps it is required for the localisation of Pso2 to the nucleus, or even, more specifically, to sites of DNA damage. An alternative is that sumoylation may repress Pso2 activity in the absence of DNA damage, perhaps by altering confirmation or substrate/ligand specificity. Indeed, the putative sumoylation of Pso2 has been observed in undamaged cells where *PSO2* is expressed at an elevated level (from the *GAL1* promoter), and a similar case of SUMO modification has previously been observed for overproduced Rad22 (homologue of *Sc*Rad52) in *S. pombe* (Ho *et al.*, 2001). It should be noted that the apparent sumoylation of Pso2 might simply be a

cellular response to the artificially high expression levels used in this study. If Pso2 does in fact have a nuclease activity, as predicted from its β-CASP domain, it is likely that the protein would be subject to stringent cellular controls to prevent inappropriate DNA digestion.

The successful purification of Pso2 direct from its native yeast provides the foundations for detailed future analysis of Pso2 function *in vitro*. One of the first applications of this protein is to be the investigation of the role of its metallo-β-lactamase hydrolytic domain. A crude assay for nuclease activity has already been performed, in which the purified (X2) Pso2 fraction was incubated with a radioactive 5' end-labelled DNA oligonucleotide in either magnesium or manganese based nuclease buffers, and subsequently resolved by denaturing PAGE (based on the *in vitro* studies of Mre11-Rad50 nuclease activity by Trujillo and Sung, 2001, and of hExo1 activity by Lee and Wilson, 1999). The initial attempt has proved inconclusive, however, there are numerous possible substrates and buffer conditions to be analysed. Given the apparent specificity of Pso2 for cross-link associated DNA structures, it is likely that such an assay will need to be highly refined to detect any activity of Pso2.

CHAPTER 6 GENERAL DISCUSSION

It has been established for some time that Pso2 is a crucial component of the cellular response to DNA interstrand cross-links, yet the exact nature of its function has remained elusive. This investigation sought to elucidate the role of Pso2, and, accordingly, to refine the current models of ICL repair, using the cross-linking agent nitrogen mustard as a paradigm. In concordance with previous genetic studies of *pso2* mutant cells (Henriques and Moustacchi, 1981), the data presented here shows *pso2* is epistatic to the NER pathway (*RAD1*, *RAD2*, *RAD3*, *RAD4*). However, in contrast to the defined ICL incision defect in NER mutants, *pso2* disruptant cells are proficient in the unhooking (incision) step of interstrand cross-link repair (Magana-Schwencke *et al.*, 1982; Wilborn and Brendel, 1989; Meniel *et al.*, 1995). Pso2 must therefore be involved in a stage of ICL repair that is downstream of the initial excision events.

Loss of *PSO2* results in an accumulation of DSBs that fail to be repaired (Ch. 3; Magana-Schwencke *et al.*, 1982; Wilborn and Brendel, 1989), implying a diminished capacity to repair cross-links by recombination (McHugh *et al.*, 2000). Hence, Pso2 is involved in the processing of an uncoupled cross-link intermediate structure, prior to further repair by the homologous recombination pathway. However, both *pso2* and NER mutants demonstrate a synergistic relationship with homologous recombination (*RAD51*, *RAD52*, *MRE11*) (Chapter 3). Although these genetic relationships seem to contradict the perceived mechanism of ICL repair by the sequential action of NER and homologous recombination, it is suggested that they are rather a reflection of the non-exclusivity of this mechanism, and that other repair pathways exist that are dependent upon NER *or* recombination. Indeed, NER factors have been implicated in some

mechanisms of ICL repair by damage bypass/PRR (Barre *et al.*, 1999; Beljanski *et al.*, 2004; Saffran *et al.*, 2004). It is also feasible that some cross-link associated DSBs may be repaired by recombination alone.

The analyses presented in Chapter 4 suggest that there is a secondary system of ICL repair, alternative to the *PSO2*-NER pathway, which is also resolved by recombination. This secondary mechanism requires the activity of both Exo1 and the MutS complexes (Msh2:Msh3 and Msh2:Msh6). It is clear that Pso2 provides a key route for ICL repair, as loss of Exo1 and MutS activity only affects viability in cells lacking Pso2 (Chapter 4). These two branches of repair must represent the only means to process a cross-link for subsequent repair by recombination, as a *pso2 msh2* double disruptant is epistatic to *rad52*.

Recent work conducted in parallel with this thesis and using the same panel of B356-7C-derived strains has provided further evidence to support an absolute requirement for homologous recombination in Pso2-dependent ICL repair (T. Ward and P. McHugh, personal communication). Cells were arrested in G1 with α-mating factor, treated with HN2, and plated on YEPD to score survival. The single mutants *pso2*, *exo1*, and *msh2* all behaved as the wild-type parent, in that stationary/G1 phase cells exhibit greater sensitivity to HN2 than in exponential phase. This growth-related resistance to HN2 is likely to result from the presence of a sister chromatid, which enables repair by homologous recombination. In contrast, the *pso2 exo1* and *pso2 msh2* strains exhibit an equivalent level of sensitivity in both growth phases, suggesting that repair by homologous recombination is totally eliminated in the absence of the Pso2- and Exo1/MutS-dependent repair sub-pathways. Furthermore, these factors are important in

the recombinational repair of non-ICL-associated DSBs, as *pso2 exo1* and *pso2 msh2* double mutant cells demonstrate an increased sensitivity to ionising radiation, and a reduced capacity for spontaneous recombination at an inverted repeat substrate (Chapter 4). This sensitivity to ionising radiation is epistatic with *rad52*, since elimination of both *pso2* and *msh2* in a *rad52* background produces an indistinguishable level of sensitivity to the *rad52* single disruptant (Chapter 4; T. Ward and P. McHugh, personal communication). Presumably, a subset of the lesions arising either spontaneously, or after exposure to ionising radiation, resemble intermediates encountered in the repair of an ICL, perhaps involving an irreversibly collapsed replication fork, or break sites associated with base damage or other modified/unusual terminal structures.

It is clear that Pso2 is involved at an intermediate stage of ICL repair, after the initial incision and unhooking of the cross-link by the NER apparatus, but prior to reconstitution of dsDNA by recombination. It is plausible that such an intermediate stage of repair may involve nucleolytic processing of the region around the unhooked cross-link in order to produce a suitable substrate for the initiation of recombination by strand invasion. Given the identification of a highly conserved hydrolytic β-lactamase domain and a DNA-specific β-CASP motif within the *PSO2* sequence (Callebaut *et al.*, 2002), and the recent demonstration that the human *PSO2*-paralogue Artemis has nuclease activity *in vitro* (Ma *et al.*, 2002), it is not inconceivable that Pso2 may act in some nucleolytic capacity in ICL repair. Furthermore, the results presented here have identified a parallel repair mechanism involving the exonuclease Exo1, and the MutS heterodimer, which is known to bind to branched DNA structures and facilitate the endonuclease activity of Rad1-Rad10 (Alani *et al.*, 1997; Sugawara *et al.*, 1997). By analogy, Pso2 may recognise and bind to the complex branched intermediate structures

arising from the NER-dependent unhooking of the cross-link, and instigate the subsequent nucleolytic processing of the gap to provide a suitable ssDNA substrate for strand invasion. This exonuclease activity may resemble that of DNA polymerase I in *E. coli* ICL repair, which proceeds in a 5'-3' direction, equivalent to *S. cerevisiae* Exo1 (Sladek *et al.*, 1989). Alternatively, Pso2 may act as a flap endonuclease, analogous to the DNA-PKcs-complexed form of human Artemis (Ma *et al.*, 2002), or the MutS-associated Rad1-Rad10 heterodimer (Sugawara *et al.*, 1997). Indeed, hairpin structures, similar to those acted upon by human Artemis, may be formed as an intermediate structure in ICL repair.

The confirmation here that NER, Pso2, and recombination act sequentially upon a DNA cross-link represents an important advance in the understanding of ICL repair in actively growing cells. Figure 6.1 outlines a putative model for ICL repair, which encompasses these new discoveries. It is proposed that Pso2 or Exo1-MutS acts upon the DNA structures arising from NER-dependent incision events, which occur throughout the cell cycle (Meniel *et al.*, 1997). However, to account for both the lack of epistasis between NER and recombination, and the complete inhibition of recombination and DSB repair in the *pso2 exo1* and *pso2 msh2* strains, it is suggested that Pso2 and Exo1-MutS can also process alternative substrates arising directly from a replication fork-associated DSB. It is not known whether these branches are co-ordinated, but the epistasis of *PSO2* with NER, and the partial DSB repair deficiency in

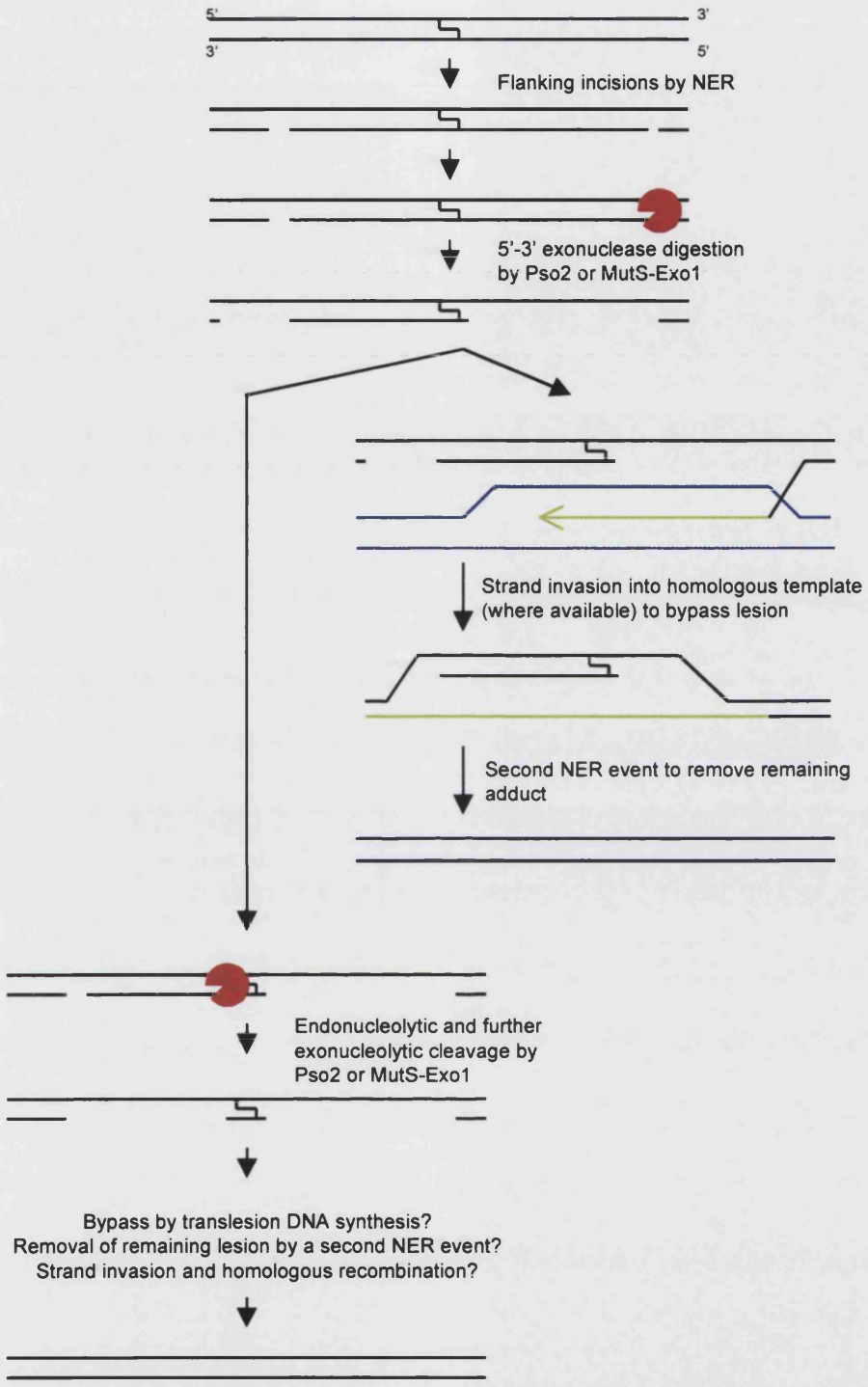

Figure 6.1 **A revised model of ICL repair in yeast,** demonstrating the proposed functions of Pso2 and MutS-Exo1 in exo- and endonucleolytic cleavage of intermediate DNA repair structures.

pso2 mutants, implies that NER-*PSO2* processing of ICLs may precede DSB repair. Furthermore, Pso2 is expected to act as the predominant factor in the processing of intermediate DNA structures, due to the absence of an increased sensitivity to ICLs in *exo1 msh2* deficient cells. In both cases, where a homologous template is available, the resulting intermediates are resolved by strand invasion and recombination across the uncoupled cross-link, with a second round of incision reactions to repair the complementary DNA strand (Fig. 6.1). The analyses of multiple gene disruptants have for the first time facilitated clarification of the complicated relationships between these different repair components, resolving the previous ambiguities which yielded predictions that NER-Pso2 and recombination represented distinct pathways of ICL repair (Grossmann *et al.*, 2001). Pso2 or MutS-Exo1 could conceivably also digest DNA 3' to the ICL, by first incising endonucleolytically (Fig. 6.1). In the absence of a suitable homologous template, it may be possible to replicate past this intermediate structure using translesion polymerases.

The conclusions drawn from this investigation regarding the mechanisms involved in ICL repair have recently been verified by two other studies in *S. cerevisiae* using a range of cross-linking agents, including cisplatin, mitomycin C, and psoralen (Beljanski *et al.*, 2004; Saffran *et al.*, 2004). Beljanski *et al.* also suggest that the relative importance of the different repair pathways in the response to cross-link damage can vary, depending on the nature of the ICL-agent. This has important implications for the elucidation of ICL repair in mammalian cells, where subtle diversions from the yeast system have already been observed, such as the enhanced involvement of XPF-ERCC1 compared to the other NER factors (Collins 1993; de Silva *et al.* 2000).

One of the remaining questions for ICL-associated DSB repair concerns the mechanism by which recombination restart can occur. Obviously, the nature of a cross-link attached to both DNA strands precludes simple recombinational bypass. However, the observation that ICL repair is more mutagenic in rapidly growing cells than in G1 phase, suggests an involvement for error-prone repair, even where substrates exist for homologous recombination (P. McHugh, unpublished observations). Furthermore, it has recently been suggested that a Rad52-dependent replication restart may occur in conjunction with damage bypass mechanisms (Schurer *et al.*, 2004). Such a system may well be suited to the bypass of an incised cross-link, hence facilitating DSB-initiated replication restart. It is hoped that further analysis of the relationship between *PSO2* and PRR, in particular the apparent epistasis with *RAD18* for nitrogen mustard sensitivity (Chapter 3), may help to elucidate this pathway of ICL repair.

Future investigation of the explicit function of Pso2 and the elucidation of ICL repair in more detail can only be achieved through biochemical analysis. The availability of yeast Pso2 protein, as produced here (Chapter 5), now enables a thorough study of its potential nuclease activity. These *in vitro* analyses should incorporate the determination of the DNA substrates acted upon by Pso2 and the manner of the nucleolytic activity (i.e. endo or exo, and directionality), as well as any protein interactions required for efficient cross-link processing. A further tool will be the use of the Pso2 purification process to provide a number of mutant Pso2 proteins, deficient in one of the conserved motifs, such as the metallo-β-lactamase and β-CASP domains. Such analysis should assist in determining the role of Pso2 in ICL repair. Ultimately, it may be possible to reconstitute *in vitro* repair at a defined ICL, and hence formulate a convincing model for the repair of DNA interstrand cross-links.

The sequence conservation of *PSO2*, especially within the putative catalytic domains, from yeast throughout higher eukaryotes implies that this is an important gene. New additions to the *PSO2* family have recently been identified in three other model organisms, namely the fission yeast *S. pombe* (Chapter 3), the fruit fly *Drosophila melanogaster* (Laurencon *et al.*, 2004), and Chicken DT40 cells (M. Takata, Kawasaki Medical University, Kurashiki, Japan, personal communication). These will no doubt prove to be essential for the extrapolation of the results observed in *S. cerevisiae*, in order to determine the extent of the functional conservation of Pso2. It is hoped that the investigation of Pso2 in model organisms will help further the understanding of human Snm1 in the repair of DNA ICL, and ultimately lead to new therapeutic strategies for the treatment of cancer.

REFERENCES

Abuin A, Zhang H, and Bradley A. **2000**. Genetic analysis of mouse embryonic stem cells bearing Msh3 and Msh2 single and compound mutations. *Mol. Cell. Biol.* **20**: 149-157

Adachi N, Ishino T, Ishii Y, Takeda S, and Koyama H. **2001**. DNA ligase IV-deficient cells are more resistant to ionizing radiation in the absence of Ku70: Implications for DNA double-strand break repair. *Proc. Natl. Acad. Sci. USA* **98**: 12109-12113

Akkari YM, Bateman RL, Reifsteck CA, Olson SB, and Grompe M. **2000**. DNA replication is required to elicit cellular responses to psoralen-induced DNA interstrand cross-links. *Mol. Cell Biol.* **20**: 8283-8289

Alani E, Lee S, Kane MF, Griffith J, and Kolodner RD. **1997**. *Saccharomyces cerevisiae MSH2*, a mispaired base recognition protein, also recognizes Holliday junctions in DNA. *J. Mol. Biol.* **265**: 289-301

Allers T and Lichten M. **2001**. Differential timing and control of noncrossover and crossover recombination during meiosis. *Cell* **106**: 47-57

Ammerer G. **1983**. Expression of genes in yeast using the *ADCI* promoter. *Methods Enzymol.* **101**: 192-201

Anderson DG and Kowalczykowski SC. **1997**. The translocating RecBCD enzyme stimulates recombination by directing RecA protein onto ssDNA in a chi-regulated manner. *Cell.* **90**: 77-86

Aravind L. **1999**. An evolutionary classification of the metallo-β-lactamase fold proteins. *In Silico Biol.* **1**:69-91

Argueso JL, Smith D, Yi J, Waase M, Sarin S, and Alani E. **2002.** Analysis of conditional mutations in the *Saccharomyces cerevisiae MLH1* gene in mismatch repair and in meiotic crossing over. *Genetics* **160**: 909-921

Ausubel FM, Brent R, Kingston RE, Moore DD, Seidman JG, Smith JA, and Struhl K (Eds.). **1993.** Unit 13.13, Preparation of Protein Extracts from Yeast. *In:* Current Protocols in Molecular Biology, John Wiley & Sons, Inc.

Averbeck D, Dardalhon M, Magana-Schwencke N, Meira LB, Meniel V, Boiteux S, and Sage E. **1992.** New aspects of the repair and genotoxicity of psoralen photoinduced lesions in DNA. *J. Photochem. Photobiol. B Biol.* **14**: 47-63

Averbeck D and Dardalhon M. **1990.** Pulsed-field electrophoresis analysis of the repair of DNA interstrand cross-links induced in *Saccharomyces cerevisiae. Yeast* **6**: S114

Bai Y and Symington LS. **1996.** A Rad52 homologue is required for *RAD51*-independent mitotic recombination in *Saccharomyces cerevisiae. Genes Dev.* **10**: 2025-2037

Bailly V, Lamb J, Sung P, Prakash S, and Prakash L. **1994.** Specific complex formation between yeast *RAD6* and *RAD18* proteins: a potential mechanism for targeting *RAD6* ubiquitin-conjugating activity to DNA damage sites. *Genes Dev.* **8**: 811-820

Balajee AS and Bohr VA. **2000.** Genomic heterogeneity of nucleotide excision repair. *Gene* **250**: 15-30. *Review.*

Bardwell AJ, Bardwell L, Tomkinson AE, and Friedberg EC. **1994**. Specific cleavage of model recombination and repair intermediates by the yeast Rad1-Rad10 DNA endonuclease. *Science* **265**: 2082-2085

Bardwell L, Cooper AJ, and Friedberg EC. **1992**. Stable and specific association between the yeast recombination and DNA repair proteins *RAD1* and *RAD10* in vitro. *Mol. Cell. Biol.* **12**: 3041-3049

Bardwell PD, Woo CJ, Wei K, Li Z, Martin A, Sack SZ, Parris T, Edelmann W, and Scharff MD. **2004**. Altered somatic hypermutation and reduced class-switch recombination in exonuclease 1-mutant mice. *Nat. Immunol.* **5**: 224-229

Barre FX, Asseline U, and Harel-Bellan A. **1999 A**. Asymmetric recognition of psoralen interstrand cross-links by the nucleotide excision repair and the error-prone pathways. *J. Mol. Biol.* **286**: 1379-1387

Barre FX, Giovannangeli C, Helene C, and Harel-Bellan A. **1999 B**. Covalent crosslinks introduced via a triple helix-forming oligonucleotide coupled to psoralen are inefficiently repaired. *Nucleic Acids Res.* **27**: 743-749

Batty DP and Wood RD. **2000**. Damage recognition in nucleotide excision repair of DNA. *Gene* **241**: 193-204. *Review.*

Becker DM, Fikes JD, and Guarente L. **1991**. A cDNA encoding a human CCAAT-binding protein cloned by functional complementation in yeast. *Proc. Natl. Acad. Sci. USA* **88**: 1968-1972

Beljanski V, Marzilli LG, and Doetsch PW. **2004**. DNA damage-processing pathways involved in the eukaryotic cellular response to anticancer DNA cross-linking drugs. *Mol Pharmacol.* **65**: 1496-1506

Berardini M, Foster PL, and Loechler EL. **1999**. DNA polymerase II (polB) is involved in a new DNA repair pathway for DNA interstrand cross-links in *Escherichia coli*. *J. Bacteriol.* **181**: 2878-82

Bessho T. **2003**. Induction of DNA replication-mediated double strand breaks by psoralen DNA interstrand cross-links. *J. Biol. Chem.* **278**: 5250-5254

Bessho T, Mu D, and Sancar A. **1997**. Initiation of DNA interstrand cross-link repair in humans: the nucleotide excision repair system makes dual incisions 5' to the cross-linked base and removes a 22- to 28-nucleotide-long damage-free strand. *Mol. Cell. Biol.* **17**: 6822-30

Bhatia PK, Verhage RA, Brouwer J, and Friedberg EC. **1996**. Molecular cloning and characterization of *Saccharomyces cerevisiae RAD28*, the yeast homolog of the human Cockayne syndrome A (CSA) gene. *J. Bacteriol.* **178**: 5977-5988

Bishop DK, Ear U, Bhattacharyya A, Calderone C, Beckett M, Weichselbaum RR and Shinohara A. **1998**. Xrcc3 is required for assembly of Rad51 complexes in vivo. *J. Biol. Chem.* **273**: 21482–21488

Blom N, Gammeltoft S, and Brunak S. **1999**. Sequence- and structure-based prediction of eukaryotic protein phosphorylation sites. *J. Mol. Biol.* **294**: 1351-1362

Bodell WJ. **1990.** Molecular dosimetry for sister-chromatid exchange induction and cytotoxicity by monofunctional and bifunctional alkylating agents. *Mutat Res.* **233**: 203-210

Boulton SJ and Jackson SP. **1996.** *Saccharomyces cerevisiae* Ku70 potentiates illegitimate DNA double-strand break repair and serves as a barrier to error-prone DNA repair pathways. *EMBO J.* **15**: 5093-5103

Brendel M and Ruhland A. **1984.** Relationships between functionality and genetic toxicology of selected DNA-damaging agents. *Mutat. Res.* **133**: 51-85

Bressan DA, Baxter BK, and Petrini JH. **1999.** The Mre11-Rad50-Xrs2 protein complex facilitates homologous recombination-based double-strand break repair in *Saccharomyces cerevisiae. Mol. Cell. Biol.* **19**: 7681-7687

Broomfield S and Xiao W. **2002.** Suppression of genetic defects within the RAD6 pathway by srs2 is specific for error-free post-replication repair but not for damage-induced mutagenesis. *Nucl. Acids Res.* **30**: 732-739

Broomfield S, Hryciw T, and Xiao W. **2001.** DNA postreplication repair and mutagenesis in *Saccharomyces cerevisiae. Mutat. Res.* **486**: 167-184. *Review.*

Caldecott K and Jeggo P. **1991.** Cross-sensitivity of gamma-ray-sensitive hamster mutants to cross-linking agents. *Mutat. Res.* **255**: 111-121

Callebaut I, Moshous D, Mornon JP, and de Villartay JP. **2002.** Metallo-beta-lactamase fold within nucleic acids processing enzymes: the beta-CASP family. *Nucleic Acids Res.* **30**: 3592-3601

Carfi A, Pares S, Duee E, Galleni M, Duez C, Frere JM, and Dideberg O. **1995.** The 3-D structure of a zinc metallo-β-lactamase from *Bacillus cereus* reveals a new type of protein fold. *EMBO J.* **14**:4914-4921

Cassier C, Chanet R, Henriques JA, and Moustacchi E. **1980.** The effects of three *PSO* genes on induced mutagenesis: a novel class of mutationally defective yeast. *Genetics* **96**: 841-857

Cassier-Chauvat C and Moustacchi E. **1988.** Allelism between *pso1-1* and *rev3-1* mutants and between *pso2-1* and *snm1* mutants in *Saccharomyces cerevisiae. Curr. Genet.* **13**:37-40

Chanet R, Cassier C, and Moustacchi E. **1985.** Genetic control of the bypass of mono-adducts and of the repair of cross-links photoinduced by 8-methoxypsoralen in yeast. *Mutat. Res.* **145**: 145-155

Chaney SG and Sancar A. **1996.** DNA repair: enzymatic mechanisms and relevance to drug response. *J. Natl. Cancer Inst.* **88**: 1346-1360. *Review.*

Chen C and Kolodner RD. **1999.** Gross chromosomal rearrangements in *Saccharomyces cerevisiae* replication and recombination defective mutants. *Nat. Genet.* **23**: 81-85

Christmann M, Tomicic MT, Roos WP, and Kaina B. **2003.** Mechanisms of human DNA repair: an update. *Toxicology* **193**: 3-34. *Review.*

Chu G and Gunderson K. **1991.** Separation of large DNA by a variable-angle contour-clamped homogeneous electric field apparatus. *Anal. Biochem.* **194**:439-446

Clark AB, Cook ME, Tran HT, Gordenin DA, Resnick MA and Kunkel TA. **1999**. Functional analysis of human MutSalpha and MutSbeta complexes in yeast. *Nucleic Acids Res.* **27**: 736-742

Cole RS, Levitan D, and Sinden RR. **1976**. Removal of psoralen interstrand cross-links from DNA of *Escherichia coli*: mechanism and genetic control. *J. Mol. Biol.* **103**: 39-59

Cole RS. **1973**. Repair of DNA containing interstrand crosslinks in *Escherichia coli*: sequential excision and recombination. *Proc. Natl. Acad. Sci. USA* **70**: 1064-1068

Collins AR. **1993**. Mutant rodent cell lines sensitive to ultraviolet light, ionizing radiation and cross-linking agents: a comprehensive survey of genetic and biochemical characteristics. *Mutat Res.* **293**: 99-118

Comess KM and Lippard SJ. **1993**. Molecular aspects of platinum-DNA interactions. *In:* Molecular Aspects of Anticancer Drug-DNA interactions, (Eds. Neidle S and Waring MJ), Macmillan Press, Houndmills, Basingstoke, UK, pp 134-168.

Cox MM, Goodman MF, Kreuzer KN, Sherratt DJ, Sandler SJ, and Marians KJ. **2000**. The importance of repairing stalled replication forks. *Nature* **404**: 37-41

Crouse GF. **2000**. Mutagenesis assays in yeast. *Methods* **22**: 116-119. *Review.*

Damia G, Imperatori L, Stefanini M, D'Incalci M. **1996**. Sensitivity of CHO mutant cell lines with specific defects in nucleotide excision repair to different anti-cancer agents. *Int. J. Cancer* **66**: 779-83

D'Amours D and Jackson SP. **2001**. The yeast Xrs2 complex functions in S phase checkpoint regulation. *Genes Dev.* **15**: 2238-2249

D'Andrea AD and Grompe M. **2003.** The Fanconi anaemia/BRCA pathway. *Nat Rev Cancer.* **3**: 23-34. *Review.*

Dardalhon M and Averbeck D. **1995.** Pulsed-field gel electrophoresis analysis of the repair of psoralen plus UVA induced DNA photoproducts in *Saccharomyces cerevisiae. Mutat. Res.* **336**: 49-60

Dardalhon M, Nohturfft A, Menial V and Averbeck D. **1994.** Repair of DNA double-strand breaks induced in *Saccharomyces cerevisiae* using different γ-ray dose rates: a pulsed-field electrophoresis analysis. *Int. J. Radiat. Biol.* **65**: 307-314

de Jager M, Wyman C, van Gent DC, and Kanaar R. **2002.** DNA end-binding specificity of human Rad50/Mre11 is influenced by ATP. *Nucl. Acids Res.* **30**: 4425-4431

de Jager M, van Noort J, van Gent DC, Dekker C, Kanaar R, and Wyman C. **2001.** Human Rad50/Mre11 is a flexible complex that can tether DNA ends. *Mol. Cell.* **8**: 1129-1135

de la Torre Ruiz MA and Lowndes NF. **2000.** *DUN1* defines one branch downstream of *RAD53* for transcription and DNA damage repair in *Saccharomyces cerevisiae. FEBS Lett.* **485**: 205-206

De Silva IU, McHugh PJ, Clingen PH, and Hartley JA. **2002.** Defects in interstrand cross-link uncoupling do not account for the extreme sensitivity of ERCC1 and XPF cells to cisplatin. *Nucleic Acids Res.* **30**: 3848-3856

De Silva IU, McHugh PJ, Clingen PH, and Hartley JA. **2000**. Defining the roles of nucleotide excision repair and recombination in the repair of DNA interstrand cross-links in mammalian cells. *Mol. Cell. Biol.* **20**: 7980-7990

Debrauwere H, Loeillet S, Lin W, Lopes J, and Nicolas A. **2001**. Links between replication and recombination in *Saccharomyces cerevisiae*: a hypersensitive requirement for homologous recombination in the absence of Rad27 activity. *Proc. Natl. Acad. Sci. USA* **98**: 8263-8269

Demuth I and Digweed M. **1998**. Genomic organization of a potential human DNA-crosslink repair gene, KIAA0086. *Mutat. Res.* **409**:11-16

Doetsch PW, Morey NJ, Swanson RL, and Jinks-Robertson S. **2001**. Yeast base excision repair: interconnections and networks. *Prog. Nucleic Acid Res. Mol. Biol.* **68**: 29-39. *Review.*

Drake JW. **1970**. *The Molecular Basis of Mutation.* Holden-Day, San Francisco, USA.

Dronkert ML and Kanaar R. **2001**. Repair of DNA interstrand cross-links. *Mutat. Res.* **486**: 217-247. *Review.*

Dronkert ML, de Wit J, Boeve M, Vasconcelos ML, van Steeg H, Tan TL, Hoeijmakers JH, and Kanaar R. **2000**. Disruption of mouse *SNM1* causes increased sensitivity to the DNA interstrand cross-linking agent mitomycin C. *Mol. Cell. Biol.* **20**: 4553-4561

Eggleston AK and West SC. **1996**. Exchanging partners: recombination in *E. coli*. *Trends Genet.* **12**: 20-26. *Review.*

Einhauer A and Jungbauer A. **2001.** The FLAG peptide, a versatile fusion tag for the purification of recombinant proteins. *J. Biochem. Biophys. Methods.* **49**: 455-465. *Review.*

Evans E, Sugawara N, Haber JE, and Alani E. **2000.** The *Saccharomyces cerevisiae* Msh2 mismatch repair protein localises to recombination intermediates in vivo. *Mol. Cell* **5**: 789-799

Evans E, Moggs JG, Hwang JR, Egly JM, and Wood RD. **1997.** Mechanism of open complex and dual incision formation by human nucleotide excision repair factors. *EMBO J.* **16**: 6559-6573

Fichtinger-Schepman AM, van Dijk-Knijnenburg HC, van der Velde-Visser SD, Berends F, and Baan RA. **1995.** Cisplatin- and carboplatin-DNA adducts: is PT-AG the cytotoxic lesion? *Carcinogenesis* **16**: 2447-2453

Fichtinger-Schepman AMJ, van der Veer JL, den Hartog JHJ, Lohman PHM, and Reedijk J. **1985.** Adducts of the antitumor drug cis-diamminedichloroplatinum(II) with DNA: formation, identification, and quantitation. *Biochemistry* **24**: 707-713

Fink D, Aebi S, and Howell SB. **1998.** The role of DNA mismatch repair in drug resistance. *Clin Cancer Res.* **4**: 1-6. *Review.*

Fiorentini P, Huang KN, Tishkoff DX, Kolodner RD, and Symington LS. **1997.** Exonuclease I of *Saccharomyces cerevisiae* functions in mitotic recombination in vivo and in vitro. *Mol. Cell. Biol.* **17**: 2764-2773

Fishman-Lobell J and Haber JE. **1992.** Removal of nonhomologous DNA ends in double-strand break recombination: the role of the yeast ultraviolet repair gene *RAD1*. *Science* **258**: 480-484

Fishman-Lobell J, Rudin N, and Haber JE. **1992.** Two alternative pathways of double-strand break repair that are kinetically separable and independently modulated. *Mol. Cell. Biol.* **12**: 1292-303

Fleer R and Brendel M. **1979.** Formation and fate of cross-links induced by polyfunctional anticancer drugs in yeast. *Mol. Gen. Genet.* **176**: 41-52

Frank-Vaillant M and Marcand S. **2001.** NHEJ regulation by mating type is exercised through a novel protein, Lif2p, essential to the ligase IV pathway. *Genes Dev.* **15**: 3005-12

Friedberg EC, Walker GC, and Siede W. **1995.** *DNA repair and Mutagenesis.* American Society for Microbiology, Washington, DC.

Garcia-Higuera I, Taniguchi T, Ganesan S, Meyn MS, Timmers C, Hejna J, Grompe M, and D'Andrea AD. **2001.** Interaction of the Fanconi anemia proteins and BRCA1 in a common pathway. *Mol. Cell.* **7**: 249-262

Gavel Y and von Heijne G. **1990.** Cleavage-site motifs in mitochondrial targeting peptides. Protein Eng. **4**: 33-37

Gavin A-C, Bosche M, Krause R, Grandi P, Marzioch M, Bauer A, Schultz J, Rick JM, Michon AM, Cruciat CM, Remor M, Hofert C, Schelder M, Brajenovic M, Ruffner H, Merino A, Klein K, Hudak M, Dickson D, Rudi T, Gnau V, Bauch A, Bastuck S, Huhse B, Leutwein C, Heurtier MA, Copley RR, Edelmann A, Querfurth E, Rybin V, Drewes

G, Raida M, Bouwmeester T, Bork P, Seraphin B, Kuster B, Neubauer G, and Superti-Furga G. **2002.** Functional organization of the yeast proteome by systematic analysis of protein complexes. *Nature* **415**: 141-147

Geigl EM and Eckardt-Schupp F. **1990.** Chromosome-specific identification and quantification of S1 nuclease-sensitive sites in yeast chromatin by pulsed-field gel electrophoresis. *Mol. Microbiol.* **4**: 801-810

Genschel J and Modrich P. **2003.** Mechanism of 5'-directed excision in human mismatch repair. *Mol. Cell* **12**: 1077-1086

Genschel J, Littman SJ, Drummond JT, and Modrich P. **1998.** Isolation of MutSbeta from human cells and comparison of the mismatch repair specificities of MutSbeta and MutSalpha. *J. Biol. Chem.* **273**: 19895-901

Godthelp BC, Wiegant WW, van Duijn-Goedhart A, Scharer OD, van Buul PP, Kanaar R, and Zdzienicka MZ. **2002.** Mammalian Rad51C contributes to DNA cross-link resistance, sister chromatid cohesion and genomic stability. *Nucleic Acids Res.* **30**: 2172-2182

Goldstein AL and McCusker JH. **1999.** Three new dominant drug resistance cassettes for gene disruption in *Saccharomyces cerevisiae*. *Yeast.* **15**: 1541-1553

Goodman LS, Wintrobe MM, Dameshek W, Goodman MJ, Gilman A, and McLennan MT. **1946.** Nitrogen Mustard Therapy. *Journal of the American Medical Association*, September 21, pp. 126-132.

Greenberg RB, Alberti M, Hearst JE, Chua MA, and Saffran WA. **2001.** Recombinational and mutagenic repair of psoralen interstrand cross-links in *Saccharomyces cerevisiae*. *J. Biol. Chem.* **276**: 31551-31560

Greene AL, Snipe JR, Gordenin DA, and Resnick MA. **1999.** Functional analysis of human FEN1 in *Saccharomyces cerevisiae* and its role in genome stability. *Hum. Mol. Genet.* **8**: 2263-2273

Gregory SM and Sweder K. **2001.** Deletion of the *CSB* homolog, *RAD26*, yields Spt- strains with proficient transcription-coupled repair. *Nucleic Acids Res.* **29**: 3080-3086

Grenson M, Mousset M, Wiame JM, and Bechet J. **1966.** Multiplicity of the amino acid permeases in *Saccharomyces cerevisiae*. I. Evidence for a specific arginine-transporting system. *Biochim. Biophys. Acta* **127**: 325-338

Grompe M and D'Andrea A. **2001.** Fanconi anemia and DNA repair. *Hum. Mol. Genet.* **10**: 2253-2259. *Review.*

Grossmann KF, Ward AM, Matkovic ME, Folias AE, and Moses RE. **2001.** *S. cerevisiae* has three pathways for DNA interstrand crosslink repair. *Mutat Res.* **487**: 73-83

Grossmann KF, Ward AM, and Moses RE. **2000.** *Saccharomyces cerevisiae* lacking Snm1, Rev3 or Rad51 have a normal S phase but arrest permanently in G2 after cisplatin treatment. *Mutat. Res.* **461**: 1-13

Guthrie C and Fink GR. **1991.** *Guide to yeast genetics and molecular biology.* Academic Press, San Diego, California.

Guzder SN, Sung P, Prakash L, and Prakash S. **1999**. Synergistic interaction between yeast nucleotide excision repair factors NEF2 and NEF4 in the binding of ultraviolet-damaged DNA. *J. Biol. Chem.* **274**: 24257-24262

Guzder SN, Sung P, Prakash L, and Prakash S. **1996**. Nucleotide excision repair in yeast is mediated by sequential assembly of repair factors and not by a pre-assembled repairosome. *J. Biol. Chem.* **271**: 8903-10

Guzder SN, Habraken Y, Sung P, Prakash L, and Prakash S. **1995**. Reconstitution of yeast nucleotide excision repair with purified Rad proteins, replication protein A, and transcription factor TFIIH. *J. Biol. Chem.* **270**: 12973-12976

Haber JE, Ira G, Malkova A, and Sugawara N. **2004**. Repairing a double-strand chromosome break by homologous recombination: revisiting Robin Holliday's model. *Philos Trans R Soc Lond B Biol Sci.* **359**: 79-86. *Review.*

Haber JE. **2000**. Partners and pathwaysrepairing a double-strand break. *Trends. Genet.* **16**: 259-64 *Review.*

Haber JE. **1998**. The many interfaces of Mre11. *Cell.* **95**: 583-586. *Review.*

Habraken Y, Sung P, Prakash L, and Prakash S. **1995**. Structure-specific nuclease activity in yeast nucleotide excision repair protein Rad2. *J. Biol. Chem.* **270**: 30194-8

Hansen WK and Kelley MR. **2000**. Review of mammalian DNA repair and translational implications. *J. Pharmacol. Exp. Ther.* **295**: 1-9. *Review.*

Haracska L, Torres-Ramos CA, Johnson RE, Prakash S, and Prakash L. **2004**. Opposing effects of ubiquitin conjugation and SUMO modification of PCNA on

replicational bypass of DNA lesions in *Saccharomyces cerevisiae*. *Mol. Cell. Biol.* **24**: 4267-4274

Haracska L, Prakash S, and Prakash L. **2000**. Replication past O(6)-methylguanine by yeast and human DNA polymerase eta. *Mol. Cell. Biol.* **20**: 8001-8007

Harfe BD and Jinks-Robertson S. **2000**. Mismatch repair proteins and mitotic genome stability. *Mut. Res.* **451**: 151-167. *Review.*

Hartley JA. **2001**. Alkylating agents. *In*: Oxford Textbook of Oncology, (Eds. Souhami RL, Tannock IF, Hohenberger P, and Horiot JC), pp. 639-654

Hartley JA, Souhami RL, and Berardini MD. **1993**. Electrophoretic and chromatographic separation methods used to reveal interstrand crosslinking of nucleic acids. *J. Chromatogr.* **618**: 277-88. *Review.*

Henriques JA, Brozmanova J, and Brendel M. **1997**. Role of *PSO* genes in the repair of photoinduced interstrand cross-links and photooxidative damage in the DNA of the yeast *Saccharomyces cerevisiae*. *J. Photochem. Photobiol. B* **39**: 185-196

Henriques JA and Moustacchi B. **1981**. Interactions between mutations for sensitivity to psoralen photoaddition (*pso*) and to radiation (*rad*) in *Saccharomyces cerevisiae*. *J. Bacteriol.* **148**: 248-256

Henriques JA and Moustacchi E. **1980**. Isolation and characterization of *pso* mutants sensitive to photo-addition of psoralen derivatives in *Saccharomyces cerevisiae*. *Genetics* **95**: 273-288

Ho JC, Warr NJ, Shimizu H, and Watts FZ. **2001.** SUMO modification of Rad22, the Schizosaccharomyces pombe homologue of the recombination protein Rad52. *Nucleic Acids Res.* **29**: 4179-4186

Ho Y, Gruhler A, Heilbut A, Bader GD, Moore L, Adams SL, Millar A, Taylor P, Bennett K, Boutilier K, Yang L, Wolting C, Donaldson I, Schandorff S, Shewnarane J, Vo M, Taggart J, Goudreault M, Muskat B, Alfarano C, Dewar D, Lin Z, Michalickova K, Willems AR, Sassi H, Nielsen PA, Rasmussen KJ, Andersen JR, Johansen LE, Hansen LH, Jespersen H, Podtelejnikov A, Nielsen E, Crawford J, Poulsen V, Sorensen BD, Matthiesen J, Hendrickson RC, Gleeson F, Pawson T, Moran MF, Durocher D, Mann M, Hogue CW, Figeys D, and Tyers M. **2002.** Systematic identification of protein complexes in Saccharomyces cerevisiae by mass spectrometry. *Nature.* **415**: 180-183, with supplementary information available at http://www.mdsproteomics.com/yeast/

Ho YP, Au-Yeung SC, and To KK. **2003.** Platinum-based anticancer agents: innovative design strategies and biological perspectives. *Med. Res. Rev.* **23**: 633-55. *Review.*

Hoege C, Pfander B, Moldovan GL, Pyrowolakis G, and Jentsch S. **2002.** RAD6-dependent DNA repair is linked to modification of PCNA by ubiquitin and SUMO. *Nature.* **419**: 135-41

Hoeijmakers JH. **2001.** Genome maintenance mechanisms for preventing cancer. *Nature* **411**: 366-374. *Review.*

Hollingsworth NM, Ponte L, and Halsey C. **1995**. *MSH5*, a novel MutS homologue facilitates meiotic reciprocal recombination between homologues in *Saccharomyces cerevisiae* but not mismatch repair. *Genes Dev.* **9**: 1728-1739

Hopfner KP, Craig L, Moncalian G, Zinkel RA, Usui T, Owen BA, Karcher A, Henderson B, Bodmer JL, McMurray CT, Carney JP, Petrini JH, and Tainer JA. **2002**. The Rad50 zinc-hook is a structure joining Mre11 complexes in DNA recombination and repair. *Nature* **418**: 562-6

Huang W, Feaver WJ, Tomkinson AE, and Friedberg EC. **1998**. The N-degron protein degradation strategy for investigating the function of essential genes: requirement for replication protein A and proliferating cell nuclear antigen proteins for nucleotide excision repair in yeast extracts. *Mutat. Res.* **408**: 183-94

Hughes TR, Roberts CJ, Dai H, Jones AR, Meyer MR, Slade D, Burchard J, Dow S, Ward TR, Kidd MJ, Friend SH, and Marton MJ. **2000**. Widespread aneuploidy revealed by DNA microarray expression profiling. *Nat. Genet.* **25**: 333-337

Ira G, Malkova A, Liberi G, Foiani M, and Haber JE. **2003**. Srs2 and Sgs1-Top3 suppress crossovers during double-strand break repair in yeast. *Cell* **115**: 401-11

Ira G and Haber JE. **2002**. Characterization of RAD51-independent break-induced replication that acts preferentially with short homologous sequences. *Mol. Cell. Biol.* **22**: 6384-92

Ivanov EL, Sugawara N, Fishman-Lobell J, and Haber JE. **1996**. Genetic requirements for the single-strand annealing pathway of double-strand break repair in Saccharomyces cerevisiae. *Genetics* **142**: 693-704

Ivanov E and Haber JE. **1995.** *RAD1* and *RAD10*, but not other excision repair genes are required for double-strand break-induced recombination in *Saccharomyces cerevisiae*. *Mol. Cell. Biol.* **15**: 2245-2251

Ivanov EL, Sugawara N, White CI, Fabre F, and Haber JE. **1994.** Mutations in *XRS2* and *RAD50* delay but do not prevent mating-type switching in *Saccharomyces cerevisiae*. *Mol. Cell. Biol.* **14**: 3414-25

Jachymczyk WJ, von Borstel RC, Mowat MR, and Hastings PJ. **1981.** Repair of interstrand cross-links in DNA of *Saccharomyces cerevisiae* requires two systems for DNA repair: the *RAD3* system and the *RAD51* system. *Mol. Gen. Genet.* **182**: 196-205

Jacobson LO, Spurr CL, Barron ESG, Smith T, Lushbaugh C, and Dick GF. **1946.** Nitrogen mustard therapy. Studies on the effect of methyl-bis (Beta-chloroethyl) amine hydrochloride on neoplastic diseases and allied disorders of the hemopoietic system. *J. Am. Med. Assoc.* **132**: 263-71

Jakupec MA, Galanski M, and Keppler BK. **2003.** Tumour-inhibiting platinum complexes--state of the art and future perspectives. *Rev Physiol Biochem Pharmacol.* **146**: 1-54. *Review.*

Jeggo PA. **1998.** Identification of genes involved in repair of DNA double-strand breaks in mammalian cells. *Radiat. Res.* **150**: S80-91. Review

Jiang L, Whiteway M, Ramos C, Rodriguez-Medina JR, and Shen SH. **2002.** The YHR076w gene encodes a type 2C protein phosphatase and represents the seventh PP2C gene in budding yeast. *FEBS Lett.* **527**: 323-325

Johnson RE, Wahington MT, Prakash S, and Prakash L. **1999**. Bridging the gap: a family of novel DNA polymerases that replicate faulty DNA. *Proc. Natl. Acad. Sci. USA* **96**: 12224-12226

Jones NJ, Cox R, and Thacker J. **1987**. Isolation and cross-sensitivity of X-ray-sensitive mutants of V79-4 hamster cells. *Mutat. Res.* **183**: 279-286

Kamemura K, Hayes BK, Comer FI, and Hart GW. **2002**. Dynamic interplay between O-glycosylation and O-phosphorylation of nucleocytoplasmic proteins: alternative glycosylation/phosphorylation of THR-58, a known mutational hot spot of c-Myc in lymphomas, is regulated by mitogens. *J. Biol. Chem.* **277**: 19229-19235

Karanjawala ZE, Adachi N, Irvine RA, Oh EK, Shibata D, Schwarz K, Hsieh CL, and Lieber MR. **2002**. The embryonic lethality in DNA ligase IV-deficient mice is rescued by deletion of Ku: implications for unifying the heterogeneous phenotypes of NHEJ mutants. *DNA Repair* **1**: 1017-26

Karran P. **2000**. DNA double strand break repair in mammalian cells. *Curr. Opin. Genet. Dev.* **10**: 144-150. *Review.*

Kaye J, Smith CA, and Hanawalt PC. **1980**. DNA repair in human cells containing photoadducts of 8-methoxypsoralen or angelicin. *Cancer Res.* **40**: 696-702

Kiakos K, Howard TT, Lee M, Hartley JA, McHugh PJ. **2002**. *Saccharomyces cerevisiae RAD5* influences the excision repair of DNA minor groove adducts. *J. Biol. Chem.* **277**: 44576-44581

Klein HL. **1998**. Different types of recombination events are controlled by the *RAD1* and *RAD52* genes of *Saccharomyces cerevisiae*. *Genetics* **120**: 367-377

Kobayashi J, Antoccia A, Tauchi H, Matsuura S, and Komatsu K. **2004**. NBS1 and its functional role in the DNA damage response. *DNA Repair* **3**: 855-61

Kraakman-van der Zwet M, Overkamp WJI, van Lange REE, Essers J, van Duijn-Goedhart A, Wiggers I, Swaminathan S, van Buul PPW, Errami A, Tan RTL, Jaspers NGJ, Sharan SK, Kanaar R and Zdzienicka MZ. **2002.** Brca2 (XRCC11) deficiency results in radioresistent DNA synthesis and a higher frequency of spontaneous deletions. *Mol. Cell. Biol.* **22**: 669–679

Kumaresan KR, Hwang M, Thelen MP, and Lambert MW. **2002**. Contribution of XPF functional domains to the 5' and 3' incisions produced at the site of a psoralen interstrand cross-link. *Biochemistry.* **41**: 890-896

Kunze R and Weil CF. **2002**. *The hAT and CACTA superfamilies of plant transposons.* p565-610. *In* Craig N, Craigie R, Gellert M, and Lambowitz A (ed.), Mobile DNA II. American Society for Microbiology, Washington, D.C.

Kuraoka I, Kobertz WR, Ariza RR, Biggerstaff M, Essigmann JM, Wood RD. **2000**. Repair of an interstrand DNA cross-link initiated by ERCC1-XPF repair/recombination nuclease. *J Biol Chem.* **275**: 26632-6

Laemmli UK. **1970**. Cleavage of structural proteins during the assembly of the head of bacteriophage T4. *Nature.* **227**: 680-5

Lage C, de Padula M, de Alencar TA, da Fonseca Goncalves SR, da Silva Vidal L, Cabral-Neto J, Leitao AC. **2003**. New insights on how nucleotide excision repair could remove DNA adducts induced by chemotherapeutic agents and psoralens plus UV-A (PUVA) in Escherichia coli cells. *Mutat Res.* **544**: 143-57

Lambert S, Mason SJ, Barber LJ, Hartley JA, Pearce JA, Carr AM, and McHugh PJ. **2003**. *Schizosaccharomyces pombe* checkpoint response to DNA interstrand cross-links. *Mol. Cell. Biol.* **23**: 4728-4737

Laurencon A, Orme CM, Peters HK, Boulton CL, Vladar EK, Langley SA, Bakis EP, Harris DT, Harris NJ, Wayson SM, Hawley RS, Burtis KC. **2004**. A large-scale screen for mutagen-sensitive loci in Drosophila. *Genetics.* **167**: 217-31

Lawrence CW and Hinkle DC. **1996**. DNA polymerase zeta and the control of DNA damage induced mutagenesis in eukaryotes. *Cancer Surv.* **28**: 21-31

Le S, Moore JK, Haber JE, and Greider CW. **1999**. *RAD50* and *RAD51* define two pathways that collaborate to maintain telomeres in the absence of telomerase. *Genetics* **152**: 143-52

Lee BI, Wilson DM 3rd. **1999**. The RAD2 domain of human exonuclease 1 exhibits 5' to 3' exonuclease and flap structure-specific endonuclease activities. *J Biol Chem.* **274**: 37763-9

Lee KJ, Huang J, Takeda Y, and Dynan WS. **2000**. DNA ligase IV and XRCC4 form a stable mixed tetramer that functions synergistically with other repair factors in a cell-free end-joining system. *J. Biol. Chem.* **275**: 34787-96

Lee SE, Bressan DA, Petrini JH, Haber JE. **2002**. Complementation between N-terminal *Saccharomyces cerevisiae mre11* alleles in DNA repair and telomere length maintenance. *DNA Repair (Amst).* **1**: 27-40

Lee SH, Altenberg GA. **2003.** Expression of functional multidrug-resistance protein 1 in *Saccharomyces cerevisiae*: effects of N- and C-terminal affinity tags. *Biochem. Biophys. Res. Commun.* **306**: 644-9

Lee SK, Yu SL, Prakash L, Prakash S. **2002.** Requirement of yeast RAD2, a homolog of human XPG gene, for efficient RNA polymerase II transcription: implications for Cockayne syndrome. *Cell* **109**: 823-34

Lewis LK, Karthikeyan G, Westmoreland JW, Resnick MA. **2002.** Differential suppression of DNA repair deficiencies of Yeast *rad50*, *mre11* and *xrs2* mutants by *EXO1* and *TLC1* (the RNA component of telomerase). *Genetics* **160**: 49-62

Lewis LK and Resnick MA. **2000.** Tying up loose ends: non-homologous end-joining in *Saccharomyces cerevisiae*. *Mut. Res.* **451**: 71-89

Li L, Moshous D, Zhou Y, Wang J, Xie G, Salido E, Hu D, de Villartay JP, and Cowan MJ. **2002.** A founder mutation in Artemis, an *SNM1*-like protein, causes SCID in Athabascan-speaking Native Americans. *J. Immunol.* **186**:6323-6329

Li L, Peterson CA, Lu X, Wei P, Legerski RJ. **1999.** Interstrand cross-links induce DNA synthesis in damaged and undamaged plasmids in mammalian cell extracts. *Mol Cell Biol.* **19**: 5619-30

Li SJ, Hochstrasser M. **1999.** A new protease required for cell-cycle progression in yeast. *Nature.* **398**: 246-51

Li X and Moses RE. **2003.** The beta-lactamase motif in Snm1 is required for repair of DNA double-strand breaks caused by interstrand crosslinks in *S. cerevisiae*. *DNA Repair* **2**:121-129

Lieber MR, Ma Y, Pannicke U, and Schwarz K. **2003**. Mechanism and regulation of human non-homologous DNA end-joining. *Nat. Rev. Mol. Cell. Biol.* **4**: 712-20. Review.

Liefshitz B, Steinlauf R, Friedl A, Eckardt-Schupp F, and Kupiec M. **1998**. Genetic interactions between mutants of the 'error-prone' repair group of *Saccharomyces cerevisiae* and their effect on recombination and mutagenesis. *Mutat Res.* **407**: 135-45.

Lindsley, J. E., and J. C. Wang. **1993**. On the coupling between ATP usage and DNA transport by yeast DNA topoisomerase II. *J. Biol. Chem.* **268**: 8096-8104

Lisby M, Rothstein R. **2004**. DNA damage checkpoint and repair centers. *Curr. Opin. Cell. Biol.* **16**: 328-34. *Review.*

Liu Y, Masson JY, Shah R, O'Regan P, and West SC. **2004**. RAD51C is required for Holliday junction processing in mammalian cells. *Science* **303**: 243-6

Loehrer PJ and Einhorn LH. **1984**. Drugs five years later. Cisplatin. *Ann Intern Med.* **100**: 704-13. *Review.*

Longtine MS, McKenzie A 3rd, Demarini DJ, Shah NG, Wach A, Brachat A, Philippsen P, and Pringle JR. **1998**. Additional modules for versatile and economical PCR-based gene deletion and modification in Saccharomyces cerevisiae. *Yeast* **14**: 953-61

Ma Y, Pannicke U, Schwarz K, and Lieber MR. **2002**. Hairpin opening and overhang processing by an Artemis/DNA-dependent protein kinase complex in nonhomologous end joining and V(D)J recombination. *Cell* **108**:781-794

Maeda D, Seki M, Onoda F, Branzei D, Kawabe Y, and Enomoto T. **2004**. Ubc9 is required for damage-tolerance and damage-induced interchromosomal homologous recombination in *S. cerevisiae*. *DNA Repair (Amst).* **3**: 335-41

Magana-Schwencke N and Averbeck D. **1991**. Repair of exogenous (plasmid) DNA damaged by photoaddition of 8-methoxypsoralen in the yeast *Saccharomyces cerevisiae*. *Mutat. Res.* **251**: 123-131

Magana-Schwencke N, Henriques JA, Chanet R, and Moustacchi E. **1982**. The fate of 8-methoxypsoralen photoinduced crosslinks in nuclear and mitochondrial yeast DNA: comparison of wild-type and repair-deficient strains. *Proc. Natl. Acad. Sci. USA* **79**: 1722-1726

Maley F, Trimble RB, Tarentino AL, and Plummer TH Jr. **1989**. Characterization of glycoproteins and their associated oligosaccharides through the use of endoglycosidases. *Anal Biochem.* **180**: 195-204. *Review.*

Malkova A, Ivanov EL, and Haber JE. **1996**. Double-strand break repair in the absence of *RAD51* in yeast: a possible role for break-induced DNA replication. *Proc. Natl. Acad. Sci. USA* **93**: 7131-6

Manivasakam P, Weber SC, McElver J, and Schiestl RH. **1995**. Micro-homology mediated PCR targeting in Saccharomyces cerevisiae. *Nucleic Acids Res.* **23**: 2799-800

Marsischky GT, T, Lee S, Griffith J, and Kolodner RD. **1999**. *Saccharomyces cerevisiae* MSH2-6 complex interacts with Holliday junctions and facilitates their cleavage by phage resolution enzymes. *J. Biol. Chem.* **274**: 7200-7206

Marsischky GT, Filosi N, Kane MF, and Kolodner R. **1996.** Redundancy of Saccharomyces cerevisiae MSH3 and MSH6 in MSH2-dependent mismatch repair. *Genes Dev.* 10: 407-420

Marti TM, Kunz C, and Fleck O. **2002.** DNA mismatch repair and mutation avoidance pathways. *J. Cell. Physiol.* **191**: 28-41. *Review.*

Martin SG, Laroche T, Suka N, Grunstein M, and Gasser SM. **1999.** Relocalization of telomeric Ku and SIR proteins in response to DNA strand breaks in yeast. *Cell* **97**: 621-33.

Masutani C, Kusumoto R, Yamada A, Dohmae N, Yokoi M, Yuasa M, Araki M, Iwai S, Takio K, and Hanaoka F. **1999.** The XPV (xeroderma pigmentosum variant) gene encodes human DNA polymerase eta. *Nature* **399**: 700-704

McGlynn P and Lloyd RG. **2002.** Recombinational repair and restart of damaged replication forks. *Nat Rev Mol Cell Biol.* **3**: 859-70. *Review.*

McHugh PJ, Spanswick VJ, and Hartley JA. **2001.** Repair of DNA interstrand crosslinks: molecular mechanisms and clinical relevance. *Lancet Oncol.* **2**: 483-90. *Review*

McHugh PJ, Sones WR, and Hartley JA. **2000.** Repair of intermediate structures produced at DNA interstrand cross-links in *Saccharomyces cerevisiae. Mol. Cell. Biol.* **20**: 3425-3433

McHugh PJ, Gill RD, Waters R, and Hartley JA. **1999.** Excision repair of nitrogen mustard-DNA adducts in *Saccharomyces cerevisiae. Nucl. Acids Res.* **27**: 3259-3266

Meetei AR, de Winter JP, Medhurst AL, Wallisch M, Waisfisz Q, van de Vrugt HJ, Oostra AB, Yan Z, Ling C, Bishop CE, Hoatlin ME, Joenje H, and Wang W. **2003**. A novel ubiquitin ligase is deficient in Fanconi anemia. *Nat. Genet.* **35**: 165-70

Meeusen S, Tieu Q, Wong E, Weiss E, Schieltz D, Yates JR, and Nunnari J. **1999**. Mgm101p is a novel component of the mitochondrial nucleoid that binds DNA and is required for the repair of oxidatively damaged mitochondrial DNA. *J. Cell. Biol.* **145**: 291-304

Mello JA, Acharya S, Fishel R, and Essigmann JM. **1996**. The mismatch repair protein hMSH2 binds selectively to DNA adducts of the anticancer drug cisplatin. *Chem. Biol.* **3**: 579-589

Meluh PB and Koshland D. **1995**. Evidence that the *MIF2* gene of *Saccharomyces cerevisiae* encodes a centromere protein with homology to the mammalian centromere protein CENP-C. *Mol. Biol. Cell.* **6**: 793-807

Memisoglu A and Samson L. **2000**. Base excision repair in yeast and mammals. *Mutat. Res.* **451**: 39-51. *Review.*

Meniel V, Magana-Schwencke, Averbeck D, and Waters R. **1997**. Preferential incision of interstrand crosss-links induced by 8-methoxypsoralen plus UVA in yeast during the cell cycle. *Mutat. Res.* **384**: 23-32

Meniel V, Magana-Schwencke N, and Averbeck D. **1995**. Preferential repair in *Saccharomyces cerevisiae rad* mutants after induction of interstrand cross-links by 8-methoxypsoralen plus UVA. *Mutagenesis* **10**: 543-548

Metzler M. **1986.** DNA adducts of medicinal drugs: some selected examples. *J. Cancer Res. Clin. Oncol.* **112**: 210-215. *Review.*

Miller RD, Prakash L, and Prakash S. **1982.** Genetic control of excision of *Saccharomyces cerevisiae* interstrand DNA cross-links induced by psoralen plus near-UV light. *Mol. Cell. Biol.* **2**:939-948

Misra RR and Vos JM. **1993.** Defective replication of psoralen adducts detected at the gene-specific level in xeroderma pigmentosum variant cells. *Mol Cell Biol.* **13**: 1002-12

Moggs JG, Szymkowski DE, Yamada M, Karran P, and Wood RD. **1997.** Differential human nucleotide excision repair of paired and mispaired cisplatin-DNA adducts. *Nucl. Acids Res. 25*: 480-490

Molloy SS, Thomas L, VanSlyke JK, Stenberg PE, and Thomas G. **1994.** Intracellular trafficking and activation of the furin proprotein convertase: localization to the TGN and recycling from the cell surface. *EMBO J.* **13**: 18-33

Moncalian G, Lengsfeld B, Bhaskara V, Hopfner KP, Karcher A, Alden E, Tainer JA, and Paull TT. **2004.** The rad50 signature motif: essential to ATP binding and biological function. *J. Mol. Biol.* **335**: 937-51

Moore CW, McKoy J, Dardalhon M, Davermann D, Martinez M, and Averbeck D. **2000.** DNA damage-inducible and RAD52-independent repair of DNA double-strand breaks in Saccharomyces cerevisiae. *Genetics* **154**: 1085-1099

Mortimer RK. **1958.** Radiobiological and genetic studies on a polyploidy series (haploid to hexaploid) of *Saccharomyces cerevisiae. Radiat. Res.* **9**: 312-326

Moshous D, Callebaut I, de Chasseval R, Corneo B, Cavazzana-Calvo M, Le Deist F, Tezcan I, Sanal O, Bertrand Y, Philippe N, Fischer A, and de Villartay JP. **2001.** Artemis, a novel DNA double-strand break repair/V(D)J recombination protein, is mutated in human Severe Combined Immune Deficiency. *Cell* **105**:177-186

Mu D, Bessho T, Nechev LV, Chen DJ, Harris TM, Hearst JE, and Sancar A. **2000.** DNA interstrand cross-links induce futile repair synthesis in mammalian cell extracts. *Mol. Cell. Biol.* **20**: 2446-54

Muller A and Fishel R. **2002.** Mismatch repair and the hereditary non-polyposis colorectal cancer syndrome (HNPCC). *Cancer Invest.* **20**: 102-109. *Review.*

Muller S, Hoege C, Pyrowolakis G, and Jentsch S. **2001.** SUMO, ubiquitin's mysterious cousin. *Nat Rev Mol Cell Biol.* **2**: 202-10. *Review.*

Nakanishi K, Taniguchi T, Ranganathan V, New HV, Moreau LA, Stotsky M, Mathew CG, Kastan MB, Weaver DT, and D'Andrea AD. **2002.** Interaction of FANCD2 and NBS1 in the DNA damage response. *Nat. Cell. Biol.* **4**: 913-20

Nelson JR, Lawrence CW, and Hinkle DC. **1996 A.** Thymine-thymine dimer bypass by yeast DNA polymerase zeta. *Science.* **272**: 1646-9

Nelson JR, Lawrence CW, and Hinkle DC. **1996 B.** Deoxycytidyl transferase activity of yeast REV1 protein. *Nature.* **382**: 729-31

Niedernhofer LJ, Odijk H, Budzowska M, van Drunen E, Maas A, Theil AF, de Wit J, Jaspers NG, Beverloo HB, Hoeijmakers JH, and Kanaar R. **2004.** The structure-specific endonuclease Ercc1-Xpf is required to resolve DNA interstrand cross-link-induced double-strand breaks. *Mol Cell Biol.* **24**: 5776-87

Niegemann E and Brendel M. **1994**. A single amino acid change in *SNM1*-encoded protein leads to thermoconditional deficiency for DNA cross-link repair in *Saccharomyces cerevisiae*. *Mutat. Res.* **315**:275-279

O'Connor PM and Kohn KW. **1990**. Comparative pharmacokinetics of DNA lesion formation and removal following treatment of L1210 cells with nitrogen mustards. *Cancer Comm.* **2**: 387-394

O'Driscoll M and Jeggo P. **2002**. Immunological disorders and DNA repair. *Mutat Res.* **509**: 109-26. *Review.*

Ojwang JO, Grueneberg DA, and Loechler EL. **1989**. Synthesis of a duplex oligonucleotide containing a nitrogen mustard interstrand DNA-DNA cross-link. *Cancer Res.* **49**: 6529-37

Palom Y, Suresh Kumar G, Tang LQ, Paz MM, Musser SM, Rockwell S, and Tomasz M. **2002**. Relative toxicities of DNA cross-links and monoadducts: new insights from studies of decarbamoyl mitomycin C and mitomycin C. *Chem. Res. Toxicol.* **15**: 1398-1406

Paques F and Haber JE. **1999**. Multiple pathways of recombination induced by double-strand breaks in *Saccharomyces cerevisiae*. *Microbiol. Mol. Biol. Rev.* **63**: 349-404. *Review.*

Pastink A and Lohman PH. **1999**. Repair and consequences of double-strand breaks in DNA. *Mutat. Res.* **428**: 141-56. *Review.*

Pathak MA and Fitzpatrick TB. **1992.** The evolution of photochemotherapy with psoralens and UVA (PUVA): 2000 BC to 1992 AD. *J. Photochem. Photobiol. B.* **14**: 3-22

Paull TT and Gellert M. **1998.** The 3' to 5' exonuclease activity of Mre 11 facilitates repair of DNA double-strand breaks. *Mol. Cell.* **1**: 969-79

Petukhova G, Van Komen S, Vergano S, Klein H, and Sung P. **1999.** Yeast Rad54 promotes Rad51-dependent homologous DNA pairing via ATP hydrolysis-driven change in DNA double helix conformation. *J. Biol. Chem* **274**: 29453-29456

Pichierri P, Averbeck D, and Rosselli F. **2002.** DNA cross-link-dependent RAD50/MRE11/NBS1 subnuclear assembly requires the Fanconi anemia C protein. *Hum. Mol. Genet.* **11**: 2531-2546

Piette J, Gamper HB, van de Vorst A, and Hearst JE. **1988.** Mutagenesis induced by site specifically placed 4'-hydroxymethyl-4,5',8-trimethylpsoralen adducts. *Nucl. Acids Res.* **16**: 9961-77.

Pinto AL and Lippard SJ. **1985.** Binding of the antitumor drug cis-diamminedichloroplatinum(II) (cisplatin) to DNA. *Biochim Biophys Acta.* **780**: 167-80. *Review.*

Prakash S and Prakash L. **2000.** Nucleotide excision repair in yeast. *Mut. Res.* **451**: 13-24. *Review.*

Prolla TA, Christie DM, and Liskay RM. **1994.** Dual requirement in yeast mismatch repair for *MLH1* and *PMS1*, two homologues of the bacterial mutL gene. *Mol. Cell. Biol.* **14**: 407-415

Pungartnik C, Picada J, Brendel M, and Henriques JA. **2002.** Further phenotypic characterisation of *pso* mutants of *Saccharomyces cerevisiae* with respect to DNA repair and response to oxidative stress. *Genet. Mol. Res.* **1**: 79-89

Qiu J, Qian Y, Chen V, Guan MX, and Shen B. **1999.** Human exonuclease 1 functionally complements its yeast homologues in DNA recombination, RNA primer removal, and mutation avoidance. *J. Biol. Chem.* **274**:17893-17900

Qiu J, Guan MX, Bailis AM, and Shen B. **1998.** *Saccharomyces cerevisiae* exonuclease-1 plays a role in UV resistance that is distinct from nucleotide excision repair. *Nuc. Acids Res.* **26**: 3077-3083

Rahn R and Patrick M. **1976.** Photochemistry of DNA: secondary structure, photosensitisation, base substitution, and exogenous molecules, in: Wang S (Ed.) *Photochemistry and Photobiology of nucleic acids.* Biology, Vol II, Academic Press, New York, 97-145

Rattray AJ and Symington LS. **1995.** Multiple pathways for homologous recombination in *Saccharomyces cerevisiae. Genetics* **139**: 45-56

Rattray AJ and Symington LS. **1994.** Use of a chromosomal inverted repeat to demonstrate that the *RAD51* and *RAD52* genes of *Saccharomyces cerevisiae* have different roles in mitotic recombination. *Genes Dev.* **10**: 2025-2037

Reagan MS, Pittenger C, Siede W, and Friedberg EC. **1995.** Characterization of a mutant strain of *Saccharomyces cerevisiae* with a deletion of the *RAD27* gene, a structural homologue of the *RAD2* nucleotide excision repair gene. *J. Bacteriol.* **177**:364-371

Reed E, Yuspa SH, Zwelling LA, Ozols RF, and Poirier MC. **1986.** Quantitation of *cis*-diamminedichloroplatinum(II)(cisplatin)-DNA-intrastrand adducts in testicular and ovarian cancer patients receiving cisplatin chemotherapy. *J. Clin. Invest.* 77: 545-550

Reenan RAG and Kolodner RD. **1992.** Characterization of insertion mutations in the *Saccharomyces cerevisiae MSH1* and *MSH2* genes: evidence for separate mitochondrial and nuclear functions. *Genetics* **132**: 975-985

Resnick MA. **1976.** The repair of double-strand breaks in DNA: a model involving recombination. *J. Theor. Biol.* **59**: 97-106

Richardson C and Jasin M. **2000.** Coupled homologous and nonhomologous repair of a double-strand break preserves genomic integrity in mammalian cells. *Mol. Cell. Biol.* **20**: 9068-75

Richie CT, Peterson C, Lu T, Hittelman WN, Carpenter PB, and Legerski RJ. **2002.** hSnm1 colocalizes and physically associates with 53BP1 before and after DNA damage. *Mol. Cell. Biol.* **22**:8635-8647

Richter D, Niegemann E, and Brendel M. **1992.** Molecular structure of the DNA cross-link repair gene *SNM1 (PSO2)* of the yeast *Saccharomyces cerevisiae*. *Mol. Gen. Genet.* **231**:194-200

Rink SM, Lipman R, Alley SC, Hopkins PB, and Tomasz M. **1996.** Bending of DNA by the mitomycin C-induced, GpG intrastrand cross-link. *Chem. Res. Toxicol.* **9**: 382-389

Rodriguez MS, Dargemont C, and Hay RT. **2001**. SUMO-1 conjugation in vivo requires both a consensus modification motif and nuclear targeting. *J. Biol. Chem.* **276**: 12654-12659

Rosenberg B, Van Camp L, Grimley EB, and Thomson AJ. **1967**. The inhibition of growth or cell division in *Eschericia coli* by different ionic species of platinum(IV) complexes. *J. Biol. Chem.* **242**: 1347-1352

Ross-Macdonald P and Roeder GS. **1994**. Mutation of a meiosis specific MutS homologue decreases crossing over but not mismatch correction. *Cell* **79**: 1069-1080

Rothfuss A and Grompe M. **2004**. Repair kinetics of genomic interstrand DNA cross-links: evidence for DNA double-strand break-dependent activation of the Fanconi anemia/BRCA pathway. *Mol. Cell. Biol.* **24**: 123-34

Ruhland A, Haase E, Siede W, and Brendel M. **1981 A.** Isolation of yeast mutants sensitive to the bifunctional alkylating agent nitrogen mustard. *Mol. Gen. Genet.* **181**: 346-51

Ruhland A, Kircher M, Wilborn F, and Brendel M. **1981 B.** A yeast mutant specifically sensitive to bifunctional alkylation. *Mutat. Res.* **91**:457-462

Ruhland A and Brendel M. **1979**. Mutagenesis by cytostatic alkylating agents in yeast strains of differing repair capacities. *Genetics* **92**:83-97

Saeki T, Machida I, and Nakai S. **1980**. Genetic control of diploid recovery after γ-irradiation in the yeast *Saccharomyces cerevisiae*. *Mutat. Res.* **73**: 251-265

Saffran WA, Ahmed S, Bellevue S, Pereira G, Patrick T, Sanchez W, Thomas S, Alberti M, and Hearst JE. **2004**. DNA Repair Defects Channel Interstrand DNA Cross-links

into Alternate Recombinational and Error-prone Repair Pathways. *J. Biol. Chem.* **279**: 36462-9

Sambrook J, Fritsch EF and Maniatis T. **1989**. *Molecular cloning: a laboratory manual.* 2nd Ed. Cold Spring Harbor Laboratory, Cold Spring Harbor, N.Y.

Sancar A. **1996**. DNA excision repair. *Annu Rev Biochem.* **65**: 43-81. *Review.*

Saparbaev M, Prakash L, and Prakash S. **1996**. Requirement of mismatch repair genes *MSH2* and *MSH3* in the *RAD1-RAD10* pathway of mitotic recombination in *Saccharomyces cerevisiae. Genetics* **142**: 727-736

Schiestl RH and Prakash S. **1988**. *RAD1*, an excision repair gene of *Saccharomyces cerevisiae*, is also involved in recombination. *Mol. Cell. Biol.* **8**:3619-3626

Schurer KA, Rudolph C, Ulrich HD, and Kramer W. **2004**. Yeast *MPH1* gene functions in an error-free DNA damage bypass pathway that requires genes from Homologous recombination, but not from postreplicative repair. *Genetics* **166**: 1673-86

Schwartz DC and Hochstrasser M. **2003**. A superfamily of protein tags: ubiquitin, SUMO and related modifiers. *Trends Biochem Sci.* **28**: 321-8. *Review.*

Shinohara A, Shinohara M, Ohta T, Matsuda S, and Ogawa T. **1998**. Rad52 forms ring structures and co-operates with RPA in single-strand DNA annealing. *Genes Cells.* **3**: 145-56

Siede W and Brendel M. **1982**. Interactions among genes controlling sensitivity to radiation (RAD) and to alkylation by nitrogen mustard (*SNM*) in yeast. *Curr. Genet.* **5**: 33-38

Signon L, Malkova A, Naylor ML, Klein H, and Haber JE. **2001.** Genetic requirements for RAD51- and RAD54-independent break-induced replication repair of a chromosomal double-strand break. *Mol. Cell. Biol.* **21**: 2048-56

Sladek FM, Munn MM, Rupp WD, Howard-Flanders P. **1989.** In vitro repair of psoralen-DNA cross-links by RecA, UvrABC, and the 5'-exonuclease of DNA polymerase I. *J Biol Chem.* **264**: 6755-65

Slater M.L. **1973.** Effect of reversible inhibition of deoxyribonucleic acid synthesis on the yeast cell cycle. *J. Bacteriol.* **113**: 263-270

Sokolsky and Alani E. **2000.** *EXO1* and *MSH6* are high copy suppressors of conditional mutations in the *MSH2* mismatch repair gene of *Saccharomyces cerevisiae.* *Genetics* **155**: 589-599

Sommers CH, Miller EJ, Dujon B, Prakash S, and Prakash L. **1995.** Conditional lethality of null mutations of *RTH1* that encodes the yeast counterpart of a mammalian 5'- to 3'-exonuclease required for lagging strand DNA synthesis in reconstituted systems. *J. Biol. Chem.* **270**: 4193-4196

Spanswick VJ, Craddock C, Sekhar M, Mahendra P, Shankaranarayana P, Hughes RG, Hochhauser D, and Hartley JA. **2002.** Repair of DNA interstrand crosslinks as a mechanism of clinical resistance to melphalan in multiple myeloma. *Blood.* **100**: 224-9

Stelter P and Ulrich HD. **2003.** Control of spontaneous and damage-induced mutagenesis by SUMO and ubiquitin conjugation. *Nature* **425**: 188-91

Strathdee G, MacKean MJ, Illand M, and Brown R. **1999.** A role for methylation of the hMLH1 promoter in loss of hMLH1 expression and drug resistance in ovarian cancer. *Oncogene* **18**: 2335-41

Sugawara N, Goldfarb T, Studamire B, Alani E, and Haber JE. **2004.** Heteroduplex rejection during single-strand annealing requires Sgs1 helicase and mismatch repair proteins Msh2 and Msh6 but not Pms1. *Proc. Natl. Acad. Sci. USA* **101**: 9315-9320

Sugawara N, Wang X, and Haber JE. **2003.** In vivo roles of Rad52, Rad54, and Rad55 proteins in Rad51-mediated recombination. *Mol. Cell.* **12**: 209-19

Sugawara N, Paques F, Colaiacovo M, and Haber JE. **1997.** Role of *Saccharomyces cerevisiae* Msh2 and Msh3 repair proteins in double-strand break-induced recombination. *Proc. Natl. Acad. Sci. USA* **94**: 9214-9.

Sugawara N and Haber JE. **1992.** Characterization of double-strand break-induced recombination: homology requirements and single-stranded DNA formation. *Mol. Cell. Biol.* **12**: 563-75

Sun X, Thrower D, Qiu J, Wu P, Zheng L, Zhou M, Bachant J, Wilson DM, and Shen B. **2003.** Complementary functions of the *Saccharomyces cerevisiae* Rad2 family nucleases in Okazaki fragment maturation, mutation avoidance, and chromosome stability. *DNA Repair* **2**: 925-40

Sung P, Guzder SN, Prakash L, and Prakash S. **1996.** Reconstitution of TFIIH and requirement of its DNA helicase subunits, Rad3 and Rad25, in the incision step of nucleotide excision repair. *J. Biol. Chem.* **271**: 10821-6

Sung P. **1994.** Catalysis of ATP-dependent homologous DNA pairing and strand exchange by yeast RAD51 protein. *Science* **265**: 1241-3

Sunters A, Springer CJ, Bagshawe KD, Souhami RL, and Hartley JA. **1992.** The cytotoxicity, DNA crosslinking ability and DNA sequence selectivity of the aniline mustards melphalan, chlorambucil and 4-[bis(2-chloroethyl)amino] benzoic acid. *Biochem. Pharmacol.* **44**: 59-64

Symington LS. **2002.** Role of *RAD52* epistasis group genes in homologous recombination and double-strand break repair. Microbiol. Mol. Biol. Rev. 66: 630-670

Symington LS, Kang LE, and Moreau S. **2000.** Alteration of gene conversion tract length and associated crossing over during plasmid gap repair in nuclease-deficient strains of *Saccharomyces cerevisiae*. *Nucl. Acids Res.* **28**: 4649-4656

Symington LS. **1998.** Homologous recombination is required for the viability of rad27 mutants. *Nucl. Acids Res.* **26**:5589-5595

Szostak JW, Orr-Weaver TL, Rothstein RJ, and Stahl FW. **1983.** The double-strand-break repair model for recombination. *Cell* **33**: 25-35

Takata M, Sasaki MS, Sonoda E, Morrison C, Hashimoto M, Utsumi H, Yamaguchi-Iwai Y, Shinohara A, and Takeda S. **1998.** Homologous recombination and non-homologous end-joining pathways of DNA double-strand break repair have overlapping roles in the maintenance of chromosomal integrity in vertebrate cells. *EMBO J.* **17**: 5497-508

Taniguchi T, Tischkowitz M, Ameziane N, Hodgson SV, Mathew CG, Joenje H, Mok SC, and D'Andrea AD. **2003**. Disruption of the Fanconi anemia-BRCA pathway in cisplatin-sensitive ovarian tumors. *Nat. Med.* **9**: 568-574

Tateishi S, Sakuraba Y, Masuyama S, Inoue H, and Yamaizumi M. **2000**. Dysfunction of human Rad18 results in defective postreplication repair and hypersensitivity to multiple mutagens. *Proc. Natl. Acad. Sci. USA* **97**: 7927-32

Tavtigian SV, Simard J, Teng DH, Abtin V, Baumgard M, Beck A, Camp NJ, Carillo AR, Chen Y, Dayananth P, Desrochers M, Dumont M, Farnham JM, Frank D, Frye C, Ghaffari S, Gupte JS, Hu R, Iliev D, Janecki T, Kort EN, Laity KE, Leavitt A, Leblanc G, McArthur-Morrison J, Pederson A, Penn B, Peterson KT, Reid JE, Richards S, Schroeder M, Smith R, Snyder SC, Swedlund B, Swensen J, Thomas A, Tranchant M, Woodland AM, Labrie F, Skolnick MH, Neuhausen S, Rommens J, and Cannon-Albright LA. **2001**. A candidate prostrate cancer susceptibility gene at chromosome 17p. *Nat. Genet.* **27**:172-180

Teo SH and Jackson SP. **1997**. Identification of *Saccharomyces cerevisiae* DNA ligase IV: involvement in DNA double-strand break repair. *EMBO J.* **16**:4788-95.

Terpe K. **2003**. Overview of tag protein fusions: from molecular and biochemical fundamentals to commercial systems. *Appl Microbiol Biotechnol.* **60**: 523-33. *Review.*

Thomas BJ and Rothstein R. **1989**. The genetic control of direct-repeat recombination in *Saccharomyces*: the effect of *rad52* and *rad1* on mitotic recombination at *GAL10*, a transcriptionally regulated gene. *Genetics* **123**: 725-738

Tishkoff DX, Boerger AL, Bertrand P, Filosi N, Gaida GM, Kane MF, and Kolodner RD. **1997 A**. Identification and characterization of *Saccharomyces cerevisiae EXO1*, a

gene encoding an exonuclease that interacts with *MSH2*. *Proc. Natl. Acad. Sci. USA* **94**: 7487-7492

Tishkoff DX, Filosi N, Gaida GM, and Kolodner RD. **1997 B.** A novel mutation avoidance mechanism dependent on *S. cerevisiae RAD27* is distinct from DNA mismatch repair. *Cell* **88**: 253-263

Toh GW and Lowndes NF. **2003.** Role of the *Saccharomyces cerevisiae* Rad9 protein in sensing and responding to DNA damage. *Biochem Soc Trans.* **31**: 242-6. *Review.*

Tomasz M. 1995. Mitomycin C: small, fast and deadly (but very selective). *Chem Biol.* **2**: 575-9. *Review.*

Tomkinson AE, Bardwell AJ, Bardwell L, Tappe NJ, and Friedberg EC. **1993.** Yeast DNA repair and recombination proteins Rad1 and Rad10 constitute a single-stranded-DNA endonuclease. *Nature* **362**:860-862

Torres-Ramos CA, Prakash S, and Prakash L. **2002.** Requirement of *RAD5* and *MMS2* for postreplication repair of UV-damaged DNA in *Saccharomyces cerevisiae. Mol. Cell. Biol.* **22**: 2419-2426

Tran PT, Simon JA and Liskay RM. **2001.** Interactions of Exo1p with components of MutLalpha in *Saccharomyces cerevisiae. Proc. Natl. Acad. Sci. USA* **98**: 9760-9765

Trujillo KM, Roh DH, Chen L, Van Komen S, Tomkinson A, and Sung P. **2003.** Yeast xrs2 binds DNA and helps target rad50 and mre11 to DNA ends. *J. Biol. Chem.* **278**: 48957-48964

Trujillo KM and Sung P. **2001.** DNA structure-specific nuclease activities in the Saccharomyces cerevisiae Rad50*Mre11 complex. *J. Biol. Chem.* **276**: 35458-35464.

Tsubouchi H and Ogawa H. **2000.** Exo1 roles for repair of DNA double-strand breaks and meiotic crossing over in *Saccharomyces cerevisiae*. *Mol. Biol. Cell* **11**: 2221-2233

Tsubouchi H and Ogawa H. **1998.** A novel *mre11* mutation impairs processing of double-strand breaks of DNA during both mitosis and meiosis. *Mol. Cell. Biol.* **18**: 260-268

Ulrich HD and Jentsch S. **2000.** Two RING finger proteins mediate cooperation between ubiquitin-conjugating enzymes in DNA repair. *EMBO J.* **19**: 3388-3397

Usui T, Ohta T, Oshiumi H, Tomizawa J, Ogawa H, and Ogawa T. **1998.** Complex formation and functional versatility of Mre11 of budding yeast in recombination. *Cell* **95**: 705-716

Valencia M, Bentele M, Vaze MB, Herrmann G, Kraus E, Lee SE, Schar P, and Haber JE. **2001.** NEJ1 controls non-homologous end joining in Saccharomyces cerevisiae. *Nature* **414**: 666-669

Vallen EA and Cross FR. **1995.** Mutations in *RAD27* define a potential link between G1 cyclins and DNA replication. *Mol. Cell. Biol.* **15**: 4291-4302

Van Gent DC, Hoeijmakers JH, and Kanaar R. **2001.** Chromosomal stability and the DNA double-stranded break connection. *Nat. Rev. Genet.* **2**: 196-206. *Review.*

van Gool AJ, Verhage R, Swagemakers SM, van de Putte P, Brouwer J, Troelstra C, Bootsma D, and Hoeijmakers JH. **1994.** *RAD26*, the functional *S. cerevisiae* homolog of the Cockayne syndrome B gene ERCC6. *EMBO J.* **13**: 5361-5369

Van Houten B, Gamper H, Holbrook SR, Hearst JE, and Sancar A. **1986.** Action mechanism of ABC excision nuclease on a DNA substrate containing a psoralen crosslink at a defined position. *Proc. Natl. Acad. Sci. USA* **83**: 8077-8081

Van Houten B, Eisen JA, and Hanawalt PC. **2002.** A cut above: discovery of an alternative excision repair pathway in bacteria. *Proc. Natl. Acad. Sci. USA.* **99**: 2581-2583

Volker M, Mone MJ, Karmakar P, van Hoffen A, Schul W, Vermeulen W, Hoeijmakers JH, van Driel R, van Zeeland AA, and Mullenders LH. **2001.** Sequential assembly of the nucleotide excision repair factors in vivo. *Mol. Cell.* **8**: 213-224

Vosseller K, Sakabe K, Wells L, and Hart GW. **2002.** Diverse regulation of protein function by O-GlcNAc: a nuclear and cytoplasmic carbohydrate post-translational modification. *Curr. Opin. Chem. Biol.* **6**: 851-857. *Review.*

Vuksanovic L and Cleaver JE. **1987.** Unique cross-link and monoadduct repair characteristics of a xeroderma pigmentosum revertant cell line. *Mutat. Res.* **184**: 255-263

Wakasugi M and Sancar A. **1998.** Assembly, subunit composition, and footprint of human DNA repair excision nuclease. *Proc. Natl. Acad. Sci. USA* **95**: 6669-6674

Wang H, Yang Y, Schofield MJ, Du C, Fridman Y, Lee SD, Larson ED, Drummond JT, Alani E, Hsieh P, and Erie DA. **2003.** DNA bending and unbending by MutS governs mismatch recognition and specificity. *Proc. Natl. Acad. Sci. USA* **100**: 14822-14827

Wang X, Peterson CA, Zheng H, Nairn RS, Legerski RJ, and Li L. **2001**. Involvement of nucleotide excision repair in a recombination-independent and error-prone pathway of DNA interstrand cross-link repair. *Mol. Cell. Biol.* **21**: 713-720

Webb BL, Cox MM, Inman RB. **1997**. Recombinational DNA repair: the RecF and RecR proteins limit the extension of RecA filaments beyond single-strand DNA gaps. *Cell.* **91**: 347-356

Weng, YS, and Nickoloff JA. **1998**. Evidence for independent mismatch repair processing on opposite sides of a double-strand break in *Saccharomyces cerevisiae*. *Genetics* **148**: 59-70

Wilborn F and Brendel M. **1989**. Formation and stability of interstrand cross-links induced by cis- and trans-diamminedichloroplatinum (II) in the DNA of *Saccharomyces cerevisiae* strains differing in repair capacity. *Curr. Genet.* **16**: 331-338

Wolter R, Siede W, and Brendel M. **1996**. Regulation of *SNM1*, an inducible *Saccharomyces cerevisiae* gene required for repair of DNA cross-links. *Mol. Gen. Genet.* **250**: 162-168

Woodgate R. **1999**. A plethora of lesion-replicating DNA polymerases. *Genes Dev.* **13**: 2191-5. *Review.*

Wu HI, Brown JA, Dorie MJ, Lazzeroni L, and Brown JM. **2004**. Genome-wide identification of genes conferring resistance to the anticancer agents cisplatin, oxaliplatin, and mitomycin C. *Cancer Res.* **64**: 3940-8

Wu L and Hickson ID. **2003**. The Bloom's syndrome helicase suppresses crossing over during homologous recombination. *Nature* **426**: 870-874

Wu X, Wilson TE, Lieber MR. **1999.** A role for FEN-1 in nonhomologous DNA end joining: the order of strand annealing and nucleolytic processing events. *Proc. Natl. Acad. Sci. USA* **96**: 1303-1308

Xiao W and Chow BL. **1998.** Synergism between yeast nucleotide and base excision repair pathways in the protection against DNA methylation damage. *Curr. Genet.* **33**: 92-99

Xiao W, Chow BL, and Rathgeber L. **1996.** The repair of DNA methylation damage in *Saccharomyces cerevisiae*. *Curr. Genet.* **30**: 461-468

Xie Y, Liu Y, Argueso JL, Henricksen LA, Kao HI, Bambara RA, and Alani E. **2001.** Identification of *rad27* mutations that confer differential defects in mutation avoidance, repeat tract instability, and flap cleavage. *Mol. Cell. Biol.* **21**: 4889-4899

Yu J, Marshall K, Yamaguchi M, Haber JE, and Weil CF. **2004.** Microhomology-dependent end joining and repair of transposon-induced DNA hairpins by host factors in *Saccharomyces cerevisiae*. *Mol. Cell. Biol.* **24**: 1351-1364.

Yu S, Owen-Hughes T, Friedberg EC, Waters R, and Reed SH. **2004.** The yeast Rad7/Rad16/Abf1 complex generates superhelical torsion in DNA that is required for nucleotide excision repair. *DNA Repair* **3**: 277-87

Zamble DB, Mu D, Reardon JT, Sancar A, and Lippard SJ. **1996.** Repair of cisplatin-DNA adducts by the mammalian excision nuclease. *Biochemistry* **35**: 10004-10013

Zdraveski ZZ, Mello JA, Marinus MG, and Essigmann JM. **2000.** Multiple pathways of recombination define cellular responses to cisplatin. *Chem. Biol.* **7**: 39-50

Zhang N, Lu X, and Legerski RJ. **2003**. Partial reconstitution of human interstrand cross-link repair in vitro: characterization of the roles of RPA and PCNA. *Biochem. Biophys. Res. Commun.* **309**: 71-78

Zhang N, Lu X, Zhang X, Peterson CA, and Legerski RJ. **2002**. hMutSbeta is required for the recognition and uncoupling of psoralen interstrand cross-links in vitro. *Mol. Cell. Biol.* **22**: 2388-97

Zhang X, Richie C, and Legerski RJ. **2002**. Translation of hSNM1 is mediated by an internal ribosome entry site that upregulates expression during mitosis. *DNA Repair (Amst).* **1**: 379-90

Zwelling LA, Anderson T, and Kohn KW. **1979**. DNA-protein and DNA interstrand cross-linking by cis- and trans-platinum(II) diamminedichloride in L1210 mouse leukaemia cells and relation to cytotoxicity. *Cancer Res.* **39**: 365-369

APPENDIX

The gene-specific sequences of primers used in the PCR-based micro-homology targeted gene deletion of *S. cerevisiae*, are detailed below. The co-ordinates given are the 5' end of each primer, according to the sequence deposited in the Genbank database. Where further sequence was required upstream of the CDS, primers were designed from the sequence deposited in the Saccharomyces Genome Database (SGD).

Primer	Gene-specific sequence (5'-3')	Co-ordinates (Genbank accession)
PSO2-DEL5'	AGC ATA CGC ACT AGT GAC TAA TTT GGG TGG TCG GTT GAT T	131
PSO2-DEL3'	TCA TAC ATT CAT ATA ATA TCC ATT ACG TAC GTA CAT CTT A	2270 (X64004)
RAD4-DEL5'	GGA CGA CAA GCA GAG ACA TAA CGA CAC TAT TTT TCC GCT AAA ATG	345
RAD4-DEL3'	AAA ACA TAC TTT CCT AAT TAT TCA AAC CGT TTC AGC CTC ATT TCA	2693 (M24928)
RAD51-DEL5'	ACG TAG TTA TTT GTT AAA GGC CTA CTA ATT TGT TAT CGT CAT ATG	1315
RAD51-DEL3'	AAG TAA ACC TGT GTA AAT AAA TAG AGA CAA GAG ACC AAA TAC CTA	2600 (M88470)

RAD52-DEL5'	AAA AGA CGA AAA ATA TAG CGG CGG GCG GGT TAC GCG ACC G	921
RAD52-DEL3'	TGA TGC AAA TTT TTT ATT TGT TTC GGC CAG GAA GCG TTT C	2520 (M10249)
EXO1-DEL5'	GCG TAG AAA GGA ATG GGT ATC CAA GGT CTT CTT CCT CAG T	521
EXO1-DEL3'	TCC GAT ATG AAA CGT GCA GTA CTT AAC TTT TAT TTA CCT T	2670 (U86134)
MRE11-DEL5'	CTC CAC TAT GGA CTA TCC TGA TCC AGA CAC AAT AAG GAT T	161
MRE11-DEL3'	TCG ACC ATT AAG TAA ACC ATA ACT AGC GTC CTC TTC GTC A	2120 (U60829)
RAD1-DEL5'	AGA GCA TTT GCT AAA TGT GTA AAA ATA ATA TTG CAC TAT C	381
RAD1-DEL3'	TCA CCA AAT GAA TAT TGT TAT TTT CAC TAT AGT TAA TCG C	3830 (M15435)
RAD27-DEL5'	TAC ATT GGA AAG AAA TAG GAA ACG GAC ACC GGA AGA AAA AAT ATG	-2
RAD27-DEL3'	CAA GGT GAA GGA CCA AAA GAA GAA AGT GGA AAA AGA ACC CCC TCA	1050 (SGD YKL113C)

MSH2-DEL5'	CTT TAT CTG CTG ACC TAA CAT CAA AAT CCT CAG ATT AAA AGT ATG	1193
MSH2-DEL3'	ATT ATC TAT CGA TTC TCA CTT AAG ATG TCG TTG TAA TAT TAA TTA	4172 (M84170)
MSH3-DEL5'	TGA ATT TTC AAT GAT AAA TAA GCT GGA ACA ATG GTG ATA G	8
MSH3-DEL3'	TGG ATA TCC AAT GAT AGT AAT TTC GCG AGT TTA TCC GTT G	3177 (M96250)
MSH6-DEL5'	AAT TTT GAC AAA GCC AAT TTG AAC TCC AAA ATG GCC CCA G	-100
MSH6-DEL3'	AAA ATC TTA CAT ACA TCG TAA ATG AAA ATA CTT AGG ATT G	4761 (SGD YDR097C)
MLH1-DEL5'	GTA AAA ATA ACA TAG ACC TAT CAA TAA CGA ATG TCT CTC A	211
MLH1-DEL3'	CTT TGG TAT TAC AGC CAA AAC GTT TTA AAG TTA ACA CCT C	2580 (U07187)

The following adapter sequences were added to the 3' end of the gene-specific sequences to form the complete primer for gene targeting. F1 (5' deletion primer) and R1 (3' deletion primer) sequences were used to amplify the KanMX4 and HIS3MX6 cassettes. URA5'/3' were used to amplify *URA3* from the pYES2 vector.

F1	CGG ATC CCC GGG TTA ATT AA
R1	GAA TTC GAG CTC GTT TAA AC
URA5'	CCT GAG CGG AAG TGT ATC GT
URA3'	AAT AAG GGC GAC ACG GAA AT

PUBLICATIONS ASSOCIATED WITH THIS THESIS

Lambert S, Mason SJ, Barber LJ, Hartley JA, Pearce JA, Carr AM, and McHugh PJ. **2003**. *Schizosaccharomyces pombe* checkpoint response to DNA interstrand cross-links. *Mol. Cell. Biol.* **23**: 4728-4737

Barber LJ, Ward T, Hartley JA, and McHugh PJ. **2004**. Overlapping roles for *PSO2/SNM1* with MutS factors and *EXO1* in DNA repair. *Mol. Cell. Biol. In press.*